THE
PHYSICAL REVIEW
A Journal of Experimental and Theoretical Physics Established by E. L. Nichols in 1893
VOL. 58, NO. 5 SEPTEMBER 1, 1940 SECOND SERIES

The Solid Angle Subtended by the Main and Shadow Cones of Cosmic Radiation

HENRY PAUL KOENIG
Massachusetts Institute of Technology, Cambridge, Massachusetts
(Received June 4, 1940)

For the calculation of the longitude and latitude effects, as well as the time variations, of charged primary cosmic radiation, the knowledge of the solid angle subtended by the main and shadow cones for all latitudes and energies is essential. This solid angle is calculated over a wide range of energy and latitude from the results of Lemaître and Vallarta, and from those of Schremp, and the results given in the form of several graphs.

IT is well known that the intensity of charged primary cosmic radiation of a given energy depends on the solid angle subtended at a given point of the earth by the allowed cone for that energy,[1] and also on the energy distribution of the primaries. As a consequence of Liouville's theorem the intensity, defined as the number of primaries of a given energy arriving at the observer per unit time, is given by the product of the number of particles of that energy multiplied by the aperture of the allowed cone at the given point and for the given energy. The knowledge of the aperture of the allowed cone is thus a matter of importance.

The theory of the allowed cone has now been pushed sufficiently far that accurate values for the aperture of the main and shadow cones can

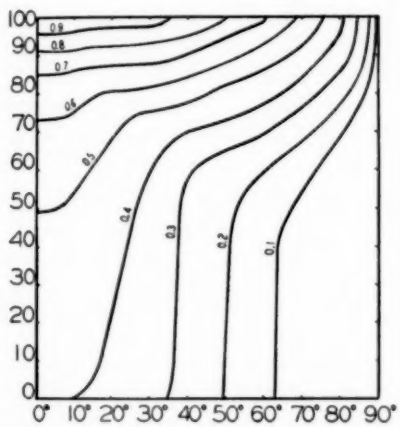

FIG. 1. The solid angle subtended by the shadow cone. Ordinates—percent; abscissas—latitude.

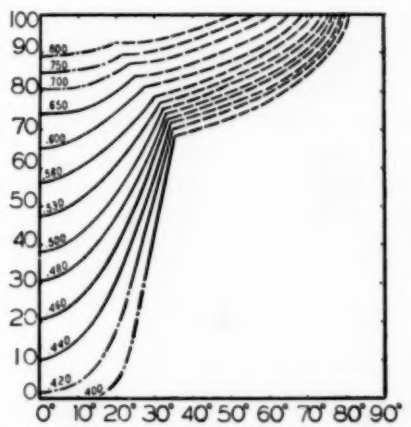

FIG. 2. The solid angle subtended by the main cone. Ordinates—percent; abscissas—latitude.

[1] G. Lemaître and M. S. Vallarta, Phys. Rev. **43**, 87 (1933); M. S. Vallarta, *An Outline of the Theory of the Allowed Cone of Cosmic Radiation* (University of Toronto Press, 1938).

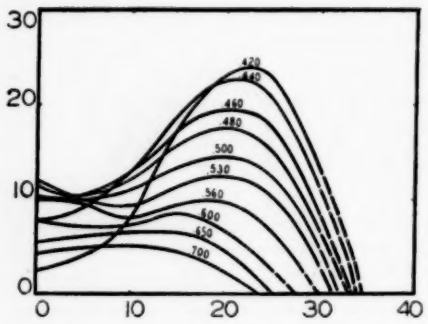

FIG. 3. The difference between the shadow cone and the main cone. Ordinates —percent; abscissas—latitude.

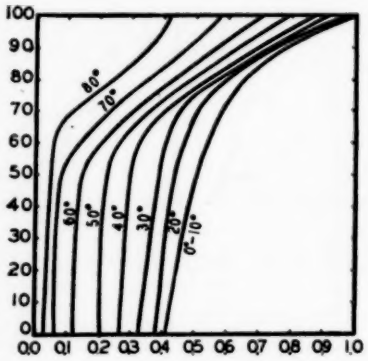

FIG. 4. The shadow cone as a function of energy for fixed latitudes, as shown. Ordinates—percent; abscissas—energy in störmers.

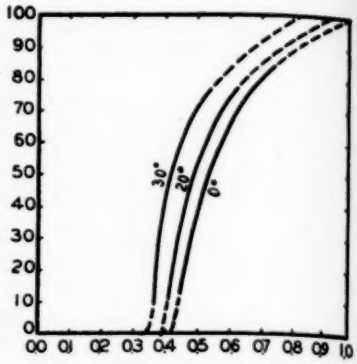

FIG. 5. The main cone as a function of energy for fixed latitudes, as shown. Ordinates—percent; abscissas—energy in störmers.

be given over a wide range of energy and latitude. An observer at a given point of the earth may define the direction of arrival of a cosmic-ray particle by using the angle θ between the tangent to the trajectory at the point of arrival and its projection on the meridian plane, and the angle η between this projection and the zenith. The solid angle subtended at the vertex by either the main or the shadow cone is then given by

$$\omega = \int\int \cos\theta d\theta d\eta,$$

the integration being extended over the boundary of the cone. This integration can be performed graphically or mechanically. The boundary of the main cone has been determined by Lemaître and Vallarta,[2] and that of the shadow cone by Schemp.[3] From their results the solid angle ω may be readily determined.

The results of this integration are shown in Figs. 1 and 2. Figure 1 gives the solid angle subtended by the shadow cone as a function of geomagnetic latitude and for different energies, the latter being expressed in Störmers.[4] It is worth recalling at this point that the shadow cone gives the upper limit of the aperture of the allowed cone for a given latitude and energy. Similarly Fig. 2 gives the solid angle subtended by the main cone as a function of latitude for different energies. The main cone gives the lower limit of the allowed cone for a given latitude and energy. The discontinuity of the curves in Fig. 2 is due to the fact that the main cone for a given energy is continued beyond a certain latitude by the shadow cone. The lowest part of certain curves (dot-dash) has been interpolated.

The difference between the main and shadow cones gives the region of penumbra. This difference is plotted in Fig. 3 for several energies as a function of latitude. The dashed part of each curve is extrapolated and doubtful. It is seen that the penumbra vanishes at high latitudes for energies higher than about 0.44 störmer. It is also worth noting that the maximum contribution of the penumbra is displaced to higher latitudes as the energy decreases.[5]

Finally, Figs. 4 and 5 give the solid angle subtended by the shadow and the main cones, respectively, as a function of energy and for a given latitude. In Fig. 4 the curve for $\lambda = 10°$ is omitted because it would be practically superposed on that for $\lambda = 0°$. These curves are very useful for the calculation of the latitude and longitude effects.

I wish to thank Professor M. S. Vallarta, who suggested this problem, for his guidance and encouragement. I am also indebted to Dr. R. A. Hutner and Dr. O. Godart for frequent discussions.

[2] G. Lemaître and M. S. Vallarta, Phys. Rev. **50**, 493 (1936).

[3] E. J. Schremp, Phys. Rev. **54**, 158 (1938); also his Ph.D. Thesis, M. I. T., 1937.

[4] For the equivalence between energy in störmers and in electron volts, see Lemaître and Vallarta, reference 1, Table VI, p. 90. For the definition, see M. S. Vallarta, reference 1, p. 7.

[5] See also R. A. Hutner, Phys. Rev. **55**, 15 (1939), Fig. 4.

The X-Ray $K\beta_{2,5}$-Emission Lines and K-Absorption Limits of Cu-Zn Alloys*

J. A. BEARDEN AND H. FRIEDMAN
Rowland Physical Laboratory, The Johns Hopkins University, Baltimore, Maryland

(Received June 17, 1940)

The shapes of the $K\beta_{2,5}$ lines of Cu and of Zn and their K-absorption edges in the pure metals and in a series of brasses have been studied with a double crystal spectrometer. Mixing Cu with Zn increases the high energy part of the emission of Cu $K\beta_{2,5}$ and decreases the corresponding part of the intensity of Zn $K\beta_2$. The magnitude of this redistribution of high energy conduction electrons between Cu and Zn is found to agree with theoretical calculations, which predict a maximum positive charge of about 10 percent of an electronic charge on a zinc atom dissolved in a Cu lattice. The present results are offered as further support for that interpretation of Cu $K\beta_{2,5}$ structure which attributes the extra low frequency emission to $3d$ band emission. In every alloy Zn $K\beta_5$ appears with very little change in width or in intensity per Zn atom, and can be definitely assigned to $3d$ quadrupole emission. No shifts of the high energy sides of the emission lines or the corresponding absorption limits greater than the experimental error have been observed with alloying, and there appears to be no evidence of any effect of crystal structure on the emission lines.

INTRODUCTION

IT has been demonstrated in recent work[1] that x-ray solid state spectroscopy in the hard x-ray region between one and two angstroms is capable of yielding considerable information about the nature of the conduction levels and higher lattice levels of metallic solids. In the work referred to, the double crystal spectrometer was applied to the study of the shapes of the $K\beta_2$- and $K\beta_5$-emission lines and the K-absorption limits of the pure elements Fe to Ge. These emission lines correspond to transitions in which electrons fall from $3d$ and $4s$ band levels into vacancies in the atomic K shells. The absorption edges result from the ejection of electrons from atomic K shells into empty levels above the Fermi surface of filled states. If one assumes a very narrow width for the K level compared to the $3d$ and $4s$ band widths, the intensity of emission or absorption at any given energy may be written as a product of density of states in the electronic bands, at the given energy, multiplied by the corresponding transition probability. The width of the emission line, where the K level is sharp, will therefore give directly the width of the electronic band.[1] The shape of the emission line will reflect the variation of density of states in the band, with modifications due to the transition probability factor. The effect of finite width of the K level can be taken into account in the manner described by Richtmyer, Barnes and Ramberg,[2] for absorption edges. In reference 1 most interest was attached to the results obtained for Cu, for which metal extensive theoretical calculations have been made. With the idea of testing some commonly held theories of the nature of binary alloys, and to check further on the correctness of the interpretation of this earlier work on pure metals, similar measurements have been carried out on a number of binary alloys. The substances chosen for study are alloys of Cu with Zn, Cu with Ni, and alloys of Ni with Zn. The selection of these alloys has again been determined by the fact that they have been the subject of much theoretical treatment and that considerable related experimental data are available on their optical constants, resistivities, specific heats, and in the case of Ni alloys, their magnetic properties.

EXPERIMENTAL

The present paper reports the results obtained for the $K\beta_{2,5}$ lines and K-absorption edges of the two component metals in alloys of Cu with Zn. The measurements were made with a Societé Genevoise precision double crystal spectrometer, which was a generous gift of Dr. A. L. Loomis.

* This research is supported by a grant-in-aid from the American Philosophical Society.

[1] W. W. Beeman and H. Friedman, Phys. Rev. **56**, 392 (1939).

[2] F. K. Richtmyer, S. W. Barnes and E. Ramberg, Phys. Rev. **46**, 843 (1934).

The constant primary voltage supply, the high voltage plant, x-ray tube and Geiger counter technique of measuring low x-ray intensities is that developed by the senior author together with Dr. C. H. Shaw. For methods employed and technique used in recording the data reference is made to previous publications.[3] During the course of the investigation no change in the properties of the crystals, from those previously reported, has been observed.

The emission measurements have been carried out for a series of four α-brasses, a β-brass, a γ-brass, and an ϵ-brass. All the alloys were made from commercial high grade cathode copper and electrolytic zinc, containing impurities to the extent of not over 0.01 percent lead and 0.01 percent iron in the alpha-alloys, and perhaps 0.02 percent lead in the beta- and gamma-alloys. The alpha- and beta-alloys were annealed repeatedly during rolling from the castings and were given a final annealing at 700°C. The gamma-alloy was sand cast and then annealed for 24 hours at 600°C. The ϵ-brass was prepared in a similar manner. Table I gives the nominal compositions by weight and by atomic number for the various alloys studied. The composition may vary by 0.25 percent from nominal.

The α-brasses have the face-centered cubic structure of pure Cu with lattice constants that increase linearly from 3.62A for the 5 percent Zn to 3.67A for the 30 percent Zn. β-brass, with the approximate composition CuZn, is a body-centered structure, forming a superlattice below about 460°C. The lattice constant is 2.95A and when the superlattice is complete the system may be described as two equivalent simple cubic lattices, one of Cu and one of Zn, with the Zn atoms, say, at the centers of the Cu cubes. The γ-brass structure is a complicated cubic lattice with the unit cell containing 52 atoms. The ϵ-brass has the zinc hexagonal structure.

TABLE I. *Composition of alloys.*

Phase	α	α	α	α	β	γ	ϵ
Zinc weight (%)	5	10	20	30	48.2	67	79.7
Zinc atomic (%)	4.9	9.8	19.7	29.4	47.5	66.4	79.2

For use as targets, the alloy samples were shaped into buttons $\frac{7}{8}$" in diameter and $\frac{3}{16}$" thick. These buttons were soldered onto the water-cooled target of the x-ray tube. The foils of α-brasses used in the absorption measurements were rolled from the buttons that had previously been used as targets. At various stages of the rolling the foils were annealed at between 500° and 600°C in an atmosphere of hydrogen.

The $K\beta_2$ and $K\beta_5$ lines in Cu and Zn are the least intense lines in the K series of these elements. H. T. Meyer[4] and J. H. Williams[5] have shown that these lines have only about 1/400 the intensity of the $K\alpha_1$ lines. With the counting technique that we have employed, however, it has been possible to obtain accurate data even with x-ray tube currents of less than 10 ma at 35 kv. In running the γ-brass the power dissipated in the target was kept below 100 watts. At greater powers, because of the poor conductivity of this alloy, there is the possibility of distilling zinc out of the target. With β-brass as the target the x-ray tube was run at 5 ma and 35 kv and careful examination of the target surface after twenty hours of operation showed no change in the surface at the focal spot, which was 4 mm in diameter. It is possible, however, that even at low power the surface of the target may have been heated to a temperature of a couple of hundred degrees during operation of the tube. This would have been sufficient to partially destroy the order of the superlattice.

In all measurements on the Zn lines, correction had to be made for the additional intensity due to the tungsten $L\beta_1$ line appearing about 2 x.u. from the peak of the $K\beta_2$ line. The vacuum conditions during operation of the tube were sufficiently good that very little intensity due to tungsten could be observed. Trouble was experienced only with the 10 percent and 5 percent Zn alloys, where because of the low Zn concentrations it was necessary to use as high as 600 watts to obtain measurable intensities,

[3] J. A. Bearden and C. H. Shaw, Phys. Rev. **48**, 18 (1935); J. A. Bearden and C. H. Shaw, Rev. Sci. Inst. **5**, 292 (1934); C. H. Shaw, Phys. Rev. **57**, 877 (1940); W. W. Beeman and H. Friedman, Phys. Rev. **56**, 392 (1939).

[4] Quoted in A. H. Compton and S. K. Allison, *X-Rays in Theory and Experiment* (D. Van Nostrand Company, 1935), p. 641.

[5] J. H. Williams, Phys. Rev. **44**, 146 (1933).

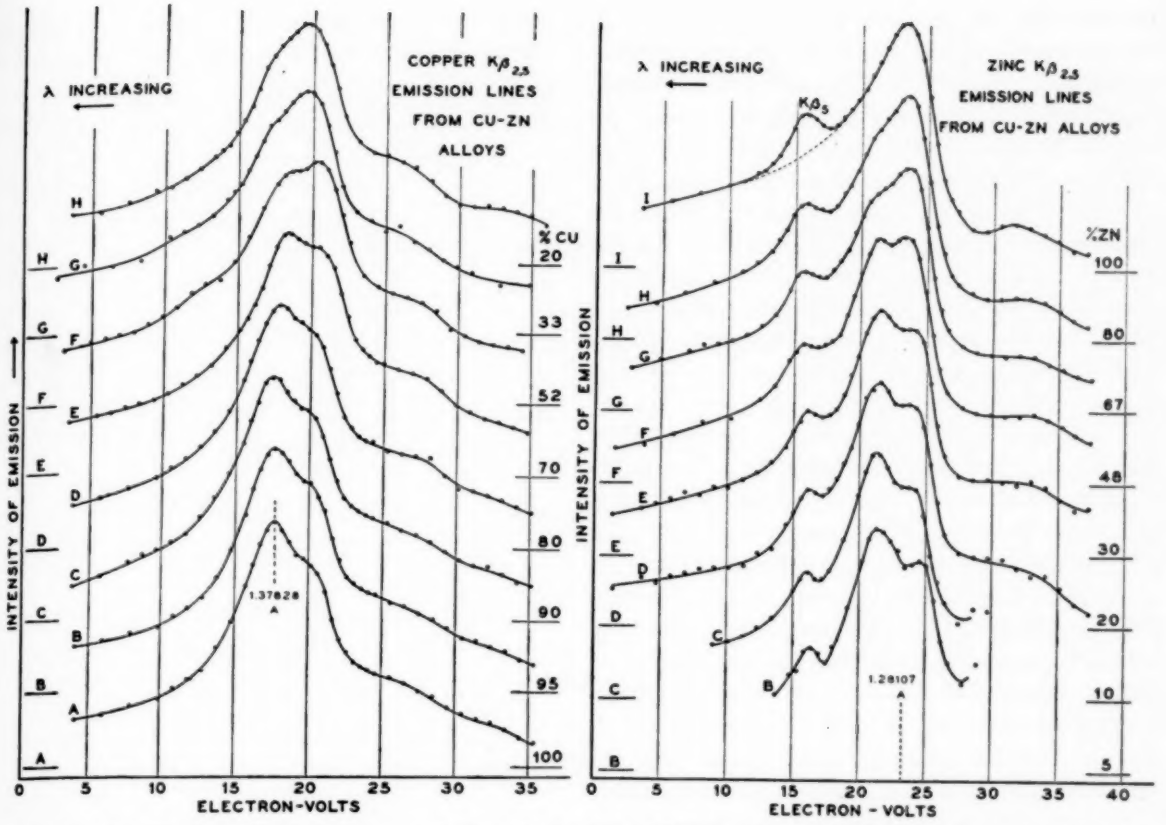

FIGS. 1 and 2. The base line for each curve is given by horizontal lines on right and left sides of the curve. The base corresponding to each curve is labeled on the left with the same letter found on the low frequency tail of the curve to which it refers, and on the right with the percentage by weight of the emitting element in that alloy target.

and in these cases the tungsten correction was probably large enough to introduce some error into the final results. The correction was determined in the following way. The tube was run overnight at low power with the target covered by a molybdenum shield. With the filament well outgassed by such treatment and with the spectrometer set for the peak of W $L\beta_1$, the first reading taken after removal of the molybdenum shield should give negligible intensity due to tungsten $L\beta_1$ and give a base from which the tungsten intensity in all succeeding runs may be measured. Successive readings on the peak of the $L\beta_1$ line in general indicated a very slow evaporation of tungsten from filament to target.

For the measurement of absorption edges, a gold disk was soldered to the target and both incident and transmitted intensities for various foils were determined over a range of from 30 to 50 volts through the edge. The results on Cu K absorption are more accurate than those on Zn, because of the much greater difficulty of measuring the Zn absorption. Zn gives only a weak absorption at the Cu edge, but Cu gives a strong absorption at the Zn edge. This, combined with the fact that the zinc percentages, in the foils studied, were low, accounts for the difficulty experienced in obtaining good data on the zinc absorption edges.

DISCUSSION

A. Widths of emission lines

From the simple free electron theory of metals, the maximum kinetic energy in the Fermi distribution would be expected to increase as Zn is added to Cu in accordance with the relation

$$E_{max} = 36.1(n_0/\Omega)^{\frac{1}{3}} \text{ ev}, \qquad (1)$$

where n_0 is the number of free electrons per atom, and Ω is the atomic volume in cubic angstrom units. If we assume one free electron

per atom of Cu and two per atom of Zn, E_{max} for Cu would be 7.0 ev and for Zn 9.5 ev. Since Ω changes very little in the series of α-brasses, E_{max} should increase almost linearly with n_0. For a 30-percent alloy the conduction band should contain 1.3 free electrons per atom. With $n_0=1.3$, formula (1) gives $E_{max}=8.0$ ev for the 30-percent Zn alloy compared to the 7.0 for pure Cu. This would lead one to expect an increase in width of the observed emission band of one volt and a corresponding shift of the high frequency side of the Cu $K\beta_2$ to shorter wave-lengths.

Figures 1 and 2 give the experimentally measured shapes for Cu and Zn $K\beta_{2,5}$ lines in the pure metals and the seven alloys. All curves have been plotted to arbitrary scales of ordinates so that they match at top and bottom. Because of the differences in intensity of satellite structure with respect to $K\beta_2$ intensity, the following arbitrary procedure has been followed in comparing widths of emission bands. The straightest portion of the slope of the high frequency side of each Cu line has been extrapolated and the width at half-maximum intensity is measured from this extrapolated slope. For Zn the high frequency slope has been similarly extrapolated and on the low frequency side, the side of the $K\beta_2$ has been extended (see curve I, Fig. 2) so as to cut off the $K\beta_5$. The widths for Zn have been measured from the high frequency extrapolation to the low frequency side of $K\beta_2$. The widths measured in this way are given in Table II.

The results listed in Table II show approximately the same widths for Cu and Zn emission bands from the same alloys. In the range of α compositions, where the crystal structure is always face-centered cubic, the width of the Cu $K\beta_{2,5}$ increases from 8.2 to 8.8 or 0.6 ev upon addition of 30 percent Zn, with roughly the same increase in width for Zn $K\beta_2$ in the same range.

Experimentally then, the widths of the emission bands attributed to conduction electrons increase with increasing n_0 but not as much as predicted on a free electron theory, nor is there any corresponding shift of the high frequency side of the Cu $K\beta_2$ in the α-brasses to higher energies by any amount greater than the experimental error of about 0.3 ev. Better agreement would be surprising, since the free electron gas model of a metal is only a very rough approximation. Still, it is interesting to see how closely the experimental widths of Cu $K\beta_{2,5}$ and Zn $K\beta_2$ correspond to the predictions of this simple theory. This seems to leave no doubt but that the above-mentioned x-ray bands are actually transitions from conduction electron levels. For no other transitions could the emission lines be expected to be as broad as observed.[6] To attempt to understand the detailed features of the curves of Figs. 1 and 2, it is necessary to resort to a more refined picture of the nature of the band electron levels involved.

TABLE II. *Half-widths of emission bands as defined above.*

Zn	Cu $K\beta_{2,5}$	Zn $K\beta_2$
0.0	8.2±0.2 ev	
5	8.3	8.4±0.3 ev
10	8.5	8.5
20	8.6	9.0
30	8.8	9.0
48	9.8	9.0
67	9.0	9.2
80	9.1	9.2
100		9.4

[6] It should be pointed out that the above procedure for measuring widths does not yield a reliable measure of the electronic band breadth in cases where the emission shows a complex structure. For example, consider a combination of a band of great breadth and low density of states with a narrow band of a very high density of states, which occupies part of the former's energy range. Such an overlapping band system might yield an emission structure which, measured across half-maximum intensity, would give a width more characteristic of the narrower band than of the wider band.

The wave-length position on the emission line corresponding to the actual limit of the Fermi distribution of a given alloy may be obtained from the wave-length position of the inflection point on its absorption limit (see references 1 and 2). (The half-maximum points in the extrapolation of the high frequency side of our lines correspond fairly closely in wave-lengths to the absorption edge inflection points.) The width of the emission band should then be measured from this point over to a point on the low frequency side of the emission corresponding to the lower limit of filled states. This latter point is more difficult to determine because the density of states on the low energy side of the electronic band is not cut off abruptly as it is at the Fermi surface. Theoretically (H. Jones and N. F. Mott, Proc. Roy. Soc. **2**, 162, 49 (1937)) the density of "p" function at the bottom of the conduction band should fall off as exp. 3/2 and reach a zero value at about 7 volts from the Fermi surface for Cu and at about 9.5 for Zn. Actually there seems to be considerable low frequency emission extending much further than given by the widths of Table I. The low frequency tails on the emission lines fall off much less rapidly than would be given by the crystal diffraction patterns or widths of the ground states. The same effect has been found (H. W. B. Skinner, *Reports on Progress in Physics* (1938), Vol. V, p. 269) in soft x-ray emission lines, and has not yet been explained.

B. Correlation of line shapes with electronic band structures

Calculations of the band structure of Cu have been carried out by Slater[7] and Krutter,[8] and an attempt has been made to correlate the observed x-ray emission structure for Cu[1] with these calculations. According to the calculations ten $3d$ electrons per atom of Cu are contained in a $3d$ band of high density of states with a double peaked structure and a spread of about 7 ev. The $4s$ band, containing 1 electron per atom, is a band of low density of states about 13 volts wide, overlapping the $3d$ band. The filled electronic levels in the $4s$ band extend about 2 ev beyond the limit of the filled $3d$ band. On the basis of these calculated results the Cu $K\beta_{2,5}$ doublet has been attributed to transitions in which electrons drop from these $3d$ and $4s$ band levels into holes in the K shells. Part of the low frequency intensity in the emission band has been attributed to electrons in the $3d$ portion of the band system and the high frequency hump has been described as emission from the filled part of the $4s$ band extending beyond the $3d$. The transitions were assumed to take place in accordance with the selection rule allowing only s to p transitions. Krutter's calculations[8] indicate that there is considerable mixing of p function in the $3d$ and $4s$ bands, enough to attribute most of the observed intensities to dipole transitions rather than quadrupole. In the case of Zn with two $4s$ electrons, the $4s$ band would be full, making Zn an insulator, if the $4s$ and $4p$ bands did not overlap slightly. This slight overlap contributes a high density of "p" function at the top of the filled electronic levels, that has been assumed responsible for the maximum intensity of emission at the high frequency side of the $K\beta_2$ line. The $K\beta_5$ line has been associated with emission from the $3d$ band of Zn, which should be expected to lie somewhat lower relative to $4s$ than the $3d$ of Cu relative to Cu $4s$.

A further development of the method of calculation used by Krutter and Slater for Cu has been carried through by Chodorow.[9] In his calculations he has partially taken into account exchange and correlation effects neglected in the earlier calculations. Exchange effects cause a contraction of the "d" wave function and a narrowing of the $3d$ band by about 1.7 ev compared to the calculations of Krutter. Furthermore, the conduction band, although very similar to one containing free electrons, is split into two sections by the perturbations of the other bands. These newer results suggest an alternative interpretation to that which assigns the low frequency extra emission in Cu $K\beta_{2,5}$ to $3d$ band emission. The experimental double structure might be interpreted as emission from a split $4s$ band and the results on the brasses could perhaps be taken as support for such an interpretation. Before attempting to prove the correctness of either one of these two possible explanations of the observed Cu $K\beta_{2,5}$ structure, it is best to consider the Zn $K\beta_5$ emission. The interpretation of this latter x-ray line is straightforward and an examination of its relation to the Zn $K\beta_2$ emission will help in settling the question of the origin of the Cu emission.

The curves in Fig. 2 all show the structure on the low frequency side, called $K\beta_5$, that has been attributed to $3d$ emission in pure Zn. No similar structure ever appears in the Cu curves of Fig. 1. If one starts with pure Zn and increases the percentage of Cu, the intensity of emission per Zn atom is lowered on the high frequency side relative to that on the low frequency side of $K\beta_2$, but there is little effect on the $K\beta_5$ structure. If the long wave-length side of the $K\beta_2$ is extrapolated as shown for the 100-percent Zn in Fig. 2, and the $K\beta_5$ intensity measured from this new base line, the resulting $K\beta_5$ lines are symmetrical lines having the half-widths given in Table III. When subtraction of 0.7 volt for crystal widths is made, the resultant half-widths are very close to the half-width of the K state alone, which has been given as 1.5 ± 0.5 ev.[1] The $3d$ levels of Zn then, in pure Zn and in the alloys, are not appreciably broadened by the lattice and the $K\beta_5$ lines are evidently quadrupole transitions of the $s\rightarrow d$ type. Electrons in the Zn $3d$ levels must remain tightly bound to their parent atoms in the lattice and cannot contribute to conduction. The peak intensities in these quadrupole transitions range from 15 percent to

[7] J. C. Slater, Phys. Rev. **49**, 537 (1936); E. Rudberg and J. C. Slater, Phys. Rev. **50**, 150 (1936).
[8] H. Krutter, Phys. Rev. **48**, 664 (1935).
[9] M. Chodorow, Phys. Rev. **55**, 675A (1939).

11 percent of the peak $K\beta_2$ intensities in going from pure zinc to 10 percent zinc. Integrated intensities due to quadrupole radiation, similar in magnitude to those found for zinc, should also be expected in Cu. However, the larger breadth of copper 3*d* in pure copper would tend to give a broad quadrupole emission with small peak intensity, rather than a narrow prominent structure like Zn $K\beta_5$. In the alloys, increasing dilution of zinc does not appreciably affect the breadth or intensity per atom of the $K\beta_5$ emission, because already in the pure metal, the overlap between 3*d* wave functions of nearest neighbors is so slight as to give no appreciable broadening of the levels. Increasing dilution of copper must be expected to narrow up the copper 3*d* band, but it is improbable that the contraction of the band would progress far enough even with low Cu concentration to ever give a 3*d* quadrupole emission from copper of similar shape and intensity per atom to that found for zinc. Support for this statement is found in the results on Cu-Ni alloys and allows of these two metals with aluminum.[10]

Returning to the curves of Figs. 1 and 2, it appears that the $K\beta_{2,5}$ structures for Cu are very similar to the $K\beta_2$ of zinc in the same alloys. As Zn is added to Cu, the high frequency intensity rises relative to the intensity on the low frequency side of the Cu emission band, and vice versa for the Zn $K\beta_2$ as Cu is added to Zn. Certainly, in pure zinc and the alloys, all the Zn emission structure to the high energy side of Zn $K\beta_5$, as well as the tail of the emission extending to low frequencies must be 4*s* band emission. The close similarity between Cu $K\beta_{2,5}$ and Zn $K\beta_2$ would make it appear then that the double structure in both cases is due to 4*s* electrons in support of Chodorow's split Cu 4*s* band. This would require that Cu 3*d* emission be spread out over most of 4*s* and so weak as not to give rise to any pronounced structure superposed on the 4*s* emission. References to Figs. 1 and 2 shows that the zinc $K\beta_2$ structure in the α-alloys has a more distinctly split appearance than the copper $K\beta_{2,5}$. A broad copper 3*d* quadrupole emission falling somewhat centrally with respect to the 4*s* band emission could produce such an effect. The main objection to this interpretation thus far is that no account has been taken of the 3*d* dipole radiation to be expected from "*p*" function mixed in the 3*d* band. The calculations of Krutter indicate enough mixing of "*p*" function near the top of the 3*d* band to give an appreciably intense 3*d* dipole intensity of small breadth, rather than a broad weak emission, and the experimental separation of the double structure is in agreement with a separation of about 1.5 to 2.5 ev predicted both by the atomic spectra data and the band calculations. The effect of diluting copper in the alloy lattice should be a narrowing of the Cu 3*d* band and with decreasing width, the amount of "*p*" function going into the description of the 3*d* band becomes less and less. It might be expected that the low frequency hump on copper, if due to 3*d* band dipole emission, would disappear with increasing dilution of copper. Experimentally it has been found that within the limits of the precision with which we could compare absolute intensities on different curves, about ten percent, there was no change in the low frequency intensity of Cu or Zn per atom in the alloy series. In the pure copper, the extra low frequency emission is only about ten or fifteen percent of the total peak intensity and even a complete disappearance of this extra intensity might be missed in our measurements. Actually, the curves do seem to indicate a loss of intensity on the low energy side of Cu, as can best be seen by comparison of curves *B* to *F* in Figs. 1 and 2. If the high energy structures of the curves are matched, it is evident that the left sides of the copper curves drop in intensity relative to their corresponding zinc curves. In curve *F*, the copper emission at the low energy side has fallen definitely below the high energy peak, while in zinc, both sides are just about equal in intensity. Since we have good reason to believe that zinc low energy 4*s* emission remains constant, the above results indicate a loss of low energy emission in copper that can best be

TABLE III. *Half-widths of* Zn $K\beta_5$ *lines in pure* Zn *and brasses.*

Zn	100	80	67	48	30	20	10	percent
Half-width	2.5	2.5	2.4	2.6	2.4	2.2	2.0	ev

[10] H. Friedman and W. W. Beeman, Phys. Rev. this issue.

attributed to decreasing 3*d* dipole emission. We might therefore conclude that the close similarity between Cu $K\beta_{2,5}$ and Zn $K\beta_2$ in all the alloys is to a great extent accidental. The low frequency structure of Zn $K\beta_2$ must be all 4*s* band emission, but that of copper $K\beta_{2,5}$ must contain appreciable 3*d* emission. Only the high kinetic energy 4*s* band electrons are completely shared and almost all the observed changes with alloying are consequently confined to the high energy portions of the emission bands.

C. Extent of sharing of high kinetic energy electrons

When Zn atoms and Cu atoms are combined to form a brass alloy, each Cu atom contributes one electron and each Zn atom contributes two electrons to the total number of conduction electrons. If these electrons are considered to form a uniform charge density distributed through the lattice, it is impossible to explain many properties of the alloys, such as conductivities, energies of superlattice formation, melting points, lattice expansions, etc.

For small amounts of Zn in solid solution in Cu, the resistance increases considerably. Part of the resistance of a dilute solid solution is due to the thermal vibrations giving rise to a definite scattering probability dependent on the temperature. In addition the periodicity of the lattice field is further disturbed by the abnormal electron distribution about each foreign atom. If upon addition of Zn to Cu, the extra 4*s* electron is considered as belonging to the lattice rather than the atom, then the increased resistance should be proportional to the scattering power of the extra field due to the Zn atoms. In calculating the resistance introduced by this extra field, Mott[11] has found that a finite resistance can be obtained only if the greater charge of the Zn atoms is shielded by part of their extra valence electrons. In other words, the Zn atoms tend to retain much of their extra charge rather than give it up to the lattice. Mott has calculated the magnitude of this screening effect and applied the results to the calculation of the charge distributions in β-brass.[12] His calculations have yielded the result that the polyhedral cell about each Cu^+ ion contains a total negative charge $-0.075\,e$ and the cell about each Zn^{++} ion is positively charged with a total $+0.075\,e$, where e is the electronic charge. That the order of magnitude of this calculation is correct was borne out by the good agreement obtained between the Madelung energy for the superlattice calculated with such charges, and the observed energy of formation of the superlattice.

In the superlattice, each Zn atom is completely surrounded with Cu as nearest neighbors, and the charge on a zinc polyhedron in this case, $0.075\,e$, is the maximum possible for a Zn-Cu alloy. The disordered alloys will give an equivalent charge on a Zn polyhedron only when the Zn is present to a small atomic percent, so that the probability of being completely surrounded by Cu is high.

Manning[13] has pointed out that a negative charge around the Cu atoms in a Cu-Zn alloy accounts for the expansion of the lattice and for the lowering of the freezing point, with addition of Zn to Cu. He has also indicated that the positive charge on Zn atomic polyhedra makes it possible to explain some apparent discrepancies between the coefficients of diffusion in Cu of the elements following Cu in the periodic table and of Cu itself diffusing in Cu.

The data presented in Figs. 1 and 2 are in agreement with the above theories that Zn loses electronic charge to Cu in a brass alloy, and offer some quantitative support for Mott's calculation of the magnitude of the charge on an atomic polyhedron. The electrons that leave Zn for Cu in the alloys must be the high kinetic energy electrons, near the top of the conduction band. If then the intensity of the low frequency portion of the Cu emission and of the Zn $K\beta_2$ emission is assumed to be constant throughout the alloy series, the peak intensity per atom of Cu on the high frequency side increases by about 30 percent of its mean value in going from 100 percent Cu to 0 percent Cu, and for Zn the intensity on the high frequency side decreases by about the same amount in going from 100 percent Zn to 0 percent Zn. The fact that the β-brass does not show the maximum sharing of electrons may be taken as indication that even

[11] N. F. Mott, Proc. Camb. Phil. Soc. **32**, 282 (1936).
[12] N. F. Mott, Proc. Phys. Soc. **49**, 258 (1937).
[13] M. F. Manning, Phys. Rev. **55**, 682A (1939).

with the x-ray tube operating at low power, the surface of the target is heated sufficiently to destroy the ordered structure.[14] According to the above-mentioned calculation by Mott, the maximum charge lost by a Zn atom in a Cu-Zn alloy should be about 0.1 *e*. If the experimental data is to be compared with this result, one should consider not the change in peak intensity but the change in integrated intensity due to 4*s* emission. This latter change is of the order of 5 percent if one compares the pure metal emission of Cu atoms with emission from Cu atoms when they occur in greatest dilution in Zn. Since the total integrated intensity under the $K\beta_2$ curve is given by two conduction electrons per atom in pure zinc, a loss of 5 percent in integrated intensity indicates a loss of 0.1 electronic charge.

The result that the peak of $K\beta_5$ in Zn does not appreciably change its position relative to the high frequency side of $K\beta_2$ in the entire alloy series might be taken as further indirect evidence for the small sharing of conduction electrons between Cu and Zn in an alloy. Reference to Bacher and Goudsmit's atomic spectra terms[15] gives the following energy relations:

Zn II $3d^9 4s^2$ lies 7.6–8.1 volts above $3d^{10}4s$

Zn III $3d^9 4s$ lies 9.9 volts above $3d^{10}$.

Zn II has the same nuclear field as Zn III but one external 4*s* electron has been added on and the shielding effect of this electron is sufficient to raise the 3*d* levels of Zn II two ev relative to those of Zn III. If this atomic data may be applied to the alloys, one should expect the separation of 3*d*, given by Zn $K\beta_5$, and 4*s* given by $K\beta_2$, to change by about 2 ev between pure Zn and Zn in dilute solution in Cu, assuming Zn to lose all of its extra electron to Cu. If, however, as predicted by Mott's calculation, the maximum loss of charge is only about 10 percent of an electron, the greatest shift expected would be of the order of 0.2 ev, which agrees with the observations of Fig. 2.

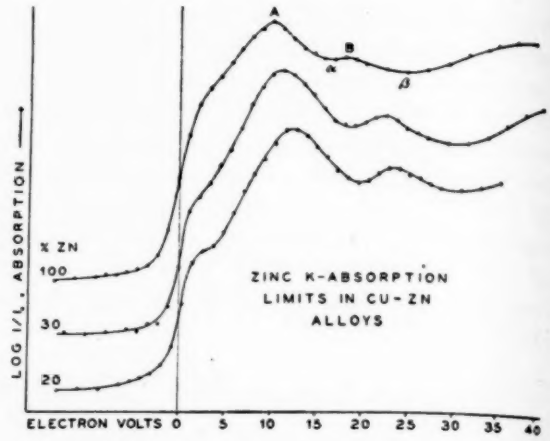

FIG. 3. Ordinates of all curves are expanded so as to have the same height from top to bottom. Curves are not corrected for second-order radiation. Zero abscissa corresponds to the wave-length of the pure metal absorption edge.

D. Absorption limits

Figure 3 shows the results obtained for the Cu *K*-absorption limits in pure Cu and in 90 percent Cu, 80 percent Cu, and 70 percent Cu α-brasses. Figure 4 shows the corresponding data for the Zn *K*-absorption limits in pure Zn, 30 percent Zn and 20 percent Zn. Copper and zinc in the same alloys show very similar absorption near the edge.

The ordinate of the inflection point (marked *L* on the 100 percent Cu curve in Fig. 3) of the initial absorption jump contour, is a measure of the density of states into which the initial absorption takes place. It has been assumed[1] that the initial absorption in Cu takes place into empty "*p*" states in a part of the 4*s* band where "*p*" function is decreasing slowly with increasing energy. The addition of Zn to Cu in the α-brasses should push the absorption at first to lower densities of "*p*" function. Experimentally, with increasing zinc content, the initial Cu absorption (measured by the ordinate *L* in Fig. 3) decreases more and more slowly in the ratio 5.2 : 4.8 : 4.5 : 4.4 from 100 percent Cu to 70 percent Cu. The initial Zn absorption

[14] With the x-ray tube powers employed, and the known width of the focal spot, we have calculated a surface temperature for the β-brass alloy target of about 400 to 500°C. The measurements could be carried out with thinner alloy samples and lower powers so as not to raise the surface temperature above 50°C. However, with the technique employed in these measurements, we have not been able to heat treat the β-brass to restore a completely ordered structure after soldering the alloy sample in place on the target. The solder diffuses through a thin sample rather quickly. We plan to alter the experimental procedure now used in such a manner as to assure complete ordering of the β-brass during measurements, and the results then obtained would offer a direct check on our above interpretation.

[15] R. F. Bacher and S. Goudsmit, *Atomic Energy States* (McGraw-Hill, 1932).

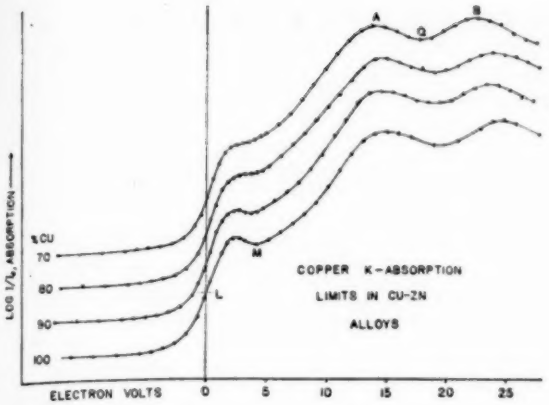

FIG. 4. Ordinates of all curves are expanded so as to have the same height from top to bottom. Curves are not corrected for second-order radiation. Zero abscissa corresponds to the wave-length of the pure metal absorption edge.

increases in the three curves of Fig. 4 in the ratio 7.0 : 7.1 : 10.2. An increasing density of "p" function near the top of the 4s band could be expected only if the 4p band overlapped the 4s band, since the top of the 4s band is pure "s" function. The above-mentioned experimental data indicate that for the 30 percent Zn alloy the surface of the Fermi distribution is situated in a region of electronic states where the 4s band is overlapped by 4p. In pure Cu, the dip marked M in Fig. 3 has been attributed to a gap or very slight overlap between 4s and 4p bands. With increasing Zn content this minimum in absorption washes out. At 10 percent Zn there is still a slight dip in the Cu absorption, but at 20 percent and 30 percent Zn in both the Cu and Zn absorption edges, the dip is no longer present. If the interpretation of the dip for pure Cu is correct, the data show that addition of Zn to Cu has the effect of causing a greater overlap of 4s and 4p bands.

The secondary absorption structures for Cu K absorptions all look like those of pure Cu, as would be expected on a free electron picture, since there is no change in lattice structure. But the corresponding Zn secondary structures bear closer resemblance to that of pure Zn in its hexagonal lattice, than to pure Cu. Evidently the atomic field and not the lattice type is the more important factor in determining secondary absorption structure even out to 30 volts. No shift of the edges greater than the experimental error of 0.3 volt has been detected, in agreement with the data on emission.

Work on the optical constants of brasses[16] shows absorption limits in the neighborhood of 5500 angstroms. These absorptions have been interpreted as due to transitions from filled 3d levels of Cu to the empty states above the Fermi surface. In the range of α-brasses up to 25 atomic percent Zn no shift of this absorption greater than 0.4 ev has been observed.

CONCLUSION

All the data on emission and absorption indicate no shift of the Fermi surface on alloying comparable to the shift expected on a simple free electron theory. Addition of Zn to Cu, however, does produce, in emission band structures, evidence of an increased number of high kinetic energy electrons about Cu and a corresponding decrease about Zn. This charge transfer is not nearly as large as expected for a complete sharing of valence electrons between Cu and Zn, but is in agreement with an alloy picture in which each component maintains a very large percentage of its valence charge.

It is a pleasure to acknowledge our indebtedness to Mr. Cyril S. Smith of the American Brass Company for carefully preparing the alloys used in this work. We are also grateful to the American Philosophical Society for a grant-in-aid, and to members of the Baltimore-Washington solid state seminar for valuable discussions and suggestions.

[16] Lowery, Wilkinson and Smare, Proc. Phys. Soc. **49**, 345 (1937).

The K-Absorption Edges and $K\beta_{2,5}$-Emission Lines of Two Zn-Ni Alloys*

J. A. BEARDEN AND W. W. BEEMAN
Rowland Physical Laboratory, The Johns Hopkins University, Baltimore, Maryland

(Received June 17, 1940)

A double crystal spectrometer has been used to measure the shapes of the $K\beta_{2,5}$-emission lines and the K-absorption edges of zinc and nickel in two zinc-nickel alloys containing 17 percent zinc and 30 percent zinc by weight, respectively. These lines arise from transitions of valence and 3d electrons into the empty K shell. In the two alloys the zinc emission line and absorption edge are shifted about a volt toward lower energies and the line is narrowed. Nickel is changed only slightly. The results indicate that the higher energy valence electrons of zinc are shared with nickel and probably go into $3d$ states about the nickel atoms.

INTRODUCTION

THE metals of the first transition group have an unfilled $3d$ band which is responsible for their ferromagnetism, high electronic specific heats and low conductivities.[1] In nickel this band lacks completion by only 0.6 electron per atom and therefore is filled in an alloy of nickel with 60 atomic percent copper or 30 atomic percent zinc, assuming that the $4s$ electrons of copper and zinc are completely shared. There is much evidence, based on the magnetic properties of these alloys, that such a sharing of electrons actually takes place. A full discussion may be found in reference 1. Later work[2] has made it doubtful if the sharing is really complete, but there can be no doubt that it is considerable and also that the degree of filling of the $3d$ band is one of the most important factors in determining the magnetic, electrical, and thermal properties of these alloys.

We have made x-ray measurements on two zinc-nickel alloys containing 17 percent zinc and 30 percent zinc by weight, respectively. They are two of those used by Dr. Wheeler of Vassar College in her recent work[2] on the paramagnetic susceptibilities of a series of copper-nickel and zinc-nickel alloys. The reader is referred to her paper[2] for details of their preparation and heat treatment. The present paper seems to be the first report on the x-ray spectra of this alloy series. Both of the present alloys crystallize in the face-centered cubic system, as does pure nickel. The limit of solubility of zinc in the nickel lattice is about 39 percent zinc at room temperatures, and the solution is not accompanied by any great distension of the lattice. The lattice constant increases by less than 2 percent in going from pure nickel to the 30-percent zinc alloy.

Our experimental procedure was the same as that described in the preceding paper on the brasses[3] except that smaller pieces, about 0.03 cm thick and 0.6 cm in diameter, were soldered to the copper target for the measurement of emission lines. The same precautions as before[3] were observed in correcting for the W $L\beta_1$ line which is just on the high frequency side of Zn

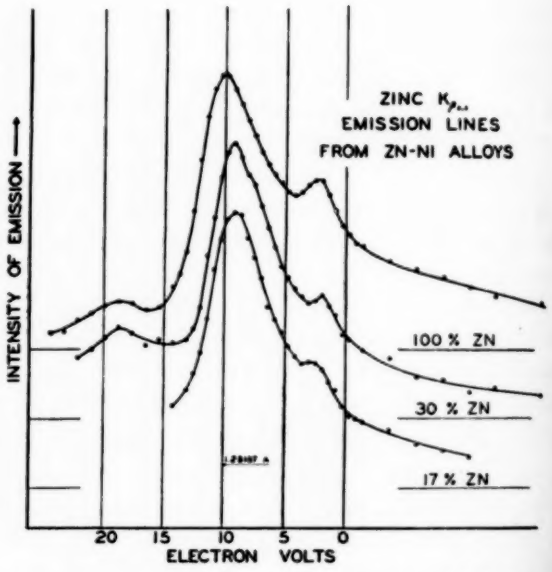

FIG. 1. Zinc $K\beta_{2,5}$-emission lines from zinc-nickel alloys.

* This research was supported by a grant-in-aid from the American Philosophical Society.

[1] N. F. Mott and H. Jones, *Properties of Metals and Alloys* (Oxford Press, 1936), p. 189.

[2] Mary A. Wheeler, Phys. Rev. **56**, 1137 (1939).

[3] J. A. Bearden and H. Friedman, Phys. Rev., preceding paper.

$K\beta_2$. Another tungsten line, $L\alpha_2$, interferes with the measurements on Ni $K\beta_5$, but its intensity is too low to cause any error. However, the same procedure was followed of outgassing the filament while shielding the target with a molybdenum plate. None of the emission lines was run with more than 300 watts expended in the target. Absorption foils were rolled to a thickness of approximately 0.001 cm and absorption measurements were made as previously described.[3]

Experimental Results

The experimental results are shown in Figs. 1 to 3. The scale of intensity of each emission curve, Figs. 1 and 2, has been adjusted so that they have the same height. Successive curves are displaced vertically and the zeros of emission indicated by the two horizontal lines under each curve.

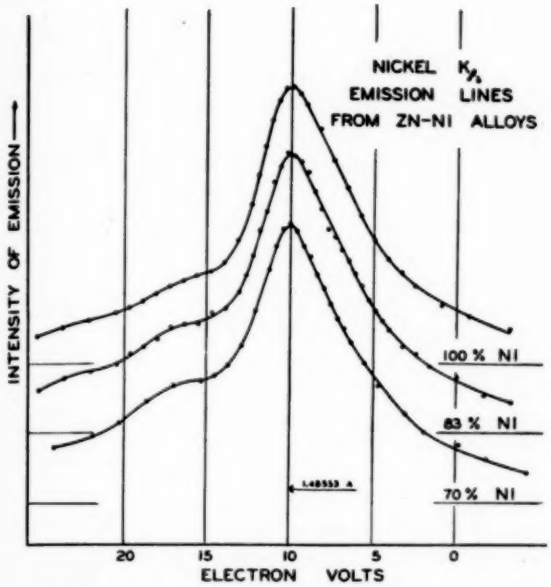

Fig. 2. Nickel $K\beta_5$-emission lines from zinc-nickel alloys.

No shifts of the peak of the nickel line were observed, but the main peak of the zinc line in the alloys was shifted about 0.9 ev toward lower energies with respect to that of pure zinc. The low frequency zinc peak due to $3d$ emission is not shifted by more than 0.3 ev. We have also measured the widths at half-maximum, and the asymmetries of these lines, and obtained the data shown in Table I. The asymmetry is defined as the part of the width at half-maximum

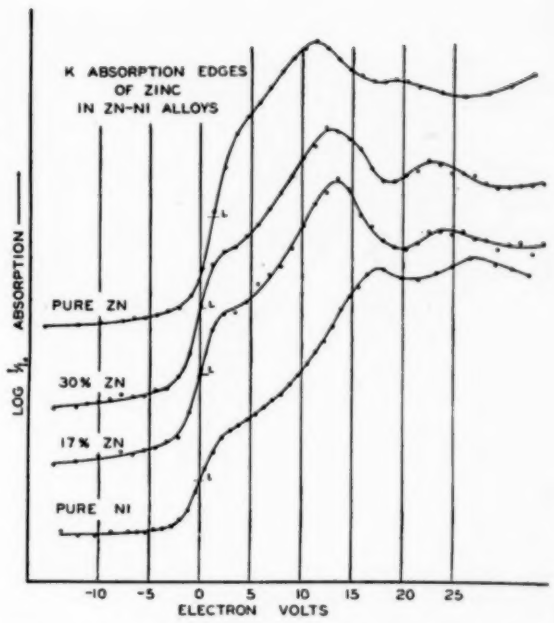

Fig. 3. The K-absorption edges of pure nickel and of zinc from zinc-nickel alloys.

on the low frequency side of the peak of the line divided by the part on the high frequency side. It is one for a symmetrical line.

In both nickel and zinc there is considerable satellite intensity, so half-widths have been measured to the projection of the straight part of the high frequency side of the line as described in reference 3. This involved only small corrections. The low frequency $3d$ peak of the zinc line also was subtracted before making half-width measurements. No corrections have been made in the tabulated half-widths for the crystal or the width of the K excited state.

Only four absorption edges are shown in Fig. 3, as the nickel edge in the alloys is indistinguishable from that of pure nickel. However, the zinc edge, just as with the emission line, shows marked changes from the pure metal to the alloy, notably a shift to lower energies of 1.3 ev of the point L marking the top of the Fermi distribution.[4] The absolute wave-lengths corresponding to the point L are, pure zinc 1.2807A, pure nickel, 1.4852A.

It is believed that the errors in the absolute energies of the peaks of the lines and the tops of the Fermi distributions are no greater than

[4] W. W. Beeman and H. Friedman, Phys. Rev. **56**, 392 (1939).

± 0.3 ev, while the half-widths of the lines are probably correct to ± 0.2 ev.

Discussion

The narrowing of the zinc line and the shift to lower energies of its main peak are most easily explained as results of the loss of higher energy zinc electrons to the empty states in the narrow $3d$ band of nickel. However, this evidence is not conclusive, as the same effects would be produced if alloying merely cut down the intensity of emission on the high frequency side of the zinc line, perhaps by changing the transition probability, without actually ionizing the zinc atom. Farineau[5] has published some soft x-ray lines involving the valence electrons of nickel and aluminum in a series of nickel-aluminum alloys. His voltage resolving power is greater that that obtainable in the hard x-ray region, and he was able to show that the aluminum line from alloys of increasing nickel content does not shift or narrow if one measures along the bottom of the line but rather that the intensity of high energy emission is greatly reduced.

Better evidence for a lowering of the top of the Fermi distribution as nickel is alloyed with zinc is furnished by the shift of the zinc absorption edge. This amounts to 1.3 ev according to our measurements, and there can be no serious error due to the finite width of the K excited state and the crystals, as the method of determining[4] the point L takes into account these factors. It is quite conceivable that the change from the hexagonal close-packed structure of pure zinc to the face-centered cubic lattice of the alloys could cause such a shift, but this is not likely in view of the results of Bearden and Friedman,[3] who found no displacement of the zinc edge in the α-brasses, which have also a face-centered cubic lattice but no holes in the $3d$ band.

The results on nickel indicate that the electrons lost by zinc go into a band in which the density of states is high and the probability of transitions to or from the K shell low. These are both characteristics one would expect of the nickel $3d$ band. The first conclusion may be understood by the following reasoning. If the energy densities of states at the highest filled levels were the same in zinc and nickel, the shifts of the absorption edges due to taking a certain number of electrons from zinc and placing them around nickel would be inversely proportional to the atomic concentrations of the elements and in opposite directions. This would predict a displacement of the nickel edge of about 0.6 ev toward higher energies in the 70 percent Ni alloy. No shift was observed, indicating that the nickel lattice can accommodate a considerable number of electrons without greatly increasing the energy of the highest filled level. On the other hand, the transition probability to these states must be low because in nickel they are empty and contributing to the intensity of the initial absorption, while in the alloys they are filled and make no contribution to the absorption. Experimentally no change in the appearance of the absorption edge is detectable. The fact that only minor changes occur in the nickel emission line is in agreement with the above conclusions. Most of the structure of both the emission line and absorption edge of nickel must be due to the $4s$ band which overlaps the $3d$. As long as there are empty states in the $3d$ band, however, very few electrons will go into the $4s$ band and the changes in the emission and absorption spectra with alloying will be slight.

It is not possible to say just what fraction of an electron per zinc atom is lost to the lattice in these alloys, but it must be greater than the 0.1 electron per atom which zinc[3] loses when completely surrounded by copper, since no shift of the zinc absorption edge is observed in any of the brasses. On the other hand, the ionization of the zinc in the present alloys is almost certainly not as great as the 1.4 electron per atom which it would lose if the $4s$ electrons were completely shared with the nickel. The

Table I. *Widths at half-maximum and asymmetry of zinc line from alloys.*

Line	Width in ev	Asymmetry
100 Ni	7.1	1.7
83 Ni	7.4	1.5
70 Ni	7.6	1.4
100 Zn	9.4	2.8
30 Zn	7.2	1.8
17 Zn	7.2	1.7

[5] J. Farineau, J. de phys. et rad. **10**, 327 (1939).

simple free electron theory would predict in this case a lowering of the top of the Fermi distribution of about 3.4 ev, but no shift of the zinc absorption edge or narrowing of the line of this magnitude is observed. Wheeler[2] found that the paramagnetic suceptibilities of these alloys do not approach zero as the concentration of zinc approaches 30 atomic percent, which would seem to show that some 3d states remain unfilled even when the total number of electrons in the lattice is sufficient to fill them. One would expect this if the sharing is incomplete, i.e., if after a certain ionization of the zinc core is reached it is energetically more favorable for electrons to shield the zinc than to go into nickel 3d states. It is interesting to note that Wheeler always found a higher paramagnetic susceptibility for a zinc-nickel alloy containing X atomic percent zinc than for a copper-nickel alloy containing $2X$ atomic percent copper. If sharing were complete there would be the same number of electrons in the $3d$ band in each case; however, one would expect greater deviations from complete sharing with zinc because of its higher charge. There is x-ray data in agreement with the results of Wheeler, Farineau and Morand[5,6] and Friedman and Beeman[7] have published some emission lines from nickel in nickel-aluminum and nickel-copper alloys which indicate that when nickel is present in concentrations of less than 50 percent, its 3d band narrows and the highest $3d$ levels are reduced to somewhat lower energies. This would tend to give a more complete filling of the band in the nickel-copper than in the nickel-zinc alloys.

[6] J. Farineau and M. Morand, J. de phys. et rad. 9, 447 (1938).

[7] H. Friedman and W. W. Beeman, Phys. Rev., following paper.

Some conclusions of interest can be drawn from the remaining data, particularly the widths and asymmetries of the zinc lines. The observed narrowing of the zinc line in the alloys would be expected simply because of the partial ionization of the zinc atom, but a decrease in width of 2.2 ev is more than can be accounted for in this way. In addition, the fact that the asymmetry decreases rather than increases with alloying shows that the larger part of this narrowing is due to a loss of intensity on the low frequency side of the line. A glance at Fig. 1 makes this apparent. The 3d peak is seen to be much further down the low frequency side of the line in the alloys than in pure zinc, indicating that the $4s$ emission at the same wave-length as the 3d peak is less intense in the alloys relative to the main peak of the line. The reason for this is probably that the stronger field of zinc lowers its $4s$ band sufficiently with respect to that of nickel so that the least energetic zinc $4s$ electrons cannot escape from their parent atom at all when zinc is largely surrounded by nickel, as in the present alloys. Under these circumstances they would behave very much as atomic $4s$ electrons and have no chance of making a transition to the K shell.

It is to be noted that here, as with the brasses, the zinc $3d$ electrons appear to be tightly bound and but little affected by alloying. No sign of emission due to them is found in the nickel lines.

We wish to thank Dr. Mary A. Wheeler for kindly lending us the alloys used in this research, and the members of the Baltimore-Washington solid-state seminar for numerous discussions of the material involved. The financial assistance given by the American Philosophical Society is greatly appreciated.

Copper and Nickel X-Ray $K\beta_2$- and $K\beta_5$-Emission Lines and K-Absorption Limits in Cu-Ni Alloys*

H. FRIEDMAN AND W. W. BEEMAN
Rowland Physical Laboratory, The Johns Hopkins University, Baltimore, Maryland
(Received June 17, 1940)

The shapes of the Cu $K\beta_{2,5}$ lines and Ni $K\beta_5$ lines from Cu-Ni alloys vary smoothly with composition. The trend with increasing percentage of the emitting atoms is always toward a flattening out of the peaks of the lines. To explain the observed shapes it has been proposed that the major effect of alloying is a loss of $3d$ band dipole radiation with increasing dilution of the emitting atom. The absorption limits, in contrast to the emission lines, show no influence of alloying. The Cu K limit continues to look like that of pure Cu even when the emitting atom is almost completely surrounded by nickel nearest neighbors, and similarly no changes are observed in the nickel edges even down to 21 percent nickel.

THE $K\beta_5$ line of pure Ni and the $K\beta_{2,5}$ line of pure Cu, as well as their K-absorption limits have been previously measured.[1,2] The present paper reports an extension of these measurements to three alloys of Cu and Ni having the compositions by weight 30 percent Cu—70 percent Ni, 54 percent Cu—46 percent Ni, 79 percent Cu—21 percent Ni. Cu and Ni form a complete series of solid solutions with the face-centered cubic structure. Furthermore, the lattice constant decreases linearly, with increasing Ni content, by only 2 percent. Pure Cu has a constant of 3.59A and Ni, 3.52A. The effect of alloying on the $K\beta_2$ and $K\beta_5$ lines and on the K-absorption limits can therefore be studied independently of crystal structure changes over the entire range of composition.

An explanation of the shape of the pure Cu $K\beta_{2,5}$ emission has been given[2] based on the results of calculations by Krutter and Slater (Fig. 1) of the electronic $3d$ and $4s$ energy bands of Cu. The extra emission on the low frequency side was attributed to the $3d$ band. Slater,[3] in calculating the ferromagnetism and electronic specific heat of Ni, extrapolated the Cu band calculations to the case of Ni and obtained order of magnitude agreement with experiment. This extrapolation consisted of lowering the surface of the Fermi distribution down to where the Cu band system would be filled with ten electrons per atom. The effect of cutting off the portion of filled states in the $4s$ band extending beyond the limit of $3d$ would be to give a nickel $K\beta_5$ line

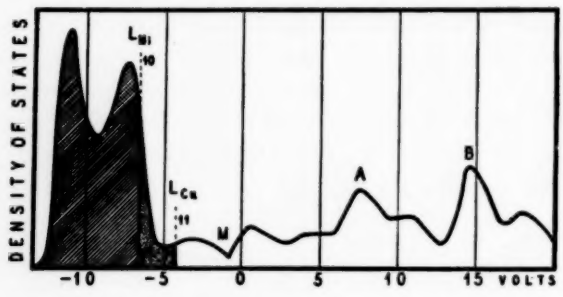

FIG. 1. Density of states as a function of energy in Cu. Lines labeled L_{Ni} and L_{Cu} give the energies to which the bands are filled in Ni (assuming same energy levels as for copper) and in Cu by 10 and 11 band electrons per atom, respectively.

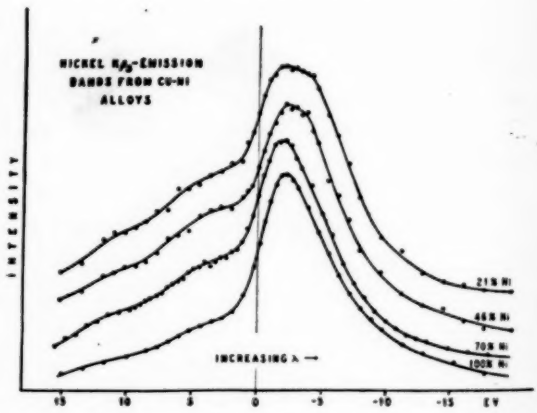

FIG. 2.

* This research was supported by a grant-in-aid from the American Philosophical Society.

[1] J. A. Bearden and C. H. Shaw, Phys. Rev. **48**, 18 (1935).

[2] W. W. Beeman and H. Friedman, Phys. Rev. **56**, 392 (1939).

[3] J. C. Slater, Phys. Rev. **49**, 537 (1936).

with no hump like that found for Cu $K\beta_{2,5}$ on the high frequency side. If the experimentally observed Ni $K\beta_5$ is drawn in on the Cu $K\beta_{2,5}$ with the copper low frequency peak matching the nickel peak, the extra emission on the copper may be attributed to emission from the portion of the band system between L_{Ni} and L_{Cu} in Fig. 1. In alloying copper and nickel, one might therefore expect the addition of copper to nickel to produce simply a filling in on the high frequency side of Ni $K\beta_5$ corresponding to a raising of the surface of the Fermi distribution beyond the limit of the $3d$ band. The nickel K-absorption edges, correspondingly, would be expected to follow the surface of the Fermi distribution to higher energies with increasing copper content. The experimental results reported here, however, are considerably more complex, and evidently the direct extrapolation of the copper band system to nickel and the above simple picture of the effect of alloying are unjustified. In the following we shall give a description of the experimental data, a comparison with other related data, and lastly an attempt to explain this variety of experimental material.

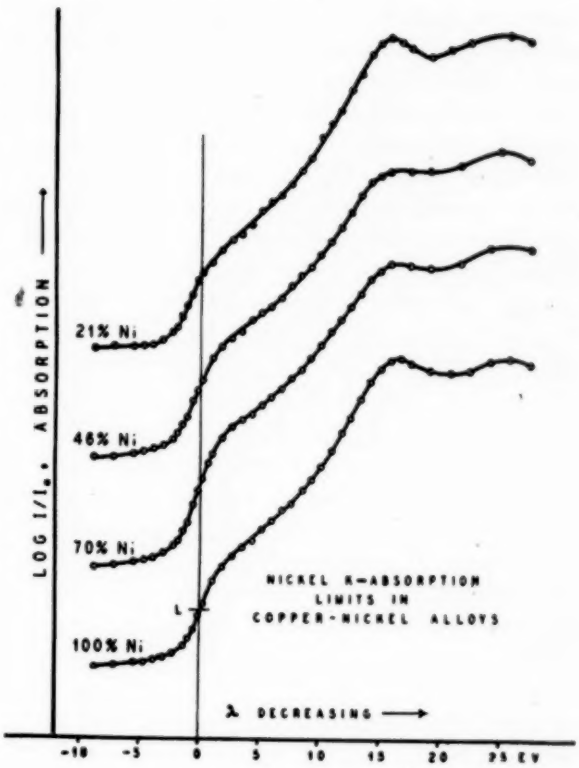

FIG. 4.

EXPERIMENTAL

The double crystal spectrometer and the technique of intensity recording is fully described in reference 3 of a preceding paper.[4] Specific precautions taken for nickel $K\beta_5$ measurements because of the W $L\alpha_2$ line on its high frequency side are described in the preceding

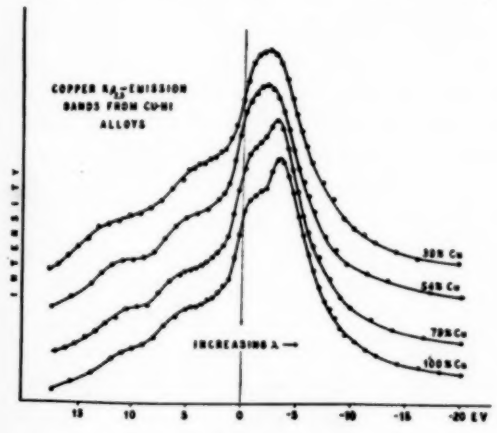

FIG. 3.

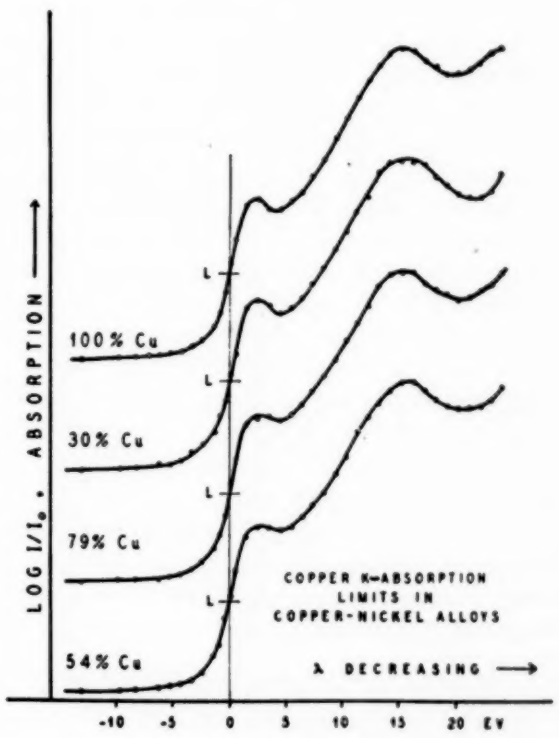

FIG. 5.

[4] J. A. Bearden and H. Friedman, Phys. Rev. this issue.

paper by Bearden and Beeman[5] on nickel-zinc alloys. The measurements shown in Figs. 2, 3, 4, and 5 are the results on a set of alloys supplied us by the American Platinum Company. Target samples were about 1 mm thick, and foils for absorption measurements were rolled from the above samples to a thickness of about 0.001 cm. As a check on the alloys used, the measurements have been repeated with two duplicate sets of alloys, one loaned us by Dr. Mary Wheeler[6] of Vassar College, and the other by Dr. B. Kurrelmeyer[7] of Brooklyn College. Measurements on all three sets agree within the experimental error.

Figures 2, 3, 4, and 5 give, respectively, the nickel $K\beta_5$ emission for pure nickel and the three alloys, the copper $K\beta_{2,5}$ emission for pure copper and the alloys, and the corresponding nickel and copper K-absorption limits. The abscissae are labeled positively and negatively with respect to a zero corresponding to a transition of a K electron of the pure metal into the lowest empty levels of the valence electron band system. The zero is determined by matching the initial absorption rise to an arctangent curve as described in reference 1. Positive abscissae correspond to unfilled levels above the Fermi distribution, and negative abscissae to filled levels below the surface of the Fermi distribution. The scales of ordinates have been adjusted so that all curves have the same total height from top to bottom, and successive curves have been displaced equal distances vertically to facilitate comparison.

The experimental results indicate that the copper absorption begins at the same energy, within a probable error of 0.3 ev, in the pure metal and in the alloys. Three of the nickel curves of Fig. 4 fall together within the 0.3 ev limit, but the low nickel percentage nickel K edge appears to be displaced at the inflection point L by 0.8 ev from the pure nickel edge. This displacement is very uncertain because of the considerable difficulty experienced in obtaining sufficiently good data on such a low percentage nickel alloy to make possible an accurate determination of the inflection point L. Repeated measurements on this nickel K edge in 21 percent nickel have, however, indicated a mean value for the L abscissa much closer to that found for the alloys with higher percentages of nickel than is indicated in Fig. 4.

TABLE I. *Widths of* Ni $K\beta_5$ *and* Cu $K\beta_{2,5}$ *lines at half-maximum.*

PERCENT Ni	Cu WIDTH	Ni WIDTH
0.0	8.2 ev	
21	7.8	8.8 ev
46	8.0	7.9
70	8.0	7.5
100		7.2

The emission lines show marked changes in shape but hardly any shift of the line as a whole. If one defines the center of the line as its horizontal midpoint at the half-maximum intensity, then any shifts of the center are less than one-half ev for both copper and nickel. The widths of the lines measured in the manner described in reference 4 are given in Table I.

Only in nickel is any trend noticed. The copper widths are equal within the experimental error.

DISCUSSION

I. Emission lines

The work of Farineau on the $L\alpha$-emission lines of copper and nickel in alloys with each other and with aluminum[8,9] shows quite definitely that the $3d$ bands of these elements tend to narrow up when the distance between like atoms is increased by alloying. The magnitude of this narrowing is not easy to estimate quantitatively, but appears from his microphotometer traces to be in the neighborhood of from 25 to 30 percent for the smallest concentrations. It generally is not very noticeable until the emitting atom is reduced to a concentration of less than 50 percent, and the nickel line actually appears to widen when the nickel is present in large amounts in a copper-nickel or aluminum-nickel alloy. Farineau has attributed this initial widening to the filling of the empty states in the nickel $3d$ band by the valence electrons of the other component of the alloy.

Comparing our results with the data of Farineau, it appears at first that a consistent

[5] J. A. Bearden and W. W. Beeman, Phys. Rev., preceding paper.
[6] Mary A. Wheeler, Phys. Rev. **56**, 1137 (1939).
[7] W. H. Keesom and B. Kurrelmeyer, Phys. Rev. **57**, 1068A (1940).
[8] J. Farineau and M. Morand, J. de phys. et rad. **9**, 447 (1938).
[9] J. Farineau, J. de phys. et rad. **10**, 327 (1939).

interpretation of both sets of experimental evidence would not be easy to attain. In contrast to his data, our results for the alloys are mostly in the direction of a broadening or smearing out of the emission line structures present in the pure metals. The two sets of data can, however, be shown to agree if one ascribes the changes in appearance of the $K\beta_{2,5}$ lines in the alloys to a loss of $3d$ emission. This can be seen as follows. The narrow low frequency peak in copper has been ascribed to $3d$ emission. It is superposed on a broad band of $4s$ emission. This same sharp $3d$ emission is present in nickel, but since the nickel $3d$ band is partially empty, the high frequency limits of the $3d$ and $4s$ emission coincide. Emission from $3d$ and $4s$ therefore adds up to give a rather sharp peaked but structureless nickel line. Now, if this $3d$ emission disappears in the alloys, there will remain only the broad $4s$ emission band, which is what the experimental results show. The nickel line appears rather flatter and broader across the top at greatest dilution of nickel than does copper in the lowest percentage copper alloy, but this is not unexpected for two reasons. First, we have measured nickel in a 21 percent nickel alloy, while our lowest percentage copper alloy contains 30 percent copper. Secondly, the nickel $3d$ emission is probably broader than that of copper, due to the greater radius of the nickel $3d$ wave functions and its loss would leave a flatter $4s$ emission. It should also be noticed that the loss of $3d$ emission does not appear to be large until the percentage of the metal concerned falls to 50 or below. This is in general agreement with Farineau's findings on the narrowing of the $3d$ band.

In seeking to explain why the narrowing of the $3d$ band should cause a disappearance of the $3d$ emission in the $K\beta_{2,5}$ lines, one is forced to the conclusion that this emission is dipole radiation resulting from a mixture of "p" function at the top of the $3d$ band. This is rather plausible. Experimentally it is clear that we are getting radiation from only a part of the $3d$ band. If one considers the $3d$ radiation of pure nickel and copper apart from the broad underlying $4s$ band radiation, and corrects the former for the width of the crystals and the K excited state (about 2 ev) it is evident that the band levels giving rise to this radiation extend over a range of not more than one ev. But Farineau's work indicates that the complete $3d$ bands of copper and nickel are between three and five ev[10] in width. It is also clear from the position of the $3d$ emission close to the high frequency side of the $K\beta_{2,5}$ line in both copper and nickel, that the states giving rise to the radiation are at the top of the $3d$ band. On theoretical grounds one would expect any admixture of "p" function in the $3d$ band to be greatest near its upper limit because there the energy of the states is more nearly that of the atomic $4p$ levels. Krutter's calculations of the band structure of copper also showed a much greater admixture of "p" function near the top than near the bottom of the $3d$ band.[11] If this interpretation of the radiation is accepted, then it is understandable enough that when like atoms are separated in a dilute alloy, the decreased interaction of similar atomic states which leads to a narrowing of the band will also lead to a reduction in the admixture of "p" function in the band.

The above hypothesis is in fairly good agreement with the experimental data on the other alloys, the greatest difficulty arising in the interpretation of the zinc $3d$ emission. The $K\beta_5$-emission line of zinc from the pure metal and its alloys indicates a $3d$ band not more than one-half volt wide, and about eight ev below the top of the Fermi distribution.[12] In the previous work the zinc $3d$ radiation has been interpreted as quadrupole because the band seems too narrow to contain any appreciable admixture of other wave functions, and also because the same line persists in the spectra of elements of higher atomic number where the $3d$ orbits must be definitely atomic in character. The zinc $3d$ radiation is affected hardly at all by alloying, another indication of the atomic character of the electrons. The question then arises why quadrupole radiation does not give definite indication of the entire extent of the copper and nickel $3d$ bands, and the answer seems to be that if the band is three to five ev wide instead of one-half ev, the emission is

[10] In arriving at these figures a correction of 1.0 ev for the width of the L_{III} excited state has been subtracted from the photographed band width.

[11] H. Krutter, Phys. Rev. **48**, 664 (1935).

[12] J. A. Bearden and H. Friedman, Phys. Rev. this issue.

spread over too great an interval to be noticeable compared to the more intense 3*d* dipole radiation. The quadrupole transition is prominent in zinc and elements of higher atomic number only because the band is narrow and therefore the density of states high. There is also the evidence of the $L\alpha$ line[13] on the width of the zinc 3*d* band. It would seem to indicate a band somewhat wider than one-half ev, perhaps as wide as 2.0 ev. Theoretically one would expect a very rapid narrowing of the 3*d* band with atomic number as soon as the 3*d* wave functions become so small that those of nearest neighbors overlap only in the region of exponential decay of the wave functions. This probably occurs near the end of the first transition group. In addition, the distance between nearest neighbors is greater in zinc than in any of the immediately preceding metals. Both factors will tend to narrow the zinc 3*d* band.

It would also be expected that the 3*d* radiation of copper and nickel, if it is dipole, would disappear in alloys of these elements with zinc. Unfortunately the zinc-nickel measurements[5] have not been carried out on alloys of sufficiently high zinc content to furnish a test. The results on the brasses,[4] while somewhat complicated, do, however, indicate a loss of 3*d* band dipole emission upon lowering the copper content of the alloys.

The emission line widths given in Table I are what one would expect from a loss of the narrow 3d emission. Because of this loss, half-width measurements are made lower on the 4*s* emission band in the alloys than in the pure metals. This probably explains the considerable widening of the nickel line. The copper line keeps about the same width throughout the series, but in copper the loss of 4*s* electrons to nickel tends to narrow the line, compensating for the other effect.

II. Absorption edges

In a previous paper[2] the *K*-absorption edges of pure copper and nickel were discussed. The experimental results on copper were found to be in good agreement with the band calculations of Krutter and Slater (Fig. 1) and the differences between copper and nickel, mainly the absence in nickel of the absorption minimum about 4 ev beyond *L* in the copper edge, seemed understandable because of the greater overlap of the nickel wave functions.

However, the curves of Figs. 4 and 5 show that no appreciable difference from the pure Cu *K*-absorption limits appears in the Cu absorption limit for any of the alloys and similarly, all the nickel curves are closely alike. These results are supported by the data of T. Hayasi[14] on the pure metals and a 50–50 Cu-Ni alloy. The above data indicate that it is not entirely correct to compare the structure of the absorption edge with the calculated bands. The failure to find any effect of alloying cannot be taken as evidence for the identity of the two band systems, since the two absorption edges are quite different, particularly the structures close to the initial absorption. It would appear, rather, that the lower energy states into which the *K* electron can be excited are determined mainly by the field of the absorbing atom itself and not by the periodic lattic field. It has been suggested by several authors[15,16] that the ionization of the *K* shell of the absorbing atom leaves its outer electrons moving in a field similar to that of the atom of next higher atomic number. As a consequence, the states which should be used in any attempted explanation of the observed absorption of pure copper are not those calculated by Krutter and Slater for the normal copper lattice, but rather the allowed states for an electron about an atom of zinc occupying one of the sites in a copper lattice. These are sometimes called reduced states. Since electrons tend to cluster around an ionized atom and shield its extra positive charge, it seems quite likely that the wave function of the ejected *K* electron does not extend any great distance from the absorbing atom and therefore that the energy distribution of the final states will not be very sensitive to whether the surrounding atoms happen to be copper or nickel. These considerations probably do not apply to absorption structure except within a very few volts of the edge, since an electron ejected with any considerable velocity

[13] J. Farineau, Ann. de physique **10**, 20 (1938).

[14] T. Hayasi, Tohoku Univ. Sci. Reports **25**, 598, 606, 661 (1936).

[15] H. W. B. Skinner, Proc. Roy. Soc. **140**, 277 (1933).

[16] F. K. Richtmyer, S. W. Barnes and E. Ramberg, Phys. Rev. **46**, 843 (1934).

cannot be thought of as remaining in the vicinity of the parent atom.[17] Even close to the edge the structure must be somewhat similar to what one would calculate for the normal lattice, since all the general features of the absorption data of reference 1 can be understood without introducing the idea of reduced states. We might expect then that absorption structure close to the edge should be less sensitive to alloying than are the emission lines, since in the final state of the emission process the K shell is filled and the structure of the line will be determined by which state of the normal lattice band is left empty. However, the failure of the copper and nickel edges to show any change at all in the copper-nickel alloys may be partly due to peculiarities of this alloy series. The two metals have about the same number of 4s electrons in the pure state, nickel 0.6 4s electron per atom and copper 1.0, necessitating very little shift of the top of the Fermi distribution on alloying. Also, the field of a copper and of a nickel atom at a neighboring lattice point should be rather similar, since the differences in the outer shells of the two atoms consist mostly of the extra 3d electrons added to copper. Their wave functions have small radii compared to the 4s so that the shielding of the extra nuclear charge of copper is good at a distance comparable to the lattice distance.

It is not surprising that in the brasses there are changes of the absorption edge with alloying[12] since the peculiarities of the copper-nickel series are absent. The brasses exist in several phases, there are considerable changes in the population of the 4s band from one end of the series to the other, and differences in the atomic fields of Cu and Zn must extend some distance from the atom because of the large radius of the 4s wave function.

The nickel absorption edges in the nickel-zinc alloys show no changes, but this is at least partly due to the absence of measurements on alloys containing a large percentage of zinc.

The failure to find a shift of the initial absorption in the copper-nickel series is in agreement with some measurements of Bor, Hobson and Wood[18] on the optical constants of the same alloys. Pure Cu has an absorption maximum beginning at about 5900A and extending to shorter wave-lengths. Mott[19] believes this absorption is due to transitions of 3d electrons to the first empty states of the 4s band. If 4s electrons are shared with Ni, this absorption should shift to larger wave-lengths in the Cu-Ni alloys. Experimentally only a very slight shift is noticed, much less than that predicted by the theory.

III. Conclusion

There now exist x-ray measurements of the band structures of the alloy systems Cu-Ni, Zn-Ni, Cu-Zn, Al-Cu, and Al-Ni, as well as a few other isolated alloys. References to the latter can be found in Skinner's review article on soft x-ray spectroscopy in the 1938 "Reports on Progress in Physics." The results indicate that in nearly all binary alloy systems the band electrons distribute themselves quite differently around the two constituents of the same alloy. Farineau[13] has reported identical emission lines from Al and Mg in Al_2Mg_3 and in Al_3Mg_2, but these appear to be the only such cases. As a rule there are great differences not only in the general appearance of the emission lines and absorption edges of the same alloy, but also in the energy breadth of the filled levels which one deduces for the two components from the widths of their emission lines. This latter is particularly well illustrated by the Al-Cu and Al-Ni series.[9] Pure Al has an emission band 11 or 12 ev wide, Cu about 8 or 9, and Ni 5 or 6 (these widths are not corrected for the lifetime of the excited state), and the bands maintain these same widths throughout the whole alloy series. The only evidence for a sharing of the higher energy electrons of Al with Cu or Ni is the reduction in the alloys of the intensity of the high frequency part of the Al line and a slight broadening of the Cu and Ni lines. There is, however, no shift of the high energy limit of the Al emission and there-

[17] However, comparing the zinc absorption edge in an α-brass or in the zinc-nickel alloys with the edges of Cu or Ni, one sees differences in the shape of the curves as much as 15 or 20 ev from the initial absorption.

[18] J. Bor, A. Hobson and C. Wood, Phys. Soc. Proc. 51, 942 (1939).

[19] N. F. Mott and H. Jones, *Properties of Metals and Alloys* (Oxford Press, 1935).

fore no evidence for a lowering of the absolute energy of the top of the Fermi distribution with alloying. This is the same kind of behavior as that exhibited by the zinc line in the brasses[12] which was there discussed from the viewpoint of the shielding of the zinc ion by the lattice electrons, leading to a much smaller residual positive charge about the zinc than would be the case with complete sharing and therefore a smaller than anticipated reduction in the intensity of the high frequency side of the line. The data seem to show that when metals of high and low valence are alloyed the charge density around the atoms of higher valency is decreased somewhat compared to what it would be in the pure metal, but that the energy of the highest filled states is decreased hardly at all. These facts may be summarized by stating that the differences in the average internal potentials of two metals are at least as important as are differences in the kinetic energies at the top of the Fermi distribution in determining how their filled levels will adjust themselves when the two are alloyed. Ordinarily only the latter difference is considered, but the experimental results indicate that the smaller average potential of the higher valence metal of a binary alloy lowers the energy of the whole band about as fast as its extra valence electrons raise the kinetic energy of the highest filled levels. The total energy of the highest filled levels therefore does not change with alloying. Such an assumption explains not only the failure to find any shifts of absorption edges or emission lines, but also the existence of emission lines with quite different widths from the two components of the same alloy. The electrons about the atom of higher valence have a wider distribution in energy because of the lower potential. The above discussion properly applies only to conduction electrons. Empty states in the $3d$ band in nickel may be favorable enough energetically to permit a considerable ionization of an element of higher valency. An actual lowering of the Fermi distribution was found in the Ni-Zn series although Farineau does not find it in the Ni-Al alloys.

A second conclusion which is well substantiated by all the data is that the atomic $3d$ states of copper and nickel are broadened mainly by interaction with the $3d$ states of identical neighboring atoms and only slightly by interaction with the states of unlike atoms. Both Farineau's work and our own indicates that mere separation of like atoms produces an appreciable narrowing of the $3d$ band. The narrowing seems to be independent of what alloy of copper or nickel is used.

We are greatly indebted to Professor J. A. Bearden, under whose direction this work was carried out. It is a pleasure to acknowledge the assistance given by members of the Baltimore-Washington solid state seminar through discussion of these problems, and the financial assistance granted to Professor Bearden by the American Philosophical Society which has made the experimental measurements possible. We also wish to thank Dr. Mary Wheeler and Dr. B. Kurrelmeyer for the loan of their alloys.

The Arc Spectrum of Cobalt

HENRY NORRIS RUSSELL, ROBERT B. KING AND CHARLOTTE E. MOORE
Princeton University Observatory, Princeton, New Jersey, and Mount Wilson Observatory, Pasadena, California

(Received June 11, 1940)

The present analysis classifies 2725 lines and identifies 768 multiplets of the doublet, quartet, and sextet systems. The results are in complete agreement with Hund's theory, and indicate that all the important features of the structure of the neutral atom are now known. The results agree closely with those of Catalan and Antunes (who classified 2076 lines) except where changes in term-designations have been made on account of Zeeman data or of a new interpretation of the convergence of the components of multiple terms to their limits. The principal ionization potential is 7.84 volts. Tables are given of terms, electron configurations, and of 3007 lines, of which 91 percent are classified. Zeeman effects have been observed for 871 lines and g values derived for 270 levels. The large majority of these have nearly the theoretical values for LS coupling. There are some cases of g sharing (Table VII). The wave-length list includes measures of 1282 lines made with the interferometer by Dr. Keivin Burns of the Allegheny Observatory, which, by his generosity, are here published for the first time; and also 274 newly measured lines between λ2230 and λ1814.

1. PREVIOUS INVESTIGATIONS

THE first regularities in the arc spectrum of cobalt were detected by Walters[1] who identified the lowest terms of the quartet system. Catalan[2] in 1928 classified about 1200 lines. A thorough discussion, classifying 2076 lines, was published in 1936 by Catalan and Antunes.[3] This publication is unfortunately difficult of access in this country, and the situation is aggravated by the fact (communicated to us by Dr. Antunes) that the reprints which the authors hoped to distribute were lost in Toledo at the beginning of the Spanish War. We are very greatly indebted to Dr. Antunes for the loan of the single copy of this work in his possession —of which we have retained a photostatic copy.

The present work was begun without knowledge that this investigation was in progress, and has been extended farther with the aid of observations in the infra-red and ultraviolet. In view of the inaccessibility of the results of the earlier analysis, a detailed presentation of ours appears to be in order.

Observations of the Zeeman effect for 151 lines were given by Roth and Bartunek[4] who found g values for 93 levels. Our observations include 871 lines, and give g values for 270 levels.

Marvin[5] has made a theoretical discussion of the energy-levels in the deep configurations of Co I. We have found certain additional terms close to the positions predicted by him.

2. THE OBSERVATIONAL DATA ON WHICH THE PRESENT INVESTIGATION IS BASED

(*a*) The *wave-lengths* have been compiled from all available sources (listed in Table VIII). We are very greatly indebted to Dr. Keivin Burns for putting at our disposal a long list of unpublished determinations with the interferometer. With his generous consent, these are printed here for the first time. Dr. Burns states that these observations are good to two parts per million. They are distinguished by heavy type in the general list (Table VIII). Next in preference, in order of accuracy, come the measures of Meggers and Kiess in the infra-red, including unpublished data kindly put at our disposal; those given in the *Wavelength Table of the Massachusetts Institute of Technology;* and unpublished measures of grating spectra by Burns. The observations have been extended from λ2230 to λ1814 by measures made by one of us (C.E.M.) on a plate taken by Dr. A. G. Shen-

[1] F. M. Walters, Jr., J. Washington Acad. Sci. **14**, 407 (1924).
[2] M. A. Catalan, Zeits. f. Physik **47**, 89 (1928).
[3] M. A. Catalan and M. T. Antunes, Anal. Soc. Española de Fisica y Quimica **34**, 103–145, 207–297 (1936).
[4] F. L. Roth and P. F. Bartunek, Phys. Rev. **47**, 526 (1935).
[5] H. H. Marvin, Phys. Rev. **47**, 521 (1935).

stone with a normal-incidence vacuum spectrograph having a 2-meter glass grating ruled 30,000 lines per inch. The dispersion is 4.2A/mm.[6] Few standard lines were available, and the measures are not of high precision.

King's temperature classification[7] has been, as always, of fundamental value in the analysis.

(*b*) The observations of Zeeman effect were made by one of us (R.B.K.) but include some plates and measures made earlier by A. S. King. They were obtained with the aid of the Weiss magnet and the 15-foot concave grating spectrograph of the Mt. Wilson laboratory. The field strength was slightly in excess of 30,000 gauss. The spectrum was photographed in the second order (dispersion 1.86A/mm) from λ2200 to λ5000, and in the first order from λ5000 to λ7000.

Measurements of the Zeeman patterns were made with an ordinary comparator. Most of the complex patterns were unresolved, the *n* components usually appearing as doublets with the components widened in some degree, while the *p* components were either undisplaced, though broadened, or appeared as doublets. Measurements of displacements on complex patterns appearing as doublets were usually made on the centers of gravity of each component of the doublet. In some cases, however, the patterns were on the verge of resolution and were strongly shaded inward or outward making it difficult to locate the center of gravity. Then settings were made on the strong edges of the pattern. These should give, very nearly, the separations of the strongest components of the complex patterns. In many cases one component of a doublet pattern, or one side of a resolved pattern, was badly blended with a neighboring line. In these cases the displacement was measured between the unblended component or components and the no-field line appearing in the adjacent spectra.

The reduction of the observed Zeeman separations in angstrom units to the theoretical unit of the normal Zeeman triplet was done in the usual manner. The field strengths were determined from measurements of the patterns of the sodium D lines and of numerous normal resolved patterns of previously classified Co I lines.

TABLE I. *Observed and predicted low levels in* Co I.

CONFIG.	TERM	PRINCIPAL LEVEL	INTERVALS
$3d^74s^2$	a^4F	0	816, 591, 402
		0	*808, 594, 406*
	b^4P	15,184	590, 422
		14,955	*250, 385*
	a^2G	16,468	766
		16,051	*787*
	b^2P	20,500	715
		20,878	*787*
	a^2H	21,780	695
		20,992	*703*
	b^2D	21,920	1232
		22,962	*1168*
	^2F	*35,798*	*−320*
	^2D	*56,272*	*−352*
$3d^84s$	b^4F	3483	660, 548, 386
		3483	*662, 538, 396*
	a^2F	7442	1018
		7629	*1050*
	a^4P	13,795	241, 363
		13,857	*498, 243*
	a^2D	16,778	−307
		16,799	*−359*
	a^2P	18,389	385
		18,194	*221*
	b^2G	23,184	23
		21,294	*4*
	^2S	*47,421*	
$3d^9$	c^2D	27,497	973
		----	----

[6] A. G. Shenstone, Phil. Trans. **237**, 453 (1938).
[7] A. S. King, Astrophys. J. **42**, 347 (1915), **51**, 179 (1920) Mt. Wilson Contr. Nos. 108 and 181.

3. RESULTS OF PRESENT ANALYSES

The results of the present analysis agree in general with those of Catalan and Antunes, except among the high levels—both odd and even—where many changes in designation have been made, based largely upon Zeeman data not previously available. The number of terms identified is 99—47 belonging to the doublet system, 43 quartets, and 9 sextets—including 284 energy-levels. There are 43 more levels which have not been grouped into terms—a total of 327 levels, of which 132 are even and 195 odd.

Combinations between these account for 2725 lines—including 69 which are unresolved blends of lines which should be roughly comparable in intensity. There are also 42 faint predicted lines which are masked by strong ones. These are grouped into 768 multiplets, and 204 combinations with miscellaneous levels, observed in whole or in part. Of these 186 are doublet combinations, 197 quartets, 18 sextets, 288 doublet-

TABLE II. *Electron configurations in* Co I.*

LIMIT d^7s		a^5F	b^3F	a^5P	^3P	^3H	^1H	^3G	^1G	^3D	^1D	^3P	^1P
Added Electron	$4s$	a^4F		b^4P		a^2H		a^2G		b^2D		b^2P	
	$4p$	z^6D^0 z^6F^0 z^6G^0	x^4D^0 x^4F^0 x^4G^0	$^6S^0$ $^6P^0$ $^6D^0$	x^4S^0 x^4P^0 t^4D^0	$^4G^0$ $^4H^0$ $^4I^0$	$^2G^0$ $^2H^0$ $^2I^0$	w^4F^0 w^4G^0 $^4H^0$	$^2F^0$ $^2G^0$ $^2H^0$	w^4P^0: s^4D^0: $^4F^0$	$^2P^0$ $^2D^0$ $^2F^0$	$^4S^0$ $^4P^0$ $^4D^0$	$^2S^0$ $^2P^0$ $^2D^0$
		z^4D^0 z^4F^0 z^4G^0	z^2D^0 z^2F^0 z^2G^0	z^4S^0 z^4P^0 w^4D^0	z^2S^0: y^2P^0: v^2D^0:	w^2G^0: y^2H^0: $^2I^0$		x^2F^0: x^2G^0 z^2H^0		$^2P^0$ $^2D^0$ $^2F^0$		x^2S^0: w^2P^0: $^2D^0$	

LIMIT d^8		a^3F	^1P	^1G	^1D
Added Electron	$4s$	b^4F a^2F	a^4P a^2P	b^2G	a^2D
	$4p$	y^4D^0 y^4F^0 y^4G^0	y^4S^0 y^4P^0 v^4D^0	u^2F^0 v^2G^0 x^2H^0:	z^2P^0 x^2D^0 w^2F^0:
		y^2D^0 y^2F^0 y^2G^0	y^2S^0: x^2P^0: w^2D^0:		

LIMIT d^7s		a^5F		b^3F	
Added Electron	$5s$	e^6F	f^4F	h^4F	g^2F
	$4d$	e^6P e^6D f^6F e^6G e^6H	f^4P f^4D i^4F f^4G f^4H	^4P ^4D ^4F ^4G ^4H	^2P ^2D ^2F ^2G ^2H

LIMIT d^8		a^3F	
Added Electron	$5s$	e^4F	e^2F
	$4d$	e^4P e^4D g^4F e^4G e^4H	e^2P e^2D f^2F e^2G e^2H

*A colon denotes that the assignment of the electron configuration is doubtful.

quartet, and 66 quartet-sextet intercombinations (while 13 are double intercombinations, between doublets and sextets).

The terms and unclassified levels are listed in Table IV. Some of the higher ones are incomplete—the components of small J value having eluded search.

4. ELECTRON CONFIGURATIONS

The *electron-configurations* for the low even terms can be assigned with certainty. Marvin's theoretical study is conclusive,—especially his prediction of the terms a^2H and b^2G close to the positions in which they were later found by Catalan and Antunes and by us, as shown in Table I, where the third column gives the level of the leading component and the next the term intervals—the observed values being in Roman type and the calculated in italics.

Marvin assigns b^2D to $3d^9$; but it fits his prediction for $3d^74s^2$ satisfactorily, and the recently discovered c^2D falls naturally in the other place.

The three remaining terms from the "low" configurations all lie so high that there is little or no hope of finding their combinations.

The odd configurations $3d^74s4p$ and $3d^84p$ give a great number of terms, forming triads, each of which should have its terms roughly at the same level and combine strongly with the related even low term. Many of these triads can be identified with certainty. Among the terms of small L value, especially in the doublets, there is a good deal of mutual perturbation and sharing of relationships, which make assignment difficult.

Among the high even terms, which are also included in the table, the "families" having the same limit-term in Co II are usually clearly separated, and assignments are rarely doubtful.

TABLE III. *Ionization potential of* Co I.

DESIG.	LEVEL	EST. n^*	TERM	Co II	$^4F_4$–$^3F_4$	FINAL n^*
a^4F	0	1.278	67,188	3350	63,838	1.281
e^6F	45,676	2.277	21,165	3350	63,493	2.276
f^4F	47,524	2.386	19,276	3350	63,450	2.382
e^6H	53,822	2.892	13,121	3350	63,593	2.901
a^4F	0	1.226	73,009	9813	63,193	1.223
h^4F	52,864	2.308	20,600	9813	63,651	2.316
b^4F	3483	1.350	60,213	0	63,696	1.352
a^3F	7442	1.387	57,043	950	63,535	1.387
e^4F	44,782	2.420	18,738	0	63,520	2.421
e^3F	45,924	2.450	18,282	950	63,336	2.433
e^4H	51,142	2.975	12,399	0	63,709	2.978

TABLE IV. Co I *terms*.

CONFIG.	TERM	OBS. g	C. AND A.
d^8s	$a^2P_{1\frac{1}{2}}$ 18,389.57	1.33	Id
	$a^2P_{\frac{1}{2}}$ 18,775.01	0.69	Id
d^7s^2	$b^2P_{1\frac{1}{2}}$ 20,500.71	1.29	Id
	$b^2P_{\frac{1}{2}}$ 21,215.90	0.68	Id
$d^8(^3F)4d$	$e^4P_{1\frac{1}{2}}$ 51,200.60	1.38:	$e^4P_{1\frac{1}{2}}$
	$e^4P_{\frac{1}{2}}$ 52,041.14:	0.48:	$e^4P_{\frac{1}{2}}$
d^8s	$a^2D_{2\frac{1}{2}}$ 16,778.16	1.28	Id
	$a^2D_{1\frac{1}{2}}$ 16,470.60	1.09	Id
d^7s^2	$b^2D_{2\frac{1}{2}}$ 21,920.09	1.24	Id
	$b^2D_{1\frac{1}{2}}$ 23,152.57	0.79	Id
d^9	$c^2D_{2\frac{1}{2}}$ 27,497.06	1.20	
	$c^2D_{1\frac{1}{2}}$ 28,470.51	0.82	
$d^8(^3F)4d$	$e^2D_{2\frac{1}{2}}$ 52,460.10	0.92	Id
	$e^2D_{1\frac{1}{2}}$ 53,343.27	0.80	Id
d^8s	$a^2F_{3\frac{1}{2}}$ 7442.41	1.16	Id
	$a^2F_{2\frac{1}{2}}$ 8460.81	0.86	Id
$d^8(^3F)5s$	$e^4F_{3\frac{1}{2}}$ 45,924.98	1.14	Id
	$e^4F_{2\frac{1}{2}}$ 46,746.00	0.49:	Id
$d^8(^3F)4d$	$f^4F_{3\frac{1}{2}}$ 52,095.00	1.11	Id
	$f^4F_{2\frac{1}{2}}$ 52,970.62	1.13	Id
$d^8s(^3F)5s$	$g^2F_{3\frac{1}{2}}$ 52,763.68	0.93	$e^2G_{3\frac{1}{2}}$
	$g^2F_{2\frac{1}{2}}$ 53,704.14	0.98	Id
d^7s^2	$a^2G_{4\frac{1}{2}}$ 16,467.90	1.11	Id
	$a^2G_{3\frac{1}{2}}$ 17,233.68	0.90	Id
d^8s	$b^2G_{4\frac{1}{2}}$ 23,184.23	1.11	
	$b^2G_{3\frac{1}{2}}$ 23,207.76	0.87	
$d^8(^3F)4d$	$e^2G_{4\frac{1}{2}}$ 52,156.46	1.12	Id
	$e^2G_{3\frac{1}{2}}$ 52,856.68	0.92	$g^2F_{3\frac{1}{2}}$
d^7s^2	$a^4H_{3\frac{1}{2}}$ 21,780.47	1.09	Id
	$a^2H_{4\frac{1}{2}}$ 22,475.36	0.94	Id
$d^8(^3F)4d$	$e^2H_{4\frac{1}{2}}$ 52,113.91	1.13	Id
	$e^2H_{3\frac{1}{2}}$ 52,775.47	0.97	Id
d^8s	$a^4P_{2\frac{1}{2}}$ 13,795.52	1.64	Id
	$a^4P_{1\frac{1}{2}}$ 14,036.28	1.72	Id
	$a^4P_{\frac{1}{2}}$ 14,399.28	2.66	Id
d^7s^2	$b^4P_{2\frac{1}{2}}$ 15,184.04	1.50	Id
	$b^4P_{1\frac{1}{2}}$ 15,774.04	1.47	Id
	$b^4P_{\frac{1}{2}}$ 16,195.68	2.68	Id
$d^8(^3F)4d$	$e^4P_{2\frac{1}{2}}$ 51,042.26	1.59	Id
	$e^4P_{1\frac{1}{2}}$ 52,033.26	1.40	$e^2P_{1\frac{1}{2}}$
	$e^4P_{\frac{1}{2}}$ 52,915.92:		$e^2P_{\frac{1}{2}}$
$d^7s(^3F)4d$	$f^4P_{2\frac{1}{2}}$ 53,936.68	1.46	$f^4F_{4\frac{1}{2}}$
	$f^4P_{1\frac{1}{2}}$		
	$f^4P_{\frac{1}{2}}$		
$d^8(^3P)5s$	$g^4P_{2\frac{1}{2}}$ 56,545.51:		$42_{2\frac{1}{2}}$*
	$g^4P_{1\frac{1}{2}}$		
	$g^4P_{\frac{1}{2}}$		
$d^8(^3F)4d$	$e^4D_{3\frac{1}{2}}$ 51,052.98	1.45	Id
	$e^4D_{2\frac{1}{2}}$ 51,560.76	1.18	Id
	$e^4D_{1\frac{1}{2}}$ 52,264.49:		Id
	$e^4D_{\frac{1}{2}}$ 52,634.62	1.58:	Id
$d^7s(^3F)4d$	$f^4D_{3\frac{1}{2}}$ 53,702.13	1.39	$e^2P_{1\frac{1}{2}}$
	$f^4D_{2\frac{1}{2}}$ 54,282.73:		$i^4F_{3\frac{1}{2}}$
	$f^4D_{1\frac{1}{2}}$		
	$f^4D_{\frac{1}{2}}$		
d^7s^2	$a^4F_{4\frac{1}{2}}$ 0.00	1.32	Id
	$a^4F_{3\frac{1}{2}}$ 816.00	1.27	Id
	$a^4F_{2\frac{1}{2}}$ 1406.84	1.05	Id
	$a^4F_{1\frac{1}{2}}$ 1809.33	0.42	Id
d^8s	$b^4F_{4\frac{1}{2}}$ 3482.82	1.34	Id
	$b^4F_{3\frac{1}{2}}$ 4142.66	1.25	Id
	$b^4F_{2\frac{1}{2}}$ 4690.18	1.04	Id
	$b^4F_{1\frac{1}{2}}$ 5075.83	0.40	Id
$d^8(^3F)5s$	$e^4F_{4\frac{1}{2}}$ 44,782.13	1.33	Id
	$e^4F_{3\frac{1}{2}}$ 45,105.59	1.21	Id
	$e^4F_{2\frac{1}{2}}$ 45,876.58	1.01	Id
	$e^4F_{1\frac{1}{2}}$ 46,375.17	0.44	Id
$d^7s(^5F)5s$	$f^6F_{5\frac{1}{2}}$ 47,524.47	1.33	Id
	$f^6F_{4\frac{1}{2}}$ 48,201.60	1.27	Id
	$f^6F_{3\frac{1}{2}}$ 48,718.57	1.04	Id
	$f^6F_{1\frac{1}{2}}$ 49,078.43	0.36	Id
$d^8(^3F)4d$	$g^4F_{4\frac{1}{2}}$ 51,170.14	1.34	Id
	$g^4F_{3\frac{1}{2}}$ 51,199.58	1.16	Id
	$g^4F_{2\frac{1}{2}}$ 52,070.00	1.08	Id
	$g^4F_{1\frac{1}{2}}$ 52,702.76	0.76:	$e^4G_{2\frac{1}{2}}$
$d^7s(^5F)5s$	$h^6F_{5\frac{1}{2}}$ 52,864.41	1.26	Id
	$h^6F_{4\frac{1}{2}}$ 53,694.57	1.28:	Id
	$h^6F_{3\frac{1}{2}}$ 54,258.75	0.98:	Id
	$h^6F_{1\frac{1}{2}}$ 54,426.64		Id
$d^7s(^5F)4d$	$i^6F_{5\frac{1}{2}}$ 53,788.78	1.27	$e^6D_{4\frac{1}{2}}$
	$i^6F_{4\frac{1}{2}}$ 54,477.07		$f^6F_{4\frac{1}{2}}$
	$i^6F_{3\frac{1}{2}}$ 54,904.99	0.85	$f^6F_{3\frac{1}{2}}$
	$i^6F_{1\frac{1}{2}}$		
$d^8(^3F)4d$	$e^4G_{5\frac{1}{2}}$ 51,203.75	1.21	Id
	$e^4G_{4\frac{1}{2}}$ 51,267.93	1.13	Id
	$e^4G_{3\frac{1}{2}}$ 52,162.02	1.13	Id
	$e^4G_{2\frac{1}{2}}$ 52,772.30	0.74	$g^4F_{1\frac{1}{2}}$
$d^7s(^5F)4d$	$f^6G_{5\frac{1}{2}}$ 53,511.83	1.32	$f^6F_{5\frac{1}{2}}$
	$f^6G_{4\frac{1}{2}}$ 54,158.17	1.25:	$f^6F_{4\frac{1}{2}}$
	$f^6G_{3\frac{1}{2}}$ 54,514.67	1.23:	$f^6F_{3\frac{1}{2}}$
	$f^6G_{1\frac{1}{2}}$ 55,165.63:		$f^6F_{1\frac{1}{2}}$
$d^8(^3F)4d$	$e^4H_{6\frac{1}{2}}$ 51,142.53	1.21	Id
	$e^4H_{5\frac{1}{2}}$ 51,174.28	1.13	Id
	$e^4H_{4\frac{1}{2}}$ 52,121.21	0.96	Id
	$e^4H_{3\frac{1}{2}}$ 52,716.70	0.93	Id
$d^7s(^5F)4d$	$f^6H_{6\frac{1}{2}}$ 53,618.08	1.22	$e^6H_{5\frac{1}{2}}$
	$f^6H_{5\frac{1}{2}}$ 54,315.67	1.18	$e^6H_{4\frac{1}{2}}$
	$f^6H_{4\frac{1}{2}}$ 54,860.93	1.10:	$f^4F_{3\frac{1}{2}}$
	$f^6H_{3\frac{1}{2}}$ 55,268.75		$e^6H_{3\frac{1}{2}}$
	$g^6H_{6\frac{1}{2}}$ 57,922.06		
	$g^6H_{5\frac{1}{2}}$ 58,441.03		
	$g^6H_{4\frac{1}{2}}$ 58,673.73		
	$g^6H_{3\frac{1}{2}}$ 59,314.82:		
$d^7s(^5F)4d$	$e^6P_{3\frac{1}{2}}$ 53,789.12	1.81	
	$e^6P_{2\frac{1}{2}}$ 54,445.61	1.67	$f^4D_{2\frac{1}{2}}$
	$e^6P_{1\frac{1}{2}}$ 54,949.97	1.44:	Id
$d^7s(^5F)4d$	$e^6D_{4\frac{1}{2}}$ 53,725.20	1.44	$e^4G_{5\frac{1}{2}}$
	$e^6D_{3\frac{1}{2}}$ 54,352.30	1.48	Id
	$e^6D_{2\frac{1}{2}}$ 54,946.90	1.47:	Id
	$e^6D_{1\frac{1}{2}}$ 55,407.10:	2.14	
	$e^6D_{\frac{1}{2}}$		
$d^7s(^5F)5s$	$e^6F_{5\frac{1}{2}}$ 45,676.00	1.48	Id
	$e^6F_{4\frac{1}{2}}$ 46,223.01	1.43	Id
	$e^6F_{3\frac{1}{2}}$ 46,706.83	1.40	Id
	$e^6F_{2\frac{1}{2}}$ 47,090.65	1.32	Id
	$e^6F_{1\frac{1}{2}}$ 47,364.73	1.09	Id
	$e^6F_{\frac{1}{2}}$ 47,528.44	−0.71	Id
$d^7s(^5F)4d$	$f^6F_{5\frac{1}{2}}$ 53,660.37	1.44	$31_{2\frac{1}{2}}$*
	$f^6F_{4\frac{1}{2}}$ 54,356.45	1.36	$e^4G_{4\frac{1}{2}}$
	$f^6F_{3\frac{1}{2}}$ 54,896.57	1.27	$e^4G_{3\frac{1}{2}}$
	$f^6F_{2\frac{1}{2}}$ 55,283.02	1.17	$e^4G_{2\frac{1}{2}}$
	$f^6F_{1\frac{1}{2}}$ 55,577.28:	1.07	$f^4D_{\frac{1}{2}}$
	$f^6F_{\frac{1}{2}}$		
$d^7s(^5F)4d$	$e^4G_{6\frac{1}{2}}$ 53,728.36:	1.35	33*
	$e^4G_{5\frac{1}{2}}$ 54,367.43	1.32	$f^4G_{5\frac{1}{2}}$
	$e^4G_{4\frac{1}{2}}$ 54,682.91	1.23	†
	$e^4G_{3\frac{1}{2}}$ 54,989.62:	1.23	$f^4G_{4\frac{1}{2}}$
	$e^4G_{2\frac{1}{2}}$ 55,449.97	1.25	$f^4D_{3\frac{1}{2}}$
	$e^4G_{\frac{1}{2}}$ 55,389.73		Id
$d^7s(^5F)4d$	$e^4H_{7\frac{1}{2}}$ 53,822.08	1.34	
	$e^4H_{6\frac{1}{2}}$ 54,452.38	1.29	$f^4H_{5\frac{1}{2}}$
	$e^4H_{5\frac{1}{2}}$ 54,947.68	1.22	$f^4H_{4\frac{1}{2}}$
	$e^4H_{4\frac{1}{2}}$ 55,312.96		$f^4H_{3\frac{1}{2}}$
	$e^4H_{3\frac{1}{2}}$ 55,520.64	0.94	$f^4G_{3\frac{1}{2}}$
	$e^4H_{2\frac{1}{2}}$ 55,555.34		
	$1_{2\frac{1}{2}}$ 54,561.74	1.36:	$e^4P_{2\frac{1}{2}}$
	$2_{2\frac{1}{2}}$ 55,078.76	1.46:	$f^4P_{1\frac{1}{2}}$
	$3_{2\frac{1}{2}}$ 55,223.14	1.14	$f^4D_{2\frac{1}{2}}$
	$4_{2\frac{1}{2}}$ 55,598.74		$f^4H_{2\frac{1}{2}}$
	$5_{1\frac{1}{2},2\frac{1}{2}}$ 55,721.01		$f^4G_{2\frac{1}{2}}$
	$6_{\frac{1}{2}}$ 55,826.81		$f^4P_{\frac{1}{2}}$
$d^7s(^3P)4p$:	$z^4S^0_{1\frac{1}{2}}$ 44,454.51	2.10	$z^2P^0_{1\frac{1}{2}}$
$d^8(^3P)4p$:	$y^4S^0_{1\frac{1}{2}}$ 47,977.94	2.05	
$d^7s(^3P)4p$:	$z^4S^0_{1\frac{1}{2}}$ 48,026.34	1.70	$w^2P^0_{1\frac{1}{2}}$
	$w^4S^0_{1\frac{1}{2}}$ 48,837.72	1.50:	$^4D^0_{\frac{1}{2}}$
$d^8(^1D)4p$	$z^2P^0_{1\frac{1}{2}}$ 43,537.71	1.19	$y^2P^0_{1\frac{1}{2}}$
	$z^2P^0_{\frac{1}{2}}$ 43,130.24	0.71	Id
$d^7s(^3P)4p$:	$y^2P^0_{1\frac{1}{2}}$ 46,685.43	1.33	$w^4D^0_{1\frac{1}{2}}$
	$y^2P^0_{\frac{1}{2}}$ 47,091.14	0.63	$w^4D^0_{\frac{1}{2}}$
$d^8(^3P)4p$:	$z^4P^0_{1\frac{1}{2}}$ 48,334.37	1.39	$w^2P^0_{1\frac{1}{2}}$
	$z^4P^0_{\frac{1}{2}}$ 48,160.43:	1.20	
$d^7s(^3P)4p$:	$w^4P^0_{1\frac{1}{2}}$ 49,025.42	0.94	$54^0_{1\frac{1}{2}}$
	$w^2P^0_{\frac{1}{2}}$ 49,754.73	1.24	
	$v^2P^0_{1\frac{1}{2}}$ 50,925.11	1.32	$103^0_{1\frac{1}{2}}$
	$v^2P^0_{\frac{1}{2}}$ 50,945.47	0.74	†
$d^7s(^5F)4p$	$z^6D^0_{2\frac{1}{2}}$ 33,462.83	1.20	Id
	$z^6D^0_{1\frac{1}{2}}$ 34,352.42	0 82	Id
$d^8(^3F)4p$	$y^4D^0_{2\frac{1}{2}}$ 36,092.44	1.19	Id
	$y^4D^0_{1\frac{1}{2}}$ 36,875.13	0.81	Id
$d^8(^1D)4p$	$z^2D^0_{2\frac{1}{2}}$ 43,921.89	1.23	Id
	$z^2D^0_{1\frac{1}{2}}$ 43,911.36	1.13	Id
$d^8(^3P)4p$:	$w^2D^0_{2\frac{1}{2}}$ 45,688.15	1.19	$y^4P^0_{1\frac{1}{2}}$
	$w^2D^0_{1\frac{1}{2}}$ 46,454.95	0.85	$v^2D^0_{1\frac{1}{2}}$
$d^7s(^3P)4p$:	$v^2D^0_{2\frac{1}{2}}$ 46,671.94	1.21	$x^4P^0_{1\frac{1}{2}}$
	$v^2D^0_{1\frac{1}{2}}$ 46,186.41	1.18	$w^2D^0_{1\frac{1}{2}}$
	$u^2D^0_{2\frac{1}{2}}$ 53,195.98	1.16	†
	$u^2D^0_{1\frac{1}{2}}$ 53,074.92	0.81	
$d^7s(^3F)4p$	$z^4F^0_{3\frac{1}{2}}$ 31,871.15	1.18	Id
	$z^4F^0_{2\frac{1}{2}}$ 32,781.71	0.88	Id
$d^8(^3F)4p$	$y^4F^0_{4\frac{1}{2}}$ 35,450.56	1.12	Id
	$y^4F^0_{3\frac{1}{2}}$ 36,329.86	0.96:	Id
$d^7s(^2G)4p$:	$z^2F^0_{3\frac{1}{2}}$ 43,555.22	1.24	$w^2P^0_{1\frac{1}{2}}$
	$z^2F^0_{2\frac{1}{2}}$ 43,425.71	1.02	$w^2P^0_{\frac{1}{2}}$
$d^8(^1D)4p$:	$u^2F^0_{3\frac{1}{2}}$ 47,225.11	1.25	$v^2P^0_{1\frac{1}{2}}$
	$u^2F^0_{2\frac{1}{2}}$ 47,128.96	0.83	$v^2P^0_{\frac{1}{2}}$
	$v^2F^0_{3\frac{1}{2}}$ 48,317.17	1.18	$u^4D^0_{1\frac{1}{2}}$
	$v^2F^0_{2\frac{1}{2}}$ 48,615.56:		$t^4D^0_{\frac{1}{2}}$
$d^8(^1G)4p$	$u^2F^0_{3\frac{1}{2}}$ 50,578.73	1.15	
	$u^2F^0_{2\frac{1}{2}}$ 50,712.45	0.91	†
	$t^2F^0_{2\frac{1}{2}}$ 51,896.75:	1.15:	
	$t^2F^0_{1\frac{1}{2}}$ 52,796.13	0.92:	†
	$s^2F^0_{2\frac{1}{2}}$ 53,103.78	1.16	†
	$s^2F^0_{1\frac{1}{2}}$ 53,146.91:		
$d^7s(^3F)4p$	$z^6G^0_{4\frac{1}{2}}$ 31,699.69	1.11	Id
	$z^6G^0_{3\frac{1}{2}}$ 32,733.07	0.91	Id
$d^8(^3F)4p$	$y^6G^0_{4\frac{1}{2}}$ 33,439.72	1.16	Id
	$y^6G^0_{3\frac{1}{2}}$ 34,133.59	0 95	Id
$d^7s(^2G)4p$	$z^2G^0_{4\frac{1}{2}}$ 46,032.10	1.12	$z^2H^0_{4\frac{1}{2}}$
	$z^2G^0_{3\frac{1}{2}}$ 45,766.63	0.93	
$d^7s(^3H)4p$:	$w^6G^0_{4\frac{1}{2}}$ 50,593.38	1.10	$101^0_{4\frac{1}{2}}$
	$w^6G^0_{3\frac{1}{2}}$ 50,611.22	0.82	
$d^8(^1G)4p$	$v^2G^0_{4\frac{1}{2}}$ 53,276.02	1.03	$102^0_{4\frac{1}{2}}$
	$v^2G^0_{3\frac{1}{2}}$ 53,373.53	0.86	
$d^7s(^3G)4p$	$z^4H^0_{5\frac{1}{2}}$ 45,540.28	1.12	Id
	$z^4H^0_{4\frac{1}{2}}$ 45,111.48	0.90	
$d^7s(^3H)4p$:	$y^4H^0_{5\frac{1}{2}}$ 50,375.91	1.09:	
	$y^4H^0_{4\frac{1}{2}}$ 50,210.80	0.91	
$d^8(^1G)4p$:	$z^2H^0_{5\frac{1}{2}}$ 50,703.08	1.08	
	$z^2H^0_{4\frac{1}{2}}$ 50,902.61	0.98	
$d^7s(^5P)4p$	$z^6S^0_{2\frac{1}{2}}$ 40,621.62	2.03	Id
$d^8(^3P)4p$	$y^4S^0_{1\frac{1}{2}}$ 46,562.87	1.25	$z^4P^0_{1\frac{1}{2}}$
$d^7s(^3P)4p$	$z^4S^0_{1\frac{1}{2}}$ 48,753.72	1.75	$t^2D^0_{1\frac{1}{2}}$

* Level rejected by Catalan and Antunes.

† Level regarded as doubtful by C. and A. and not given designation.

TABLE IV.—*Concluded.*

CONFIG.	TERM		OBS. g	C. AND A.
$d^7s(^3P)4p$	$z^4P^0_{3½}$	41,968.89	1.63	Id
	$z^4P^0_{2½}$	41,982.66	1.73	Id
	$z^4P^0_{1½}$	41,969.90	2.51	Id
$d^8(^2P)4p$	$y^4P^0_{2½}$	44,480.14	1.55	$w^4P^0_{2½}$
	$y^4P^0_{1½}$	44,658.03	1.62	$z^2P^0_{1½}$
	$y^4P^0_{½}$	44,857.57	2.44	$z^2S^0_{½}$
$d^7s(^3P)4p$	$z^4P^0_{2½}$	46,002.83	1.54	$w^2D^0_{2½}$
	$z^4P^0_{1½}$	45,904.68	1.68	$y^4P^0_{1½}$
	$z^4P^0_{½}$	45,957.29	2.48	$y^4P^0_{½}$
$d^7s(^3D)4p$:	$w^4P^0_{3½}$	51,160.03	1.51:	$8S^0_{3½}$
	$w^4P^0_{2½}$	52,014.45	1.68	†
	$w^4P^0_{1½}$	52,355.12	2.40	†
$d^7s(^3F)4p$	$z^4D^0_{3½}$	29,294.52	1.43	Id
	$z^4D^0_{2½}$	29,948.76	1.35	Id
	$z^4D^0_{1½}$	30,443.63	1.18	Id
	$z^4D^0_{½}$	30,742.65	−0.01	Id
$d^8(^2F)4p$	$y^4D^0_{3½}$	32,027.50	1.41	Id
	$y^4D^0_{2½}$	32,654.50	1.39	Id
	$y^4D^0_{1½}$	33,150.68	1.20	Id
	$y^4D^0_{½}$	33,449.18	0.01	Id
$d^7s(^3F)4p$	$z^4D^0_{3½}$	39,649.16	1.41	Id
	$z^4D^0_{2½}$	40,345.95	1.35	Id
	$z^4D^0_{1½}$	40,827.77	1.24	Id
	$z^4D^0_{½}$	41,101.80	−0.03	Id
$d^7s(^3P)4p$	$w^4D^0_{3½}$	43,398.62	1.33	$z^2F^0_{3½}$
	$w^4D^0_{2½}$	43,242.95	1.17	$z^2F^0_{2½}$
	$w^4D^0_{1½}$	43,263.57	1.16	$z^2F^0_{1½}$
	$w^4D^0_{½}$	43,435.58	0.14	$y^2F^0_{½}$
$d^8(^2P)4p$	$t^4D^0_{3½}$	45,971.19	1.42	$w^2D^0_{2½}$
	$t^4D^0_{2½}$	46,329.63	1.36	$w^4D^0_{2½}$
	$t^4D^0_{1½}$	46,260.02	1.48	$P^0_{1½}$
	$t^4D^0_{½}$	46,502.15	0.16	$x^1P^0_{1}$
	$u^4D^0_{3½}$	46,872.74	1.30	$t^4D^0_{3½}$
	$u^4D^0_{2½}$	47,393.93	1.28	$t^4D^0_{2½}$
	$u^4D^0_{1½}$	47,612.18	1.12	$t^4D^0_{1½}$
	$u^4D^0_{½}$	47,905.26	0.01	$t^4D^0_{½}$
$d^7s(^3P)4p$	$t^4D^0_{3½}$	48,217.32	1.19	$u^2D^0_{2½}$
	$t^4D^0_{2½}$	48,443.76	1.34	$u^2D^0_{1½}$
	$t^4D^0_{1½}$	48,546.07	1.05	$u^4D^0_{1½}$
	$t^4D^0_{½}$	48,571.77	0.36:	$u^4D^0_{½}$
$d^7s(^3D)4p$:	$s^4D^0_{3½}$	50,741.66		Id
	$s^4D^0_{2½}$	51,139.38	1.33:	Id
	$s^4D^0_{1½}$	51,847.27		Id
	$s^4D^0_{½}$	52,264.01:		

CONFIG.	TERM		OBS. g	C. AND A.
$d^7s(^5F)4p$	$z^6F^0_{5½}$	28,345.86	1.35	Id
	$z^6F^0_{4½}$	28,777.27	1.24	Id
	$z^6F^0_{3½}$	29,216.37	1.03	Id
	$z^6F^0_{2½}$	29,563.17	0.42	Id
$d^8(^3F)4p$	$y^4F^0_{4½}$	32,841.99	1.32	Id
	$y^4F^0_{3½}$	33,466.87	1.16	Id
	$y^4F^0_{2½}$	33,945.90	0.95	Id
	$y^4F^0_{1½}$	34,196.21	0.47	Id
$d^7s(^5F)4p$	$z^6F^0_{5½}$	41,225 76	1.35	Id
	$z^6F^0_{4½}$	41,918.41	1.24	Id
	$z^6F^0_{3½}$	42,434.23	1.04	Id
	$z^6F^0_{2½}$	42,796.67	0.44	Id
$d^7s(^5G)4p$	$w^6F^0_{6½}$	43,295.32	1.32	†
	$w^6F^0_{5½}$	43,847.98	1.20	$v^2F^0_{3½}$
	$w^6F^0_{4½}$	44,201.92	0.95	$v^2F^0_{2½}$
	$w^6F^0_{3½}$	44,555.71	0.44	$w^4F^0_{3½}$
	$v^6F^0_{6½}$	54,791.2		
	$v^6F^0_{5½}$	55,314.04:		
	$v^6F^0_{4½}$	55,684.7		
	$v^6F^0_{3½}$	55,622.84		
$d^7s(^5F)4p$	$z^6G^0_{6½}$	28,845.22	1.27	Id
	$z^6G^0_{5½}$	29,269.73	1.19	Id
	$z^6G^0_{4½}$	29,735.18	1.01	Id
	$z^6G^0_{3½}$	30,102.96	0.58	Id
$d^8(^3F)4p$	$y^4G^0_{5½}$	32,430.59	1.28	Id
	$y^4G^0_{4½}$	32,464.73	1.17	Id
	$y^4G^0_{3½}$	33,173.36	1.03	Id
	$y^4G^0_{2½}$	33,674.38	0.72	Id
$d^7s(^5F)4p$	$z^4G^0_{5½}$	41,528.53	1.31	Id
	$z^4G^0_{4½}$	42,269.32	1.18	Id
	$z^4G^0_{3½}$	42,811.44	0.98	Id
	$z^4G^0_{2½}$	43,199.65	0.83	Id
$d^7s(^5G)4p$	$w^4G^0_{6½}$	43,952.06:		
	$w^4G^0_{5½}$	44,183.34	1.18	$w^4F^0_{4½}$
	$w^4G^0_{4½}$	44,394.47	1.00	$w^4F^0_{3½}$
	$w^4G^0_{3½}$	44,568.47	0.70	
$d^7s(^5F)4p$	$z^6D^0_{4½}$	24,627.79	1.57	Id
	$z^6D^0_{3½}$	25,269.25	1.56	Id
	$z^6D^0_{2½}$	25,739.93	1.66	Id
	$z^6D^0_{1½}$	26,063.11	1.88	Id
	$z^6D^0_{½}$	26,250.49	3.37	Id

CONFIG.	TERM		OBS. g	C. AND A.
$d^7s(^5F)4p$	$z^6F^0_{5½}$	23,611.78	1.46	Id
	$z^6F^0_{4½}$	23,855.62	1.49	Id
	$z^6F^0_{3½}$	24,326.11	1.40	Id
	$z^6F^0_{2½}$	24,733.28	1.33	Id
	$z^6F^0_{1½}$	25,041.16	1.10	Id
	$z^6F^0_{½}$	25,232.79	−0.61	Id
$d^7s(^5F)4p$	$z^6G^0_{6½}$	25,138.88	1.40	Id
	$z^6G^0_{5½}$	25,568.68	1.34	Id
	$z^6G^0_{4½}$	25,937.59	1.29	Id
	$z^6G^0_{3½}$	26,232.05	1.15	Id
	$z^6G^0_{2½}$	26,450.02	0.88	Id
	$z^6G^0_{1½}$	26,597.64	−0.01	Id
	$1^0_{½}$	41,041.43	1.40	
	$2^0_{½}$	41,104.96	1.34:	
	$3^0_{½}$	42,988.12		
	$4^0_{½}$	43,969.90		
	$5^0_{½}$	44,381.32:		
	$6^0_{½}$?	47,839.15		
	$7^0_{½}$	48,828.87		
	$8^0_{½}$	48,851.58:		
	$9^0_{½,4½}$	49,197.74:		
	$10^0_{½}$	49,484.05	1.25:	$11^0_{½}$
	$11^0_{½}$	49,847.08	1.09	
	$12^0_{½}$	50,105.05	0.70:	$8^0_{½}$
	$13^0_{½,4½}$	50,738.20		
	$14^0_{½}$	50,806.55		
	$15^0_{½}$	51,184.63		
	$16^0_{½}$	51,863.18		
	$17^0_{½}$	51,989.31:		
	$18^0_{½}$	52,476.64		
	$19^0_{½}$	52,498.17		
	$20^0_{½,2½}$	52,526.04		
	$21^0_{½,4½}$	53,065.96:		
	$22^0_{½}$	53,463.10		
	$23^0_{½}$	54,165.35	1.36	
	$24^0_{½}$	54,398.60		
	$25^0_{½}$	54,874.08		
	$26^0_{½}$	54,932.32		
	$27^0_{½}$	55,061.49	1.66:	
	$28^0_{½}$	55,120.30:		
	$29^0_{½}$	55,387.11:		
	$30^0_{½}$	55,508.78		
	$31^0_{½}$	55,737.87		
	$32^0_{½}$	55,818.91	1.31:	
	$33^0_{½,2½}$	55,922.3		
	$34^0_{½,2½}$	56,101.84:		
	$35^0_{½,3½}$	56,222.04:		
	$36^0_{½,4½}$	58,187.39		
	$37^0_{½,3½}$	59,388.89		

Table II shows the assignments finally adopted. Terms predicted by theory but not found are denoted by the absence of small letters. Most of these terms are either very high, or would combine feebly, if at all, with the low level (e.g. the $^6S^0$, $^6P^0$, $^6D^0$, $^4H^0$). The most notable missing terms are the two $^2I^0$ terms, which are probably represented by observed lines with no satellites to identify them (§9). Most of the unassigned terms are odd, and all but two lie between 50,000 and 55,000 where the lower terms of the $5p$ configurations should be expected.

5. SERIES LIMITS

The convergence of the components of the terms of Co I to the components of the limit terms in Co II is of interest. Catalan and Antunes have shown[8] that, among the terms which have $d^8\,{}^3F$ as limit, the quartet and doublet components of lowest J go to $^3F_2$, those of next higher J to $^3F_3$, leaving two high J quartet components for $^3F_4$. This "inverted" convergence was found by one of us[9] for the limit $d^9\,{}^2D$ in Ni II. In Ni I, inverted convergence appears also in the terms having $d^8s\,{}^2F$ as limit, though that to $d^8s\,{}^4F$ is normal, but in Co I the convergence to $d^7s\,{}^3F$ is "normal." The combinations of all four components of h^4F with x^4G^0 are much stronger than those of g^2F, and the reverse is true for z^2F^0, z^2G^0; hence the doublet and quartet levels are correctly identified. But $h^4F_{4½}$, $g^2F_{3½}$ are close together; also $h^4F_{3½}$, $g^2F_{2½}$,

[8] Reference 3, pp. 132–134.
[9] H. N. Russell, Phys. Rev. **34**, 821 (1929).

and $h^4F_{2\frac{1}{2}}$, $h^4F_{1\frac{1}{2}}$. This suggests strongly that the convergence to $d^7s\ ^5F$ should be normal. Catalan and Antunes concluded that it is inverted, and found it difficult to distinguish the sextets and quartets in this pentad by means of the line-intensities. Working on the assumption of normal arrangement, we have been able to arrange the levels into a pentad of terms which combine much more strongly with z^6D^0, z^6F^0, z^6G^0 than with any quartet, and another pentad which combine more strongly with the quartets than the sextets. The ten leading components of these terms all lie between 53,511 and 53,936, the second components between 54,158 and 54,477, and so on.

In consequence of this reinterpretation of the situation, our values for the leading components of the sextet pentad, e^6P, e^6D, f^6F, e^6G, e^6H differ from those of the previous authors. Two of them were rejected as not real levels by them, and two not given at all; yet all are determined by good combinations except $e^6H_{7\frac{1}{2}}$ which gives a single very strong line with the right Zeeman pattern. The components of small L and J in this pentad give faint lines, and some of them could not be identified. A level of 54,282 which we have placed in this pentad as $f^4D_{2\frac{1}{2}}$ is classified by Catalan and Antunes as $d^8(^3F)6s\ ^4F_{3\frac{1}{2}}$. It gives no combinations with levels having $J=4\frac{1}{2}$. If their interpretation is correct it seems to us very improbable that the $^4F_{4\frac{1}{2}}$ component, for which they searched in vain, should be missing, as, especially in high series members, it should give stronger lines.

6. Ionization Potential

The available series consist of only two members (4*s* and 5*s*). The best way to determine the ionization potential is that developed by Catalan and Antunes[10] and independently by Meggers and Russell[11]— estimating the Rydberg denominators n^* by comparison with neighboring elements. Reliable values of n^* are known for Mn, Ni, Cu and Zn, so that those for Co can be interpolated with security. Table III gives the results. Only the components of largest J in the terms, and of greatest L in the pentads, need be used. The error of the estimated term value is proportional to $\Delta n^*/n^{*3}$ so that the low terms give poor determinations. Adding this to the level of Co I, and subtracting the height of the limiting level in Co II above the ground-level, we obtain the level of $^3F_4$ above $^4F_{4\frac{1}{2}}$. The mean for the terms for which $n^*>2$ is 63,536 corresponding to an ionization potential of 7.84 volts with an estimated probable error of ± 0.02. The values of n^* corresponding to this limit are given in the last column. The agreement with the estimated values is very close. Catalan and Antunes, by the same method, find 63,339, (7.82 volts). They prefer the value 63,312 obtained from their 6*s* term by a Hicks formula. The level $g^4P_{2\frac{1}{2}}$, if in series with $b^4P_{2\frac{1}{2}}$, should give Δn^* about 1.10. This would place the limit at 75,000 above $^4F_{4\frac{1}{2}}$, or 11,500 above $^3F_4$ of Co II. The still undiscovered term $d^8\ ^3P$ should lie at about this level.

7. Term Table

Table IV gives the term values which have been finally adopted. These were obtained by the usual process of convergent approximation, finding mean values for the odd terms from their combinations with the low even ones, etc. In taking these means, values derived from Burns' interferometer measures were given triple weight, and discordant combinations with deviations of 0.1 cm^{-1} or more were disregarded if better data were available. A colon denotes that the term value is determined with inferior accuracy, but not that the reality of the level itself is doubted.

The term v^4F^0 is doubtful. It gives a good multiplet with b^4F, but its combinations with a^4F are polar lines in the arc, and were originally attributed to Co II.

The term designations given by Catalan and Antunes are listed in the last column, "Id" meaning that they are identical with ours, and a blank that the level does not appear in their list. The numerous differences in assignment arise among the odd terms mainly from the present availability of Zeeman data; among the high even terms, from our reinterpretation of the convergence to the d^7s limits (§5). Three levels which they rejected as not real are restored to our list, and also nine which they regarded as doubtful. Thirty-three energy levels for which

[10] Reference 3, pp. 139–140.

[11] W. F. Meggers and H. N. Russell, J. Research Nat. Bur. Stand. **17**, 190 (1936); (RP 906).

TABLE V. *Zeeman patterns of* Co I.

λ	Zeeman Effect Observed	Zeeman Effect Calculated
6872.32	(1.37)1.35	(1.34)1.34
6814.95	(0.43)1.34	(0.41)1.32
6771.04	(0.36)1.43	(0.33)1.42
6632.43	(–)1.09	(0)1.10
6595.86	(–)0.91	(0)0.86*s*
6591.83	(–)0.96	(0)0.98*s*
6563.40	(–)1.10	(0)1.11
6490.34	(–)0.94	(0)0.99
6477.86	(–)0.83	(0)0.88
6454.99	(–)1.17	(0)1.16
6451.13	(–)1.15	(0)1.19
6450.23	(–)1.16	(0)1.17 (0.03)0.90
6431.07	(?)1.03	(0)1.02
6430.34	(–)1.10?	(0)1.12
6429.91	(–)0.90	(0)0.92
6421.70	(–)0.85	(0)0.80*s*
6417.82	(–)0.78	(0)0.85
6395.15	(–)0.61	(0)0.55
6351.44	(?)0.97?	(0.26)1.02
6347.84	(–)1.15	(0.12)1.14
6340.80	(–)1.15:	(0)1.23
6320.41	(–)1.05	(0)1.14
6314.52	(–)1.06	(*0.08*, 0.25, 0.42) 0.71 . . . *1.55*
6313.03	(–)1.25	(0)1.16
6282.63	(–)0.90*A*	(0)0.79*s*
6273.02	(–)1.13	(0.35)0.96 (0)1.14
6271.47	(–)1.15?	(0)1.03
6257.57	(–)0.86	(0)0.88
6249.50	(–)1.11	(0.22)1.14
6247.28	(–)1.09:	(0)1.02
6246.38	(–)1.36:	(0)1.49
6232.44	(–)1.20	(0)1.21
6230.96	(0.71)*0.44*, 1.83	(0.74)*0.44*, 1.92
6223.35	(?)1.01:	(0.76)1.22
6211.19	(–)1.42	(0)1.37
6193.54	(–)1.02:	(0)1.01
6189.00	(0.54)1.48	(0.63)1.50
6181.00	(?)1.21:	(0.41)1.34
6122.64	(–)1.24	(0.09)1.22
6116.99	(1.33)1.35	(1.33)1.33
6107.93	(?)1.06	(0.57)1.06
6100.77	(–)1.24?:	(0)0.89
6093.14	(0.81)1.43	(0.76)1.45
6086.66	(–)1.21	(0.07)1.22
6082.43	(–)1.34	(0.07)1.34
6070.67	(–)0.79	(0.01)0.80
6049.11	(–)1.12	(0)0.87
6007.69	(0.46)1.08	(0.37)1.04
6006.35	(–)1.18	(0.03)1.12
6000.66	(–)1.05	(0.04)1.02
5991.89	(–)1.23	(0.18)1.24
5984.25	(–)1.18	(0)1.12 (0)2.15
5984.09		(0.03)0.43
5946.48	(–)0.41	(0)1.30
5935.39	(–)1.32:	(0.15)0.92
5915.55	(–)0.93	(0.19)1.14
5890.48	(–)1.17	(0)1.37
5877.42	(–)1.29	(0)1.08?
5876.10	(–)0.80	(0)1.53
5846.57	(–)1.65	(0.30)1.19
5830.07	(–)1.20	(0)1.92*s*
5826.29	(–)2.09?:	(0.56)1.02
5790.08	(0.59:)?	(0.56)1.02
5774.37	(?)0.99:	(0)0.71
5770.44	(–)0.71	(0)1.11
5750.95	(–)1.12:	(0)1.11
5706.16	(–)1.20:	(1.18)0.76?
5703.03	(?)0.76?:	(0)1.67*s*
5659.12	(–)1.66:	(0)0.80*s*
5651.73	(–)0.82:	(0)0.90
5647.23	(–)1.10	(0)1.08
5637.73	(–)1.12	(0)1.16
5636.12	(–)1.08	(0)1.06
5616.07	(–)1.05	(0)1.08
5598.47	(–)0.55	(0)0.60
5590.74	(0.45)0.98	(0.38)0.96
5558.82	(–)0.85	(0.04)0.84
5546.96	(–)1.50?:	(0)1.42
5545.93	(–)1.12	(0.38)1.10
5524.99	(–)1.25	(0)1.30
5523.31	(–)0.86	(0)0.87*s*
5515.99	(?)1.08:	(0.28)1.02
5489.66	(–)1.18	(0)1.09
5488.12	(–)1.58*s*?	(0)1.57*s*
5483.96	(–)1.19	(0)1.16
5483.35	(–)1.10	(0)1.12
5477.08	(–)1.08	(0)1.07*s*
5470.46	(–)0.92	(0)0.94
5469.30	(0.72)1.59:	(0.66)1.35
5454.57	(–)1.33	(0.07)1.33
5452.30	(–)0.57	(0)0.54*s*
5444.58	(–)1.04	(0)0.96
5437.00	(–)0.82	(0)0.84
5434.57	(0.84:)1.12:	(0.79)0.90
5431.02	(–)0.67?:	(0)0.48*s*
5413.73	(0.78)1.13	(0.77)1.14
5408.11	(0.68:)?	(0.73)1.07
5407.52	(?)1.43	(*0.20*, 0.61, 1.02) 0.11 . . . *2.15*
5402.00	(0.41)0.68:	(0.41)0.62
5399.76	(–)0.94	(0.07)0.94
5393.72	(–)1.83:	(0)1.52
5390.47	(–)1.35	(0)1.40
5381.77	(–)1.11	(0)1.14*s*
5381.10	(0.68?:)?	(0.91)1.14
5369.59	(–)0.87*i*	(0)0.89*s*
5368.90	(–)0.93	(0)0.91*s*
5366.74	(?)1.01:	(0.15)1.14
5364.81	(1.35:)	(1.15)0.77
5362.78	(–)1.15	(0)1.04*s*
5359.20	(–)0.56	(0)0.61
5358.01	(?)0.88	(0)0.84
5353.50	(–)1.06	(0)1.06 (0)0.92
5352.04	(–)1.14	(0)1.14
5349.09	(–)1.16	(0)1.05
5347.49	(?)1.06:	(0.09)1.14
5343.38	(–)1.18:	(0)1.04
5342.70	(–)1.01	(0)1.02
5341.32	(–)1.16	(0.15)1.14
5339.52	(–)0.86	(0.09)0.94
5336.16	(–)1.16?:	(0)1.18
5334.82	(–)1.37?:	(0)1.15 (0)1.39*s*
5333.64	(0.87:)?	(0.67)1.20
5331.45	(0.74)?	(0.73)*0.47*, 1.93
5325.94	(–)1.03:	(0)0.91
5325.27	(–)1.22	(0.31)1.24
5321.71	(?)0.70	(0.44)0.82
5316.77	(–)1.15	(0.15)1.15
5312.65	(–)0.97	(0)0.90
5310.21	(?)0.76	(0.46)0.84
5301.04	(0.60)1.45	(0.55)1.52
5292.20	(–)1.19:	(0)1.38
5287.78	(–)1.30	(0.46)1.28
5283.48	(?)1.01	(0.24)1.07
5280.63	(–)1.07	(0)1.05
5276.18	(–)0.86	(0)0.84
5268.49	(–)0.80	(0)0.74
5266.50	(–)1.09	(0)1.09
5266.30	(–)0.88	(0)0.94*s*
5257.62	(–)1.18	(0)1.18
5254.65	(–)1.47	(0.12)1.43
5250.00	(–)1.35?	(0)1.45*s*
5247.92	(1.38)1.32	(1.33)1.33
5237.08	(–)1.35	(0)1.38*s*
5235.18	(–)0.92	(0)0.82
5230.21	(0.78)1.45	(0.73)1.46
5222.49	(–)1.06	(0)1.10*s*
5219.00	(?)1.80?:	(0)1.97*s*
5212.69	(–)1.33	(0.07)1.34
5210.83	(?)0.83	(0.78)0.78
5210.04	(–)1.16	(0)1.10
5183.53	(–)1.15	(0)1.20
5176.08	(–)1.22	(0.20)1.24
5166.06	(–)1.22:	(0)1.22*s*
5156.36	(–)1.11	(0)1.14*s*
5154.07	(–)1.00	(0)1.04
5146.75	(–)1.28	(0.09)1.26
5133.46	(–)1.20	(0)1.22*s*
5126.20	(–)1.07	(0.02)1.04
5124.71	(?)1.26	(0)1.36
5122.76	(–)0.37	(0.08)0.39
5108.90	(–)1.17	(0.07)1.12
5094.95	(–)1.30	(0)1.26
5087.85	(?)1.74:	(0)1.04
4993.00	(?)1.06:	(0.22)1.29
4986.44	(?)1.48:	(0.85)1.44
4979.94	(–)0.97	(0)0.97
4928.29	(?)1.00:	(0.52)1.36 (0)1.02
4924.99	(–)0.86	(0)1.62
4918.26	(?)0.47	(0.07)1.26
4915.96	(?)0.86:	(0)0.87
4914.71	(?)0.81:	
4907.58	(?)0.84:	(0)0.84
4904.17	(–)0.89:	(0.56)0.99
4899.52	(0.46)0.85:	(0.39)0.95
4886.99	(–)1.06	(0.04)1.12
4882.70	(0.77)1.13:	(0.74)1.28
4881.31	(?)0.93	
4867.87	(–)1.19*A*?	(0)1.18
4855.59	(?)0.59	(0)1.50
4849.31	(?)0.97:	(0.90)1.16
4843.45	(1.13)1.10	(0.96)1.10
4840.25	(–)1.12*A*?	(0)1.14
4815.90	(?)0.93	(0.48)0.96
4813.96	(1.71)0.56	(1.54)0.54
4813.47	(–)1.06*A*?	(0)1.10 (0)1.56
4795.85	(0.86:)1.00:	(0.74)1.06
4792.85	(–)0.93*A*?	(0)0.94
4785.07	(0.71)?	(0.74)1.06
4781.43	(0.81)1.36:	(0.78*s*)1.35
4779.97	(–)0.71	(0)0.72
4778.23	(–)0.93	(0.22)0.93
4776.31	(0.36)0.36	(0.36)0.36
4771.10	(–)1.24	(0)1.20
4768.07	(–)0.98	(0)1.08
4767.14	(–)0.82	(0)0.82
4756.72	(–)1.50?:	(0)1.42
4754.35	(–)0.50	(0)0.48*s*
4749.68	(–)1.33	(0)1.28
4737.76	(1.14)1.10	(0.93)1.14
4734.82	(1.15)1.18	(1.14)*0.05*, 2.22
4727.93	(0.76)?	(0.85)1.46
4718.47	(–)1.18	(0)1.06
4698.38	(2.05)1.32	(2.04)1.33
4693.19	(–?, *1.17*) 0.68, *1.49*, 2.16?	(0.40, *1.19*) 0.69, *1.48*, 2.28
4682.36	(0.75)1.49C?	(0.74)1.49
4663.40	(0.48)1.49	(0.47)1.48
4657.39	(1.37:)0.50:, *3.11*:	(1.30)0.58, *3.18*
4654.83	(?)0.95:	(0.22)0.93
4644.31	(–)0.86:	(0)0.82
4629.35	(0.35)1.54	(0.52)1.50
4625.76	(0.41)1.15	(0.37)1.26
4596.90	(–)1.27	(0)1.23
4594.63	(–)1.44	(0.06)1.44
4581.59	(–)1.44	(0)1.46 – –
4580.13	(–)1.26	(0)1.24
4570.02	(–)1.24	(0)1.18
4566.61	(0.75:)0.76:	(0.74)0.78
4565.57	(–)1.45	(0)1.48
4564.15	(–)0.92	(0)0.95
4552.44	(0.51?)?	(0.38)0.38, 1.14
4549.65	(–)1.46	(0)1.49 (0)0.60
4545.98	(–)1.35	(0)1.32
4545.23	(–)0.80:	(0)0.80?
4543.81	(–)1.24	(0.02)1.24
4540.78	(–?)1.00:	(0)0.86
4533.98	(–)1.50	(0)1.48
4530.94	(–)1.56	(0.09)1.47
4527.91	(–)1.62:	(0)1.87
4517.09	(0.87)–?, *1.95*	(0.84)0.24, *1.93*
4500.56	(–)0.96:	(0)0.86
4494.74	(–)1.01	(0)0.98
4483.91	(–)0.68	(0.05)0.66
4478.31	(–)1.09	(0.01)1.10
4471.80	(–)1.06	(0)1.14
4471.55	(–)1.33	(0.02)1.32
4469.54	(–)1.46	(0.22)1.46
4466.88	(–)1.42	(0)1.40
4431.60	(–)0.96	(0.18)0.90
4421.33	(–)1.56	(0)1.53
4417.39	(–)1.51	(0)1.51
4404.93	(0.25?)	(0.22)0.90, 1.35
4402.67	(–)1.23	(0)1.18
4395.87	(–)0.83?	(0)0.99*s*
4391.89	(–)1.22	(0.18)1.22
4391.56	(–)1.52	(0)1.50
4387.91	(–)1.20:	(0)1.32
4380.07	(–)1.34	(0.04)1.34
4379.26	(?)0.50	(0)0.58
4375.54	(–)1.13	(0.04)1.12
4374.91	(–)1.65	(0)1.64
4373.63	(–)0.99	(0)0.90
4371.13	(–)1.58	(0)1.57
4339.62	(0.24)1.23	(0.14)1.24
4331.23	(–)1.12	(0)1.13*s*
4310.09	(1.05:)1.80:	(0.91)1.60
4303.23	(–?, *1.10*)?	(0.34, *1.02*) 0.08, *0.76*, 1.44
4292.25	(–)0.96	(0)0.96

TABLE V.—*Continued.*

λ	Zeeman Effect Observed	Zeeman Effect Calculated
4287.38	(–)1.16	(0.38)1.18
4285.78	(0.77)1.15:	(0.70*s*)1.19
4276.10	(–)0.95	(0)0.98*s*
4268.03	(–)0.60	(0)0.68
4252.30	(0.62)1.34	(0.38)1.33
4248.18	(0.81)?	(0.76)1.06
4207.61	(?)1.14	(0.13)1.10
4190.71	(0.53)1.47	(0.63)1.40
4187.24	(–)1.55	{(0)1.54 / (0.38)1.34}
4179.22	(–)0.94	(0)0.92
4170.88	(–)1.09	(0)1.08*s*
4162.16	(–)1.24	(0)1.29
4158.42	(–)0.84	(0)0.86
4150.42	(–)1.42	(0)1.49
4139.45	(–, *1.41*)1.56:	(0.47, *1.41*) 0.62, *1.56*, 2.50
4122.27	(–)1.08	(0)1.02
4121.31	(–)1.08	(0)1.02
4118.77	(–)0.95	(0)0.97
4110.53	(–)0.88	(0.04)0.87
4104.74	(–)0.75?	(0.01)0.70
4104.41	(0.23)1.19	(0.21)1.16
4092.84	(0.33)?	(0.32)*0.89*, 2.36
4092.38	(–)1.18	(0.06)1.17
4086.30	(–)1.31	(0)1.30
4082.59	(–)0.44	(0.03)0.41
4081.44	(–)1.11?	(0)0.99
4077.40	(0.40:)1.30	(0.33)1.30
4068.54	(–)1.29	(0)1.26
4066.36	{(0.90*o*) / (0.79*g*)}1.26*C*	{(0.87*s*) / (0.74*g*)}1.28
4058.60	(0.72)*0.53*, 1.88:	(0.72)*0.52*, 1 96
4058.18	(–)1.24	(0.03)1.24
4057.19	(*0.25*, 0.74)1.45:	(*0.23*, 0.69)0.19, 0.65, 1.11, *1.57*
4056.97	(–)1.37	(0)1.39
4053.91	(0.38)0.47	(0.28)0.42
4052.91	(–)1.29	(0.22)1.30
4045.38	(–)$^{1.47o}_{1.34g}$ *B*?	{(0)1.45*s* / (0)1.24*g*}
4035.54	(–)1.10?	(0)1.08
4027.03	(–)1.33	(0)1.28
4023.39	(0.83)	(0.79)1.75
4020.89	(–)1.33	(0.04)1.34
4013.94	(1.34)1.33	(1.36)1.32
4010.93	(?)0.87?	(0.44)1.32
4003.59	(0.29)0.91, *1.49*	(0.25)0.93, *1.43*
3997.90	(–)1.87*o*, *B*	(0)1.91*s*
3995.30	(–)1.20	(0)1.18
3991.68	(–)0.96	(0)0.97
3991.52	(–)1.17	(0)1.16
3990.29	(0.35)1.35	(0.32)1.36
3987.11	(–)1.54	(0)1.52
3979.51	(–)1.38	(0)1.36*s*
3978.86	(–)1.26?	(0)1.26
3978.65	(–)1.05	(0)1.08
3977.75	(–)0.95?	(0)0.99
3977.18	(0.23)1.35	(0.22)0.90, *1.35*
3974.72	(0.64*o*)1.32*C*?	(0.64*s*)1.34
3972.50	(–)1.25	{(0)1.25 / – –}
3969.11	(–)1.15	(0)1.12
3960.99	(–)0.91	(0)0.89
3957.92	(0.54, *0.86*) –, –, 1.20, –, –	(0.16, 0.47, *0.78*) 0.57, 0.88, *1.20*, 1.51, 1.82
3952.91	{(0.90*o*) / (0.74*g*)}1.05	{(0.87*s*) / (0.74*g*)}1.04
3947.12	(0.74)0.87?, 2.25?	(0.75)0.72, *2.22*
3946.63	(–)1.25	(0)1.24
3945.32	(*0.13*, –, –)1.81*o*, *B*	(*0.14*, 0.42, 0.70) 0.46 . . . *1.86*
3942.68	(–)1.26	(0)1.28
3941.72	(–)1.14	(0)1.11
3940.88	(0.41?, *1.21*) 0.00, *0.80*, 1.67	(0.39, *1.17*) 0.01, *0.79*, 1.57
3938.85	(–)1.26	(0)1.27
3935.96	(–)1.89*o*, *B*	(0)1.88*s*
3935.28	(0.57)?	(0.55)1.48
3929.25	(–)1.31	(0.30)1.31
3925.15	(0.34)–?, *1.70*	(0.32)1.00, *1.65*
3922.75	(–)0.89	(0.20)0.90
3917.11	(0.26)1.20	(0.28)1.23
3909.93	(–)1.40	(0)1.38
3906.28	(0.86*o*)1.37*C*	(0.12, 0.36, *0.60*) 0.65, 0.89, *1.15*, 1.37, 1.61
3898.48	(–)1.69?	(0)1.70
3894.97	(0.20)0.24, *0.66*	(0.20)0.20, *0.60*
3894.07	(–)1.02	(0)1.06
3892.11	(–)1.23	(0.15)1.24
3885.27	(0.34)1.13	(0.38)1.10
3884.60	(*0.22*, 0.67)1.51?	(*0.21*, 0.60) 0.28 . . . *1.45*
3881.86	(–)$^{0.94g}_{0.75i}$ *A*	(0)$^{0.94g}_{0.83s}$
3878.75	(–)2.53	(0.08)2.60
3876.83	(0.49)*1.22*, 2.38:?	{(0.55)1.26 / (0.48)*1.25*, 2.20}
3873.95	(–)1.14	(0)1.12
3873.12	(–)1.24	(0)1.18
3861.16	(–)0.80	(0)0.89
3851.84	(0.63)1.16	(0.62)1.07
3850.09	(?, 1.74)1.84?	
3845.46	(–)1.23	(0)1.16
3843.69	(–)0.49?	(0)0.56
3842.04	(–)1.08	(0)1.06*s*
3841.45	(–)1.14	(0)1.16
3835.90	(–)1.27	(0.06)1.27
3823.52	(?)1.19*o*, *B*?	
3819.90	(–)1.21	(0)1.15
3817.94	(–)1.30	(0.06)1.31
3816.87	(–)1.02?	(0)0.75
3816.45	(–)1.65?	(0)1.75
3816.31	(0.51)*1.00*, –?	(0.52)*0.95*, 2.00
3814.45	(0.34)1.65	(0.36)1.60
3813.92	(–)1.09?	(0.03)1.24
3812.47	(0.34)1.58?	(0.31)*1.72*, 2.35
3808.10	(*0.18*, –, –, –)?	(0.16*s*)1.92
3805.77	(0.54)?	(0.44*s*)1.48
3797.44	(0.92)0.76	(0.91)0.77
3795.85	(0.42?)1.61?	(0.44)1.29
3783.73	(?)0.43?	(0.98)1.06
3777.54	(0.46)1.27	(0.28*s*)1.23
3774.59	(–)1.34	(0)1.37
3760.40	(0.42)1.98:	(0.44)1.88
3755.44	(–)1.40	(0)1.39
3754.34	(*0.22*, 0.71)?	(*0.23*, 0.69) *0.14* . . . 1.52
3752.78	(–)0.55	(0)0.60
3751.62	(0.39)1.17	(0.57)1.15
3749.93	(0.18)1.31*o*	(0.19)0.90, *1.28*
3745.49	{(0.82*o*) / (0.66*g*)}1.01*C*	{(0.73*s*) / (0.62*g*)}1.06
3740.18	(*0.23*, 0.66)	(*0.13*, 0.39) *0.44* . . . 1.22
3735.92	(–)1.44	(0)1.42*s*
3734.13	(–)1.12	(0)1.23
3733.48	(–)1.16	(0)1.14*s*
3732.39	(–)1.53*B*	(0.28)1.56
3731.26	(–)1.10	(0.10)1.12
3730.47	(–)1.36	(0)1.33
3728.84	(0.50)1.21	(0.51)1.19
3726.65	(*0.24*, 0.63)	(*0.20*, 0.59) *1.06* . . . 2.23
3712.17	(–)$^{0.73g}_{0.36i}$	(0)$^{0.72g}_{0.34s}$
3711.64	(0.99)1.67	(0.98)1.69
3708.82	(–)1.12	(*0.04*, 0.11) *0.92* . . . 1.13
3707.46	(0.45)0.62, *1.54*	(0.47)0.61, *1.56*
3704.06	(–)1.82*o*, *B*	(0)1.77*s*
3702.23	(–)0.93*B*?	(0)0.98
3693.47	(–)1.09	(0.14)1.14
3693.10	(–)1.10	(0)1.10
3690.71	(–)$^{0.84g}_{0.70i}$ *A*	(0)$^{0.88g}_{0.66s}$
3686.47	(0.39)–?, 1.78	(0.36)1.04, *1.75*
3684.96	(0.50)1.26:, *2.07*:	(0.50)1.18, *2.17*
3684.47	(–)1.41	(0)1.39
3683.04	(–)1.25	(0.11)1.26
3676.55	(–)1.04	(0)1.04
3670.04	(1.25)1.40	(1.27)1.41
3662.15	(–)1.13	(0)1.08
3660.69	(0.58:)?	(0.66)1.49
3657.91	(0.17)1.22*o*	(0.18)0.87, *1.24*
3656.96	(*0.19*, 0.53, –) –?, 2.20:	(*0.18*, 0.55, 0.92) 0.49 . . . *2.34*
3654.44	(0.37)1.10, *1.90*	(0.38)1.09, *1.85*
3652.54	(–)1.73*o*, *B*	(0)1.72*s*
3651.25	(–)0.93	(0)0.88
3649.32	(–)1.02	(0)1.04
3648.14	(–)0.83	(0.15)0.84
3647.65	(*0.31*, 0.91) –?, 0.73, 1.37, *1.96*	(*0.30*, 0.91)0.11, 0.72, 1.33, *1.94*
3647.08	(0.26)–, 0.94, *1.50*	(0.25)0.93, *1.42*
3643.18	(–)1.10	(0.06)1.11
3641.78	(–)1.30	(0)1.34
3639.44	(*0.22*, 0.55) *0.51*, 0.81, –	(*0.15*, 0.45)*0.72* 1.02, 1.32, 1.62
3638.34	(–)0.98	(0)0.91*s*
3637.31	(0.40)?	(0.40)1.09, *1.83*
3636.71	(0.42)1.34	(0.44)1.32
3634.71	(–)0.86	(0)0.82
3633.34	(0.57)1.18?	(0.18, *0.53*) 1.16, *1.51*, 1.86
3632.83	(–)1.14	(0)1.01
3631.94	(0.20)1.10	(0.21)*1.08*, 1.49
3631.39	(–)1.50	(0)1.49
3627.80	(–)0.91	(0)0.86
3624.33	(0.47)1.31?	(0.47)*1.26*, 2.19
3620.42	(–)1.85*o*, *B*?	(0)1.86*s*
3619.28	(–)1.18	(0.41)1.09
3615.38	(–)0.55*i*, *A*	(0)$^{0.35s}_{0.68g}$
3611.70	(–)0.92	(0)0.93*s*
3609.75	(–)1.21	(0)1.17
3605.37	(0.18)1.20	(0.21)1.22
3605.01	(–)0.80	(0)0.84
3604.46	(–)0.95	(0.11)0.92
3602.07	(–)0.40	(0)0.42
3600.80	(0.53)1.41?	(0.14, *0.42*) 1.05, *1.33*, 1.61
3596.51	(–)1.25	(0.21)1.26
3594.87	(–)1.01	{(0.04)1.04 / (0)1.00}
3591.74	(0.19)1.35	(0.14)1.34
3587.18	(?)0.95	(0.22)0.91
3586.08	(–)0.94	(0)0.90
3585.80	(*0.19*, –)0.74	(*0.17*, 0.51)0.77, 1.11, 1.45, 1.79
3585.15	(0.46)1.34*C*	(0.47)1.33
3581.87	(0.33)0.92?, 1.67?	(0.32)1.01, *1.85*
3579.02	(–)1.52	(0)1.50*s*
3578.90	(–)1.24	(0)1.32*s*
3569.37	(–)1.23	(0.12)1.14
3564.94	(–)0.77	(0)0.75
3564.11	(–)0.86	(0)0.89
3562.09	(0.66)0.61, 1.05, 1.52	(0.24, *0.72*) 0.61, *1.09*, 1.57
3560.89	(0.40, *1.21*) 0.00, *0.78*, 1.59	(0.40, *1.20*) 0.00, *0.80*, 1.60
3558.77	(0.34)1.02	{(0.35)0.96 / (0.45)1.39}
3552.98	(0.51)1.34?	(0.48)1.30
3552.72	(0.47)	(0.46*s*)2.05
3550.59	(*0.34*, 0.93) 0.73, 1.32, *1.97*	(*0.31*, 0.94)0.10, 0.73, 1.36, *1.99*
3548.43	(–)1.60	(0.02)1.64
3546.70	(–)1.51	(0)1.50*s*
3543.25	(–)$^{1.05g}_{0.87i}$ *A*	(0)$^{1.12g}_{0.90s}$
3534.76	(–)1.20	{(0)1.12 / (0.24)1.19}
3533.35	(–)0.70	(0)0.70
3530.55	(–)0.75?	(0.03)0.66
3529.81	(–)1.04	(0)1.03
3529.03	(–)0.98	(0)0.96
3527.94	(–)1.31	(0)1.24
3526.84	(–)1.35	(0.11)1.34
3525.87	(0.23)?	(*0.15*, 0.46) 1.03 . . . *1.96*
3522.85	(–)0.97	(0)0.93
3521.56	(–)1.58*B*	(0)1.62
3520.07	(0)1.55	(0)1.57
3518.34	(–)0.94	(0)0.94*s*
3513.47	(–)1.11	(0)1.05
3512.64	(–)1.02	(0)0.92
3510.42	(0.53)?	(0.47)1.35
3506.31	(–)1.20	(0)1.08
3504.72	(0.32)1.15	(0.49)1.12
3503.71	(–)0.95?	(0.09)0.92
3495.68	(–)0.84*B*	(0)0.96
3491.31	(0.49?, *1.23*) 0.00, *0.78*, 1.58	(0.38, *1.14*) 0.04, *0.80*, 1.58
3490.73	(*0.20*, 0.56, 0.92) 2.17*o*, *B*?	(*0.18*, 0.55, 0.92) 2.17*s*
3489.39	(–)1.15	(0)1.12
3487.71	(–)0.42*i*, *A*	(0)0.45*i*
3485.70	(0.34)1.19?	(0.32)*1.15*, 1.78
3485.36	(–)1.16	(0)1.14
3483.41	(–)1.45*B*	(0)1.44
3480.01	(*0.19*, 0.62)	(*0.19*, 0.56) 0.95 . . . *2.06*
3478.74	(0.66)?	(0.59)1.36
3478.55	(*0.23*, 0.62) 0.00, *0.43*, 0.84	(*0.25*, 0.75)*0.08*, 0.58, 1.08, 1.58
3477.83	(–)1.25	(0.22)1.26
3476.36	(0.25:)1.18	(0.24)1.19

TABLE V.—*Continued.*

λ	Zeeman Effect Observed	Calculated
3474.53	(0.38)1.13?	(0.35)1.12
3474.01	(-)1.40	(0)1.46 (0)1.31
3471.38	(-)1.32	(0.09)1.33
3469.68	(-)1.08	(0)1.04$_s$
3465.79	(-)1.17	(0)1.16
3463.49	(-)1.08	(0.75)*0.41*, 1.91
3462.80	(*0.26*, 0.80) 0.69, 1.24, *1.80*	(*0.27*, 0.82)0.13, 0.68, 1.23, *1.78*
3461.17	(-)1.14	(0)1.15
3458.02	(-)1.20$_o$, *B*?	(0.20)1.24
3456.92	(0.83$_o$)?*C*	(0.91$_s$)1.14
3456.52	(-)1.06	(0.04)1.08
3455.23	(-)0.66$_o$, *B*	(0)0.63$_s$
3453.51	(-)1.19	(0)1.15
3448.35	(-)1.20	(0.03)1.14
3446.08	(-)1.05	(0)1.06
3443.64	(0.64)1.15	(0.65)1.14
3442.91	(-)0.95	(0)0.95 (1.33)1.33
3438.90	(-)1.01	(0)1.02
3438.71	(-)1.10	(0)1.14
3435.75	(0.38)1.50	(0.48)1.50
3433.04	(-)0.46	(0.10)0.44
3432.31	(-)0.89?	(0)0.98
3431.58	(-)1.14	(0)1.17
3428.22	(-)1.12	(0)1.15 (1.11)1.42
3426.45	(-)1.42	(0)1.42
3424.50	(-)1.58	(0)1.60
3422.90	(*0.28*?, 0.95?)0.63?:	(*0.28*, 0.83)*0.34*, 0.89, 1.44, 1.99
3421.62	(?)1.30?	(0)1.34$_s$
3420.79	(0.56)1.45	(0.57)1.41
3420.47	(0.78)?	(0.79)1.44
3417.67	(0.50)1.21	(0.50)1.20
3417.15	(0.32:)0.98	(0.20)1.00
3414.73	(*0.60*)	(0.63$_s$)0.61$_s$
3409.17	(0.28)1.26	(0.26)1.20
3406.89	(0.28)1.09	(0.36)2.01
3405.12	(-)1.37	(0.07)1.33
3402.06	(0.72)0.96	(0.26)0.94
3401.91	(0.31?, 0.89?)0.22?	(*0.32*, 0.95) *0.50*...2.19
3401.61	(0.34:)0.17?	(0.35$_s$)0.03$_s$
3400.47	(0.80:)	(0.79)0.93, *2.51*
3395.37	(-)0.83	(0)0.84
3390.79	(-)0.46	(0)0.48
3390.39	(0.69)0.39	(0.70)*0.39*, 1.78
3388.16	(0.32, 0.83)0.76 1.34, 1.93*	(*0.29*, 0.86)0.19 0.76, 1.33, *1.90*
3385.21	(*0.26*, 0.78, 1.30) 0.43, 0.95, 1.49, 2.02, *2.58*	(*0.26*, 0.79, 1.32) -0.07, 0.46, 0.99, 1.52, 2.05, *2.58*
3383.90	(1.06)1.45	(1.07)1.42
3382.07	(0.37)1.01, *1.77*	(0.35)1.04, *1.74*
3381.49	(-)1.11	(0.04)1.12
3378.73	(-)0.89	(0)0.97$_s$
3378.35	(-)0.39	(0)0.30
3377.06	$(-)^{0.94g}_{0.71i}$ *A*?	$(0)^{0.94g}_{0.56s}$
3376.20	(-)1.35	(0)1.32
3374.30	(0.65)1.35	(0.86)1.42
3373.96	(1.26)?	(1.35)1.33
3373.22	(0.20)1.08	(0.19)*1.14*, 1.51
3370.32	(-)1.23	(0)1.22
3367.11	(*0.12*,-,-,-)2.37$_o$, *B*	(0.15$_i$)2.42$_s$
3365.01	(0.61)*0.94*?, 2.25?	(0.50)*1.18*, 2.18 (0.32)1.00, *1.64*
3364.25	(0.13)1.15	(0.13)1.14
3363.76	(0.61)0.65:	(0.97)1.40
3362.79	(0.44)1.39	(0.78)1.46
3361.55	(-)0.58*A*	(0)0.26
3359.28	(-)1.17	(0)0.74
3358.00	$(-)^{1.73?}_{1.18?}$	(0)1.36 (0)1.14
3356.84	(-)1.11	(0)1.10
3356.46	(-)1.26	(0)1.30
3355.11	(-)0.58	(0.16)0.52
3354.37	(-)2.18$_o$, *B*	(0)2.00$_s$
3351.53	(-)1.36	(0.07)1.34
3348.11	(-)1.57	(0)1.56
3347.57	(-)0.66	(0)0.66
3346.93	(-)1.42	(0.19)1.46
3342.73	(-)1.26	(0)1.24
3341.94	$(-)^{0.92g}_{0.78i}$ *A*	$(0)^{0.98g}_{0.77s}$
3341.34	(-)1.04	(0)1.02
3339.78	(0.41)0.94	(*0.16*, 0.48...1.12) *0.87*...2.61
3338.51	(-)1.31	(0.08)1.36
3337.17	$(0.66)^{1.30g}_{0.74i}$ *A*?	$(0.67)^{1.25g}_{0.53s}$
3334.14	$(-)^{2.09o}_{1.72g}$ *B*	$(0)^{1.97s}_{1.66g}$ (0.34)0.97
3333.38	(1.06)	(1.05)1.10 (0)0.80
3329.46	(-)1.44	(0.24)1.44
3329.01	(-)-?, 1.28, -?	(0)1.29
3328.20	(0.44)1.31	(0.51)1.28
3326.99	(-)1.45	(0.09)1.45
3326.56	(-)1.04?	(0)0.65
3325.24	(0.60)*0.90*, 2.04?	(0.60)*0.88*, 2.08
3322.19	(-)1.10	(0.22)1.17 (0.30)1.07
3321.91	(-)1.34	(0)1.35$_s$
3319.82	(-)1.52	(0)1.50
3319.47	(-)1.04	(0)1.05
3319.15	(-)1.06	(0)1.06
3318.39	(0.91)0.82, 1.71?	(0.21, 0.62, *1.03*) 0.62, 1.03, *1.44*, 1.85, 2.26
3315.03	(0.66)1.36	(0.42$_s$)1.19 – – (0)0.37
3314.07	(-)0.88	(0.03)0.86 (1.37)0.77, *3.51* – –
3313.11	(1.47)0.77	(0)1.88
3312.82	(0.46)1.46	(0.51)*0.96*, 1.97
3312.14	(0.51)*0.95*, 2.00?	(0.31)1.40
3308.81	(-)1.40	(0)1.25
3308.48	(-)1.24	(0)1.60
3307.15	(-)1.60	(0)1.50$_s$
3306.40	(-)1.55	(0)1.22
3305.73	(-)1.20	
3305.10	(0.49:)0.39 or 1.12	(0)1.00
3304.79	(?)1.31?	(0)0.98$_s$
3304.11	(-)0.61?	(0.52)*1.10*, 2.14
3303.88	(0.50)*1.15*, 2.07?	(1.26)1.42
3298.68	(1.26)1.40	(0.84)0.23, *1.91*
3294.53	(0.80)1.87	
3294.09	(?)1.36?	(0.98)1.06
3293.86	(0.92:)0.44?	$(0)^{0.93g}_{0.63s}$
3293.21	$(-)^{1.01g}_{0.64i}$ *A*?	(0.72)*0.53*, 1.96
3292.08	(0.73)0.55	(0)1.36
3287.57	(-)1.37	(0.41)1.32
3287.19	(0.39)1.32	(0)1.42
3283.77	(-)1.46	(0)1.17$_s$
3283.46	(-)1.13	(0)1.28
3283.32	(-)1.26	(0.01)1.48
3279.25	(-)1.47	(0.67)*0.65*, 2.00
3278.84	(0.67)0.68	(0.48)1.42
3277.66	(0.19)1.43	(0.68)1.34
3277.30	(0.65)1.33	$(0)^{0.94g}_{0.56s}$
3276.48	$(-)^{0.95g}_{0.72i}$ *A*	(0)1.28
3271.77	(-)1.26	(0.38)1.34
3270.19	(-)1.30	(0)0.50$_s$
3268.89	(?)0.60:	(0)1.28
3265.35	(-)1.29	(0.18)0.91, *1.27* (0)1.86 (0)1.31
3264.84	(0.22)0.87?, *1.29*	(0.14)1.67
3264.71	(-)1.62	(0.55)1.14
3263.21	(0.30)1.18	$(0)^{0.64g}_{0.44s}$
3260.81	$(-)^{0.67g}_{0.44i}$ *A*	(0.87)1.16
3258.41	(0.99)1.16?	(0.20)1.60
3258.03	(-)1.57	(0)1.37
3254.20	(-)1.39	(0.66)0.81, *1.12*
3253.41	(?)0.76?	(0)1.68
3251.65	(-)1.68?	(0)1.32$_s$
3249.99	(-)1.29	(0)1.32 (0)0.45
3247.17	(-)1.31	(0.31)1.36
3246.99	(0.28)1.35	(0.09)1.52
3243.84	(-)1.51	(0.36)*1.36*, 2.08
3243.57	(0.33)1.34	$(0)^{0.83g}_{0.55s}$
3237.02	$(-)^{0.86g}_{0.68i}$ *D*	(1.02)1.65
3235.78	(?)1.65	(0)1.08 (0)1.02
3235.53	(-)0.99*A*?	(0.20)1.40
3234.11	(-)1.33?	(0)1.42
3232.87	(-)1.49	(0)1.22
3227.75	(-)1.17	(0.28)0.97
3226.98	(0.35)1.03	(0)1.74
3224.63	(-)1.79	
3219.15	(0.16)1.20	(0.26)1.22
3216.99	(-)1.47	(0)1.52
3210.85	(-)1.15	
3210.21	(-)1.10	(0.04)1.10
3205.88	(-)1.06	(0)1.06
3203.02	(0.53)1.29	(0.41)1.34
3199.32	(0.79)1.25	(0.74)1.22
3198.66	$(-)^{1.65o}_{1.51g}$ *B*	$(0)^{1.80s}_{1.38g}$
3196.42	(?)1.18	(0.17)1.20
3193.16	(0.29)1.20	(0.38)1.18
3192.22	(0.43)-, 1.06, *1.90*	(0.42)1.05, *1.89*
3191.29	(-)0.68	(0)0.74
3190.91	(-)0.63	(0)0.70
3189.75	(1.20)0.00, *0.80*, 1.60	(0.39, *1.17*) 0.03, *0.81*, 1.59
3188.37	(*0.32*, 0.91)*0.00*, 0.53, 1.11, 1.73	(*0.52*, 0.96)-*0.13* 0.51, 1.15, 1.79
3186.35	(0.41)0.97	(0.37)0.96
3185.94	(-)1.74	(0)1.69
3182.11	(0.78)*0.35*, 1.88	(0.78)*0.34*, 1.90
3180.29	(0.54)0.61?, *1.84*, 2.61?	(0.54)0.55, *1.63*
3177.26	(-)0.93	
3174.90	(0.68)1.29	(0.64)1.36
3174.14	(-)1.03	(0)1.22
3173.14	(0.48)1.30	(0.49)*1.19*, 2.17
3169.76	(-)1.05	(0)1.06
3168.06	(-)1.17?	(0)1.20
3161.65	(-)1.17	(0)1.14
3159.66	(0.18)0.57	(0)0.52 (0.17)1.00
3158.77	$(-)^{0.98g}_{0.85i}$ *A*	$(0)^{1.00g}_{0.82s}$
3154.79	(-)1.06	(0)1.05
3154.67	(-)1.07	(0)1.06
3152.70	(1.32)1.33	(1.34)1.34
3152.12	(?)1.82?	(0.88)1.02
3149.31	(-)0.90	(0)0.94
3147.06	(-)1.03	(0)1.00
3145.02	(0.65)?	(0.74)*0.44*, 1.92
3140.71	(0.50)2.15?	(0.49)2.19
3139.94	(-)1.08	(0)1.12 (0.49)1.30
3137.75	(0.64)0.94	(0.59)*0.89*, 2.07
3137.32	$(-)^{1.16o}_{0.99g}$ *B*	$(0)^{1.17s}_{0.94g}$
3129.48	(1.66)?	(1.67$_s$)1.16
3127.25	(-)1.79	(0)1.72
3126.72	(-)1.46	(0)1.53
3121.56	(-)1.42*B*?	(0)1.41
3121.41	(-)1.24	(0)1.16
3118.24	(-)1.38	(0)1.44$_s$
3113.47	(-)1.54	(0)1.58$_s$
3110.82	(?)1.64	(0)1.74$_s$
3109.50	(0.80)*0.95*, 1.48 1.99	(0.27, *0.81*) 0.91, *1.45*, 1.99 (0)1.48
3107.54	(-?)0.71	(0.02)0.71
3107.04	(-)1.13	(0)1.14
3105.92	(?)1.55?	(0)1.61
3103.98	(-?)1.55	(0.22)1.59
3103.73	(0.45)1.38	(0.48)1.39
3102.40	(0.32)1.60	(0.34)1.60
3099.66	(-)1.42	(0)1.41
3098.19	(0.74)0.89	(0.72)0.88
3096.70	(1.07)0.77, *1.45*	(0.33, *0.99*) 0.76, *1.48*, 2.08
3096.40	(0.66)*0.70*, -?	(0.66)*0.66*, 1.99
3095.71	(-)0.86*iA*?	(0)0.82$_s$
3090.25	(0.83)0.24?	(0.82)*0.23*, 1.86
3089.59	(0.60)1.11	(0.71)1.15
3088.67	(-)0.70	(0)0.58 (0)0.98
3087.80	(1.24)1.54	(1.16)1.52
3086.77	(-)0.45	(0.07)0.44
3086.39	$(-)^{2.17o}_{2.05g}$ *B*	$(0)^{2.33s}_{1.98g}$
3082.61	(-)1.14	(0)1.10$_s$
3079.39	(-)1.66	(0.56)1.24 (0)1.76
3073.52	(0.67)1.11, *1.48*, 1.90	(0.24, *0.71*)1.01, *1.48*, 1.95
3072.34	(0.32)0.97	(0.25$_s$)1.00
3071.95	(0.58)-, *0.83*, -	(0.56)0.62
3064.37	(-)1.00	(0)0.97
3062.19	(-)1.29	(0)1.36
3061.82	(0.30)1.21	(0.32)1.22
3060.04	(-)1.20	(0)1.25
3056.66	(?)1.21	(0)1.21

* Zeeman pattern from Rybar, Physik. Zeits. **12**, 889 (1911).

TABLE V.—*Concluded.*

λ	Zeeman Effect Observed	Calculated
3054.72	(–)0.75	(0)0.70*s*
3050.93	(–)1.90*B*?	(0)1.93
3050.49	(0.66)0.88, *1.28* 1.73	(0.21, *0.63*) 0.84, *1.26*, 1.68
3048.88	(*0.30*, 0.87) 0.72, 1.33, *1.95*	(*0.29*, 0.87)0.18, 0.76, 1.34, *1.98*
3048.10	(0.40?)0.94, *2.05*	(0.55)0.91, *2.02*
3044.00	(–)1.32	(0)1.32 – –
3042.48	(*0.30*, 0.82, 1.33) 0.43, 0.95, 1.52, 2.08, *2.60*	(*0.27*, 0.82, 1.37) –0.11, 0.44, 0.99, 1.54, 2.09, *2.64*
3040.81	(?)1.42:	(0.94)1.42
3039.56	(–)1.80	(0)1.87
3038.30	(?)0.71	(0)0.68*s*
3034.43	(–)1.39?	(0)1.39*s*
3031.28	(0.40)1.58	(0.39)1.61
3028.18	(–)1.45	
3026.37	$(-)^{0.72g}_{0.49i}$ *A*	$(0)^{0.80g}_{0.41s}$
3023.59	(–)1.50	(0)1.46
3022.35	(–)0.87	(0)0.88
3017.54	(–)2.02*o*, *B*	(0)2.07*s*
3017.25	(–)0.78:	(0)0.78
3015.68	(–)1.60	(0)1.58
3013.59	(–)2.31*o*, *B*	(0)2.34*s*
3006.52	(–)1.18	(0.74)1.20
3005.97	(–)1.48	
3005.76	(0.45)1.41	(0.35)1.42
3000.54	(0.98)1.18*C*	(0.94)1.11
2999.71	(–)1.98	(0)2.15*s*
2996.94	(?)0.90	(0)0.95
2996.54	(–)2.01	(0)2.18*s*
2995.24	(?)1.05	(0)1.09
2995.15	(–)0.87	(0.24)0.86
2989.59	(0.64)1.24	(0.59)1.24
2987.16	$(-)^{1.94o}_{1.65g}$ *B*	$(0)^{1.88s}_{1.60g}$
2982.26	(–)0.43	(0)0.42
2978.95	(0.80:)1.91	(0.72)1.96
2978.01	(–)1.33	(0)1.32
2977.46	(0.60:)1.40:	(0.84)1.42
2975.46	(0.64)1.15	(0.78)1.46
2971.36	(?)1.05?	
2969.61	(–)1.33	(0)1.32
2957.67	(–)0.95	(0)0.99
2955.38	(0.67)0.78	
2936.54	(–)1.15	(0)1.21 – –
2929.50	(–)1.11	(0.04)1.10
2928.81	(?)2.52	(0)2.62*s*
2927.66	(–)1.23	(0)1.25
2919.55	(–)0.75	(0)0.78
2911.56	(?)1.10:	(0)1.17
2907.67	(?)1.36	(0.50)1.40
2903.19	(0.50)1.04	(0.48)1.04
2899.81	(–)1.22	(0)1.18
2892.24	(–)1.21	
2886.44	(0.26)1.19	(0.44)1.20
2885.30	(?)1.49	(0.66)1.49
2882.21	(0.71)1.05	(0.73)1.07 (0.31)1.12
2878.55	(0.70)*0.69*, 2.03	(0.68)*0.64*, 2.00
2872.49	(–)0.75	(0)0.64
2862.60	(0.22)0.96	(0.20)1.00
2859.65	(–)2.02:	(0)1.87
2850.94	(0.58:)0.67	(0.55)0.62
2850.04	(–)0.64*A*?	(0)0.61
2842.38	(0.35)–, 1.10 *1.85*	(0.36)1.10, *1.83*
2837.15	$(-)^{1.02g}_{0.85i}$ *A*	$(0)^{0.98g}_{0.68s}$
2833.92	(–)1.32	(0)1.37
2828.46	(–)0.85	
2826.79	(–?)1.13	(0)1.12*s*
2823.64	(–)1.22	
2821.74	(?)0.95	(0)0.97*s*
2820.00	(–)0.63	(0)0.66 (0)1.67
2818.59	(?)1.10?	(0)1.23
2815.55	(0.57)1.29	(0.56*s*)1.33
2814.97	(–)1.77:	(0)1.66
2803.77	(0.81)1.15	(0.77*s*)1.20
2797.08	(–)1.60	(0.20)0.90 (0)1.64
2792.43	(–)1.22	(0)1.15
2785.89	(–?)0.43	(0)0.43*s*
2778.81	(–)1.54	(0.02)1.50
2774.96	(–)0.56	(0)0.51
2772.69	(–)1.15	
2766.38	(–)0.87	(0)0.89
2766.21	(–)0.88	(0.12)0.88
2764.18	(–)1.17	(0)1.22
2763.06	(–)0.97	
2761.36	(–)1.06	(0)1.00*s*
2758.53	(?)1.62	(0.29)1.58
2752.07	(–)0.79	(0)0.79 (0)0.86*s*
2746.02	(–)1.16	(0.12)1.18
2745.09	(–)1.24	(0.26)1.22
2740.45	(–)1.05	(0)1.07
2731.11	(0.39)0.95	(0.39)0.95
2728.75	(–)1.00	(0)1.02
2722.10	(–)1.29	(0)1.27*s*
2719.58	(–?)1.37	(0)1.42
2715.98	(–)1.07	(0.30)1.07
2695.84	(–)1.49	(0)1.52
2685.33	(–)1.52	(0)1.49
2679.75	(–)0.91	(0)1.02
2673.91	(?)1.23	(0)1.22
2661.71	(–)1.30	(0)1.24
2650.26	(–)0.42	(0.06)0.42
2649.93	(–)0.64	(0)0.62
2648.63	(–)0.95	(0)1.04 (0.04)1.34
2646.41	(–)1.23	(0.03)1.24
2629.97	(0.77)1.30	(0.74)1.33
2627.63	(–)1.14	(0)1.17*s*
2623.44	(–)1.88	(0)1.94*s*
2622.43	(–)0.91	(0)0.90
2617.85	(1.11)0.87?	(1.07)0.78
2613.49	(–)1.26	
2606.12	(–)0.51	(0)0.53*s*
2600.97	(–)1.63	(0)1.69*s*
2591.68	(–)0.89	(0)0.86*s*
2590.59	(–)1.07	(0)1.05
2585.33	(–)0.78	(0.07)0.84
2574.35	(0.58)1.34	(0.49*s*)1.34
2572.23	(–)1.52	(0)1.49
2567.34	(0.74)1.19	(0.75*s*)1.20
2562.12	(?)0.00, *0.83*, 1.64	(0.41, *1.23*) 0.01, *0.83*, 1.65
2556.76	(–)1.73	(0)1.35
2555.07	$(-)^{1.79o}_{1.57g}$ *B*	$(0)^{1.78s}_{1.36g}$
2553.33	(–)1.43	(0)1.44
2553.00	(–)1.37	(0)1.40
2549.29	(*0.49*, 1.45) *0.50*, 1.40, –?	(*0.49*, 1.47)–*0.42*, 0.56, 1.54, 2.52
2548.33	(–)1.06	(0)1.04*s*
2544.25	(–)1.53?	(0)0.53
2536.50	(–)1.21	(0.03)1.24
2535.96	(–)0.91	(0)0.91
2535.35	(0.50:)1.16	(0.41)1.23
2532.17	(–)0.46	(0.06)0.42
2531.35	(–)0.95	(0)0.92
2528.96	(–)1.12:	(0)1.07*s*
2521.36	(–)1.20	(0)1.16
2513.11	(–)1.21	(0)1.28
2512.90	(–)1.30	(0.26)1.20
2507.67	(–)–?, 2.00	(0)1.94*s*
2506.87	(0.77)?	(0.74)0.87
2504.51	(–)1.24	(0)1.36
2496.71	(–)1.04	(0)1.06
2495.55	(–)1.69	(0)1.62
2494.73	(–)1.51	(0)1.52
2493.93	(–)0.74	(0)0.72
2489.24	(?)0.62	(0)0.62*s*
2483.61	(0.70)1.11	(0.74)1.12
2476.64	(–)1.54	(0)1.58
2476.43	(–)1.43	
2473.90	(–)1.51	(0)1.49
2472.92	(?)2.29	(0)2.62*s*
2467.68	(–)1.51	(0)1.48
2460.80	(–)1.95*o*, *B*	(0)1.97*s*
2460.19	(?)1.64	(0)1.64
2456.23	(0.67)1.25	(0.72*s*)1.26
2441.04	(?)1.03	
2435.09	(–)1.07	
2432.21	(–)*0.96*?, 1.56?	(0.09)1.26
2429.22	(–)0.44*A*	(0)0.37*s*
2428.59	(–)1.39	
2426.99	(–)1.52	
2424.93	(–)1.31	(0.11)1.33
2422.56	(–)1.65	(0.04)1 65
2413.18	(–)0.45	(0)0.46
2410.50	(–)0.80	
2402.16	(–)1.54	(0)1.47 (0)1.56
2402.05		
2384.85	(?)1.48	(0)1.46
2380.48	(0.69)1.12	(0.86)1.12 (0)0.82
2369.67	(–)1.07	(0)1.11
2365.05	(0.54:)1.25	(0.52)1.25
2350.28	(–)1.47	(0)1.51

i Inside component.
o Outside component.
g Center of gravity of pattern.
s Strongest component calculated.
: Doubtful value.

A *n* component shaded outward.
B *n* component shaded inward.
C *p* component shaded inward.
D *p* component shaded outward.

we have given term designations are not given by Catalan and Antunes. Each of the low terms b^2G and c^2D accounts for 42 lines. Most of the higher levels are confirmed by from three to ten combinations; $g^4H_{6\frac{1}{2}}$ and $x^2H_{5\frac{1}{2}}{}^0$ have but two, and $e^6H_{7\frac{1}{2}}$ only one (§5).

Six levels to which they have given designations (in the pentads discussed in §5) are placed in our list of unclassified levels—either because of irregular intensities in the multiplets or because other levels, in a more probable position, were discovered. We have been constrained to reject as unreal five of their high odd levels (four in this pentad) and the low c^2D at 22,247, 23,392, which they regarded as doubtful. Of our 37 unclassified odd levels, all but two are new. More than two-thirds of these depend on the new measures in the ultraviolet.

8. Zeeman Data

The observed separations are given in Table V. The g values given in Table IV were found from

TABLE VI. *The g sums for* Co I.

CONFIG.		d^7s, d^8s, d^9	$d^8(^3F)$, $d^7s(^5F)$, $d^7s(^3F)+4p$	OTHER ODD TERMS	HIGH EVEN TERMS	ALL TERMS
J = ½	N	4	5	13	1	23
	O	6.71	2.73	17.80	−0.71	26.53
	T	6.67	2.67	17.33	−0.67	26.00
1½	N	9	11	19	7	46
	O	9.33	9.55	24.63	7.30	50.81
	T	9.33	9.33	25.07	7.33	51.06
2½	N	8	16	15	15	54
	O	9.81	17.26	17.79	17.39	62.25
	T	9.71	16.85	17.89	17.55	62.02
3½	N	5	16	12	18	51
	O	5.45	19.24	13.55	21.70	59.94
	T	5.40	19.14	13.74	21.27	59.55
4½	N	5	11	8	14	38
	O	5.82	14.18	8.54	17.13	45.67
	T	5.80	14.00	8.56	17.49	45.85
5½	N	1	5	2	9	17
	O	1.09	6.66	2.20	11.38	21.33
	T	1.09	6.62	2.18	11.36	21.34
6½	N		1		4	5
	O		1.40		5.06	6.46
	T		1.39		5.13	6.51
7½	N				1	1
	O				1.34	1.34
	T				1.33	1.33
All	N	32	65	69	69	235
	O	38.21	71.02	84.51	80.59	274.33
	T	38.00	70.00	84.77	80.79	273.56

these in the usual manner, starting with the unresolved patterns, and then using the formulae of Shenstone and Blair[12] in the case of unresolved patterns, when it appeared probable that the mean of a blend had been observed; or sometimes the formulae for the strongest line when this was probably observed. The computed patterns are derived from these empirical g values. For unresolved patterns, the center of gravity of the group is usually given. When the strongest component is entered instead, it is denoted by s. When two assignments are given in Table VIII, both calculated patterns are entered here.

The accuracy of the g values may be estimated by comparison with those of Roth and Bartunek.[13] Grouping the levels according to their J values the mean differences in the sense authors' values minus those of R and B are as follows in units of 0.01.

J	½	1½	2½	3½	4½	5½	6½
No.	7	20	26	21	15	6	1
Alg. mean	−4.3	−1.7	+0.8	+0.4	−0.5	+0.6	(+2)
Arith. mean	±5.7	±3.5	±2.5	±1.5	±1.4	±1.0	(±2)
Comp.	6.8	3.4	2.3	1.7	1.4	1.1	

The accuracy increases steadily with J, which is to be expected, for the displacement of the strongest n component of a resolved pattern is $J_1g_1-J_2g_2$ and that of an unresolved blend is $\frac{1}{2}\{(J+1)g_1-J_2g_2\}$. The observations therefore determine, on the average, the value of $(J+x)g$, where x should be of the order of ½. The values of $6.8/(J+\frac{1}{2})$ are given in the last line and closely represent the observed mean discordances. The average value of J is 2.9, corresponding to a discordance of ±0.02 in the g values. If the two sets of determinations were of equal accuracy, the probable error of either would be ±0.012, confirming Roth and Bartunek's statement: "Most of the g factors are estimated to be reliable to about 0.01."

Most of the g values are in good agreement with those derived from the elementary theory (LS coupling). The g sums for various configurations are given in Table VI. Here for each group of configurations N is the number of levels of given J for which reliable g values were derived (omitting the doubtful values marked with colons in Table IV), O the sum of the observed g values, and T that of those from LS coupling. For the first two sets of configurations g values have been found for all the levels, so that the g sum test is strictly applicable. For the others some levels are missing and the test is not exact. The excess of O above T for the first two sets suggests that the observed values may be about one percent too great; but the others do not confirm this.

TABLE VII. *Conspicuous examples of the sharing of g values.*

TERM	LEVEL	$O-T$	TERM	LEVEL	$O-T$
$b^4P_{1\frac{1}{2}}$	15,774	−0.26	$y^4S^0_{1\frac{1}{2}}$	46,562	−0.75
$a^2D_{1\frac{1}{2}}$	16,470	+0.29	$v^4D^0_{1\frac{1}{2}}$	46,260	+0.28
			$v^2D^0_{1\frac{1}{2}}$	46,186	+0.38
$b^4P_{2\frac{1}{2}}$	15,184	−0.10			
$a^2D_{2\frac{1}{2}}$	16,778	+0.08	$e^2D_{2\frac{1}{2}}$	52,460	−0.28
			$f^2F_{2\frac{1}{2}}$	52,970	+0.27
$x^2F^0_{2\frac{1}{2}}$	43,425	+0.16			
$w^4D^0_{2\frac{1}{2}}$	43,242	−0.20	$g^2F_{3\frac{1}{2}}$	52,763	−0.21
			$e^4H_{3\frac{1}{2}}$	52,716	+0.26

[12] A. G. Shenstone and H. A. Blair, Phil. Mag. **8**, 765 (1929); H. N. Russell, Phys. Rev. **36**, 1590 (1930).
[13] F. L. Roth and P. F. Bartunek, Phys. Rev. **47**, 526 (1935).

TABLE VIII. *Arc spectrum of cobalt* (Co I).

Ref.	λ *IA*	Int.–*TC*	Wave No. Vac.	Multiplet Designation
1	11,894.93	10	8404.65	$c^2D_{1\frac{1}{2}} - y^2D^0_{1\frac{1}{2}}$
1	11,630.93	40	8595.41	$c^2D_{2\frac{1}{2}} - y^2D^0_{2\frac{1}{2}}$
1	11,508.4	6*h*	8686.9	$b^2G_{4\frac{1}{2}} - z^2F^0_{3\frac{1}{2}}$
1	11,402.20	3*h*	8767.84	
1	11,318.27	40	8832.85	$c^2D_{2\frac{1}{2}} - y^2F^0_{3\frac{1}{2}}$
1	11,305.0	2*h*	8843.2	$b^2G_{4\frac{1}{2}} - y^4D^0_{3\frac{1}{2}}$
1	11,158.6	2	8959.2	$b^4P_{1\frac{1}{2}} - z^6F^0_{2\frac{1}{2}}$
1	11,106.34	8	9001.40	$y^2D^0_{1\frac{1}{2}} - e^4F_{2\frac{1}{2}}$
1	11,094.7	3*h*	9010.8	
1	11,091.94	50	9013.09	$y^2D^0_{2\frac{1}{2}} - e^4F_{3\frac{1}{2}}$
1	11,085.4	1*h*?	9018.4	$w^4D^0_{3\frac{1}{2}} - e^6G_{3\frac{1}{2}}$?
1	11,018.1	1*h*?	9073.5	$z^4P^0_{2\frac{1}{2}} - e^4P_{2\frac{1}{2}}$
1	11,015.9	2*h*	9075.3	$w^4D^0_{\frac{1}{2}} - f^6F_{1\frac{1}{2}}$?
1	10,957.0	2*h*	9124.1	$x^4F^0_{3\frac{1}{2}} - e^4P_{2\frac{1}{2}}$
1	10,946.88	10*h*	9132.52	
1	10,935.42	4	9142.10	$b^4P_{2\frac{1}{2}} - z^6F^0_{3\frac{1}{2}}$
1	10,805.9	10*h*	9251.7	$x^4F^0_{4\frac{1}{2}} - e^4F_{4\frac{1}{2}}$
1	10,785.4	3*h*	9269.3	$a^2D_{1\frac{1}{2}} - z^6D^0_{2\frac{1}{2}}$
1	10,771.3	1?	9281.4	$x^4F^0_{3\frac{1}{2}} - e^4F_{3\frac{1}{2}}$
1	10,739.0	6*h*	9309.3	$x^2F^0_{3\frac{1}{2}} - h^4F_{4\frac{1}{2}}$
1	10,713.4	1	9331.6	$y^2F^0_{2\frac{1}{2}} - e^4F_{3\frac{1}{2}}$
1	10,692.6	3*h*	9349.7	$x^4F^0_{3\frac{1}{2}} - e^4G_{4\frac{1}{2}}$
1	10,681.82	30*h*	9359.14	
1	10,660.17	30	9378.14	$c^2D_{2\frac{1}{2}} - y^2D^0_{1\frac{1}{2}}$
1	10,561.3	2	9465.9	$w^4D^0_{3\frac{1}{2}} - h^4F_{4\frac{1}{2}}$
1	10,521.3	3*h*	9501.9	$b^2D_{1\frac{1}{2}} - y^4D^0_{2\frac{1}{2}}$
1	10,471.96	15	9546.69	$y^2F^0_{2\frac{1}{2}} - e^4F_{2\frac{1}{2}}$
1	10,447.39	4*h*	9569.15	$w^4F^0_{4\frac{1}{2}} - h^4F_{4\frac{1}{2}}$
1	10,442.11	20	9573.99	$b^2G_{4\frac{1}{2}} - z^6F^0_{4\frac{1}{2}}$
1	10,398.38	4*h*	9614.25	$x^4G^0_{5\frac{1}{2}} - e^4H_{6\frac{1}{2}}$
1	10,382.16	50	9629.27	$b^2D_{1\frac{1}{2}} - z^6F^0_{2\frac{1}{2}}$
1	10,367.95	2	9642.47	$x^4F^0_{2\frac{1}{2}} - e^4D_{2\frac{1}{2}}$
1	10,364.4	1	9645.8	$x^4G^0_{4\frac{1}{2}} - e^4H_{5\frac{1}{2}}$
1	10,354.45	60	9655.04	$y^2F^0_{3\frac{1}{2}} - e^4F_{3\frac{1}{2}}$
1	10,348.1	1?	9661.0	$x^4F^0_{2\frac{1}{2}} - f^2F_{2\frac{1}{2}}$
1	10,335.39	4*h*	9672.85	$w^4D^0_{2\frac{1}{2}} - e^4P_{2\frac{1}{2}}$
1	10,332.66	3*h*	9675.40	$x^4G^0_{4\frac{1}{2}} - e^4G_{4\frac{1}{2}}$
1	10,276.80	4*h*	9728.00	$x^4F^0_{3\frac{1}{2}} - e^4G_{4\frac{1}{2}}$
1	10,172.85	20*h*	9827.39	$x^4F^0_{4\frac{1}{2}} - e^4D_{3\frac{1}{2}}$
1	10,167.58	200	9832.48	$y^2D^0_{2\frac{1}{2}} - e^2F_{3\frac{1}{2}}$
1	10,154.90	2	9844.77	$x^4G^0_{4\frac{1}{2}} - e^2H_{5\frac{1}{2}}$
1	10,152.95	4	9846.66	$w^4F^0_{3\frac{1}{2}} - h^4F_{3\frac{1}{2}}$
1	10,131.37	2	9867.63	$b^4P_{\frac{1}{2}} - z^6D^0_{1\frac{1}{2}}$?
1	10,128.06	150	9870.86	$y^2D^0_{1\frac{1}{2}} - e^2F_{2\frac{1}{2}}$
1	10,111.0	1*h*	9887.5	$x^4G^0_{4\frac{1}{2}} - e^2G_{4\frac{1}{2}}$
1	10,105.43	2	9892.96	$x^4G^0_{4\frac{1}{2}} - e^4G_{3\frac{1}{2}}$
1	10,092.1	3*h*	9906.0	$x^4F^0_{3\frac{1}{2}} - e^4F_{3\frac{1}{2}}$?
1	10,078.62	100	9919.28	$a^2H_{5\frac{1}{2}} - z^6G^0_{4\frac{1}{2}}$
1	10,052.98	8	9944.58	$x^4F^0_{4\frac{1}{2}} - e^4F_{4\frac{1}{2}}$
1	10,048.80	3	9948.71	$x^4F^0_{4\frac{1}{2}} - e^4H_{5\frac{1}{2}}$
1	10,046.31	150	9951.18	$b^2D_{2\frac{1}{2}} - z^2F^0_{2\frac{1}{2}}$
1	10,031.45	5	9965.92	$b^4P_{1\frac{1}{2}} - z^6D^0_{2\frac{1}{2}}$
1	10,021.47	4*h*	9975.84	$x^4F^0_{3\frac{1}{2}} - e^4G_{3\frac{1}{2}}$
1	10,019.08	30*h*	9978.22	$x^4F^0_{4\frac{1}{2}} - e^4G_{5\frac{1}{2}}$
1	10,007.80	3	9989.47	$a^2H_{4\frac{1}{2}} - y^4G^0_{4\frac{1}{2}}$
2	9952.2	3*h*	10,045.3	$y^2F^0_{2\frac{1}{2}} - e^4F_{1\frac{1}{2}}$ $x^4G^0_{3\frac{1}{2}} - e^2G_{3\frac{1}{2}}$
2	9940.69	2	10,056.91	$w^4F^0_{2\frac{1}{2}} - h^4F_{2\frac{1}{2}}$
2	9918.1	1	10,079.8	$w^4D^0_{1\frac{1}{2}} - e^2D_{1\frac{1}{2}}$
2	9912.73	10	10,085.28	$b^4P_{2\frac{1}{2}} - z^6D^0_{3\frac{1}{2}}$
2	9909.52	1*h*	10,088.54	$w^4F^0_{2\frac{1}{2}} - f^4P_{2\frac{1}{2}}$
2	9890.92	30	10,107.51	$b^2D_{2\frac{1}{2}} - y^4D^0_{3\frac{1}{2}}$
2	9859.90	1	10,139.31	$x^2F^0_{3\frac{1}{2}} - h^4F_{3\frac{1}{2}}$
2	9852.5	1	10,146.9	$x^2F^0_{3\frac{1}{2}} - f^4D_{2\frac{1}{2}}$
2	9847.7	2	10,151.9	$x^4F^0_{3\frac{1}{2}} - e^4F_{2\frac{1}{2}}$
2	9823.52	4*h*	10,176.86	$x^4F^0_{3\frac{1}{2}} - f^2F_{3\frac{1}{2}}$?
2	9798.37	2*h*	10,202.98	$x^4F^0_{3\frac{1}{2}} - e^4H_{4\frac{1}{2}}$?
2	9785.39	40	10,216.52	$w^4F^0_{4\frac{1}{2}} - f^4G_{5\frac{1}{2}}$
2	9769.0	1*h*	10,233.66	$x^2F^0_{2\frac{1}{2}} - i^4F_{3\frac{1}{2}}$
2	9764.53	5*h*	10,238.34	$x^2F^0_{2\frac{1}{2}} - e^2G_{3\frac{1}{2}}$?
2	9746.02	100	10,257.79	$a^2H_{4\frac{1}{2}} - z^2G^0_{3\frac{1}{2}}$
2	9735.53	2	10,268.84	$x^2F^0_{2\frac{1}{2}} - h^4F_{3\frac{1}{2}}$
2	9729.54	3	10,275.16	$w^4F^0_{3\frac{1}{2}} - i^4F_{4\frac{1}{2}}$
2	9696.60	5	10,310.07	$b^2D_{1\frac{1}{2}} - z^2D^0_{2\frac{1}{2}}$ $w^4F^0_{2\frac{1}{2}} - f^4G_{3\frac{1}{2}}$
2	9694.0	2	10,312.8	$w^4F^0_{2\frac{1}{2}} - f^4G_{3\frac{1}{2}}$
2	9678.21	10*h*	10,329.66	$x^4F^0_{2\frac{1}{2}} - g^2F_{3\frac{1}{2}}$
2	9670.20	2	10,338.21	$x^4F^0_{3\frac{1}{2}} - e^4G_{3\frac{1}{2}}$
2	9659.94	3	10,349.20	$w^4F^0_{1\frac{1}{2}} - i^4F_{2\frac{1}{2}}$
2	9629.83	3*h*	10,381.56	
2	9613.46	4	10,399.23	$w^4F^0_{4\frac{1}{2}} - h^4F_{5\frac{1}{2}}$
2	9606.52	5	10,406.74	$w^4F^0_{4\frac{1}{2}} - f^4D_{3\frac{1}{2}}$
2	9597.90	200	10,416.09	$y^2F^0_{2\frac{1}{2}} - e^2F_{2\frac{1}{2}}$
2	9592.3	2*h*	10,422.2	$x^4F^0_{3\frac{1}{2}} - e^2G_{3\frac{1}{2}}$?
2	9585.28	2	10,429.81	$w^4F^0_{4\frac{1}{2}} - e^6D_{4\frac{1}{2}}$
2	9580.63	3	10,434.87	$w^4F^0_{3\frac{1}{2}} - f^4D_{2\frac{1}{2}}$
2	9569.00	5*h*	10,447.55	
2	9548.66	4	10,469.80	
2	9544.52	300	10,474.35	$y^2F^0_{2\frac{1}{2}} - e^2F_{2\frac{1}{2}}$
2	9527.17	10*h*	10,493.42	$w^4F^0_{4\frac{1}{2}} - i^4F_{4\frac{1}{2}}$
2	9517.33	1	10,504.27	$w^4F^0_{3\frac{1}{2}} - e^6D_{3\frac{1}{2}}$ $x^4G^0_{3\frac{1}{2}} - g^2F_{3\frac{1}{2}}$?
2	9513.42	1	10,508.59	$w^4F^0_{3\frac{1}{2}} - f^4F_{4\frac{1}{2}}$
2	9482.75	1	10,542.57	$x^4F^0_{3\frac{1}{2}} - e^4F_{3\frac{1}{2}}$
2	9470.74	2	10,555.94	$b^4P_{2\frac{1}{2}} - z^6D^0_{3\frac{1}{2}}$
2	9454.23	3*h*	10,574.38	$w^4D^0_{3\frac{1}{2}} - e^4P_{2\frac{1}{2}}$
2	9442.34	4*h*	10,587.69	$x^4G^0_{4\frac{1}{2}} - e^6G_{5\frac{1}{2}}$?
2	9435.70	3	10,595.15	$x^4G^0_{4\frac{1}{2}} - h^4F_{4\frac{1}{2}}$
2	9428.8	1	10,602.9	$x^2F^0_{3\frac{1}{2}} - f^4G_{4\frac{1}{2}}$
2	9422.60	3*h*	10,609.87	$w^4F^0_{4\frac{1}{2}} - f^4G_{5\frac{1}{2}}$
2	9406.12	4*h*	10,628.46	
2	9395.11	2	10,640.92	$x^4P^0_{2\frac{1}{2}} - e^4P_{2\frac{1}{2}}$
2	9356.98	200	10,684.28	$a^2H_{5\frac{1}{2}} - y^4G^0_{4\frac{1}{2}}$
2	9351.06	3	10,691.04	
2	9347.88	2*h*	10,694.68	$w^4F^0_{3\frac{1}{2}} - f^4F_{3\frac{1}{2}}$
2	9344.93	20	10,698.06	$a^2H_{4\frac{1}{2}} - y^4G^0_{5\frac{1}{2}}$
2	9340.54	3*h*	10,703.09	$w^4F^0_{4\frac{1}{2}} - i^4F_{5\frac{1}{2}}$
2	9319.53	2	10,727.21	$w^4F^0_{3\frac{1}{2}} - f^4F_{3\frac{1}{2}}$
2	9280.42	5	10,772.42	$y^2F^0_{2\frac{1}{2}} - e^4F_{3\frac{1}{2}}$
2	9262.5	2	10,793.3	$b^2D_{1\frac{1}{2}} - y^4F^0_{2\frac{1}{2}}$
2	9258.18	4	10,798.30	$x^4F^0_{4\frac{1}{2}} - e^4H_{5\frac{1}{2}}$
2	9245.60	1	10,812.99	$b^2D_{2\frac{1}{2}} - z^2G^0_{3\frac{1}{2}}$
2	9233.64	1	10,827.00	$a^2P_{1\frac{1}{2}} - z^4F^0_{2\frac{1}{2}}$
2	9207.96	1	10,857.19	$x^4F^0_{4\frac{1}{2}} - e^2H_{4\frac{1}{2}}$
2	9204.11	5	10,861.73	$b^2D_{2\frac{1}{2}} - z^2F^0_{2\frac{1}{2}}$
2	9185.95	2	10,883.21	$x^4G^0_{4\frac{1}{2}} - h^4F^0_{3\frac{1}{2}}$
2	9181.75	5	10,888.19	$x^4F^0_{4\frac{1}{2}} - e^2H_{4\frac{1}{2}}$
2	9177.93	20	10,892.72	$x^4G^0_{5\frac{1}{2}} - g^4F^0_{4\frac{1}{2}}$
2	9165.52	2	10,907.46	$x^4F^0_{4\frac{1}{2}} - g^4F^0_{3\frac{1}{2}}$
2	9133.24	6	10,946.02	$x^4F^0_{3\frac{1}{2}} - h^4F^0_{4\frac{1}{2}}$
2	9130.50	2	10,949.30	$b^2G_{4\frac{1}{2}} - y^2G^0_{3\frac{1}{2}}$
2	9111.64	1	10,971.96	$y^2G^0_{3\frac{1}{2}} - e^4F_{3\frac{1}{2}}$
2	9095.37	50	10,991.59	$a^2H_{4\frac{1}{2}} - y^4F^0_{3\frac{1}{2}}$
2	9071.35	4*h*	11,020.70	
2	9052.44	2	11,043.72	$b^2D_{1\frac{1}{2}} - y^4F^0_{1\frac{1}{2}}$
2	9040.0	1	11,058.9	$x^4G^0_{5\frac{1}{2}} - h^4F^0_{5\frac{1}{2}}$
2	9037.87	50	11,061.52	$a^2H_{5\frac{1}{2}} - y^4F^0_{4\frac{1}{2}}$
3	9032.70	1	11,067.86	$x^2D^0_{2\frac{1}{2}} - e^4G_{3\frac{1}{2}}$?
2	8986.51	3	11,124.74	
2	8972.89	7	11,141.63	$w^4F^0_{3\frac{1}{2}} - e^4G_{4\frac{1}{2}}$
2	8958.37	15	11,159.68	$y^4F^0_{2\frac{1}{2}} - e^4F_{3\frac{1}{2}}$
2	8953.72	2	11,165.48	$w^4F^0_{3\frac{1}{2}} - 5_{3\frac{1}{2}}$
2	8939.14	5	11,183.69	$w^4D^0_{2\frac{1}{2}} - h^4F^0_{3\frac{1}{2}}$
2	8926.21	50	11,199.89	$b^2D_{2\frac{1}{2}} - z^2D^0_{2\frac{1}{2}}$
2	8904.63	30	11,227.03	$x^4G^0_{5\frac{1}{2}} - h^4F^0_{4\frac{1}{2}}$
2	8892.49	1	11,242.36	$x^4D^0_{4\frac{1}{2}} - e^4F^0_{3\frac{1}{2}}$
2	8888.70	8*h*	11,247.15	$x^4G^0_{5\frac{1}{2}} - e^2H^0_{4\frac{1}{2}}$
2	8878.28	3	11,260.35	$x^4F^0_{3\frac{1}{2}} - h^4F^0_{3\frac{1}{2}}$
2	8870.70	8	11,269.98	$x^4F^0_{3\frac{1}{2}} - g^2F^0_{3\frac{1}{2}}$
2	8856.56	3	11,287.96	
2	8850.70	30	11,295.44	$y^2F^0_{3\frac{1}{2}} - e^2F^0_{3\frac{1}{2}}$
2	8837.90	4*h*	11,311.80	
2	8835.21	20	11,315.25	$y^4F^0_{4\frac{1}{2}} - e^4F_{4\frac{1}{2}}$
4	8819.11*v*	100	11,335.90	$x^4G^0_{5\frac{1}{2}} - h^4F^0_{4\frac{1}{2}}$
2	8779.20	3	11,387.44	$w^4F^0_{4\frac{1}{2}} - e^4G^0_{5\frac{1}{2}}$
2	8774.71	2	11,393.26	$x^4D^0_{3\frac{1}{2}} - e^4F^0_{3\frac{1}{2}}$
2	8772.04	2	11,396.73	$w^4F^0_{3\frac{1}{2}} - 4_{3\frac{1}{2}}$
2	8766.55	4*h*	11,403.87	$x^4D^0_{3\frac{1}{2}} - e^4D^0_{3\frac{1}{2}}$
2	8759.58	3	11,412.94	
2	8750.13	60	11,425.27	$x^4G^0_{4\frac{1}{2}} - h^4F^0_{4\frac{1}{2}}$
2	8745.56	8	11,431.24	$y^4G^0_{3\frac{1}{2}} - e^4F^0_{3\frac{1}{2}}$?
2	8744.37	10	11,432.80	
2	8733.27	40	11,447.32	$x^4G^0_{5\frac{1}{2}} - h^4F^0_{5\frac{1}{2}}$
2	8722.12	2	11,461.96	$x^4F^0_{3\frac{1}{2}} - h^4F^0_{3\frac{1}{2}}$
2	8678.65	3	11,519.37	$x^4G^0_{4\frac{1}{2}} - i^4F^0_{4\frac{1}{2}}$
2	8675.02	20	11,524.19	$z^2D^0_{2\frac{1}{2}} - e^4F^0_{3\frac{1}{2}}$
4	8661.06*v*	60	11,542.76	$b^2D_{2\frac{1}{2}} - z^2D^0_{3\frac{1}{2}}$
2	8658.14	3	11,546.66	$b^2D_{2\frac{1}{2}} - y^4F^0_{3\frac{1}{2}}$
2	8655.73	3*h*	11,549.87	$x^4F^0_{4\frac{1}{2}} - e^2H^0_{4\frac{1}{2}}$
2	8648.79	4	11,559.14	$a^2P_{1\frac{1}{2}} - z^6D^0_{2\frac{1}{2}}$
3	8596.09	3*h*	11,630.00	$x^4F^0_{4\frac{1}{2}} - h^4F^0_{4\frac{1}{2}}$
4	8589.78*v*	50	11,638.55	$y^4F^0_{4\frac{1}{2}} - e^4F^0_{4\frac{1}{2}}$ $x^4F^0_{4\frac{1}{2}} - h^4F^0_{4\frac{1}{2}}$
4	8586.68*v*	30	11,642.75	$z^2D^0_{2\frac{1}{2}} - e^4F^0_{3\frac{1}{2}}$
4	8575.32*v*	50	11,658.17	$a^2H_{4\frac{1}{2}} - y^4G^0_{5\frac{1}{2}}$
4	8574.46*v*	50	11,659.34	$a^2H_{5\frac{1}{2}} - y^4G^0_{5\frac{1}{2}}$
3	8569.72	18	11,665.79	$y^2G^0_{4\frac{1}{2}} - e^4F^0_{4\frac{1}{2}}$ $x^4G^0_{5\frac{1}{2}} - i^4F^0_{5\frac{1}{2}}$
5	8559.07	10	11,680.31	$y^4F^0_{3\frac{1}{2}} - e^4F^0_{3\frac{1}{2}}$
5	8513.52	5*h*	11,742.80	$y^2G^0_{4\frac{1}{2}} - e^4F^0_{3\frac{1}{2}}$
5	8489.50	30	11,776.02	$x^4F^0_{4\frac{1}{2}} - h^4F^0_{4\frac{1}{2}}$
3	8478.45	8	11,791.37	$y^2G^0_{4\frac{1}{2}} - e^4F^0_{4\frac{1}{2}}$ $x^4F^0_{3\frac{1}{2}} - h^4F^0_{4\frac{1}{2}}$
3	8454.71	1	11,824.48	$w^4D^0_{3\frac{1}{2}} - 3_{3\frac{1}{2}}$
3	8409.03	10*Wh*	11,888.71	$x^4G^0_{5\frac{1}{2}} - f^4G^0_{4\frac{1}{2}}$
4	8379.44*v*	35	11,930.69	$y^4F^0_{3\frac{1}{2}} - e^4F^0_{3\frac{1}{2}}$

TABLE VIII.—*Continued.*

Ref.	λ *IA*	Int.–*TC*	Wave No. Vac.	Multiplet Designation
4	8378.34*v*	50	11,932.26	$y^4G_{3\frac{1}{2}} - e^4F_{3\frac{1}{2}}$
4	8372.79*v*	80*h*	11,940.18	$y^4F_{4\frac{1}{2}} - e^4F_{4\frac{1}{2}}$
5	8345.55	20*h*	11,979.15	$y^4F_{3\frac{1}{2}} - e^4F_{3\frac{1}{2}}$
5	8342.63	50*Wh*	11,983.33	$x^4G_{5\frac{1}{2}} - f^4G_{5\frac{1}{2}}$
5	8331.69	20	11,999.07	$a^2D_{2\frac{1}{2}} - z^4F^o_{3\frac{1}{2}}$
3	8318.55	5*Wh*	12,018.03	$x^4F^o_{4\frac{1}{2}} - f^4D_{3\frac{1}{2}}$
5	8315.35	20	12,022.66	$z^2D^o_{2\frac{1}{2}} - e^4F_{3\frac{1}{2}}$
5	8301.45	5*h*	12,042.79	$x^4F^o_{3\frac{1}{2}} - i^4F_{3\frac{1}{2}}$
4	8298.95*v* §§	60*h*	12,046.41	$x^4G_{4\frac{1}{2}} - f^4H_{4\frac{1}{2}}$
4	8296.82*v*	50*h*	12,049.50	$x^4G_{5\frac{1}{2}} - f^4H_{4\frac{1}{2}}$
5	8283.48	50*h*	12,068.90	$x^4G_{5\frac{1}{2}} - f^4H_{5\frac{1}{2}}$
3	8275.55	8*h*	12,080.47	$x^4F^o_{5\frac{1}{2}} - f^4G_{5\frac{1}{2}}$
5	8272.38	5*h*	12,085.10	$x^4G_{3\frac{1}{2}} - f^4F_{3\frac{1}{2}}$
5	8269.38	80*h*	12,089.48	$x^4G_{3\frac{1}{2}} - f^4H^o_{4\frac{1}{2}}$
3	8243.38	1	12,127.62	$x^4F^o_{3\frac{1}{2}} - 1z_{3\frac{1}{2}}$
4	8208.57*v*	80	12,179.05	$y^4F^o_{3\frac{1}{2}} - e^4F_{3\frac{1}{2}}$
4	8192.97*v*	125	12,202.24	$y^4G_{5\frac{1}{2}} - e^4F_{5\frac{1}{2}}$
5	8189.32	10*h*	12,207.68	$x^4G_{4\frac{1}{2}} - i^4F_{3\frac{1}{2}}$
5	8167.88	20*Wh*	12,239.71	$x^4F^o_{5\frac{1}{2}} - f^4G_{4\frac{1}{2}}$
5	8160.65	40	12,250.57	$y^4G_{3\frac{1}{2}} - e^4F_{3\frac{1}{2}}$
3	8154.31	10*h*	12,260.09	$x^4G_{3\frac{1}{2}} - i^4F_{4\frac{1}{2}}$
4	8151.95*v*	60	12,263.64	$y^4F^o_{4\frac{1}{2}} - e^4F_{3\frac{1}{2}}$
5	8150.19	50	12,266.29	$b^2G_{4\frac{1}{2}} - y^2F^o_{3\frac{1}{2}}$
5	8140.43	40	12,280.99	$b^2P_{1\frac{1}{2}} - z^2F^o_{2\frac{1}{2}}$
5	8137.08	80	12,286.05	$x^4F^o_{4\frac{1}{2}} - f^4G_{5\frac{1}{2}}$
4	8116.37*v*	80	12,317.40	$y^4G_{4\frac{1}{2}} - e^4F_{4\frac{1}{2}}$
5	8114.04	10*h*	12,320.93	$x^4G_{2\frac{1}{2}} - e^4H_{3\frac{1}{2}}$
3	8112.13	5*Wh*	12,323.83	$z^2F^o_{3\frac{1}{2}} - e^4F_{3\frac{1}{2}}$
4	8093.932*v*	8–III	12,351.54	$y^4G_{3\frac{1}{2}} - e^4F_{4\frac{1}{2}}$
5	8085.54	5*h*	12,364.36	$x^4F^o_{3\frac{1}{2}} - f^4D_{2\frac{1}{2}}$
3	8082.60	1	12,368.86	$x^4F^o_{3\frac{1}{2}} - f^4G_{2\frac{1}{2}}$
5	8080.23	60	12,372.49	$z^2G^o_{3\frac{1}{2}} - e^4F_{3\frac{1}{2}}$
5	8066.49	60	12,393.56	$z^2D^o_{1\frac{1}{2}} - e^2F_{2\frac{1}{2}}$
3	8062.98	5*Wh*	12,398.96	$x^4G_{2\frac{1}{2}} - 4z_{2\frac{1}{2}}$
4	8055.996*v*	2–*V*	12,409.71	$y^4F^o_{5\frac{1}{2}} - e^4F_{5\frac{1}{2}}$
3	8053.50	2*h*	12,413.55	$\begin{cases} z^2D^o_{2\frac{1}{2}} - e^4F_{3\frac{1}{2}} \\ x^4G_{4\frac{1}{2}} - e^4G_{4\frac{1}{2}} \end{cases}$
5	8050.76	5*Wh*	12,417.77	$x^4D^o_{2\frac{1}{2}} - g^2F_{3\frac{1}{2}}$
4	8043.306*v*	2–*V*	12,429.28	$y^4F^o_{3\frac{1}{2}} - e^4F_{3\frac{1}{2}}$
5	8041.37	20	12,432.28	$b^2D_{2\frac{1}{2}} - z^2D^o_{3\frac{1}{2}}$
5	8037.64	10*h*	12,438.04	$\begin{cases} a^2D_{2\frac{1}{2}} - z^4F^o_{3\frac{1}{2}} \\ x^4F^o_{3\frac{1}{2}} - f^4F_{4\frac{1}{2}} \end{cases}$
4	8029.217*v*	80	12,451.10	$y^4D^o_{3\frac{1}{2}} - e^4F_{3\frac{1}{2}}$
5	8024.73	40	12,458.05	$y^4F^o_{3\frac{1}{2}} - e^2F_{3\frac{1}{2}}$
4	8022.087*v*	40	12,462.16	$z^2D^o_{2\frac{1}{2}} - e^2F_{2\frac{1}{2}}$
5	8017.86	15*h*	12,468.73	$x^4F^o_{4\frac{1}{2}} - h^4F_{3\frac{1}{2}}$
5	8016.56	15*h*	12,470.76	$x^4F^o_{3\frac{1}{2}} - i^4F_{2\frac{1}{2}}$
5	8012.99	20*Wh*	12,476.31	$x^4F^o_{4\frac{1}{2}} - f^4D_{3\frac{1}{2}}$
4	8007.239*v*	5–*V*	12,485.27	$y^2G^o_{4\frac{1}{2}} - e^2F_{3\frac{1}{2}}$
5	7998.09	12*h*	12,499.55	$x^4F^o_{4\frac{1}{2}} - e^4D_{4\frac{1}{2}}$
5	7996.80	10*h*	12,501.57	$\begin{cases} a^2G_{4\frac{1}{2}} - z^4G^o_{3\frac{1}{2}} \\ x^4G^o_{3\frac{1}{2}} - e^4H_{4\frac{1}{2}} \end{cases}$
4	7987.36*v*	5–III	12,516.34	$a^2D_{2\frac{1}{2}} - z^4D^o_{3\frac{1}{2}}$
3	7984.22	1	12,521.27	$x^4G^o_{3\frac{1}{2}} - 5z_{3\frac{1}{2}}$
5	7980.57	3*h*	12,526.99	$x^4F^o_{3\frac{1}{2}} - e^4P^o_{2\frac{1}{2}}$?
5	7966.08	40	12,549.77	$y^4F^o_{4\frac{1}{2}} - e^2F_{3\frac{1}{2}}$
3	7962.40	3*Wh*	12,555.58	$x^4F^o_{3\frac{1}{2}} - e^4G_{3\frac{1}{2}}$
5	7960.55	25*h*	12,558.50	$x^4F^o_{3\frac{1}{2}} - i^4F_{3\frac{1}{2}}$
5	7957.76	40*h*	12,562.90	$x^4F^o_{4\frac{1}{2}} - i^4F_{4\frac{1}{2}}$
4	7926.525*v*	3–*V*	12,612.40	$y^2G^o_{3\frac{1}{2}} - e^2F_{3\frac{1}{2}}$
5	7919.48	15*h*	12,623.62	$x^2D^o_{2\frac{1}{2}} - g^4P^o_{2\frac{1}{2}}$
3	7912.90	1	12,634.12	$x^2D^o_{1\frac{1}{2}} - g^4P^o_{2\frac{1}{2}}$
4	7908.679*v*	6–III?	12,640.86	$y^4G^o_{4\frac{1}{2}} - e^4F_{3\frac{1}{2}}$
3	7907.14	1	12,643.32	$x^4F^o_{3\frac{1}{2}} - 1z_{2\frac{1}{2}}$
5	7885.25	10*Wh*	12,678.43	$x^4G^o_{4\frac{1}{2}} - e^4H_{5\frac{1}{2}}$
5	7877.49	20	12,690.91	
5	7873.32	10*h*	12,697.63	$w^4F^o_{4\frac{1}{2}} - g^4P^o_{2\frac{1}{2}}$
4	7871.370*v*	2–*V*	12,700.78	$y^4G^o_{3\frac{1}{2}} - e^4F_{4\frac{1}{2}}$
4	7869.868*v*	2–*V*	12,703.20	$y^4G^o_{3\frac{1}{2}} - e^4F_{2\frac{1}{2}}$
3	7866.10	1	12,709.29	$x^4G^o_{3\frac{1}{2}} - e^4H_{3\frac{1}{2}}$
5	7859.39	10*Wh*	12,720.14	$x^4G^o_{4\frac{1}{2}} - e^4G_{4\frac{1}{2}}$
4	7855.821*v*	40*h*	12,725.92	$y^4D^o_{3\frac{1}{2}} - e^4F_{2\frac{1}{2}}$
5	7843.64	12	12,745.68	$a^2D_{1\frac{1}{2}} - z^4F^o_{2\frac{1}{2}}$
4	7839.997*v*	40	12,751.60	$y^4G^o_{5\frac{1}{2}} - e^2F_{3\frac{1}{2}}$
4	7838.121*v*	3–*V*	12,754.66	$y^4D^o_{3\frac{1}{2}} - e^4F_{4\frac{1}{2}}$
3	7822.12	2*Wh*	12,780.74	$x^4F^o_{4\frac{1}{2}} - f^4F_{3\frac{1}{2}}$
3	7818.25	5*h*	12,787.07	$\begin{cases} x^4G^o_{3\frac{1}{2}} - f^4H_{4\frac{1}{2}} \\ x^4G^o_{3\frac{1}{2}} - 4z_{3\frac{1}{2}} \end{cases}$
3	7817.15	1	12,788.87	$x^4F^o_{2\frac{1}{2}} - 3z_{2\frac{1}{2}}$
5	7810.30	10*h*	12,800.09	$y^4F^o_{2\frac{1}{2}} - e^2F_{2\frac{1}{2}}$
5	7809.24	20	12,801.83	$a^2G_{4\frac{1}{2}} - z^4G^o_{4\frac{1}{2}}$
5	7794.13	5*h*	12,826.64	$a^2G_{4\frac{1}{2}} - z^4D^o_{3\frac{1}{2}}$
3	7786.63	1	12,839.00	$x^4G^o_{5\frac{1}{2}} - e^4G_{5\frac{1}{2}}$
5	7764.02	12	12,876.38	$x^4D^o_{1\frac{1}{2}} - g^2F_{2\frac{1}{2}}$
5	7743.27	4	12,910.89	$z^2F^o_{3\frac{1}{2}} - e^4F_{4\frac{1}{2}}$
5	7735.45	10*h*	12,923.94	$x^4G^o_{3\frac{1}{2}} - e^4H_{4\frac{1}{2}}$
5	7734.23	40	12,925.98	$y^4D^o_{2\frac{1}{2}} - e^4F_{1\frac{1}{2}}$
5	7725.95	12	12,939.84	$b^2D_{1\frac{1}{2}} - y^2D^o_{2\frac{1}{2}}$
4	7712.661*v*	6–III	12,962.13	$b^2P_{1\frac{1}{2}} - z^2D^o_{2\frac{1}{2}}$
5	7704.92	12	12,975.16	$a^2H_{4\frac{1}{2}} - y^2F^o_{3\frac{1}{2}}$
5	7701.90	12	12,980.24	$b^2P_{1\frac{1}{2}} - y^4F^o_{1\frac{1}{2}}$
5	7695.94	10*h*	12,990.29	$x^2F^o_{3\frac{1}{2}} - g^4P^o_{2\frac{1}{2}}$
3	7685.65	1	13,007.69	$z^2F^o_{3\frac{1}{2}} - g^4P^o_{2\frac{1}{2}}$
5	7648.08	12*h*	13,071.59	$y^4G^o_{2\frac{1}{2}} - e^2F_{2\frac{1}{2}}$
3	7641.43	1	13,082.96	$y^4F^o_{4\frac{1}{2}} - e^2F_{3\frac{1}{2}}$
3	7637.63	4	13,089.47	
5	7634.50	3	13,094.84	$z^2F^o_{3\frac{1}{2}} - e^4F_{3\frac{1}{2}}$
5	7618.64	2	13,122.09	$b^2G_{4\frac{1}{2}} - y^2F^o_{3\frac{1}{2}}$
3	7616.13	1	13,126.42	$x^4F^o_{4\frac{1}{2}} - e^4D_{3\frac{1}{2}}$
5	7610.24	2–IV	13,136.58	$b^2P_{1\frac{1}{2}} - z^2D^o_{1\frac{1}{2}}$
3	7606.30	2–V	13,143.38	$\begin{cases} z^2F^o_{3\frac{1}{2}} - e^4F_{3\frac{1}{2}} \\ z^2G^o_{3\frac{1}{2}} - e^4F_{2\frac{1}{2}} \end{cases}$
3	7604.30	1	13,146.84	$w^4D^o_{2\frac{1}{2}} - g^4P^o_{2\frac{1}{2}}$
3	7600.11	1	13,154.09	$x^4G^o_{4\frac{1}{2}} - e^4G_{4\frac{1}{2}}$?
3	7594.18	1	13,164.36	$x^4F^o_{4\frac{1}{2}} - 4z_{4\frac{1}{2}}$
5	7590.57	2–III	13,170.62	$a^2D_{2\frac{1}{2}} - z^4D^o_{2\frac{1}{2}}$
3	7588.71	1	13,173.85	$b^2P_{1\frac{1}{2}} - y^4G^o_{2\frac{1}{2}}$
5	7586.72	20	13,177.31	$b^2D_{1\frac{1}{2}} - y^2F^o_{2\frac{1}{2}}$
3	7578.34	1	13,191.88	$z^2G^o_{4\frac{1}{2}} - e^2F_{3\frac{1}{2}}$
5	7564.96	20	13,215.21	$x^4D^o_{3\frac{1}{2}} - h^4F_{4\frac{1}{2}}$
5	7561.06	15	13,222.03	$y^4D^o_{2\frac{1}{2}} - e^4F_{2\frac{1}{2}}$
5	7559.65	15	13,224.49	$y^4D^o_{1\frac{1}{2}} - e^4F_{1\frac{1}{2}}$
4	7553.970*v*	4–IV	13,234.43	$z^2F^o_{3\frac{1}{2}} - e^4F_{3\frac{1}{2}}$
5	7533.48	1–IV	13,270.43	$y^4D^o_{2\frac{1}{2}} - e^2F_{2\frac{1}{2}}$
5	7526.29	2	13,283.11	$z^2D^o_{2\frac{1}{2}} - e^2F_{2\frac{1}{2}}$
3	7524.07	1	13,287.03	$x^4F^o_{3\frac{1}{2}} - 5z_{3\frac{1}{2}}$
3	7515.28	1	13,302.56	$w^4D^o_{3\frac{1}{2}} - g^4P^o_{2\frac{1}{2}}$
5	7502.72	3*h*	13,324.84	$x^4D^o_{4\frac{1}{2}} - h^4F_{4\frac{1}{2}}$
5	7489.37	10	13,348.59	$x^4D^o_{3\frac{1}{2}} - h^4F_{3\frac{1}{2}}$
3	7484.00	1	13,358.16	$x^4D^o_{2\frac{1}{2}} - g^2F_{2\frac{1}{2}}$
3	7478.77	3	13,367.51	$b^4P_{\frac{1}{2}} - z^4F^o_{1\frac{1}{2}}$
3	7471.21	1	13,381.03	$y^4F^o_{4\frac{1}{2}} - e^4F_{4\frac{1}{2}}$
4	7457.342*v*	6–V	13,405.92	$z^2G^o_{4\frac{1}{2}} - e^4F_{3\frac{1}{2}}$
5	7443.43	10*h*	13,430.97	$x^4D^o_{4\frac{1}{2}} - h^4F_{3\frac{1}{2}}$
5	7437.16	1–III*A*	13,442.29	$b^4P_{1\frac{1}{2}} - z^4F^o_{2\frac{1}{2}}$
5	7429.00	10	13,457.05	$x^4F^o_{4\frac{1}{2}} - e^4G_{4\frac{1}{2}}$
4	7417.38*v*	10–II	13,478.14	$a^2D_{2\frac{1}{2}} - z^4D^o_{2\frac{1}{2}}$
3	7406.23	1	13,498.43	$c^2D_{2\frac{1}{2}} - z^4P^o_{2\frac{1}{2}}$
3	7398.72	1	13,512.14	$c^2D_{1\frac{1}{2}} - z^4P^o_{1\frac{1}{2}}$
4	7388.689*v*	5–III	13,530.48	$b^2D_{2\frac{1}{2}} - y^2F^o_{3\frac{1}{2}}$
3	7365.77	1	13,572.58	$y^4G^o_{3\frac{1}{2}} - e^2F_{3\frac{1}{2}}$
4	7354.579*v*	3–III	13,593.23	$b^4P_{2\frac{1}{2}} - z^4F^o_{3\frac{1}{2}}$
5	7353.47	25	13,595.28	$y^4D^o_{3\frac{1}{2}} - e^2F_{2\frac{1}{2}}$
3	7351.55	1	13,598.83	$x^4D^o_{1\frac{1}{2}} - h^4F_{1\frac{1}{2}}$
3	7349.68	1	13,602.29	$x^4F^o_{3\frac{1}{2}} - e^4H_{3\frac{1}{2}}$
5	7315.73	25	13,665.42	$a^2D_{2\frac{1}{2}} - z^4D^o_{1\frac{1}{2}}$
3	7307.86	1	13,680.13	$x^4F^o_{3\frac{1}{2}} - 4z_{3\frac{1}{2}}$
5	7285.28#	4–IV	13,722.53	$b^2D_{1\frac{1}{2}} - y^2D^o_{1\frac{1}{2}}$
5	7263.58	6	13,763.53	$x^4F^o_{4\frac{1}{2}} - e^4G_{4\frac{1}{2}}$?
5	7250.12	1–III*A*	13,789.08	$b^4P_{1\frac{1}{2}} - z^4F^o_{1\frac{1}{2}}$
5	7217.34	8	13,851.71	$b^2P_{1\frac{1}{2}} - z^2D^o_{1\frac{1}{2}}$
4	7193.56*v*	4–V	13,897.50	$y^4D^o_{2\frac{1}{2}} - e^2F_{2\frac{1}{2}}$
3	7185.63	1Cr?	13,912.84	$x^4D^o_{2\frac{1}{2}} - h^4F_{2\frac{1}{2}}$
3	7173.37	1	13,936.61	$x^4D^o_{2\frac{1}{2}} - f^4D_{2\frac{1}{2}}$
4	7159.153*v*	6–V	13,964.29	$z^2F^o_{2\frac{1}{2}} - e^2F_{2\frac{1}{2}}$
4	7154.688*v*	8–II	13,973.00	$a^2D_{1\frac{1}{2}} - z^4D^o_{1\frac{1}{2}}$
4	7134.290*v*	5–V	14,012.96	$z^2G^o_{3\frac{1}{2}} - e^2F_{2\frac{1}{2}}$
5	7124.47	1–III	14,032.27	$b^4P_{2\frac{1}{2}} - z^4F^o_{2\frac{1}{2}}$
3	7117.91	2	14,045.20	$x^4D^o_{3\frac{1}{2}} - h^4F_{3\frac{1}{2}}$
6	7113.98	1	14,052.96	$x^4D^o_{2\frac{1}{2}} - f^4D_{2\frac{1}{2}}$
4	7113.538*v*	5–V	14,053.84	$z^2F^o_{3\frac{1}{2}} - e^2F_{3\frac{1}{2}}$
5	7102.55	25	14,075.58	
3	7101.77	1	14,077.12	$x^4D^o_{1\frac{1}{2}} - i^4F_{2\frac{1}{2}}$
3	7097.84	1	14,084.92	$y^2G^o_{4\frac{1}{2}} - f^4F_{4\frac{1}{2}}$
5	7094.53	1–IV	14,091.49	$y^4D^o_{3\frac{1}{2}} - e^2F_{2\frac{1}{2}}$
4	7084.974*v*	100–I	14,110.49	$b^4P_{2\frac{1}{2}} - z^4D^o_{2\frac{1}{2}}$
5	7079.20	10	14,122.00	$x^4D^o_{4\frac{1}{2}} - e^6P^o_{3\frac{1}{2}}$
5	7070.41	20	14,139.56	$x^4D^o_{3\frac{1}{2}} - i^4F_{4\frac{1}{2}}$
5	7055.88	25	14,168.68	$x^4D^o_{2\frac{1}{2}} - f^4G_{3\frac{1}{2}}$
4	7054.042*v*	10–III	14,172.37	$b^2D_{2\frac{1}{2}} - y^2D^o_{2\frac{1}{2}}$
4	7052.872*v*	60–I	14,174.72	$b^4P_{1\frac{1}{2}} - z^4D^o_{2\frac{1}{2}}$
5	7042.58	5*h*	14,195.43	$y^4D^o_{2\frac{1}{2}} - e^4F_{4\frac{1}{2}}$
5	7032.52	25	14,215.74	$x^4D^o_{2\frac{1}{2}} - 1z_{2\frac{1}{2}}$
4	7027.797*v*	6–V	14,225.29	$z^2G^o_{4\frac{1}{2}} - e^4F_{3\frac{1}{2}}$
4	7016.602*v*	35–I	14,247.99	$b^4P_{1\frac{1}{2}} - z^4D^o_{1\frac{1}{2}}$
5	7015.18	5	14,250.88	$x^4D^o_{1\frac{1}{2}} - 2z_{1\frac{1}{2}}$
5	7004.81	3–III	14,271.98	$a^2D_{1\frac{1}{2}} - z^4D^o_{1\frac{1}{2}}$
5	6997.22	4*d*–V	14,287.45	$x^4D^o_{2\frac{1}{2}} - f^4P^o_{2\frac{1}{2}}$
3	6977.02	1	14,328.82	$b^4P_{1\frac{1}{2}} - z^4G^o_{2\frac{1}{2}}$
3	6972.70	1	14,337.70	$x^4D^o_{1\frac{1}{2}} - f^4G_{2\frac{1}{2}}$
5	6946.31	10	14,392.17	$a^2P_{1\frac{1}{2}} - z^2F^o_{2\frac{1}{2}}$
5	6937.81	4–III	14,409.80	$b^2D_{2\frac{1}{2}} - y^2F^o_{2\frac{1}{2}}$
5	6910.84	15	14,466.04	$a^2G_{4\frac{1}{2}} - z^2G^o_{4\frac{1}{2}}$
5	6908.08	30	14,471.81	$c^2D_{2\frac{1}{2}} - z^4P^o_{2\frac{1}{2}}$
3	6906.39	1	14,475.36	$x^4D^o_{3\frac{1}{2}} - f^4F_{4\frac{1}{2}}$
5	6901.52	5	14,485.57	$c^2D_{2\frac{1}{2}} - z^4P^o_{1\frac{1}{2}}$
4	6872.32*v*	40–I	14,547.01	$b^4P_{\frac{1}{2}} - z^4D^o_{\frac{1}{2}}$
5	6864.91	10	14,562.82	$z^4P^o_{1\frac{1}{2}} - g^4P^o_{2\frac{1}{2}}$

§§ Error of +1A assumed in λ published in M. I. T. list.

Line double-Burns.

TABLE VIII.—*Continued.*

REF.	λ *IA*	INT.–*TC*	WAVE NO. VAC.	MULTIPLET DESIGNATION
5	6858.38	25	14,576.69	$z^4P^o_{2\frac{1}{2}} - g^4P_{2\frac{1}{2}}$
5	6846.97	25	14,600.98	$x^4D^o_{2\frac{1}{2}} - e^6D_{2\frac{1}{2}}$
3	6845.66	10	14,603.77	$x^4D^o_{2\frac{1}{2}} - e^6P_{1\frac{1}{2}}$
5	6838.11	15	14,619.89	
3	6829.92	1	14,637.43	$a^2G_{3\frac{1}{2}} - z^2F^o_{3\frac{1}{2}}$
5	6826.96	3	14,643.77	$x^4D^o_{3\frac{1}{2}} - e^6G_{3\frac{1}{2}}$
5	6819.53	20	14,659.73	$c^2D_{1\frac{1}{2}} - z^2P^o_{1\frac{1}{2}}$
4	6814.950*v*	40–I	14,669.58	$b^4P_{1\frac{1}{2}} - z^4D^o_{1\frac{1}{2}}$
5	6808.94	25*h*	14,682.53	$y^4F^o_{4\frac{1}{2}} - f^4F_{4\frac{1}{2}}$
3	6807.43	1	14,685.78	$y^2D^o_{2\frac{1}{2}} - e^4D_{2\frac{1}{2}}$
5	6799.40	6*h*	14,703.13	$x^4D^o_{3\frac{1}{2}} - e^6D_{3\frac{1}{2}}$
3	6792.35	1	14,718.39	$y^4D^o_{2\frac{1}{2}} - e^2F_{2\frac{1}{2}}$
5	6789.26	15	14,725.09	$x^4D^o_{\frac{1}{2}} - 6_{\frac{1}{2}}$
5	6784.85	25	14,734.66	$y^4F^o_{3\frac{1}{2}} - f^4F_{3\frac{1}{2}}$
3	6778.06	1	14,749.42	$x^4D^o_{1\frac{1}{2}} - f^6F_{1\frac{1}{2}}$
4	6771.040*v*	50–I	14,764.71	$b^4P_{2\frac{1}{2}} - z^4D^o_{2\frac{1}{2}}$
5	6767.394	15	14,772.67	$y^4F^o_{2\frac{1}{2}} - f^4F_{2\frac{1}{2}}$
5	6758.10	25	14,792.99	$c^2D_{1\frac{1}{2}} - w^4D^o_{1\frac{1}{2}}$
5	6756.57	25	14,796.33	$x^4D^o_{2\frac{1}{2}} - e^4P_{2\frac{1}{2}}$
5	6742.17	5	14,827.93	$x^4D^o_{2\frac{1}{2}} - z^4F_{3\frac{1}{2}}$
5	6722.71	4	14,870.85	$y^2F^o_{2\frac{1}{2}} - e^2P_{1\frac{1}{2}}$
5	6720.95	4	14,874.75	$z^2F^o_{2\frac{1}{2}} - e^2F_{2\frac{1}{2}}$
5	6717.64	5*h*	14,882.08	$y^4F^o_{1\frac{1}{2}} - f^4F_{1\frac{1}{2}}$
5	6712.71	8*h*	14,893.01	$x^4D^o_{1\frac{1}{2}} - 5_{1\frac{1}{2}\cdot 2\frac{1}{2}}$
5	6703.92	15	14,912.53	$x^4D^o_{2\frac{1}{2}} - 1_{2\frac{1}{2}}$
3	6700.99	1	14,919.06	$b^4P_{2\frac{1}{2}} - z^4G^o_{3\frac{1}{2}}$
5	6692.87	4	14,937.15	$x^4D^o_{2\frac{1}{2}} - f^6F_{2\frac{1}{2}}$
4	6684.875*v*	30	14,955.02	$b^2D_{2\frac{1}{2}} - y^2D^o_{1\frac{1}{2}}$
5	6684.08	30	14,956.80	
3	6682.30	1*w*	14,960.78	$y^2D^o_{2\frac{1}{2}} - e^4D_{2\frac{1}{2}}$
3	6680.35	1	14,965.15	$c^2D_{1\frac{1}{2}} - w^4D^o_{1\frac{1}{2}}$
4	6678.818*v*	5–II	14,968.58	$b^4P_{1\frac{1}{2}} - z^4D^o_{\frac{1}{2}}$
3	6672.96	2	14,981.72	$a^4P_{2\frac{1}{2}} - z^4F^o_{3\frac{1}{2}}$
5	6665.29	4	14,998.97	$x^4D^o_{1\frac{1}{2}} - 6_{\frac{1}{2}}$
5	6663.72	3*h*	15,002.50	$z^4G^o_{2\frac{1}{2}} - e^4F_{2\frac{1}{2}}$
5	6652.29	3*h*	15,028.28	$y^4G^o_{3\frac{1}{2}} - f^4F_{3\frac{1}{2}}$
3	6649.97	5	15,033.52	$x^1D^o_{2\frac{1}{2}} - e^6G_{3\frac{1}{2}}$
5	6645.33	4*h*	15,044.01	$y^4G^o_{3\frac{1}{2}} - f^4F_{3\frac{1}{2}}$
10	6644.03	1	15,046.96	$z^4G^o_{3\frac{1}{2}} - e^4F_{4\frac{1}{2}}$
3	6638.40	1	15,059.72	$y^4G^o_{4\frac{1}{2}} - f^4F_{4\frac{1}{2}}$
5	6635.12	25*h*	15,067.16	$c^2D_{1\frac{1}{2}} - z^2F^o_{1\frac{1}{2}}$
4	6632.438*v*	15–II	15,073.26	$a^2P_{1\frac{1}{2}} - z^2D^o_{2\frac{1}{2}}$
4	6623.780*v*	2–III?	15,092.96	$a^2D_{2\frac{1}{2}} - z^2F^o_{3\frac{1}{2}}$
6	6623.36	1	15,093.92	$y^4G^o_{5\frac{1}{2}} - f^4F_{4\frac{1}{2}}$
4	6617.572*v*	3*n*–V	15,107.12	$y^2D^o_{2\frac{1}{2}} - g^4F_{3\frac{1}{2}}$
4	6617.126*v*	6*n*–V	15,108.14	$y^2D^o_{2\frac{1}{2}} - e^2P_{1\frac{1}{2}}$
4	6595.869*v*	12–V	15,156.83	$z^4D^o_{2\frac{1}{2}} - e^4F_{3\frac{1}{2}}$
7	6591.834	15	15,166.10	$y^2D^o_{1\frac{1}{2}} - e^2P_{1\frac{1}{2}}$
3	6588.02	1	15,174.88	$x^4D^o_{2\frac{1}{2}} - e^6H_{3\frac{1}{2}}$?
4	6579.373*v*	15	15,194.83	$y^2D^o_{1\frac{1}{2}} - g^4F_{2\frac{1}{2}}$
4	6563.403*v*	40–II	15,231.80	$a^2G_{4\frac{1}{2}} - e^2G^o_{4\frac{1}{2}}$
8	6554.840	2*n*	15,251.70	$y^4F^o_{3\frac{1}{2}} - f^4F_{2\frac{1}{2}}$
8	6554.382	2*n*	15,252.76	$x^4D^o_{3\frac{1}{2}} - 4_{2\frac{1}{2}}$
4	6551.466*v*	3–III	15,259.55	$b^4P_{2\frac{1}{2}} - z^4D^o_{1\frac{1}{2}}$
3	6540.64	1	15,284.81	$a^2P_{1\frac{1}{2}} - y^4G^o_{2\frac{1}{2}}$
5	6535.13	2*h*	15,297.69	$x^4D^o_{3\frac{1}{2}} - e^6D_{3\frac{1}{2}}$
5	6517.00	3*h*	15,340.25	$x^4D^o_{3\frac{1}{2}} - e^6G_{3\frac{1}{2}}$
4	6508.785*v*	5*h*	15,359.62	$y^4F^o_{4\frac{1}{2}} - f^4F_{3\frac{1}{2}}$
4	6504.213*v*	15	15,370.41	$z^4G^o_{4\frac{1}{2}} - e^4F_{3\frac{1}{2}}$
3	6502.29	1	15,374.96	$x^4D_{2\frac{1}{2}} - 5_{1\frac{1}{2}\cdot 2\frac{1}{2}}$
3	6496.18	1	15,389.42	$y^2D^o_{1\frac{1}{2}} - e^2D_{1\frac{1}{2}}$
4	6490.344*v*	6–III	15,403.26	$a^2G_{4\frac{1}{2}} - z^2F^o_{3\frac{1}{2}}$
8	6483.305	1*n*	15,419.98	$z^2F^o_{2\frac{1}{2}} - f^4F_{3\frac{1}{2}}$
7	6482.806	2*h*	15,421.17	$a^2P_{\frac{1}{2}} - y^4F^o_{1\frac{1}{2}}$
4	6477.861*v*	10–V	15,432.94	$z^4D^o_{1\frac{1}{2}} - e^4F_{2\frac{1}{2}}$
4	6474.558*v*	25*w*	15,440.81	$c^2D_{1\frac{1}{2}} - x^2D^o_{1\frac{1}{2}}$
4	6470.128*v*	3	15,451.38	$c^2D_{1\frac{1}{2}} - x^2D^o_{2\frac{1}{2}}$
4	6463.060*v*	25*h*	15,468.28	$y^2D^o_{2\frac{1}{2}} - e^4D_{2\frac{1}{2}}$
4	6454.998*v*	40–III	15,487.60	$z^4D^o_{3\frac{1}{2}} - e^4F_{4\frac{1}{2}}$
4	6451.136*v*	3*n*–V	15,496.87	$y^4D^o_{3\frac{1}{2}} - f^4F_{4\frac{1}{2}}$
4	6450.230*v*	80–I	15,499.05	$a^4P_{2\frac{1}{2}} - z^4D^o_{3\frac{1}{2}}$ $(a^2G_{4\frac{1}{2}} - z^2G^o_{4\frac{1}{2}})$
4	6444.678*v*	2–V	15,512.40	$z^4G^o_{4\frac{1}{2}} - e^4F_{4\frac{1}{2}}$
5	6439.171	80	15,525.67	
4	6431.075*v*	5*h*	15,545.21	$y^4G^o_{3\frac{1}{2}} - f^4F_{3\frac{1}{2}}$
7	6430.342	2–V	15,546.98	$y^4D^o_{2\frac{1}{2}} - f^4F_{2\frac{1}{2}}$
4	6429.913*v*	4–III	15,548.02	$a^2G_{4\frac{1}{2}} - z^2F^o_{3\frac{1}{2}}$
5	6425.115	5	15,559.63	$a^2G_{4\frac{1}{2}} - y^4D^o_{3\frac{1}{2}}$
4	6421.703*v*	2–V	15,567.90	$y^4D^o_{1\frac{1}{2}} - f^4F_{2\frac{1}{2}}$
5	6417.824	15–III	15,577.31	$a^2P_{\frac{1}{2}} - z^2D^o_{1\frac{1}{2}}$
9	6414.67	1	15,584.97	$y^2D^o_{1\frac{1}{2}} - e^2D_{2\frac{1}{2}}$
4	6407.510*v*	1	15,602.38	$y^2F^o_{3\frac{1}{2}} - e^4D_{3\frac{1}{2}}$
5	6396.524	2–V	15,629.18	$y^4D^o_{2\frac{1}{2}} - f^4F_{1\frac{1}{2}}$
4	6395.158*v*	8–V	15,632.52	$z^4D^o_{\frac{1}{2}} - e^4F_{1\frac{1}{2}}$
5	6386.69	5*h*	15,653.25	$z^2F^o_{2\frac{1}{2}} - f^4F_{3\frac{1}{2}}$
3	6366.20	1*w*	15,703.62	$y^2F^o_{2\frac{1}{2}} - e^4P_{1\frac{1}{2}}$
8	6352.751	2*h*	15,736.87	$y^4G^o_{4\frac{1}{2}} - f^4F_{3\frac{1}{2}}$
4	6351.448*v*	2–V	15,740.10	$y^2F^o_{3\frac{1}{2}} - g^4F_{2\frac{1}{2}}$
4	6347.843*v*	10–V	15,749.04	$y^2F^o_{3\frac{1}{2}} - g^4F_{3\frac{1}{2}}$
4	6340.805*v*	10	15,766.52	$c^2D_{2\frac{1}{2}} - w^4D^o_{1\frac{1}{2}}$

REF.	λ *IA*	INT.–*TC*	WAVE NO. VAC.	MULTIPLET DESIGNATION
4	6337.963*v*	5	15,773.59	$z^4G^o_{4\frac{1}{2}} - e^4F_{3\frac{1}{2}}$
8	6322.919	2*h*	15,811.12	$z^4D^o_{3\frac{1}{2}} - e^4F_{3\frac{1}{2}}$
4	6320.418*v*	8–IV	15,817.37	$y^2F^o_{3\frac{1}{2}} - e^4G_{4\frac{1}{2}}$
8	6318.551	4*n*	15,822.05	$z^4G^o_{4\frac{1}{2}} - e^2F_{3\frac{1}{2}}$
5	6315.779	2*h*	15,828.99	$b^2P_{1\frac{1}{2}} - y^2F^o_{2\frac{1}{2}}$
4	6314.528*v*	50	15,832.13	$y^2F^o_{2\frac{1}{2}} - e^4G_{3\frac{1}{2}}$
4	6313.032*v*	50	15,835.88	$z^4G^o_{4\frac{1}{2}} - e^4F_{3\frac{1}{2}}$
3	6302.50	1	15,862.34	$x^4G^o_{5\frac{1}{2}} - g^4H_{4\frac{1}{2}}$
3	6296.96	2*h*	15,876.30	$a^2D_{2\frac{1}{2}} - y^4D^o_{2\frac{1}{2}}$
4	6291.829*v*	5	15,889.24	$z^4F^o_{4\frac{1}{2}} - e^4F_{3\frac{1}{2}}$
4	6282.636*v*	40–I	15,912.49	$a^4P_{1\frac{1}{2}} - z^4D^o_{1\frac{1}{2}}$
3	6278.19	1	15,923.76	$z^4S^o_{1\frac{1}{2}} - g^4P_{1\frac{1}{2}}$
4	6276.608*v*	40	15,927.78	$z^4D^o_{2\frac{1}{2}} - e^4F_{2\frac{1}{2}}$ $(y^4D^o_{1\frac{1}{2}} - f^4F_{1\frac{1}{2}})$
5	6275.133#	25	15,931.52	$z^4D^o_{1\frac{1}{2}} - e^4F_{1\frac{1}{2}}$
5	6273.026	4–III?	15,936.87	$z^2F^o_{2\frac{1}{2}} - f^4F_{2\frac{1}{2}}$ $z^4G^o_{3\frac{1}{2}} - e^4F_{4\frac{1}{2}}$ $a^2G_{4\frac{1}{2}} - y^4G^o_{5\frac{1}{2}}$ $a^4P_{2\frac{1}{2}} - z^4G^o_{3\frac{1}{2}}$
7	6271.900	1	15,939.73	$y^2D^o_{2\frac{1}{2}} - e^4P_{1\frac{1}{2}}$
4	6271.472*v*	5	15,940.82	$a^2D_{2\frac{1}{2}} - z^2G^o_{3\frac{1}{2}}$
3	6265.97	1	15,954.82	$a^2P_{1\frac{1}{2}} - z^2D^o_{1\frac{1}{2}}$ $(a^2G_{4\frac{1}{2}} - y^4G^o_{5\frac{1}{2}})$
5	6262.825	5*h*	15,962.82	
4	6257.578*v*	6–III	15,976.22	$z^4D^o_{2\frac{1}{2}} - e^4F_{2\frac{1}{2}}$
4	6257.066*v*	3	15,977.52	$y^2D^o_{2\frac{1}{2}} - g^4F_{3\frac{1}{2}}$
5	6253.940	2*h*	15,985.51	$z^2G^o_{3\frac{1}{2}} - f^4F_{3\frac{1}{2}}$
4	6249.504*v*	8–II	15,996.86	$a^2G_{4\frac{1}{2}} - y^4G^o_{4\frac{1}{2}}$
4	6247.284*v*	8	16,002.54	$y^2D^o_{2\frac{1}{2}} - f^4F_{3\frac{1}{2}}$
4	6246.389*v*	5*h*	16,004.83	$z^4F^o_{3\frac{1}{2}} - e^4F_{4\frac{1}{2}}$
4	6232.440*v*	2–IV?	16,040.65	$c^2D_{2\frac{1}{2}} - z^2F^o_{3\frac{1}{2}}$
5	6230.968	10–III	16,044.44	$a^4P_{\frac{1}{2}} - z^4D^o_{\frac{1}{2}}$
4	6223.355*v*	10	16,064.07	$y^4D^o_{3\frac{1}{2}} - f^4F_{4\frac{1}{2}}$
5	6222.329	3	16,066.72	$a^4P_{1\frac{1}{2}} - z^4G^o_{2\frac{1}{2}}$
4	6211.197*v*	2–IV?	16,095.51	$y^2D^o_{1\frac{1}{2}} - f^4F_{2\frac{1}{2}}$
5	6205.503	3*h*	16,110.28	$y^4F^o_{3\frac{1}{2}} - e^4D_{2\frac{1}{2}}$
5	6203.701	2*h*	16,114.96	$x^4G^o_{5\frac{1}{2}} - g^4H_{5\frac{1}{2}}$
5	6197.837	5*h*	16,130.21	$y^4F^o_{4\frac{1}{2}} - e^4D_{3\frac{1}{2}}$
4	6193.540*v*	15	16,141.40	$z^4G^o_{5\frac{1}{2}} - e^4F_{5\frac{1}{2}}$
4	6189.005*v*	10–IIA	16,153.23	$a^4P_{2\frac{1}{2}} - z^4D^o_{2\frac{1}{2}}$
3	6181.90	1	16,171.79	$x^4G^o_{4\frac{1}{2}} - g^4H_{4\frac{1}{2}}$
4	6181.008*v*	10*h*	16,174.13	$y^4D^o_{3\frac{1}{2}} - f^4F_{4\frac{1}{2}}$
5	6175.029	2	16,189.79	$z^4G^o_{5\frac{1}{2}} - e^4F_{5\frac{1}{2}}$
3	6171.43	1	16,199.23	$x^4D^o_{3\frac{1}{2}} - g^4P_{2\frac{1}{2}}$
3	6168.86	2*h*	16,205.97	$a^2G_{4\frac{1}{2}} - y^2G^o_{4\frac{1}{2}}$
3	6160.04	1	16,229.18	$a^2G_{4\frac{1}{2}} - z^2D^o_{3\frac{1}{2}}$
3	6158.53	2*h*	16,233.16	$a^2G_{4\frac{1}{2}} - y^4F^o_{4\frac{1}{2}}$
3	6146.38	3*h*	16,265.25	$a^2G_{4\frac{1}{2}} - z^2G^o_{4\frac{1}{2}}$
7	6143.764	5*h*	16,272.17	$z^4G^o_{5\frac{1}{2}} - e^4F_{4\frac{1}{2}}$
5	6132.410	10*h*	16,302.30	$z^4D^o_{1\frac{1}{2}} - e^2F_{2\frac{1}{2}}$
3	6130.41	1	16,307.62	$a^4P_{2\frac{1}{2}} - z^4G^o_{3\frac{1}{2}}$
4	6129.118*v*	20*w*	16,311.06	$a^2D_{1\frac{1}{2}} - z^2F^o_{2\frac{1}{2}}$
4	6128.214*v*	5	16,313.46	$z^4F^o_{4\frac{1}{2}} - e^4F_{3\frac{1}{2}}$
4	6122.640*v*	8–IV?	16,328.31	$z^4F^o_{4\frac{1}{2}} - e^4F_{4\frac{1}{2}}$
4	6116.994*v*	8–I	16,343.38	$a^4P_{\frac{1}{2}} - z^4D^o_{\frac{1}{2}}$
4	6107.937*v*	2–V	16,367.62	$y^2D^o_{2\frac{1}{2}} - e^2D_{2\frac{1}{2}}$
5	6105.470	10*h*	16,374.23	$a^2G_{4\frac{1}{2}} - y^4F^o_{4\frac{1}{2}}$
4	6100.778*v*	4*h*	16,386.83	$y^2F^o_{3\frac{1}{2}} - e^4H_{4\frac{1}{2}}$
8	6098.270	3	16,393.56	$x^4G^o_{5\frac{1}{2}} - g^4H_{4\frac{1}{2}}$
4	6093.144*v*	10–I	16,407.35	$a^4P_{1\frac{1}{2}} - z^4D^o_{1\frac{1}{2}}$
4	6086.663*v*	7–II?	16,424.83	$c^2D_{2\frac{1}{2}} - z^2D^o_{2\frac{1}{2}}$
5	6083.283	2*h*	16,433.96	$y^2F^o_{3\frac{1}{2}} - g^2F_{3\frac{1}{2}}$
4	6082.431*v*	15–III	16,436.25	$z^4F^o_{4\frac{1}{2}} - e^4F_{4\frac{1}{2}}$
4	6070.671*v*	2–V	16,468.09	$y^2D^o_{1\frac{1}{2}} - e^2D_{1\frac{1}{2}}$
4	6058.233*v*	3	16,501.90	$z^2G^o_{4\frac{1}{2}} - f^4F_{3\frac{1}{2}}$
4	6049.110*v*	6–V	16,526.79§	$y^2F^o_{3\frac{1}{2}} - e^2G_{4\frac{1}{2}}$
4	6015.384*v*	2	16,619.45	$y^2F^o_{3\frac{1}{2}} - g^4F_{3\frac{1}{2}}$
4	6013.653*v*	30†	16,624.23	$y^2D^o_{2\frac{1}{2}} - e^4H_{4\frac{1}{2}}$
4	6011.402*v*	2*h*	16,630.46	$z^4D^o_{2\frac{1}{2}} - e^4F_{3\frac{1}{2}}$
4	6007.690*v*	5–V	16,640.73	$y^2F^o_{3\frac{1}{2}} - f^2F_{3\frac{1}{2}}$
4	6006.352*v*	5–IV?	16,644.44	$y^2F^o_{3\frac{1}{2}} - f^2F_{2\frac{1}{2}}$
4	6005.030*v*	8	16,648.11	$a^4P_{2\frac{1}{2}} - z^4D^o_{3\frac{1}{2}}$
4	6002.459*v*	2	16,655.24	$z^4G^o_{4\frac{1}{2}} - e^2F_{3\frac{1}{2}}$
4	6000.668*v*	5–I	16,660.21§	$z^4F^o_{3\frac{1}{2}} - e^4F_{3\frac{1}{2}}$?
4	5996.915*v*	2	16,670.63	$y^2F^o_{3\frac{1}{2}} - e^4H_{4\frac{1}{2}}$
3	5993.48	1	16,680.19	$a^2D_{2\frac{1}{2}} - y^4D^o_{3\frac{1}{2}}$
4	5991.890*v*	20–III	16,684.62	$a^2D_{2\frac{1}{2}} - z^2D^o_{2\frac{1}{2}}$
3	5990.46	1	16,688.60	$a^2D_{2\frac{1}{2}} - y^4F^o_{3\frac{1}{2}}$
3	5989.58	1	16,691.05	$y^4D^o_{3\frac{1}{2}} - f^4F_{3\frac{1}{2}}$
8	5984.582	4*n*	16,704.99	$c^2D_{2\frac{1}{2}} - w^4F^o_{3\frac{1}{2}}$
4	5984.253*v*	3–III?	16,705.91	$y^2F^o_{3\frac{1}{2}} - e^2G_{4\frac{1}{2}}$
4	5984.092*v*	3–III?	16,706.36	$a^4P_{1\frac{1}{2}} - z^4D^o_{\frac{1}{2}}$
4	5983.278*v*	2	16,708.63	$z^4F^o_{3\frac{1}{2}} - e^2F_{3\frac{1}{2}}$
4	5981.990*v*	3*h*	16,712.22	$a^2G_{4\frac{1}{2}} - y^4F^o_{5\frac{1}{2}}$
5	5965.661	2*h*	16,757.96	$z^4D^o_{2\frac{1}{2}} - e^4F_{3\frac{1}{2}}$
11	5965.040	2*h*	16,759.72	$z^4F^o_{4\frac{1}{2}} - e^4F_{4\frac{1}{2}}$
3	5963.39	1	16,764.35	$y^2D^o_{2\frac{1}{2}} - e^2G_{3\frac{1}{2}}$
3	5951.73	2	16,797.20	$z^4D^o_{2\frac{1}{2}} - e^2F_{2\frac{1}{2}}$
4	5946.484*v*	5–III	16,812.01	$z^4F^o_{4\frac{1}{2}} - e^4F_{4\frac{1}{2}}$
7	5940.424	1	16,829.16	$y^2D^o_{2\frac{1}{2}} - g^2F_{3\frac{1}{2}}$
10	5939.86	1	16,830.76	$z^4G^o_{5\frac{1}{2}} - e^4F_{4\frac{1}{2}}$

† Wave-length 6013.582 (M. I. T.).

§ Line probably a blend.

TABLE VIII.—*Continued.*

Ref.	λ *IA*	Int.–*TC*	Wave No. Vac.	Multiplet Designation
4	5935.391*v*	6–III	16,843.44	$b^4P_{2\frac{1}{2}} - y^4D^o_{3\frac{1}{2}}$
10	5923.13	1	16,878.30	$y^2D^o_{2\frac{1}{2}} - f^2F_{3\frac{1}{2}}$
5	5922.365	3	16,880.48	$b^4P_{1\frac{1}{2}} - y^4D^o_{2\frac{1}{2}}$
3	5916.88	2*h*	16,896.13	$x^4D^o_{3\frac{1}{2}} - g^4P_{2\frac{1}{2}}$
4	5915.551*v*	10–III	16,899.92	$a^2G_{3\frac{1}{2}} - y^2G^o_{3\frac{1}{2}}$
4	5905.584*v*	2*h*	16,928.45	$z^4D^o_{3\frac{1}{2}} - e^4F_{4\frac{1}{2}}$
4	5890.487*v*	12–III	16,971.83	$a^2G_{4\frac{1}{2}} - y^2G^o_{4\frac{1}{2}}$
4	5886.52	1	16,983.27	$c^2D_{2\frac{1}{2}} - y^4P^o_{2\frac{1}{2}}$
3	5883.421*v*	3	16,992.22	$a^2D_{1\frac{1}{2}} - z^2D^o_{2\frac{1}{2}}$
4	5881.077	2–I?	16,998.99	$a^2G_{4\frac{1}{2}} - y^4F^o_{3\frac{1}{2}}$
5	5878.047	1	17,007.75	$b^4P_{1\frac{1}{2}} - z^2F^o_{2\frac{1}{2}}$
11	5877.427*v*	4*h*	17,009.54	$y^2F^o_{3\frac{1}{2}} - e^2D_{2\frac{1}{2}}$
4	5876.102*v*	4*h*	17,013.38	$y^2F^o_{2\frac{1}{2}} - e^2D_{1\frac{1}{2}}$
4	5846.575*v*	2–V	17,099.30	$z^4F^o_{3\frac{1}{2}} - e^4F_{3\frac{1}{2}}$
4	5834.628*v*	1	17,134.32	$y^2G^o_{3\frac{1}{2}} - e^4G_{4\frac{1}{2}}$
4	5830.070*v*	4–V	17,147.71	$z^4F^o_{4\frac{1}{2}} - e^2F_{3\frac{1}{2}}$
4	5826.299*v*	3	17,158.81	$z^4F^o_{3\frac{1}{2}} - e^4F_{4\frac{1}{2}}$
3	5818.09	2	17,183.02	$z^4F^o_{4\frac{1}{2}} - e^2F_{3\frac{1}{2}}$
3	5806.34	1	17,217.79	$c^2D_{1\frac{1}{2}} - w^2D^o_{2\frac{1}{2}}$
3	5793.92	1Fe?	17,254.70	$y^4F^o_{3\frac{1}{2}} - e^2P_{1\frac{1}{2}}$
4	5790.084*v*	2	17,266.13	$y^2F^o_{3\frac{1}{2}} - e^4H_{4\frac{1}{2}}$
4	5774.375*v*	2	17,313.10	$y^2F^o_{3\frac{1}{2}} - g^2F_{3\frac{1}{2}}$
4	5770.443*v*	2–V	17,324.90	$y^2F^o_{4\frac{1}{2}} - e^2H_{4\frac{1}{2}}$
3	5768.71	1	17,330.10	$z^4F^o_{4\frac{1}{2}} - e^4F_{5\frac{1}{2}}$
3	5760.39	1	17,355.13	$z^4G^o_{5\frac{1}{2}} - e^4F_{5\frac{1}{2}}$?
11	5754.079	1	17,374.17	$y^2F^o_{3\frac{1}{2}} - g^2F_{3\frac{1}{2}}$
5	5752.883	2*h*	17,377.78	$z^4G^o_{5\frac{1}{2}} - e^4F_{4\frac{1}{2}}$
5	5750.952	2	17,383.61	$y^2D^o_{1\frac{1}{2}} - h^4F_{2\frac{1}{2}}$
10	5741.50	1	17,412.23	$z^4D^o_{3\frac{1}{2}} - e^4F_{3\frac{1}{2}}$
5	5740.986	2*h*	17,413.79	$y^2F^o_{4\frac{1}{2}} - h^4F_{4\frac{1}{2}}$
3	5739.59	1	17,418.03	$a^2D_{2\frac{1}{2}} - y^4F^o_{3\frac{1}{2}}$
3	5736.52	1	17,427.35	$y^2G^o_{4\frac{1}{2}} - e^4D_{3\frac{1}{2}}$
3	5734.25	1	17,434.25	$c^2D_{2\frac{1}{2}} - x^4P^o_{2\frac{1}{2}}$
3	5733.28	1	17,437.20	$z^4G^o_{4\frac{1}{2}} - e^4F_{3\frac{1}{2}}$
3	5730.45	1	17,445.81	$z^4F^o_{3\frac{1}{2}} - e^4F_{4\frac{1}{2}}$
3	5720.80	1	17,475.24	$a^2D_{1\frac{1}{2}} - y^4F^o_{2\frac{1}{2}}$
10	5715.91	1	17,490.19	$z^4F^o_{4\frac{1}{2}} - e^4F_{5\frac{1}{2}}$
4	5706.160*v*	1	17,520.07	$y^2F^o_{3\frac{1}{2}} - f^2F_{3\frac{1}{2}}$
5	5703.031	2*h*	17,529.68	$z^4F^o_{3\frac{1}{2}} - e^2F_{2\frac{1}{2}}$
3	5696.75	1	17,549.01	$b^4P_{2\frac{1}{2}} - z^2G^o_{3\frac{1}{2}}$
5	5688.593	2–II	17,574.17	$a^2D_{2\frac{1}{2}} - z^2D^o_{3\frac{1}{2}}$
11	5688.169	1	17,575.48	$y^4F^o_{4\frac{1}{2}} - e^4F_{3\frac{1}{2}}$
3	5686.96	3	17,579.22	$z^4F^o_{4\frac{1}{2}} - e^2F_{3\frac{1}{2}}$
3	5684.69	1	17,586.24	$y^4F^o_{3\frac{1}{2}} - e^4D_{3\frac{1}{2}}$
10	5681.04	1	17,597.54	$b^4P_{2\frac{1}{2}} - z^2F^o_{2\frac{1}{2}}$
11	5679.637	1	17,601.89	$y^2D^o_{2\frac{1}{2}} - h^4F_{3\frac{1}{2}}$?
3	5676.49	2	17,611.64	$y^2D^o_{2\frac{1}{2}} - g^2F_{2\frac{1}{2}}$
5	5675.421	3*h*	17,614.96	$y^4F^o_{3\frac{1}{2}} - e^4D_{2\frac{1}{2}}$
4	5659.121*v*	3–II	17,665.70	$a^2G_{4\frac{1}{2}} - y^2G^o_{3\frac{1}{2}}$
3	5656.10	1	17,675.13	$b^2D_{1\frac{1}{2}} - x^4D^o_{1\frac{1}{2}}$
5	5651.734	3*h*	17,688.79	$\left\{\begin{matrix} b^4P_{1\frac{1}{2}} - z^2D^o_{2\frac{1}{2}} \\ z^2D^o_{1\frac{1}{2}} - e^2P_{1\frac{1}{2}} \end{matrix}\right.$
4	5647.234*v*	12–II	17,702.88	$a^2P_{1\frac{1}{2}} - y^2D^o_{2\frac{1}{2}}$
5	5643.087	5*h*	17,715.89	$c^2D_{1\frac{1}{2}} - z^2D^o_{1\frac{1}{2}}$
5	5642.542	2*h*	17,717.60	$z^2D^o_{2\frac{1}{2}} - g^4F_{3\frac{1}{2}}$
5	5639.991	1–III*A*	17,725.62	$a^2D_{1\frac{1}{2}} - y^4F^o_{2\frac{1}{2}}$
4	5637.734*v*	3–V	17,732.71	$y^4F^o_{4\frac{1}{2}} - g^4F_{5\frac{1}{2}}$
4	5636.455*v*	1	17,736.73	$z^2D^o_{2\frac{1}{2}} - g^4F_{3\frac{1}{2}}$
4	5636.128*v*	3–V	17,737.77	$z^2D^o_{2\frac{1}{2}} - e^2P_{1\frac{1}{2}}$
5	5627.726	2	17,764.25	$y^2G^o_{4\frac{1}{2}} - e^4G_{5\frac{1}{2}}$
5	5616.077	5	17,801.09	$y^4F^o_{3\frac{1}{2}} - e^4G_{4\frac{1}{2}}$
9	5602.26	1	17,845.00	$y^4F^o_{4\frac{1}{2}} - e^2P_{1\frac{1}{2}}$
5	5598.478	50Ca?	17,857.05	$b^2G_{4\frac{1}{2}} - 19^o_{3\frac{1}{2}}$
4	5594.778*v*	2	17,868.86	$y^4G^o_{5\frac{1}{2}} - e^4P_{2\frac{1}{2}}$
10	5593.13	1	17,874.13	$z^4F^o_{3\frac{1}{2}} - e^4F_{3\frac{1}{2}}$
5	5592.185	2	17,877.15	$z^4F^o_{4\frac{1}{2}} - e^4F_{4\frac{1}{2}}$
4	5590.744*v*	10–II	17,881.75	$a^2D_{1\frac{1}{2}} - z^2D^o_{1\frac{1}{2}}$
3	5589.27	1*g*?	17,886.47	$y^4G^o_{5\frac{1}{2}} - e^4D_{3\frac{1}{2}}$
3	5581.28	2	17,912.08	$z^2D^o_{2\frac{1}{2}} - e^4D_{1\frac{1}{2}}$
11	5576.045	1	17,928.89	$y^2F^o_{3\frac{1}{2}} - h^4F_{3\frac{1}{2}}$
9	5573.65	1	17,936.60	$y^2G^o_{4\frac{1}{2}} - g^4F_{3\frac{1}{2}}$
11	5569.678	1Fe?	17,949.39	$b^2D_{1\frac{1}{2}} - x^4D^o_{1\frac{1}{2}}$?
3	5565.87	1	17,961.67	$y^2G^o_{4\frac{1}{2}} - f^2F_{3\frac{1}{2}}$?
3	5563.69	1	17,968.71	$z^4F^o_{3\frac{1}{2}} - e^2F_{2\frac{1}{2}}$
4	5558.825*v*	2–III?	17,984.42	$c^2D_{1\frac{1}{2}} - w^2D^o_{1\frac{1}{2}}$
5	5546.968	4	18,022.88	$y^2G^o_{4\frac{1}{2}} - e^4G_{4\frac{1}{2}}$
4	5545.937*v*	2–III?	18,026.22	$y^4G^o_{4\frac{1}{2}} - g^4F_{3\frac{1}{2}}$
9	5544.28	1	18,031.61	$c^2D_{1\frac{1}{2}} - v^4D^o_{1\frac{1}{2}}$
11	5533.070	1	18,068.14	$y^4F^o_{4\frac{1}{2}} - e^4D_{3\frac{1}{2}}$
4	5530.780*v*	10–II	18,075.62	$a^4P_{2\frac{1}{2}} - z^2F^o_{2\frac{1}{2}}$
3	5527.19	1	18,087.36	$y^4F^o_{2\frac{1}{2}} - e^4P_{1\frac{1}{2}}$
11	5525.674	1	18,092.33	$c^2D_{1\frac{1}{2}} - y^4S^o_{1\frac{1}{2}}$
4	5524.990*v*	4–V	18,094.55	$y^4G^o_{5\frac{1}{2}} - e^4G_{4\frac{1}{2}}$
7	5523.968	1	18,097.92	$z^2D^o_{2\frac{1}{2}} - e^4D_{2\frac{1}{2}}$
4	5523.310*v*	8–II?	18,100.07	$a^2P_{1\frac{1}{2}} - y^2D^o_{1\frac{1}{2}}$
4	5515.990*v*	3*h*	18,124.09	$y^4F^o_{3\frac{1}{2}} - g^4F_{3\frac{1}{2}}$
3	5508.29	1	18,149.43	$y^4F^o_{4\frac{1}{2}} - f^2F_{3\frac{1}{2}}$?
3	5503.23	1	18,166.11	$y^2D^o_{2\frac{1}{2}} - h^4F_{2\frac{1}{2}}$
11	5501.511	1	18,171.79	$b^4P_{1\frac{1}{2}} - y^4F^o_{2\frac{1}{2}}$
11	5497.557	1	18,184.86	$y^4F^o_{4\frac{1}{2}} - f^4G_{5\frac{1}{2}}$
4	5495.682*v*	2–III?	18,191.06	$c^2D_{2\frac{1}{2}} - w^2D^o_{2\frac{1}{2}}$
4	5489.666*v*	5–III?	18,211.00	$y^4F^o_{4\frac{1}{2}} - e^4D_{3\frac{1}{2}}$
4	5488.121*v*	1	18,216.12	$y^4F^o_{3\frac{1}{2}} - e^4G_{4\frac{1}{2}}$
4	5483.962*v*	10–V	18,229.94	$z^4D^o_{2\frac{1}{2}} - f^4F_{3\frac{1}{2}}$
4	5483.354*v*	40–I	18,231.96	$a^4P_{2\frac{1}{2}} - y^4D^o_{2\frac{1}{2}}$
9	5479.74	1	18,243.99	$y^4F^o_{4\frac{1}{2}} - h^4F_{3\frac{1}{2}}$
4	5477.089*v*	5–V	18,252.82	$z^4D^o_{3\frac{1}{2}} - f^4F_{3\frac{1}{2}}$
5	5476.906	400*w*Ni	18,253.42	$(y^4F^o_{3\frac{1}{2}} - g^2F_{2\frac{1}{2}})$
10	5476.47	<1	18,254.88	$z^4G^o_{4\frac{1}{2}} - f^4F_{4\frac{1}{2}}$
4	5470.460*v*	4–V	18,274.92	$z^4D^o_{1\frac{1}{2}} - f^4F_{2\frac{1}{2}}$
5	5469.305	4–III*A*	18,278.79	$b^4P_{2\frac{1}{2}} - z^2D^o_{2\frac{1}{2}}$
9	5457.45	1	18,318.50	$y^4F^o_{3\frac{1}{2}} - e^4D_{3\frac{1}{2}}$
4	5454.573*v*	20–V	18,328.16	$y^4F^o_{4\frac{1}{2}} - g^4F_{4\frac{1}{2}}$
4	5453.338*v*	1	18,332.31	$y^4F^o_{4\frac{1}{2}} - e^4H_{5\frac{1}{2}}$
4	5452.305*v*	3–V	18,335.78	$z^4D^o_{2\frac{1}{2}} - f^4F_{1\frac{1}{2}}$
9	5447.93	1	18,350.51	$z^2D^o_{2\frac{1}{2}} - g^4F_{1\frac{1}{2}}$
4	5444.585*v*	20–IV?	18,361.78	$y^4F^o_{4\frac{1}{2}} - e^4G_{5\frac{1}{2}}$
4	5437.002*v*	3–III?	18,387.39	$y^4G^o_{5\frac{1}{2}} - e^4D_{4\frac{1}{2}}$
4	5434.576*v*	2–III?	18,395.60	$y^4G^o_{5\frac{1}{2}} - g^4F_{5\frac{1}{2}}$
4	5431.027*v*	2–V	18,407.62	$c^2D_{2\frac{1}{2}} - x^4P^o_{1\frac{1}{2}}$
10	5428.00	0	18,417.89	$z^2F^o_{3\frac{1}{2}} - g^4F_{3\frac{1}{2}}$
12	5427.39	2	18,419.96	$z^2D^o_{1\frac{1}{2}} - e^4G_{2\frac{1}{2}}$
12	5427.21	2	18,420.57	$y^4G^o_{3\frac{1}{2}} - f^2F_{3\frac{1}{2}}$
4	5426.734*v*	1	18,422.18	$b^4P_{1\frac{1}{2}} - y^4F^o_{1\frac{1}{2}}$
4	5425.621*v*	4	18,425.96	$\left\{\begin{matrix} y^4F^o_{4\frac{1}{2}} - e^4G_{4\frac{1}{2}} \\ (b^2D_{2\frac{1}{2}} - x^4D^o_{2\frac{1}{2}}) \end{matrix}\right.$
9	5421.98	1	18,438.34	$y^4F^o_{3\frac{1}{2}} - e^4D_{2\frac{1}{2}}$
7	5413.734	2–V	18,466.42	$z^4G^o_{5\frac{1}{2}} - f^4F_{5\frac{1}{2}}$
5	5408.119	2–III?	18,485.59	$a^2P_{1\frac{1}{2}} - y^2D^o_{1\frac{1}{2}}$
4	5407.520*v*	5–V	18,487.64	$y^4G^o_{5\frac{1}{2}} - e^4G_{5\frac{1}{2}}$
4	5402.000*v*	3–V	18,506.53	$y^4F^o_{4\frac{1}{2}} - g^4F_{4\frac{1}{2}}$
4	5399.762*v*	10	18,514.20	$y^4F^o_{3\frac{1}{2}} - e^2D_{2\frac{1}{2}}$
5	5393.729	3*h*	18,534.91	$z^2G^o_{4\frac{1}{2}} - e^4G_{4\frac{1}{2}}$
12	5390.81	2	18,544.95	$y^4D^o_{3\frac{1}{2}} - g^4F_{3\frac{1}{2}}$
4	5390.478*v*	2–IV?	18,546.09	$y^4D^o_{2\frac{1}{2}} - e^2P_{1\frac{1}{2}}$
4	5381.776*v*	6–V	18,576.07	$y^4F^o_{3\frac{1}{2}} - e^4G_{3\frac{1}{2}}$
5	5381.105	5–III	18,578.39	$b^4P_{1\frac{1}{2}} - z^2D^o_{2\frac{1}{2}}$
9	5378.20	1	18,588.42	$y^4G^o_{4\frac{1}{2}} - e^4D_{3\frac{1}{2}}$
4	5373.958*v*	1	18,603.10	$y^4F^o_{3\frac{1}{2}} - g^4F_{3\frac{1}{2}}$
9	5372.75	1	18,607.32	$z^2D^o_{2\frac{1}{2}} - g^4F_{2\frac{1}{2}}$
7	5370.350	1	18,615.60	$z^4G^o_{5\frac{1}{2}} - f^4F_{5\frac{1}{2}}$
4	5369.591*v*	20–I	18,618.23	$a^4P_{1\frac{1}{2}} - y^4D^o_{2\frac{1}{2}}$
4	5368.904*v*	30	18,620.61	$c^2D_{1\frac{1}{2}} - y^2P^o_{1\frac{1}{2}}$
4	5366.743*v*	5	18,628.11	$y^4F^o_{4\frac{1}{2}} - f^2F_{3\frac{1}{2}}$
4	5364.816*v*	4	18,634.80	$z^4D^o_{1\frac{1}{2}} - f^4F_{1\frac{1}{2}}$
4	5362.781*v*	15–III	18,641.87	$y^2G^o_{4\frac{1}{2}} - e^2H_{4\frac{1}{2}}$
4	5359.200*v*	6–III?	18,654.33	$y^4F^o_{3\frac{1}{2}} - e^4H_{4\frac{1}{2}}$
5	5358.923	2–IV	18,655.29	$y^2G^o_{4\frac{1}{2}} - f^2F_{3\frac{1}{2}}$
9	5358.01	1	18,658.47	$c^2D_{1\frac{1}{2}} - w^4F^o_{2\frac{1}{2}}$
4	5353.500*v*	25–III	18,674.19	$\left\{\begin{matrix} y^2G^o_{4\frac{1}{2}} - e^2H_{5\frac{1}{2}} \\ (a^2D_{2\frac{1}{2}} - y^2F^o_{3\frac{1}{2}}) \end{matrix}\right.$
4	5352.046*v*	20–III	18,679.26	$z^4G^o_{5\frac{1}{2}} - f^4F_{4\frac{1}{2}}$
4	5349.091*v*	4–V	18,689.58	$y^4F^o_{3\frac{1}{2}} - e^2G_{4\frac{1}{2}}$?
4	5347.499*v*	4–V	18,695.15	$y^4F^o_{4\frac{1}{2}} - e^4G_{5\frac{1}{2}}$
4	5344.570*v*	10	18,705.39	$y^4G^o_{4\frac{1}{2}} - g^4F_{4\frac{1}{2}}$
4	5343.383*v*	20–III	18,709.55	$y^4G^o_{4\frac{1}{2}} - e^4H_{5\frac{1}{2}}$
4	5342.703*v*	50–III	18,711.93	$y^4G^o_{5\frac{1}{2}} - e^4H_{6\frac{1}{2}}$
4	5341.328*v*	7–V	18,716.74	$y^2G^o_{4\frac{1}{2}} - e^2G_{4\frac{1}{2}}$
5	5339.528	4–V	18,723.05	$y^2G^o_{3\frac{1}{2}} - e^2G_{3\frac{1}{2}}$
7	5337.330	1*n*	18,730.76	$y^2G^o_{4\frac{1}{2}} - h^4F_{4\frac{1}{2}}$
4	5336.163*v*	3–V	18,734.86	$y^4G^o_{4\frac{1}{2}} - g^4F_{3\frac{1}{2}}$
4	5334.821*v*	6–V	18,739.57	$\left\{\begin{matrix} y^4G^o_{5\frac{1}{2}} - g^4F_{4\frac{1}{2}} \\ (y^4G^o_{4\frac{1}{2}} - e^4G_{4\frac{1}{2}}) \end{matrix}\right.$
4	5333.647*v*	5–III	18,743.70	$y^4G^o_{5\frac{1}{2}} - e^4H_{5\frac{1}{2}}$
4	5332.652*v*	5–III	18,747.20	$z^4F^o_{4\frac{1}{2}} - f^4F_{4\frac{1}{2}}$
4	5331.456*v*	15–II	18,751.40	$a^4P_{1\frac{1}{2}} - y^4D^o_{1\frac{1}{2}}$
10	5329.82	1	18,757.16	$y^4F^o_{2\frac{1}{2}} - g^4F_{1\frac{1}{2}}$?
9	5328.01	2–V	18,763.53	
5	5326.247	3–IV	18,769.74	$z^4D^o_{2\frac{1}{2}} - f^4F_{2\frac{1}{2}}$
4	5325.949*v*	4–III	18,770.79	$y^4F^o_{3\frac{1}{2}} - e^4H_{5\frac{1}{2}}$
4	5325.276*v*	10–III	18,773.16	$y^4G^o_{4\frac{1}{2}} - e^4G_{4\frac{1}{2}}$
4	5321.719*v*	2–V	18,785.71	$y^4G^o_{3\frac{1}{2}} - e^2D_{2\frac{1}{2}}$
4	5316.772*v*	7–III	18,803.19	$y^4G^o_{4\frac{1}{2}} - e^4G_{4\frac{1}{2}}$
4	5312.650*v*	8–III	18,817.78	$y^4F^o_{4\frac{1}{2}} - g^2F_{3\frac{1}{2}}$
4	5310.219*v*	20	18,826.39	$y^4F^o_{3\frac{1}{2}} - e^4G_{3\frac{1}{2}}$
10	5308.55	1	18,832.31	$y^2F^o_{3\frac{1}{2}} - f^4D_{3\frac{1}{2}}$?
4	5307.208*v*	0	18,837.07	$y^2G^o_{3\frac{1}{2}} - f^2F_{2\frac{1}{2}}$
4	5301.042*v*	15–II	18,858.98	$a^4P_{2\frac{1}{2}} - y^4D^o_{2\frac{1}{2}}$
7	5292.203	1*n*	18,890.48	$y^4D^o_{1\frac{1}{2}} - e^2P_{1\frac{1}{2}}$
13	5290.49	0	18,896.60	$y^4G^o_{3\frac{1}{2}} - g^4F_{3\frac{1}{2}}$
4	5287.785*v*	5–V	18,906.26	$y^4D^o_{2\frac{1}{2}} - e^4D_{2\frac{1}{2}}$
5	5287.574	3–V	18,907.02	$z^4D^o_{2\frac{1}{2}} - f^4F_{2\frac{1}{2}}$
9	5286.48	1	18,910.93	$y^4F^o_{3\frac{1}{2}} - e^2G_{3\frac{1}{2}}$
9	5284.08	1	18,919.52	$y^4D^o_{3\frac{1}{2}} - g^4F_{3\frac{1}{2}}$
4	5283.487*v*	4–V	18,921.64	$y^4G^o_{3\frac{1}{2}} - f^2F_{2\frac{1}{2}}$
4	5280.631*v*	20–III	18,931.88	$z^4G^o_{4\frac{1}{2}} - f^4F_{3\frac{1}{2}}$
4	5276.183*v*	8–V	18,947.84	$y^4G^o_{5\frac{1}{2}} - e^4H_{4\frac{1}{2}}$
4	5268.498*v*	10–III	18,975.48	$z^4G^o_{5\frac{1}{2}} - f^4F_{5\frac{1}{2}}$
4	5266.506*v*	25–II	18,982.65	$a^2G_{4\frac{1}{2}} - y^2F^o_{3\frac{1}{2}}$
4	5266.302*v*	10–II?	18,983.39	$z^4G^o_{4\frac{1}{2}} - f^4F_{3\frac{1}{2}}$
4	5265.786*v*	4–V	18,985.25	$z^4F^o_{3\frac{1}{2}} - f^4F_{2\frac{1}{2}}$
11	5265.523	1	18,986.20	$\left\{\begin{matrix} a^4P_{2\frac{1}{2}} - z^2F^o_{2\frac{1}{2}} \\ y^2D^o_{2\frac{1}{2}} - 2_{1\frac{1}{2}} \end{matrix}\right.$

TABLE VIII.—*Continued.*

Ref.	λ *IA*	Int.–*TC*	Wave No. Vac.	Multiplet Designation
9	5264.83	1	18,988.69	$y^4G_{2\frac{1}{2}} - e^4G_{3\frac{1}{2}}$
4	5264.203*v*	2–IV	18,990.96	$z^2D^0_{1\frac{1}{2}} - e^2D_{1\frac{1}{2}}$
6	5262.48	2	18,997.17	$z^2D^0_{2\frac{1}{2}} - e^2D_{2\frac{1}{2}}$
4	5257.621*v*	10–III	19,014.73	$y^4D^0_{3\frac{1}{2}} - e^4P_{2\frac{1}{2}}$
4	5254.652*v*	8–IV	19,025.48	$y^4D^0_{2\frac{1}{2}} - e^4D_{2\frac{1}{2}}$
10	5253.84	1	19,028.42	$y^4G_{2\frac{1}{2}} - g^4F_{1\frac{1}{2}}$
4	5250.003*v*	7–V	19,042.32	$y^4G_{2\frac{1}{2}} - e^4H_{3\frac{1}{2}}$
4	5247.921*v*	15–II	19,049.88	$a^4P_{1\frac{1}{2}} - y^4D^0_{\frac{1}{2}}$
10	5243.541	1	19,065.79	$c^2D_{2\frac{1}{2}} - y^4S^0_{1\frac{1}{2}}$
4	5237.085*v*	5	19,089.29	$y^4G^0_{2\frac{1}{2}} - g^2F_{3\frac{1}{2}}$
4	5235.188*v*	15–II	19,096.21	$a^2G_{3\frac{1}{2}} - y^2F^0_{2\frac{1}{2}}$
9	5234.67	1	19,098.10	$y^4G_{2\frac{1}{2}} - e^4G_{2\frac{1}{2}}$
10	5230.363	1	19,113.82	$y^4D^0_{1\frac{1}{2}} - e^4D_{1\frac{1}{2}}$
4	5230.210*v*	25–II	19,114.38	$a^4P_{1\frac{1}{2}} - y^4D^0_{1\frac{1}{2}}$
4	5222.490*v*	4–IV	19,142.64	$y^4D^0_{2\frac{1}{2}} - g^4F_{4\frac{1}{2}}$
10	5221.243	1	19,147.21	$y^4F^0_{1\frac{1}{2}} - e^2D_{1\frac{1}{2}}$
4	5219.008*v*	2–V	19,155.41	$z^4F^0_{1\frac{1}{2}} - f^4F_{2\frac{1}{2}}$
4	5214.751*v*	1	19,171.05	$z^2F^0_{2\frac{1}{2}} - e^4P_{2\frac{1}{2}}$
10	5214.440	0	19,172.19	$y^4D^0_{2\frac{1}{2}} - g^4F_{3\frac{1}{2}}$
4	5212.699*v*	25–III	19,178.59	$z^4F^0_{4\frac{1}{2}} - f^4F_{4\frac{1}{2}}$
4	5211.832*v*	3–IV	19,181.78	$z^2F^0_{3\frac{1}{2}} - e^4D_{3\frac{1}{2}}$
10	5211.714	2	19,182.22	$y^4G^0_{3\frac{1}{2}} - e^2G_{3\frac{1}{2}}$
4	5210.834*v*	3–IV	19,185.46	$y^4D^0_{\frac{1}{2}} - e^4D_{1\frac{1}{2}}$
4	5210.042*v*	3–IV	19,188.38	$c^2D_{2\frac{1}{2}} - y^2P^0_{1\frac{1}{2}}$
4	5192.358*v*	4–V	19,253.73	$y^4D^0_{\frac{1}{2}} - g^4F_{1\frac{1}{2}}$
9	5183.53	1	19,286.52	$y^4G^0_{2\frac{1}{2}} - e^2D_{2\frac{1}{2}}$?
9	5183.04	1	19,288.34	$z^2F^0_{2\frac{1}{2}} - g^4F_{2\frac{1}{2}}$
9	5180.13	1	19,299.18	$z^2F^0_{3\frac{1}{2}} - g^4F_{4\frac{1}{2}}$
9	5179.66	1	19,300.92	$z^2D^0_{2\frac{1}{2}} - g^2F_{3\frac{1}{2}}$
10	5177.585	1*n*	19,308.66	$y^4F^0_{3\frac{1}{2}} - e^2H_{4\frac{1}{2}}$
10	5177.363	1*n*	19,309.49	$y^4D^0_{1\frac{1}{2}} - e^2D_{2\frac{1}{2}}$
4	5176.085*v*	20–III	19,314.26	$a^2D_{2\frac{1}{2}} - y^2D^0_{2\frac{1}{2}}$
6	5173.48	0	19,323.98	$y^2G^0_{4\frac{1}{2}} - g^4F_{3\frac{1}{2}}$
4	5172.292*v*	2	19,328.42	$z^2F^0_{3\frac{1}{2}} - g^4F_{3\frac{1}{2}}$
4	5166.060*v*	2–V	19,351.74	$z^2D^0_{1\frac{1}{2}} - g^2F_{2\frac{1}{2}}$
4	5165.156*v*	3–IV?	19,355.12	$a^4P_{2\frac{1}{2}} - y^4D^0_{1\frac{1}{2}}$
4	5158.854*v*	2–IV?	19,378.77	$y^4D^0_{2\frac{1}{2}} - e^4P_{1\frac{1}{2}}$
5	5158.431	2–IV?	19,380.36	$z^2F^0_{2\frac{1}{2}} - e^4G_{3\frac{1}{2}}$
4	5156.366*v*	10–IV?	19,388.12	$z^2G^0_{3\frac{1}{2}} - e^4H_{4\frac{1}{2}}$
12	5154.87	3	19,393.74	$z^2D^0_{2\frac{1}{2}} - e^2G_{3\frac{1}{2}}$
4	5154.070*v*	8–IV?	19,396.75	$z^2F^0_{3\frac{1}{2}} - e^4G_{4\frac{1}{2}}$
4	5149.796*v*	4–II	19,412.85	$a^4P_{1\frac{1}{2}} - y^4D^0_{\frac{1}{2}}$
4	5149.108*v*	2–IV?	19,415.45	$y^4D^0_{2\frac{1}{2}} - g^4F_{2\frac{1}{2}}$
4	5146.753*v*	15–IV?	19,424.33	$z^4F^0_{3\frac{1}{2}} - f^4F_{3\frac{1}{2}}$
5	5145.512	2–IV?	19,429.01	$z^2G^0_{4\frac{1}{2}} - e^4G_{5\frac{1}{2}}$
4	5142.471*v*	3	19,440.50	$y^4D^0_{2\frac{1}{2}} - f^2F_{2\frac{1}{2}}$
9	5141.03	1	19,445.95	$y^2F^0_{3\frac{1}{2}} - f^4F_{2\frac{1}{2}}$
11	5135.543	1	19,466.73	$y^4D^0_{\frac{1}{2}} - e^4P_{1\frac{1}{2}}$
4	5133.467*v*	15–V	19,474.60	$z^2G^0_{4\frac{1}{2}} - e^4H_{5\frac{1}{2}}$
4	5126.201*v*	10–IV?	19,502.20	$z^4F^0_{2\frac{1}{2}} - f^4F_{2\frac{1}{2}}$
4	5125.715*v*	7–IV?	19,504.05	$z^2G^0_{4\frac{1}{2}} - e^4G_{5\frac{1}{2}}$
4	5124.718*v*	2–IV?	19,507.85	$y^4F^0_{1\frac{1}{2}} - g^2F_{2\frac{1}{2}}$
4	5122.767*v*	8–IV?	19,515.28	$z^4F^0_{1\frac{1}{2}} - f^4F_{1\frac{1}{2}}$
5	5113.232	6–IV?	19,551.67	$a^2D_{2\frac{1}{2}} - y^2F^0_{2\frac{1}{2}}$
4	5108.903*v*	10–V	19,568.24	$z^2G^0_{4\frac{1}{2}} - e^4G_{4\frac{1}{2}}$
9	5108.27	1	19,570.66	$y^2G^0_{3\frac{1}{2}} - g^2F_{2\frac{1}{2}}$
10	5103.11	1	19,590.45	$y^4G^0_{3\frac{1}{2}} - g^2F_{2\frac{1}{2}}$
7	5100.034	1*N*	19,602.27	$y^4G^0_{3\frac{1}{2}} - e^4H_{4\frac{1}{2}}$
9	5098.02	1	19,610.01	$y^4D^0_{2\frac{1}{2}} - e^4D_{1\frac{1}{2}}$
4	5094.955*v*	8–III	19,621.81	$a^2D_{1\frac{1}{2}} - y^2D^0_{2\frac{1}{2}}$
10	5091.282	1	19,635.97	$b^4F_{2\frac{1}{2}} - z^6F^0_{3\frac{1}{2}}$
4	5087.858*v*	3–V	19,649.18	$y^4G^0_{4\frac{1}{2}} - e^2H_{5\frac{1}{2}}$
10	5085.695	1	19,657.53	$b^4F_{1\frac{1}{2}} - z^6F^0_{2\frac{1}{2}}$
4	5077.410*v*	3–III?	19,689.61	$z^2F^0_{2\frac{1}{2}} - e^4D_{2\frac{1}{2}}$
9	5076.83	1	19,691.86	$y^4G^0_{4\frac{1}{2}} - e^2G_{4\frac{1}{2}}$
9	5067.55	2–IV?	19,727.92	$c^2D_{2\frac{1}{2}} - w^2F^0_{3\frac{1}{2}}$
11	5059.849	1	19,757.94	$y^4F^0_{3\frac{1}{2}} - g^2F_{3\frac{1}{2}}$?
11	5057.990	1	19,765.20	$y^4D^0_{1\frac{1}{2}} - e^4P_{1\frac{1}{2}}$
11	5050.601	1	19,794.12	$a^2H_{4\frac{1}{2}} - x^4G^0_{4\frac{1}{2}}$
7	5034.970	1*N*	19,855.57	$z^4F^0_{4\frac{1}{2}} - f^4F_{4\frac{1}{2}}$
12	5034.06	3	19,859.16	$a^2D_{1\frac{1}{2}} - y^2F^0_{2\frac{1}{2}}$
7	5033.36	1*N*	19,861.92	$z^4F^0_{2\frac{1}{2}} - f^4F_{1\frac{1}{2}}$
4	5022.118*v*	2	19,906.38	$z^2D^0_{1\frac{1}{2}} - h^4F_{2\frac{1}{2}}$
4	5013.326*v*	1*n*	19,941.29	$z^4F^0_{2\frac{1}{2}} - f^4F_{2\frac{1}{2}}$
4	5007.286*v*	5	19,965.35	$b^4F_{1\frac{1}{2}} - z^6F^0_{1\frac{1}{2}}$
10	5004.187	1	19,977.71	$b^2D_{1\frac{1}{2}} - z^2F^0_{1\frac{1}{2}}$
10	5000.877	1	19,990.93	$z^6G^0_{3\frac{1}{2}} - e^6F_{4\frac{1}{2}}$
4	4993.006*v*	5	20,022.44	$y^4F^0_{4\frac{1}{2}} - h^4F_{4\frac{1}{2}}$
4	4988.035*v*	10	20,042.40	$z^2G^0_{4\frac{1}{2}} - e^2H_{5\frac{1}{2}}$
4	4987.853*v*	2–IA	20,043.13	$b^4F_{2\frac{1}{2}} - z^6F^0_{2\frac{1}{2}}$
4	4986.443*v*	10	20,048.80	$b^2D_{2\frac{1}{2}} - z^4F^0_{2\frac{1}{2}}$
10	4983.04	1	20,062.49	$\begin{cases} b^2D_{2\frac{1}{2}} - z^4F^0_{1\frac{1}{2}} \\ y^4F^0_{1\frac{1}{2}} - h^4F_{2\frac{1}{2}} \end{cases}$
4	4981.789*v*	0	20,067.53	$y^4D^0_{2\frac{1}{2}} - f^2F_{3\frac{1}{2}}$
4	4979.944*v*	60	20,074.96	$z^2F^0_{2\frac{1}{2}} - e^2G_{3\frac{1}{2}}$
9	4974.47	1	20,097.05	$a^2D_{2\frac{1}{2}} - y^2D^0_{3\frac{1}{2}}$
4	4971.935*v*	2–IV	20,107.30	$z^6G^0_{4\frac{1}{2}} - e^6F_{5\frac{1}{2}}$
4	4971.015*v*	6	20,111.02	$b^2D_{1\frac{1}{2}} - w^4D^0_{1\frac{1}{2}}$
4	4967.902*v*	10*w*	20,123.62	$z^2G^0_{3\frac{1}{2}} - e^2G_{3\frac{1}{2}}$
5	4967.528	3	20,125.14	$y^2G^0_{3\frac{1}{2}} - h^4F_{2\frac{1}{2}}$
4	4966.581*v*	2–IA	20,128.98	$b^4F_{4\frac{1}{2}} - z^6F^0_{3\frac{1}{2}}$
11	4961.891	1	20,148.00	$y^2F^0_{2\frac{1}{2}} - 4_{2\frac{1}{2}}$
4	4959.682*v*	5	20,156.97	$b^4F_{1\frac{1}{2}} - z^6F^0_{\frac{1}{2}}$
4	4953.179*v*	2–IA	20,183.44	$b^4F_{2\frac{1}{2}} - z^6F^0_{1\frac{1}{2}}$
5	4951.828	2	20,188.95	$z^2F^0_{2\frac{1}{2}} - f^2F_{3\frac{1}{2}}$
4	4948.589*v*	4	20,202.16	$y^4D^0_{2\frac{1}{2}} - e^6G_{3\frac{1}{2}}$
5	4945.784	4	20,213.61	
9	4945.55	1	20,214.57	$b^2G_{4\frac{1}{2}} - w^4D^0_{3\frac{1}{2}}$?
7	4944.735	1*n*	20,217.90	$b^2G_{3\frac{1}{2}} - x^2F^0_{2\frac{1}{2}}$
5	4943.282	2	20,223.85	$z^2F^0_{3\frac{1}{2}} - f^2F_{3\frac{1}{2}}$
5	4942.350	2	20,227.66	$y^4F^0_{3\frac{1}{2}} - h^4F_{3\frac{1}{2}}$
9	4941.65	1	20,230.53	$y^4F^0_{1\frac{1}{2}} - h^4F_{1\frac{1}{2}}$
4	4941.354*v*	3	20,231.73	$z^2D^0_{2\frac{1}{2}} - h^4F_{3\frac{1}{2}}$
4	4936.418*v*	6	20,251.97	$(y^6G^0_{4\frac{1}{2}} - e^6H_{5\frac{1}{2}})$
5	4935.222	2	20,256.87	$z^6G^0_{3\frac{1}{2}} - e^6F_{3\frac{1}{2}}$
5	4934.065	25Ba?	20,261.63	
4	4932.883*v*	5	20,266.48	$b^4P_{2\frac{1}{2}} - y^6F^0_{3\frac{1}{2}}$
11	4931.346	1	20,272.80	$b^2D_{1\frac{1}{2}} - x^2F^0_{2\frac{1}{2}}$?
11	4930.783	3	20,275.11	
11	4928.818	1	20,283.19	$\begin{cases} b^2D_{1\frac{1}{2}} - w^4D^0_{\frac{1}{2}} \\ c^2D_{1\frac{1}{2}} - x^4S^0_{1\frac{1}{2}} \end{cases}$
4	4928.290*v*	2–III	20,285.37	$\begin{cases} z^6G^0_{4\frac{1}{2}} - e^6F_{4\frac{1}{2}} \\ z^2F^0_{3\frac{1}{2}} - e^2G_{4\frac{1}{2}} \end{cases}$
11	4925.676	1	20,296.13	$z^6G^0_{3\frac{1}{2}} - e^6F_{3\frac{1}{2}}$
4	4924.998*v*	4	20,298.93	$y^4G^0_{4\frac{1}{2}} - g^2F_{3\frac{1}{2}}$
4	4920.272*v*	1–III*A*	20,318.42	$b^4P_{1\frac{1}{2}} - y^6D^0_{2\frac{1}{2}}$
11	4918.266	2	20,326.71	$b^2P_{1\frac{1}{2}} - x^4D^0_{1\frac{1}{2}}$?
11	4915.960	3	20,336.24	$a^2H_{4\frac{1}{2}} - x^4G^0_{3\frac{1}{2}}$
11	4914.714	3	20,341.40	
4	4912.399*v*	1–IA	20,350.99	$b^4F_{2\frac{1}{2}} - z^6F^0_{1\frac{1}{2}}$
11	4910.934	4*R*	20,357.06	
4	4908.481*v*	3	20,367.23	$c^2D_{1\frac{1}{2}} - w^2S^0_{\frac{1}{2}}$
9	4907.58	1	20,370.96	$b^2G_{4\frac{1}{2}} - z^2F^0_{3\frac{1}{2}}$
5	4907.125	2	20,372.86	$b^4F_{4\frac{1}{2}} - z^6F^0_{4\frac{1}{2}}$
4	4904.172*v*	1–III	20,385.13	$b^2D_{1\frac{1}{2}} - z^2F^0_{1\frac{1}{2}}$
9	4902.52	1	20,392.00	$y^4G^0_{4\frac{1}{2}} - e^2G_{3\frac{1}{2}}$
4	4899.520*v*	2–III*A*	20,404.48	$a^2D_{1\frac{1}{2}} - y^2D^0_{1\frac{1}{2}}$
4	4897.182*v*	15	20,414.22	$z^2G^0_{4\frac{1}{2}} - e^2H_{5\frac{1}{2}}$
10	4892.76	1	20,432.67	$y^4D^0_{2\frac{1}{2}} - e^2D_{2\frac{1}{2}}$
7	4892.508	1*n*	20,433.73	$y^4G^0_{5\frac{1}{2}} - h^4F_{4\frac{1}{2}}$
4	4886.995*v*	5	20,456.78	$z^2G^0_{4\frac{1}{2}} - e^2G_{4\frac{1}{2}}$
4	4882.704*v*	2–III	20,474.76	$z^6G^0_{5\frac{1}{2}} - e^6F_{5\frac{1}{2}}$
11	4881.311	4	20,480.60	$(y^4F^0_{3\frac{1}{2}} - h^4F_{3\frac{1}{2}})$
12	4880.25	2	20,485.05	$b^4F_{2\frac{1}{2}} - z^6D^0_{3\frac{1}{2}}$
12	4878.356*v*	0	20,493.00	$z^6G^0_{3\frac{1}{2}} - e^6F_{3\frac{1}{2}}$
4	4869.377*v*	10	20,530.79	$y^4G^0_{3\frac{1}{2}} - g^2F_{3\frac{1}{2}}$
4	4867.870*v*	25–II	20,537.15	$z^6G^0_{4\frac{1}{2}} - e^6F_{5\frac{1}{2}}$
5	4863.461	5	20,555.76	$b^4P_{1\frac{1}{2}} - y^6F^0_{2\frac{1}{2}}$
4	4862.097*v*	1	20,561.53	$z^2F^0_{2\frac{1}{2}} - e^2D_{2\frac{1}{2}}$
9	4857.938	1	20,579.13	$b^4F_{2\frac{1}{2}} - z^6D^0_{2\frac{1}{2}}$
7	4855.590	1	20,589.08	$z^2F^0_{3\frac{1}{2}} - e^2D_{2\frac{1}{2}}$
4	4855.235*v*	0	20,590.58	$b^4F_{2\frac{1}{2}} - z^6F^0_{2\frac{1}{2}}$
11	4853.309	3	20,598.76	$z^2D^0_{2\frac{1}{2}} - e^4P_{2\frac{1}{2}}$
11	4851.973	1	20,604.43	$b^2P_{1\frac{1}{2}} - 2^0_{1\frac{1}{2}}$
11	4849.315	2	20,615.73	$y^4F^0_{2\frac{1}{2}} - 1_{2\frac{1}{2}}$
4	4843.454*v*	3–III	20,640.67	$z^6G^0_{3\frac{1}{2}} - e^6_{2\frac{1}{2}}$
4	4840.253*v*	25–III	20,654.32	$z^6G^0_{4\frac{1}{2}} - e^6F_{4\frac{1}{2}}$
10	4837.948	2	20,664.16	$b^4F_{1\frac{1}{2}} - z^6D^0_{2\frac{1}{2}}$
10	4834.359	—	20,679.50	$b^4P_{\frac{1}{2}} - y^6D^0_{\frac{1}{2}}$
4	4832.088*v*	0	20,689.22	$y^4D^0_{2\frac{1}{2}} - e^6H_{3\frac{1}{2}}$
10	4818.411	1	20,747.95	$y^4D^0_{3\frac{1}{2}} - e^6H_{4\frac{1}{2}}$
9	4817.43	1	20,752.17	$y^4G^0_{5\frac{1}{2}} - h^4F_{4\frac{1}{2}}$
4	4815.900*v*	1–III	20,758.77	$b^2D_{1\frac{1}{2}} - x^2D^0_{1\frac{1}{2}}$
4	4813.966*v*	2–III	20,767.11	$z^6G^0_{4\frac{1}{2}} - e^6F_{4\frac{1}{2}}$
4	4813.476*v*	20–III	20,769.22	$\begin{cases} z^6G^0_{4\frac{1}{2}} - e^6F_{5\frac{1}{2}} \\ (b^2D_{1\frac{1}{2}} - x^2D^0_{2\frac{1}{2}}) \end{cases}$
10	4808.24	1	20,791.84	$y^4F^0_{4\frac{1}{2}} - h^4F_{3\frac{1}{2}}$
10	4801.79	1	20,819.76	$z^2D^0_{2\frac{1}{2}} - f^2D_{2\frac{1}{2}}$
4	4797.835*v*	1	20,836.93	$y^4D^0_{3\frac{1}{2}} - h^4F_{4\frac{1}{2}}$
4	4797.750*v*	1	20,837.30	$c^2D_{2\frac{1}{2}} - x^2F^0_{3\frac{1}{2}}$
4	4796.378*v*	1–II*A*	20,843.26	$b^4F_{4\frac{1}{2}} - z^6F^0_{5\frac{1}{2}}$
4	4795.853*v*	2–V	20,845.54	$z^2F^0_{3\frac{1}{2}} - e^6H_{4\frac{1}{2}}$
9	4794.27	1	20,852.42	$y^4F^0_{4\frac{1}{2}} - h^4F_{5\frac{1}{2}}$
4	4792.855*v*	15–III	20,858.58	$z^6G^0_{5\frac{1}{2}} - e^6F_{5\frac{1}{2}}$
4	4785.070*v*	50	20,892.51	$z^2F^0_{3\frac{1}{2}} - g^2F_{3\frac{1}{2}}$
11	4782.561	1	20,903.47	$a^2F_{3\frac{1}{2}} - z^6F^0_{4\frac{1}{2}}$
4	4781.432*v*	3–II*A*	20,908.41	$b^4P_{2\frac{1}{2}} - y^6D^0_{3\frac{1}{2}}$
4	4779.979*v*	10–III	20,914.76	$z^6G^0_{5\frac{1}{2}} - e^6F_{5\frac{1}{2}}$
4	4778.233*v*	2–IV	20,922.41	$z^2F^0_{2\frac{1}{2}} - g^2F_{3\frac{1}{2}}$
4	4776.311*v*	6–III	20,930.83	$z^6G^0_{4\frac{1}{2}} - e^6F_{5\frac{1}{2}}$
11	4773.498	1	20,943.16	$y^4D^0_{2\frac{1}{2}} - f^2F_{2\frac{1}{2}}$
5	4771.108	6–III	20,953.65	$z^6D^0_{3\frac{1}{2}} - e^6F_{4\frac{1}{2}}$
4	4768.072*v*	5–III	20,966.99	$z^6D^0_{4\frac{1}{2}} - e^6F_{4\frac{1}{2}}$
4	4767.142*v*	100	20,971.08	$z^2G^0_{4\frac{1}{2}} - g^2F_{3\frac{1}{2}}$
11	4762.353	1Mn?	20,992.17	$z^2G^0_{4\frac{1}{2}} - e^4D_{3\frac{1}{2}}$
4	4756.722*v*	100	21,017.02	$z^2G^0_{4\frac{1}{2}} - e^4H_{5\frac{1}{2}}$
4	4754.358*v*	3–III	21,027.47	$z^6D^0_{4\frac{1}{2}} - e^6F_{5\frac{1}{2}}$
9	4751.57	1	21,039.81	$y^4D^0_{3\frac{1}{2}} - h^4F_{3\frac{1}{2}}$
4	4749.68*v*	10–III	21,048.18	$z^6D^0_{4\frac{1}{2}} - e^6F_{5\frac{1}{2}}$
4	4746.115*v*	100	21,063.99	$z^2G^0_{4\frac{1}{2}} - g^2F_{4\frac{1}{2}}$
12	4742.22	2	21,081.29	$y^4G^0_{5\frac{1}{2}} - f^4G_{4\frac{1}{2}}$
11	4738.097	1	21,099.64	$z^2F^0_{3\frac{1}{2}} - f^2F_{3\frac{1}{2}}$

TABLE VIII.—*Continued.*

Ref.	λ *IA*	Int.–*TC*	Wave No. Vac.	Multiplet Designation
4	4737.769*v*	2–II*A*	21,101.10	$b^4P_{1\frac{1}{2}} - y^2D^0_{2\frac{1}{2}}$
9	4736.22	1	21,108.00	$y^4D^0_{1\frac{1}{2}} - h^4F^0_{2\frac{1}{2}}$
4	4734.828*v*	2–III?	21,114.20	$z^6D^0_{\frac{1}{2}} - e^6F_{1\frac{1}{2}}$
4	4732.051*v*	40	21,126.59	$b^4F_{2\frac{1}{2}} - z^6D^0_{2\frac{1}{2}}$
4	4729.058	2	21,139.97	
4	4727.936*v*	3–I*A*	21,144.98	$b^4F_{4\frac{1}{2}} - z^6D^0_{4\frac{1}{2}}$
11	4727.746	1	21,145.83	$b^4P_{2\frac{1}{2}} - y^2F^0_{2\frac{1}{2}}$
4	4725.250*v*	1	21,157.00	$z^6G^0_{4\frac{1}{2}} - e^6G_{4\frac{1}{2}}$
4	4718.470*v*	50	21,187.40	$y^4G^0_{3\frac{1}{2}} - f^4H^0_{4\frac{1}{2}}$
9	4709.04	1	21,229.83	$\begin{cases} y^4G^0_{4\frac{1}{2}} - f^6F^0_{3\frac{1}{2}} \\ y^4G^0_{4\frac{1}{2}} - h^4F^0_{3\frac{1}{2}} \end{cases}$
4	4704.386*v*	3	21,250.83	$z^4D^0_{2\frac{1}{2}} - e^4F_{2\frac{1}{2}}$
11	4704.144	1	21,251.93	$z^4D^0_{2\frac{1}{2}} - e^2P_{1\frac{1}{2}}$
4	4699.180*v*	25	21,274.37	$a^2F_{2\frac{1}{2}} - z^4G^0_{3\frac{1}{2}}$
4	4698.389*v*	3–IV?	21,277.96	$z^4D^0_{\frac{1}{2}} - e^4F_{\frac{1}{2}}$
9	4697.52	1	21,281.89	$y^4D^0_{2\frac{1}{2}} - f^4F_{2\frac{1}{2}}$?
11	4697.000	1	21,284.25	$c^2D_{1\frac{1}{2}} - w^2P^0_{1\frac{1}{2}}$
4	4693.190*v*	6–IV?	21,301.53	$z^6D^0_{1\frac{1}{2}} - e^6F_{1\frac{1}{2}}$
9	4689.98	1	21,316.11	$y^4F^0_{4\frac{1}{2}} - f^4G_{4\frac{1}{2}}$
4	4688.489*v*	20	21,322.88	$b^2D_{2\frac{1}{2}} - w^4D^0_{2\frac{1}{2}}$
4	4685.858*v*	30	21,334.86	$a^2F_{3\frac{1}{2}} - z^4F^0_{3\frac{1}{2}}$
9	4683.95	1	21,343.55	$b^2D_{2\frac{1}{2}} - w^4D^0_{1\frac{1}{2}}$
4	4682.361*v*	9–III?	21,350.79	$z^6D^0_{2\frac{1}{2}} - e^6F_{2\frac{1}{2}}$
11	4677.528	1	21,372.85	$b^4F_{2\frac{1}{2}} - z^6D^0_{1\frac{1}{2}}$
5	4677.251	4	21,374.12	$b^4F_{1\frac{1}{2}} - z^6G^0_{2\frac{1}{2}}$
4	4676.705*v*	0	21,376.61	$c^2D_{1\frac{1}{2}} - 11^0_{2\frac{1}{2}}$
9	4670.92	1	21,403.09	$b^2D_{1\frac{1}{2}} - w^4F^0_{1\frac{1}{2}}$
4	4667.861*v*	10	21,417.11	
4	4663.403*v*	12–III	21,437.59	$z^6D^0_{3\frac{1}{2}} - e^6F_{2\frac{1}{2}}$
4	4657.390*v*	100	21,465.26	$z^6D^0_{\frac{1}{2}} - e^6F_{\frac{1}{2}}$
4	4654.834*v*	25	21,477.05	$z^2F^0_{2\frac{1}{2}} - h^4F_{2\frac{1}{2}}$
10	4654.519	1	21,478.50	$b^2D_{2\frac{1}{2}} - w^4D^0_{2\frac{1}{2}}$
4	4653.770*v*	1	21,481.96	$b^2P_{1\frac{1}{2}} - z^4P^0_{1\frac{1}{2}}$
11	4652.470	1	21,487.96	$a^2F_{2\frac{1}{2}} - z^4D^0_{2\frac{1}{2}}$
12	4651.84	3	21,490.87	
5	4648.652	5	21,505.61	$\begin{cases} b^2D_{2\frac{1}{2}} - x^2F^0_{2\frac{1}{2}} \\ b^2D_{1\frac{1}{2}} - y^4P^0_{1\frac{1}{2}} \end{cases}$
4	4645.153*v*	0	21,521.81	$b^4F_{1\frac{1}{2}} - z^6G^0_{1\frac{1}{2}}$
4	4644.317*v*	70	21,525.68	$z^6G^0_{2\frac{1}{2}} - h^4F^0_{2\frac{1}{2}}$
4	4643.733*v*	15	21,528.39	$c^2D_{2\frac{1}{2}} - w^2P^0_{1\frac{1}{2}}$
9	4642.79	1	21,532.76	$z^4G^0_{3\frac{1}{2}} - e^4G_{4\frac{1}{2}}$
4	4640.820*v*	10	21,541.90	$b^4F_{2\frac{1}{2}} - z^6G^0_{2\frac{1}{2}}$
9	4639.07	1	21,550.03	$y^2G^0_{4\frac{1}{2}} - e^4G_{3\frac{1}{2}}$
9	4631.10	1	21,587.12	$z^6G^0_{4\frac{1}{2}} - f^4F_{4\frac{1}{2}}$?
9	4630.52	1	21,589.82	$z^4D^0_{\frac{1}{2}} - e^4P_{1\frac{1}{2}}$
4	4629.359*v*	15–III	21,595.24	$z^6D^0_{4\frac{1}{2}} - e^6F_{4\frac{1}{2}}$
4	4628.908*v*	125	21,597.34	$b^4F_{3\frac{1}{2}} - z^6D^0_{3\frac{1}{2}}$
9	4627.44	1	21,604.19	$y^4D^0_{3\frac{1}{2}} - h^4F_{3\frac{1}{2}}$
4	4625.767*v*	2–III	21,612.00	$z^4D^0_{2\frac{1}{2}} - e^4D_{2\frac{1}{2}}$
4	4624.561*v*	10	21,617.64	$b^2D_{2\frac{1}{2}} - z^2P^0_{1\frac{1}{2}}$
4	4623.020*v*	150	21,624.84	$z^6D^0_{2\frac{1}{2}} - e^6F_{1\frac{1}{2}}$
4	4622.691*v*	30	21,626.38	$z^4D^0_{1\frac{1}{2}} - e^4F_{2\frac{1}{2}}$
4	4620.824*v*	25	21,635.12	$b^2D_{2\frac{1}{2}} - z^2F^0_{2\frac{1}{2}}$
10	4619.329	1	21,642.12	$a^2F_{2\frac{1}{2}} - z^4G^0_{2\frac{1}{2}}$
4	4614.003*v*	60	21,667.11	$y^4D^0_{3\frac{1}{2}} - h^4F_{3\frac{1}{2}}$
9	4612.41	1	21,674.58	$y^4D^0_{2\frac{1}{2}} - f^4D_{2\frac{1}{2}}$
4	4608.908*v*	8	21,691.06	$b^4P_{2\frac{1}{2}} - y^2D^0_{1\frac{1}{2}}$
4	4601.158*v*	30	21,727.59	$y^4G^0_{4\frac{1}{2}} - f^4G_{4\frac{1}{2}}$
4	4596.903*v*	5–IV	21,747.70	$z^4D^0_{\frac{1}{2}} - e^4P_{\frac{1}{2}}$
4	4594.633*v*	4–IV	21,758.45	$z^4D^0_{\frac{1}{2}} - e^4D_{\frac{1}{2}}$
11	4594.356	1	21,759.76	$b^4F_{2\frac{1}{2}} - z^4G^0_{2\frac{1}{2}}$
11	4591.375	1	21,773.89	$a^2F_{3\frac{1}{2}} - z^4F^0_{3\frac{1}{2}}$
9	4589.36	1	21,783.44	$z^4G^0_{4\frac{1}{2}} - e^4D_{3\frac{1}{2}}$
4	4588.730*v*	1–I*A*	21,786.44	$b^4F_{4\frac{1}{2}} - z^6D^0_{3\frac{1}{2}}$
4	4586.936*v*	15	21,794.96	$b^4F_{3\frac{1}{2}} - z^6G^0_{4\frac{1}{2}}$
4	4581.596*v*	20–III	21,820.36	$\begin{cases} z^6F^0_{4\frac{1}{2}} - e^6F_{4\frac{1}{2}} \\ (z^4D^0_{3\frac{1}{2}} - e^4D_{3\frac{1}{2}}) \end{cases}$
11	4581.380	1	21,821.39	$z^6D^0_{3\frac{1}{2}} - e^6F_{2\frac{1}{2}}$
11	4580.964	1	21,823.37	$z^2F^0_{2\frac{1}{2}} - h^4F_{3\frac{1}{2}}$
4	4580.139*v*	4–I*A*	21,827.30	$a^2F_{3\frac{1}{2}} - z^4G^0_{4\frac{1}{2}}$
5	4579.364	25	21,831.00	$z^2F^0_{3\frac{1}{2}} - f^4D_{3\frac{1}{2}}$
10	4577.27	1	21,840.99	$y^4F^0_{4\frac{1}{2}} - e^6G_{4\frac{1}{2}}$
4	4574.942*v*	20	21,852.10	$a^2F_{3\frac{1}{2}} - z^4D^0_{2\frac{1}{2}}$
4	4570.024*v*	2–IV	21,875.61	$z^4D^0_{2\frac{1}{2}} - e^4F_{3\frac{1}{2}}$
5	4567.533	2	21,887.54	$y^4G^0_{4\frac{1}{2}} - e^4D_{3\frac{1}{2}}$
4	4566.610*v*	100	21,891.97	$z^4D^0_{\frac{1}{2}} - e^4D_{\frac{1}{2}}$
4	4565.578*v*	15–III	21,896.91	$z^6F^0_{4\frac{1}{2}} - e^6F_{4\frac{1}{2}}$
5	4564.843	10	21,900.44	$z^4G^0_{4\frac{1}{2}} - e^4F_{4\frac{1}{2}}$
4	4564.153*v*	35	21,903.75	$b^6G_{3\frac{1}{2}} - z^6H^0_{4\frac{1}{2}}$
5	4563.989	10	21,904.53	$z^4G^0_{4\frac{1}{2}} - e^4H_{5\frac{1}{2}}$
10	4563.85	1	21,905.20	$z^4D^0_{2\frac{1}{2}} - e^4F_{3\frac{1}{2}}$
9	4563.38	1	21,907.46	$b^4F_{3\frac{1}{2}} - z^6G^0_{3\frac{1}{2}}$
9	4563.02	1	21,909.19	$y^4D^0_{2\frac{1}{2}} - f^4P_{2\frac{1}{2}}$
4	4561.948*v*	25	21,914.34	$b^2P^0_{\frac{1}{2}} - z^2P^0_{\frac{1}{2}}$
9	4561.22	1	21,917.83	$z^2F^0_{2\frac{1}{2}} - e^4P_{2\frac{1}{2}}$
9	4560.97	1	21,919.04	$a^2H_{4\frac{1}{2}} - w^4G^0_{3\frac{1}{2}}$
5	4559.123	10	21,927.91	$b^2D_{2\frac{1}{2}} - w^4F^0_{3\frac{1}{2}}$
4	4553.336*v*	25	21,955.79	$z^6G^0_{3\frac{1}{2}} - f^4F_{4\frac{1}{2}}$
4	4552.441*v*	25	21,960.10	$z^4D^0_{\frac{1}{2}} - g^4F_{1\frac{1}{2}}$
10	4550.469	<1	21,969.62	$z^6G^0_{3\frac{1}{2}} - f^4F_{3\frac{1}{2}}$
4	4549.658*v*	10–III	21,973.54	$\begin{cases} z^6F^0_{3\frac{1}{2}} - e^6F_{3\frac{1}{2}} \\ (z^4D^0_{3\frac{1}{2}} - e^4G_{4\frac{1}{2}}) \end{cases}$
10	4547.75	<1	21,982.75	$a^2F_{2\frac{1}{2}} - z^4D^0_{1\frac{1}{2}}$
11	4546.873	1	21,986.99	$c^2D_{2\frac{1}{2}} - 10^0_{2\frac{1}{2}}$
4	4545.985*v*	1–III	21,991.29	$b^2D_{2\frac{1}{2}} - x^2D^0_{1\frac{1}{2}}$
4	4545.238*v*	50	21,994.90	$z^2G^0_{4\frac{1}{2}} - h^4F_{3\frac{1}{2}}$
11	4544.541	1	21,998.27	$z^4G^0_{4\frac{1}{2}} - e^4G_{4\frac{1}{2}}$
4	4543.810*v*	6–III	22,001.82	$b^2D_{2\frac{1}{2}} - x^2D^0_{2\frac{1}{2}}$
9	4541.65	1	22,012.28	$y^4G^0_{4\frac{1}{2}} - i^4F_{5\frac{1}{2}}$
4	4540.786*v*	30	22,016.47	$z^4D^0_{3\frac{1}{2}} - e^4D_{3\frac{1}{2}}$
10	4534.353	1	22,047.70	$b^2P^0_{\frac{1}{2}} - w^4D^0_{1\frac{1}{2}}$
4	4533.985*v*	7–III	22,049.49	$z^6F^0_{3\frac{1}{2}} - e^6F_{2\frac{1}{2}}$
11	4532.605	1	22,056.20	$a^4P_{1\frac{1}{2}} - y^2D^0_{2\frac{1}{2}}$
4	4530.949*v*	30–II	22,064.26	$z^6F^0_{3\frac{1}{2}} - e^6F_{3\frac{1}{2}}$
4	4527.919*v*	2–III	22,079.03	$z^6D^0_{4\frac{1}{2}} - e^6F_{5\frac{1}{2}}$
4	4526.794*v*	2–III	22,084.52	$z^4D^0_{\frac{1}{2}} - e^4F_{1\frac{1}{2}}$
4	4526.518*v*	0	22,085.86	$b^4F_{4\frac{1}{2}} - z^6G^0_{5\frac{1}{2}}$
5	4525.787	5	22,089.43	$b^4F_{3\frac{1}{2}} - z^6G^0_{3\frac{1}{2}}$
12	4524.72	3	22,094.64	
4	4519.283*v*	40	22,121.22	$z^4D^0_{3\frac{1}{2}} - g^4F^0_{3\frac{1}{2}}$
9	4517.96	1	22,127.70	$z^2G^0_{4\frac{1}{2}} - f^4H^0_{4\frac{1}{2}}$
4	4517.094*v*	4–III	22,131.94	$z^6F^0_{5\frac{1}{2}} - e^6F_{5\frac{1}{2}}$
4	4514.177*v*	1–IV	22,146.24	$z^4D^0_{3\frac{1}{2}} - f^6F^0_{3\frac{1}{2}}$
11	4508.664	1	22,173.32	$z^4D^0_{\frac{1}{2}} - e^4P_{\frac{1}{2}}$
4	4500.562*v*	5	22,213.24	$z^4D^0_{2\frac{1}{2}} - e^4G_{3\frac{1}{2}}$
5	4499.261	3	22,219.66	$b^2P^0_{\frac{1}{2}} - w^4D^0_{\frac{1}{2}}$
4	4494.746*v*	2–IV	22,241.98	$c^2D_{1\frac{1}{2}} - w^2F^0_{2\frac{1}{2}}$
9	4493.05	1	22,250.38	$y^4D^0_{3\frac{1}{2}} - i^4F_{4\frac{1}{2}}$
5	4492.076	5	22,255.20	$\begin{cases} z^6D^0_{3\frac{1}{2}} - f^6F^0_{4\frac{1}{2}} \\ (y^4D^0_{3\frac{1}{2}} - f^4D_{3\frac{1}{2}}) \end{cases}$
5	4490.309	2	22,263.96	$z^6G^0_{4\frac{1}{2}} - f^6F_{5\frac{1}{2}}$
9	4489.40	1	22,268.46	$z^6G^0_{3\frac{1}{2}} - f^6F_{2\frac{1}{2}}$
4	4486.706*v*	50	22,281.84	$b^2D_{2\frac{1}{2}} - w^4F^0_{2\frac{1}{2}}$
4	4484.513*v*	60	22,292.73	$a^2F_{3\frac{1}{2}} - z^4G^0_{3\frac{1}{2}}$
4	4483.918*v*	3–III	22,295.69	$z^6F^0_{\frac{1}{2}} - e^6F_{\frac{1}{2}}$
5	4483.586	20*h*	22,297.34	$z^4G^0_{5\frac{1}{2}} - e^4H^0_{6\frac{1}{2}}$
11	4481.577	1	22,307.34	$b^4F_{3\frac{1}{2}} - z^6G^0_{3\frac{1}{2}}$
5	4478.657	5	22,321.87	$b^2P^0_{\frac{1}{2}} - z^2P^0_{\frac{1}{2}}$
4	4478.319*v*	4–III	22,323.56	$z^6F^0_{\frac{1}{2}} - e^6F_{1\frac{1}{2}}$
4	4477.212*v*	30*wh*	22,329.08	$\begin{cases} z^4G^0_{5\frac{1}{2}} - e^4H^0_{6\frac{1}{2}} \\ y^4D^0_{4\frac{1}{2}} - f^6F^0_{4\frac{1}{2}} \end{cases}$
4	4471.809*v*	1–III	22,356.06	$b^2G^0_{4\frac{1}{2}} - z^2H^0_{5\frac{1}{2}}$
4	4471.550*v*	5–III	22,357.36	$z^6F^0_{5\frac{1}{2}} - e^6F_{5\frac{1}{2}}$
10	4471.271	1	22,358.75	$z^4G^0_{5\frac{1}{2}} - e^4G_{4\frac{1}{2}}$
11	4471.046	1	22,359.88	$z^4G^0_{3\frac{1}{2}} - f^4F_{2\frac{1}{2}}$
4	4469.547*v*	15–III	22,367.38	$z^6F^0_{4\frac{1}{2}} - e^6F_{4\frac{1}{2}}$
9	4467.53	1	22,377.47	$y^4D^0_{\frac{1}{2}} - 6_{\frac{1}{2}}$
4	4466.881*v*	10–III	22,380.72	$z^6F^0_{3\frac{1}{2}} - e^6F_{3\frac{1}{2}}$
4	4465.817*v*	5	22,386.06	$z^4G^0_{5\frac{1}{2}} - e^4H_{4\frac{1}{2}}$
11	4460.725	1	22,411.61	$z^2F^0_{3\frac{1}{2}} - f^4D_{2\frac{1}{2}}$
4	4458.594*v*	10	22,422.32	$z^4F^0_{3\frac{1}{2}} - g^4F_{3\frac{1}{2}}$
11	4458.242	1	22,424.09	$y^4D^0_{2\frac{1}{2}} - 2_{1\frac{1}{2}}$
11	4452.166	1	22,454.70	$b^4F_{4\frac{1}{2}} - z^6G^0_{4\frac{1}{2}}$
9	4450.79	1	22,461.61	$z^6D^0_{3\frac{1}{2}} - f^4F_{3\frac{1}{2}}$
4	4445.711*v*	4–III	22,487.29	$z^6F^0_{\frac{1}{2}} - e^6F_{\frac{1}{2}}$
4	4445.049*v*	2–IV	22,490.65	$z^4F^0_{4\frac{1}{2}} - e^4G_{4\frac{1}{2}}$
4	4441.952*v*	5	22,506.33	$a^2F_{3\frac{1}{2}} - z^4D^0_{2\frac{1}{2}}$
9	4441.02	1	22,511.05	$\begin{cases} z^4D^0_{2\frac{1}{2}} - e^2D_{2\frac{1}{2}}? \\ y^4D^0_{3\frac{1}{2}} - f^4G_{3\frac{1}{2}} \end{cases}$
4	4437.872*v*	2	22,527.02	$z^4D^0_{1\frac{1}{2}} - f^4F_{2\frac{1}{2}}$
4	4436.193*v*	15	22,535.55	$\begin{cases} b^2D_{1\frac{1}{2}} - w^2D^0_{2\frac{1}{2}} \\ z^2G^0_{4\frac{1}{2}} - f^4H_{5\frac{1}{2}} \end{cases}$
4	4431.608*v*	3–III	22,558.86	$b^2G^0_{4\frac{1}{2}} - x^2G^0_{3\frac{1}{2}}$
9	4429.33	1	22,570.46	$y^4D^0_{\frac{1}{2}} - 5_{1\frac{1}{2}}$
9	4422.00	1	22,607.87	$\begin{cases} z^2F^0_{3\frac{1}{2}} - e^6G_{4\frac{1}{2}} \\ c^2D_{2\frac{1}{2}} - 12^0_{3\frac{1}{2}} \end{cases}$
4	4421.337*v*	4–III	22,611.26	$z^6F^0_{5\frac{1}{2}} - e^6F_{4\frac{1}{2}}$
9	4420.86	1	22,613.70	$z^4G^0_{\frac{1}{2}} - e^4H_{\frac{1}{2}}$
9	4420.43	1	22,615.90	$z^2G^0_{4\frac{1}{2}} - f^4H_{5\frac{1}{2}}$
10	4418.000	<1	22,628.34	$\begin{cases} z^6G^0_{3\frac{1}{2}} - f^6F_{4\frac{1}{2}} \\ y^4D^0_{3\frac{1}{2}} - f^6F_{3\frac{1}{2}} \end{cases}$
9	4417.76	1	22,629.57	$b^2P_{1\frac{1}{2}} - z^2P^0_{\frac{1}{2}}$
4	4417.398*v*	5–III	22,631.43	$z^6F^0_{5\frac{1}{2}} - e^6F_{4\frac{1}{2}}$
4	4416.482*v*	3	22,636.12	$a^2H_{4\frac{1}{2}} - z^2H^0_{4\frac{1}{2}}$
4	4412.727*v*	1	22,655.38	$z^6D^0_{4\frac{1}{2}} - f^6F_{5\frac{1}{2}}$
7	4411.786	1	22,660.21	$a^2F_{3\frac{1}{2}} - z^4G^0_{2\frac{1}{2}}$
4	4411.685*v*	0	22,660.73	$z^4G^0_{3\frac{1}{2}} - g^4F_{3\frac{1}{2}}$
9	4410.02	1	22,669.29	$z^4G^0_{3\frac{1}{2}} - e^4G_{3\frac{1}{2}}$
4	4404.932*v*	3–III	22,695.47	$b^2P_{\frac{1}{2}} - x^2D^0_{1\frac{1}{2}}$
9	4404.28	1	22,698.83	$b^2P^0_{1\frac{1}{2}} - x^4G^0_{2\frac{1}{2}}$
4	4402.674*v*	3–III	22,707.11	$z^4F^0_{4\frac{1}{2}} - e^4D_{3\frac{1}{2}}$
10	4396.717	1	22,737.88	$b^2D_{2\frac{1}{2}} - y^4P^0_{1\frac{1}{2}}$
4	4395.871*v*	1–III*A*	22,742.25	$b^2P^0_{1\frac{1}{2}} - w^4D^0_{2\frac{1}{2}}$
9	4394.54	1	22,749.15	$b^4F_{4\frac{1}{2}} - z^6G^0_{5\frac{1}{2}}$
4	4391.890*v*	3–III	22,762.86	$b^2P^0_{1\frac{1}{2}} - w^4D^0_{1\frac{1}{2}}$
4	4391.568*v*	4–III	22,764.54	$z^6F^0_{5\frac{1}{2}} - e^6F_{5\frac{1}{2}}$
4	4387.915*v*	3	22,783.49	$z^4F^0_{5\frac{1}{2}} - e^4D_{3\frac{1}{2}}$
9	4381.50	1	22,816.84	$z^4F^0_{3\frac{1}{2}} - e^4P_{1\frac{1}{2}}$
4	4380.07*v*	5–III?	22,824.28	$z^4F^0_{4\frac{1}{2}} - g^4F_{4\frac{1}{2}}$
4	4379.266*v*	1	22,828.49	$z^4F^0_{4\frac{1}{2}} - e^4H_{5\frac{1}{2}}$
9	4376.26	1	22,844.17	$z^4G^0_{4\frac{1}{2}} - e^4H_{5\frac{1}{2}}$
4	4375.540*v*	2–III	22,847.92	$b^2G^0_{4\frac{1}{2}} - x^2G^0_{4\frac{1}{2}}$
10	4375.103	1	22,850.20	$b^2D_{1\frac{1}{2}} - x^4P^0_{2\frac{1}{2}}$
4	4374.918*v*	3–III	22,851.17	$z^6F^0_{4\frac{1}{2}} - e^6F_{3\frac{1}{2}}$

TABLE VIII.—*Continued.*

Ref.	λ *IA*	Int.–*TC*	Wave No. Vac.	Multiplet Designation
4	4374.446*v*	2*wh*	22,853.64	$z^1F^0_{3\frac{1}{2}} - g^1F_{3\frac{1}{2}}$
4	4373.634*v*	6–IV	22,857.88	$z^1F^0_{4\frac{1}{2}} - e^1G_{4\frac{1}{2}}$
9	4372.08	1	22,866.00	$y^4D^0_{3\frac{1}{2}} - e^4H_{3\frac{1}{2}}$
4	4371.130*v*	5–III	22,870.96	$a^3D_{2\frac{1}{2}} - x^4D^0_{3\frac{1}{2}}$
9	4368.08	1	22,886.94	$z^5G^0_{4\frac{1}{2}} - e^5G_{4\frac{1}{2}}$
9	4367.03	1	22,892.44	$z^5G^0_{4\frac{1}{2}} - e^4G_{3\frac{1}{2}}$
4	4366.213*v*	2	22,896.73	$z^5D^0_{4\frac{1}{2}} - f^5F_{4\frac{1}{2}}$
4	4361.913*v*	2*h*	22,919.30	$a^4F_{2\frac{1}{2}} - z^5F^0_{3\frac{1}{2}}$
5	4361.031	2	22,923.94	$a^4F_{1\frac{1}{2}} - z^5F^0_{2\frac{1}{2}}$
4	4360.830*v*	10	22,924.99	$b^2P_{1\frac{1}{2}} - x^2F^0_{2\frac{1}{2}}$
4	4359.426*v*	15	22,932.38	$z^5D^0_{3\frac{1}{2}} - f^5F_{3\frac{1}{2}}$
9	4358.96	1	22,934.83	$b^2P_{1\frac{1}{2}} - w^4D^0_{2\frac{1}{2}}$
9	4358.08	1	22,939.46	$z^3F^0_{3\frac{1}{2}} - 5_{3\frac{1}{2},2\frac{1}{2}}$
5	4357.173	10	22,944.23	$y^4D^0_{2\frac{1}{2}} - 4_{2\frac{1}{2}}$
4	4356.900*v*	3	22,945.67	$z^5F^0_{2\frac{1}{2}} - e^5G_{2\frac{1}{2}}$
4	4353.824*v*	4	22,961.88	$y^4D^0_{3\frac{1}{2}} - e^5G_{3\frac{1}{2}}$?
4	4350.630*v*	1	22,978.74	$z^5D^0_{2\frac{1}{2}} - f^5F_{2\frac{1}{2}}$
9	4350.10	1	22,981.54	$z^5G^0_{2\frac{1}{2}} - e^4H_{2\frac{1}{2}}$
10	4343.724	<1	23,015.27	$z^5D^0_{1\frac{1}{2}} - f^5F_{1\frac{1}{2}}$
4	4342.486*v*	0	23,021.83	$z^5D^0_{2\frac{1}{2}} - f^5F_{2\frac{1}{2}}$
9	4341.19	1	23,028.71	$z^5G^0_{3\frac{1}{2}} - g^5F_{3\frac{1}{2}}$
7	4340.240	1*w*	23,033.75	$b^3D_{1\frac{1}{2}} - w^3D^0_{1\frac{1}{2}}$ $z^3F^0_{2\frac{1}{2}} - i^3F_{2\frac{1}{2}}$
4	4339.625*v*	5–III	23,037.01	$b^2P_{1\frac{1}{2}} - z^2F^0_{2\frac{1}{2}}$
9	4339.03	1	23,040.17	$z^5G^0_{3\frac{1}{2}} - e^5H_{4\frac{1}{2}}$
9	4337.54	2	23,048.09	$z^5F^0_{2\frac{1}{2}} - e^5D_{1\frac{1}{2}}$
9	4334.37	1	23,064.94	$a^3H_{4\frac{1}{2}} - z^3H^0_{3\frac{1}{2}}$
9	4333.14	1	23,071.49	$z^5F^0_{3\frac{1}{2}} - e^5D_{2\frac{1}{2}}$
9	4331.64	1	23,079.55	$a^4P_{2\frac{1}{2}} - y^5D^0_{1\frac{1}{2}}$
4	4331.231*v*	3–IV	23,081.66	$c^3D_{2\frac{1}{2}} - w^3F^0_{2\frac{1}{2}}$
4	4326.406*v*	0	23,107.40	$b^3D_{1\frac{1}{2}} - w^4D^0_{1\frac{1}{2}}$
9	4324.32	1	23,118.54	$z^5F^0_{2\frac{1}{2}} - e^5G_{2\frac{1}{2}}$
4	4320.385*v*	2	23,139.60	$z^5F^0_{3\frac{1}{2}} - g^5F_{3\frac{1}{2}}$
4	4313.403*v*	0	23,177.05	$b^3D_{1\frac{1}{2}} - w^4D^0_{2\frac{1}{2}}$
4	4310.093*v*	2	23,194.85	$a^3P_{1} - z^1P^0_{1}$
4	4309.437*v*	2	23,198.38	$z^5F^0_{3\frac{1}{2}} - f^5F_{4\frac{1}{2}}$
4	4307.439*v*	2–V	23,209.15	$z^5F^0_{1\frac{1}{2}} - e^5G_{2\frac{1}{2}}$
4	4303.235*v*	3–I*A*	23,231.82	$a^4F_{1\frac{1}{2}} - z^5F^0_{1\frac{1}{2}}$
4	4301.026*v*	3	23,243.75	$z^5F^0_{2\frac{1}{2}} - e^5D_{3\frac{1}{2}}$
4	4297.928*v*	2	23,260.50	$z^5D^0_{3\frac{1}{2}} - g^5F_{3\frac{1}{2}}$
4	4292.250*v*	3*h*	23,291.27	$a^3H_{4\frac{1}{2}} - x^3G^0_{3\frac{1}{2}}$
9	4291.94	1	23,292.95	$z^5F^0_{3\frac{1}{2}} - g^5F_{3\frac{1}{2}}$
7	4290.206	1	23,302.37	$b^3D_{1\frac{1}{2}} - w^3D^0_{1\frac{1}{2}}$
9	4288.54	1	23,311.42	$z^5G^0_{4\frac{1}{2}} - e^5G_{4\frac{1}{2}}$
4	4287.381*v*	2	23,317.72	$z^5F^0_{2\frac{1}{2}} - f^5F_{2\frac{1}{2}}$
4	4285.782*v*	6–I	23,326.42	$a^4F_{2\frac{1}{2}} - z^5F^0_{2\frac{1}{2}}$
10	4283.33	—	23,339.78	$b^2P_{1\frac{1}{2}} - w^4F^0_{2\frac{1}{2}}$
4	4282.567*v*	1	23,343.94	$z^5F^0_{4\frac{1}{2}} - e^5H_{4\frac{1}{2}}$
4	4276.107*v*	2	23,379.20	$z^5F^0_{3\frac{1}{2}} - e^5G_{4\frac{1}{2}}$
7	4275.069	3	23,384.88	$z^5F^0_{2\frac{1}{2}} - e^5G_{3\frac{1}{2}}$
4	4270.427*v*	2	23,410.30	$a^3F_{2\frac{1}{2}} - z^3F^0_{3\frac{1}{2}}$
4	4268.446*v*	2–III	23,421.16	$b^3P_{1\frac{1}{2}} - x^3D^0_{2\frac{1}{2}}$
5	4268.032	3*h*	23,423.43	$a^4F_{1\frac{1}{2}} - z^5F^0_{1}$
9	4267.18	1	23,428.11	$c^3D_{3\frac{1}{2}} - y^3F^0_{3\frac{1}{2}}$
10	4264.642	—	23,442.05	$b^3P_{1} - y^1P^0_{1\frac{1}{2}}$
4	4263.743*v*	2	23,447.00	$z^4G^0_{4\frac{1}{2}} - e^4H_{5\frac{1}{2}}$
10	4263.333	<1	23,449.25	$z^5D^0_{4\frac{1}{2}} - f^5F_{5\frac{1}{2}}$
4	4259.865*v*	2	23,468.34	$z^5F^0_{3\frac{1}{2}} - f^5F_{3\frac{1}{2}}$
9	4255.22	1	23,493.96	$z^4G^0_{4\frac{1}{2}} - g^5F_{5\frac{1}{2}}$
4	4252.302*v*	12–I	23,510.08	$a^4F_{3\frac{1}{2}} - z^5F^0_{2\frac{1}{2}}$
4	4248.188*v*	2–V	23,532.84	$b^2D_{1\frac{1}{2}} - y^3P^0_{1\frac{1}{2}}$
4	4245.578*v*	2–V	23,547.31	$z^5F^0_{2\frac{1}{2}} - g^5F_{2\frac{1}{2}}$
5	4241.886	2–III	23,567.81	$a^3D_{3\frac{1}{2}} - x^4D^0_{2\frac{1}{2}}$
4	4241.516*v*	2–V	23,569.86	$z^5D^0_{4\frac{1}{2}} - h^5F_{4\frac{1}{2}}$
9	4240.79	1	23,573.90	$z^5D^0_{4\frac{1}{2}} - f^5F_{5\frac{1}{2}}$
4	4238.442*v*	2	23,586.96	$z^5G^0_{4\frac{1}{2}} - e^5G_{5\frac{1}{2}}$
4	4237.341*v*	1–III	23,593.08	$a^3P_{1\frac{1}{2}} - z^5P^0_{1\frac{1}{2}}$
7	4233.996‡	2–I*A* 2–I*A*	23,611.72	$a^4F_{4\frac{1}{2}} - z^5F^0_{3\frac{1}{2}}$
4	4229.955*v*	3*h*	23,634.28	$a^4F_{2\frac{1}{2}} - z^5F^0_{1\frac{1}{2}}$
11	4228.861	1	23,640.39	$z^5F^0_{3\frac{1}{2}} - e^5G_{4\frac{1}{2}}$
9	4228.54	1	23,642.19	$c^3D_{3\frac{1}{2}} - z^5D^0_{2\frac{1}{2}}$
4	4225.110*v*	2–III	23,661.38	
4	4223.768*v*	0	23,668.89	$z^5F^0_{4\frac{1}{2}} - f^5F_{4\frac{1}{2}}$
10	4222.254	<1	23,677.39	$z^5F^0_{3\frac{1}{2}} - f^5F_{3\frac{1}{2}}$
9	4221.09	1	23,683.92	$z^5D^0_{1} - h^5F_{1\frac{1}{2}}$
4	4220.436*v*	2	23,687.59	$c^3D_{2\frac{1}{2}} - 15^0_{3\frac{1}{2}}$
7	4220.274	2	23,688.50	$b^3G_{4\frac{1}{2}} - w^4D^0_{3\frac{1}{2}}$
4	4214.872*v*	2	23,718.86	
4	4210.086*v*	0	23,745.82	$z^5D^0_{2\frac{1}{2}} - h^5F_{3\frac{1}{2}}$
9	4208.74	1	23,753.42	$z^5D^0_{3\frac{1}{2}} - f^5D_{3\frac{1}{2}}$
4	4207.611*v*	2*h*	23,759.79	$a^3H_{5\frac{1}{2}} - z^3H^0_{4\frac{1}{2}}$
11	4206.143	1	23,768.08	$b^3D_{2\frac{1}{2}} - w^3D^0_{2\frac{1}{2}}$
10	4204.85	<1	23,775.39	$z^5F^0_{4\frac{1}{2}} - e^5H_{4\frac{1}{2}}$
11	4204.057	1	23,779.87	$z^5F^0_{3\frac{1}{2}} - e^3D_{1\frac{1}{2}}$?
5	4198.425	3*h*	23,811.77	$a^4F_{3\frac{1}{2}} - z^5D^0_{4\frac{1}{2}}$
12	4197.85	2	23,815.03	$z^5D^0_{1\frac{1}{2}} - h^5F_{2\frac{1}{2}}$
9	4196.84	1	23,820.76	$z^5G^0_{4\frac{1}{2}} - e^5H_{5\frac{1}{2}}$?
9	4194.87	1–III	23,831.95	
5	4194.344	5	23,834.94	
4	4192.856*v*	3*h*	23,843.40	$a^2D_{2\frac{1}{2}} - z^4S^0_{1\frac{1}{2}}$
10	4192.473	<1	23,845.57	$z^5F^0_{1} - f^5F_{1\frac{1}{2}}$
4	4190.712*v*	20–I	23,855.60	$a^4F_{4\frac{1}{2}} - z^5F^0_{5\frac{1}{2}}$
9	4189.50	1	23,862.50	$a^4F_{2\frac{1}{2}} - z^5D^0_{3\frac{1}{2}}$
4	4187.246*v*	4–II	23,875.34	$a^2D_{1\frac{1}{2}} - x^4D^0_{1\frac{1}{2}}$ $(z^5F^0_{2\frac{1}{2}} - f^5F_{2\frac{1}{2}})$
9	4184.50	1	23,891.01	$y^4D^0_{2\frac{1}{2}} - g^5P^0_{2\frac{1}{2}}$
4	4180.695*v*	0	23,912.75	$z^5F^0_{3\frac{1}{2}} - f^5F_{4\frac{1}{2}}$
4	4179.226*v*	2–III	23,921.14	$b^3G_{3\frac{1}{2}} - w^3F^0_{3\frac{1}{2}}$
9	4177.59	1	23,930.52	$a^4F_{1\frac{1}{2}} - z^5D^0_{2\frac{1}{2}}$
4	4176.039*v*	0	23,939.42	$z^5F^0_{4\frac{1}{2}} - e^5H_{5\frac{1}{2}}$
10	4172.569	1	23,959.32	$z^5G^0_{5\frac{1}{2}} - h^5F_{4\frac{1}{2}}$
4	4170.888*v*	4	23,968.98	$z^5G^0_{4\frac{1}{2}} - g^5F_{5\frac{1}{2}}$
9	4168.44	1	23,983.05	$z^5D^0_{1\frac{1}{2}} - h^5F_{1\frac{1}{2}}$
10	4168.114	<1	23,984.93	$z^5F^0_{2\frac{1}{2}} - f^5F_{2\frac{1}{2}}$?
9	4167.85	1	23,986.45	$z^5F^0_{3\frac{1}{2}} - g^5F_{3\frac{1}{2}}$
9	4167.61	1	23,987.83	$z^5D^0_{2\frac{1}{2}} - f^5P_{2\frac{1}{2}}$
5	4162.169	2–IV	24,019.18	$z^5G^0_{5\frac{1}{2}} - h^5F_{4\frac{1}{2}}$
9	4160.70	8 Co II?	24,027.67	$c^3D_{1\frac{1}{2}} - 19^0_{2\frac{1}{2}}$
4	4158.420*v*	4–III	24,040.84	$b^3G_{4\frac{1}{2}} - w^4F^0_{4\frac{1}{2}}$
9	4156.91	1	24,049.57	$a^3D_{2\frac{1}{2}} - x^4D^0_{1\frac{1}{2}}$
10	4156.646	—	24,051.10	$b^3D_{2\frac{1}{2}} - y^4D^0_{2\frac{1}{2}}$
10	4155.97	—	24,055.01	$b^2P_{1\frac{1}{2}} - w^4F^0_{2\frac{1}{2}}$
9	4151.74	1	24,079.52	$z^5F^0_{3\frac{1}{2}} - e^5G_{4\frac{1}{2}}$
9	4151.20	1	24,082.65	$b^3D_{2\frac{1}{2}} - x^4P^0_{2\frac{1}{2}}$ $z^5D^0_{2\frac{1}{2}} - 63$
4	4150.429*v*	2–I*A*	24,087.13	$b^4F_{2\frac{1}{2}} - z^5F^0_{2\frac{1}{2}}$
4	4139.452*v*	3–III	24,151.00	$a^3D_{1\frac{1}{2}} - z^5S^0_{1\frac{1}{2}}$
10	4138.393	1	24,157.18	$b^3P_{1\frac{1}{2}} - y^4P^0_{2\frac{1}{2}}$
5	4132.155	4–I	24,193.64	$a^2F_{2\frac{1}{2}} - y^4D^0_{3\frac{1}{2}}$
9	4131.85	3–V	24,195.43	
7	4130.538	1*w*	24,203.12	$b^4F_{3\frac{1}{2}} - z^5F^0_{4\frac{1}{2}}$
5	4122.271	2–III	24,251.66	$a^3H_{5\frac{1}{2}} - x^3G^0_{4\frac{1}{2}}$
4	4121.318*v*	60–II	24,257.26	$a^5F_{2\frac{1}{2}} - z^5G^0_{2\frac{1}{2}}$
4	4118.774*v*	50–II	24,272.25	$a^5F_{3\frac{1}{2}} - z^5G^0_{3\frac{1}{2}}$
4	4110.532*v*	25–I	24,320.91	$a^5F_{2\frac{1}{2}} - z^5F^0_{2\frac{1}{2}}$
5	4110.073	5*h*	24,323.63	$z^4G^0_{5\frac{1}{2}} - h^5F_{4\frac{1}{2}}$
7	4109.706	1*d*–(I*A*)	24,325.80	$a^4F_{4\frac{1}{2}} - z^5F^0_{5\frac{1}{2}}$ $c^3D_{1\frac{1}{2}} - f^5F^0_{2\frac{1}{2}}$
11	4108.488	1	24,333.01	$a^4F_{3\frac{1}{2}} - z^5D^0_{3\frac{1}{2}}$
9	4108.34	1	24,333.89	$z^5D^0_{2\frac{1}{2}} - f^5D_{2\frac{1}{2}}$
10	4106.462	<1	24,345.02	$z^5F^0_{3\frac{1}{2}} - f^5F_{3\frac{1}{2}}$
10	4106.306	<1	24,345.94	$z^5F^0_{4\frac{1}{2}} - f^5F_{5\frac{1}{2}}$
4	4104.743*v*	4–III	24,355.21	$a^2P_{1} - z^2P^0_{1}$
4	4104.418*v*	2–III	24,357.14	$a^2D_{1\frac{1}{2}} - z^4D^0_{1\frac{1}{2}}$
4	4097.193*v*	2	24,400.09	$z^5D^0_{3\frac{1}{2}} - h^5F_{4\frac{1}{2}}$
4	4095.925*v*	2–V	24,407.64	$z^5D^0_{2\frac{1}{2}} - f^5D_{3\frac{1}{2}}$
5	4093.053	2–V	24,424.77	$z^5G^0_{4\frac{1}{2}} - h^5F_{5\frac{1}{2}}$
5	4092.848	3–III	24,426.00	$b^4P_{1\frac{1}{2}} - z^4S^0_{1\frac{1}{2}}$
4	4092.386*v*	25–I	24,428.75	$a^2F_{2\frac{1}{2}} - z^2F^0_{3\frac{1}{2}}$
5	4090.354	20*h*	24,440.89	
4	4088.291*v*	1–I*A*	24,453.22	$a^4F_{3\frac{1}{2}} - z^5D^0_{4\frac{1}{2}}$
9	4086.92	1	24,461.42	$z^5D^0_{1\frac{1}{2}} - i^5F_{2\frac{1}{2}}$?
4	4086.300*v*	15–II	24,465.14	$b^4P_{2\frac{1}{2}} - z^4D^0_{3\frac{1}{2}}$
4	4084.113*v*	2	24,478.24	$z^5F^0_{2\frac{1}{2}} - h^5F_{3\frac{1}{2}}$
9	4083.63	1–IV	24,481.13	
4	4082.593*v*	2–I*A*	24,487.35	$b^4F_{1\frac{1}{2}} - z^5F^0_{1\frac{1}{2}}$
4	4081.440*v*	2–V	24,494.27	$z^5D^0_{3\frac{1}{2}} - i^5F_{4\frac{1}{2}}$
9	4079.42	1	24,506.39	$z^5D^0_{1\frac{1}{2}} - e^5P^0_{1\frac{1}{2}}$
5	4077.406	2–V	24,518.49	$z^5F^0_{4\frac{1}{2}} - h^5F_{5\frac{1}{2}}$
11	4077.382	2–III	24,518.64	
4	4076.565*v*	3*h*	24,523.56	$z^4G^0_{5\frac{1}{2}} - h^4F_{5\frac{1}{2}}$
4	4076.124*v*	3–I*A*	24,526.21	$b^4F_{3\frac{1}{2}} - z^5F^0_{3\frac{1}{2}}$
4	4069.540*v*	1–IV	24,565.89	$z^5D^0_{3\frac{1}{2}} - f^5G_{4\frac{1}{2}}$
4	4068.541*v*	8–II	24,571.92	$b^4P_{1\frac{1}{2}} - x^4D^0_{2\frac{1}{2}}$
4	4066.365*v*	15–I	24,585.07	$a^2F_{2\frac{1}{2}} - y^4D^0_{3\frac{1}{2}}$
4	4063.174*v*	3*h*	24,604.38	$b^4F_{3\frac{1}{2}} - z^5D^0_{4\frac{1}{2}}$ $c^3D_{3\frac{1}{2}} - w^3D^0_{3\frac{1}{2}}$
9	4061.76	1	24,612.94	$z^5D^0_{2\frac{1}{2}} - 1_{2\frac{1}{2}}$
10	4059.321	1–(I*A*)	24,627.73	$a^4F_{4\frac{1}{2}} - z^5D^0_{4\frac{1}{2}}$
7	4058.762	1	24,631.12	$a^3D_{1\frac{1}{2}} - z^5D^0_{1\frac{1}{2}}$
4	4058.600*v*	6–II	24,632.11	$b^4P_{1\frac{1}{2}} - x^4D^0_{1\frac{1}{2}}$
4	4058.183*v*	8–I	24,634.64	$b^4F_{3\frac{1}{2}} - z^5F^0_{3\frac{1}{2}}$
4	4057.195*v*	5–I	24,640.63	$a^4F_{1\frac{1}{2}} - z^5G^0_{2\frac{1}{2}}$
5	4056.979	2–V	24,641.95	$z^5D^0_{4\frac{1}{2}} - f^5P^0_{3\frac{1}{2}}$
4	4054.618*v*	2–(I*A*)	24,656.30	$a^4F_{3\frac{1}{2}} - z^5D^0_{3\frac{1}{2}}$
4	4053.918*v*	1–IV	24,660.55	$a^3P_{1} - w^4D^0_{1}$
4	4052.912*v*	3–III	24,666.68	$z^4G^0_{5\frac{1}{2}} - f^4G_{4\frac{1}{2}}$
4	4049.283*v*	4	24,688.78	$b^2P_{1} - x^4P^0_{1\frac{1}{2}}$
4	4045.386*v*	20–I	24,712.56	$a^2F_{2\frac{1}{2}} - y^4G^0_{3\frac{1}{2}}$
4	4040.794*v*	2–III	24,740.65	$a^2P_{1\frac{1}{2}} - z^2P^0_{1}$
5	4040.647	2	24,741.55	$b^2P_{1} - x^4P^0_{1\frac{1}{2}}$
4	4038.963*v*	0	24,751.86	$b^2D_{2\frac{1}{2}} - z^2D^0_{2\frac{1}{2}}$
4	4037.198*v*	2	24,762.68	$a^2P_{1} - z^2P^0_{1}$
4	4036.763*v*	0	24,765.35	$b^2D_{2\frac{1}{2}} - y^2P^0_{1\frac{1}{2}}$
4	4035.542*v*	8–III	24,772.84	$z^4G^0_{5\frac{1}{2}} - f^4H_{4\frac{1}{2}}$
5	4034.490	250*r* Mn	24,779.30	$(z^4G^0_{4\frac{1}{2}} - f^4G_{4\frac{1}{2}})$
4	4027.032*v*	10–I	24,825.19	$a^4F_{2\frac{1}{2}} - z^5G^0_{3\frac{1}{2}}$
10	4025.497	1	24,834.66	$z^4D^0_{3\frac{1}{2}} - f^5F_{4\frac{1}{2}}$
4	4023.399*v*	4–III	24,847.61	$b^4P_{1\frac{1}{2}} - z^4S^0_{1\frac{1}{2}}$

‡ Coincides with V I.

TABLE VIII.—*Continued.*

Ref.	λ *IA*	Int.–*TC*	Wave No. Vac.	Multiplet Designation
4	4020.898*v*	20–I	24,863.06	$b^4F_4 - z^4F^o_4$
4	4019.288*v*	5–I	24,873.02	$\begin{cases} b^4F_3 - z^4F^o_3 \\ (b^4F_4 - z^4D^o_3) \end{cases}$
5	4019.140	5	24,873.94	$a^2P_1 - w^4D^o_1$
7	4016.830	2–V	24,888.24	$z^4G_4 - f^4G_4$
4	4015.222*v*	2	24,898.21	
4	4013.942*v*	7–II	24,906.15	$b^4P_1 - x^4D^o_1$
4	4012.143*v*	2	24,917.32	$z^4F^o_4 - h^4F_4$
4	4011.089*v*	2–I*A*	24,923.86	$a^4F_3 - z^4D^o_3$
4	4010.931*v*	3*h*	24,924.85	$z^4F^o_3 - f^4D_3$
4	4007.923*v*	1–III	24,943.55	$z^4G^o_3 - i^4F_4$
11	4007.273	1	24,947.60	$z^4G^o_3 - e^6G_4$
4	4003.596*v*	2–III	24,970.51	$b^2P_1 - z^2D^o_1$
11	3999.180	1	24,998.08	$z^4D^o_2 - e^6D_3$
7	3998.554	1*n*	25,001.99	$a^2F_3 - z^2D^o_3$
4	3997.901*v*	40–II	25,006.08	$a^2F_3 - y^4F^o_3$
11	3997.051	1	25,011.40	$z^4F^o_4 - i^4F_4$
4	3995.306*v*	60–II	25,022.32	$a^2F_3 - y^4G^o_4$
4	3994.542*v*	6–I	25,027.11	$b^4F_4 - z^4G^o_5$
9	3992.36	1	25,040.79	$z^4D^o_3 - e^6G_4$
10	3992.014	1	25,042.95	$a^4F_3 - z^6G^o_3$
5	3991.831	15	25,044.10	$b^2P_1 - z^4D^o_1$
4	3991.684*v*	6–I	25,045.03	$b^4F_3 - z^6G^o_3$
4	3991.528*v*	4–IV	25,046.00	$z^6G^o_4 - f^4H^o_5$
4	3990.299*v*	6–II	25,053.72	$b^4P_1 - x^4D^o_1$
11	3989.687	1	25,057.56	$z^4D^o_2 - e^6D_3$?
4	3988.884*v*	2	25,062.61	$z^6G^o_3 - f^6G_3$
4	3987.117*v*	6–I	25,073.71	$b^4F_3 - z^4F^o_3$
7	3985.449	2*h*	25,084.21	$z^6D^o_4 - 6_4$
4	3979.518*v*	10–I	25,121.59	$a^4F_4 - z^6G^o_4$
5	3978.864	4–V	25,125.72	$z^6G^o_3 - f^4H_4$
4	3978.650*v*	10–I	25,127.07	$b^4F_3 - z^4G^o_4$
9	3977.75	1	25,132.76	$b^2G_4 - y^2F^o_3$
4	3977.184*v*	3–III	25,136.33	$a^2P_1 - x^2D^o_1$
4	3975.320*v*	3–III	25,148.12	$a^2P_1 - z^2P^o_1$
4	3974.726*v*	10–I	25,151.88	$b^4F_3 - z^4D^o_3$
5	3973.561	15Ni?	25,159.25	$z^4F^o_3 - f^4P_3$
4	3973.144*v*	10–II	25,161.89	$b^4P_2 - x^4D^o_2$
4	3972.506*v*	6–III	25,165.93	$\begin{cases} z^4F^o_4 - f^6G_4 \\ (z^4G^o_3 - f^4H_3) \end{cases}$
4	3969.116*v*	8–III	25,187.43	$b^2P_1 - w^2D^o_2$
9	3968.61	1–II*A*	25,190.64	$\begin{cases} a^2D_3 - z^4P^o_3 \\ a^4F_3 - z^6G^o_3 \end{cases}$
10	3966.438	—	25,204.43	$a^2D_3 - z^4P^o_3$
4	3965.236*v*	2–II*A*	25,212.07	$a^2F_3 - y^4D^o_2$
7	3965.011	1–II*A*	25,213.50	$a^2F_3 - y^4G^o_3$
4	3960.997*v*	6–II	25,239.05	$b^2P_1 - w^2D^o_1$
9	3958.60	1	25,254.34	$z^6G^o_3 - e^6G_3$
4	3957.928*v*	15–II	25,258.62	$b^4F_3 - z^4D^o_2$
7	3957.629	10	25,260.53	$z^4F^o_3 - i^4F_3$
9	3956.59	1	25,267.17	$z^4D^o_3 - 1_2$
4	3956.270*v*	15	25,269.21	$a^4F_4 - z^6D^o_4$
4	3954.954*v*	1	25,277.62	$z^4D^o_1 - 5_{1,2}$
7	3953.612	1*n*	25,286.20	$b^2P_1 - y^4D^o_1$
5	3952.917	25–II	25,290.64	$a^2F_4 - z^2G^o_4$
5	3952.326	8–I	25,294.42	$b^4F_4 - z^4F^o_3$
4	3951.717*v*	4*h*	25,298.32	$z^4F^o_2 - f^4G_3$
4	3947.125*v*	3–II	25,327.75	$b^4P_1 - x^4D^o_1$
4	3946.633*v*	2–II	25,330.91	$b^4P_1 - 2^o_2$
4	3945.326*v*	15–I	25,339.30	$a^2F_3 - z^2F^o_3$
5	3944.950	1–IV	25,341.72	$z^4F^o_4 - i^4F_4$
9	3944.41	1	25,345.19	$z^4F^o_2 - 1_2$
4	3942.684*v*	2–IV	25,356.28	$z^4F^o_4 - f^4D_3$
4	3941.728*v*	20–II	25,362.43	$b^4F_4 - z^4G^o_4$
4	3940.887*v*	12–I	25,367.84	$b^4F_4 - z^4D^o_3$
9	3939.07	2–V	25,379.54	$z^4F^o_4 - e^6D_4$?
4	3938.856*v*	3–V	25,380.92	$z^4F^o_3 - f^4G_4$
5	3937.949	7*h*	25,386.76	$z^4F^o_4 - e^4P_3$
4	3935.964*v*	30–II	25,399.58	$a^2F_3 - y^4F^o_4$
5	3935.287	1–III	25,403.94	$b^2P_1 - x^4P^o_1$
4	3934.712*v*	1–III	25,407.65	$b^2G_3 - z^2F^o_3$
4	3933.918*v*	6–I	25,412.78	$b^4F_3 - z^4G^o_3$
5	3933.654	80Ca?	25,414.48	
7	3933.159	1*n*	25,417.69	$z^4G^o_3 - e^6H_3$
10	3930.076	1	25,437.63	$b^4P_2 - z^4S^o_1$
4	3929.256*v*	3–III	25,442.93	$z^4F^o_4 - i^4F_4$
4	3925.151*v*	3–III	25,469.54	$b^2P_1 - y^2P^o_1$
4	3922.755*v*	7–I	25,485.10	$a^2F_3 - y^4F^o_3$
4	3921.104*v*	1–IV	25,495.83	$z^4G^o_3 - 4_2$
4	3920.729*v*	4–II	25,498.27	$a^2D_3 - z^4P^o_2$
5	3920.581	2–III	25,499.23	$a^2D_3 - z^4P^o_1$
4	3920.135*v*	2–III	25,502.13	$b^2P_1 - x^4P^o_2$
5	3919.635	4	25,505.38	$z^4F^o_3 - f^4D_2$
10	3918.627	1	25,511.94	$a^2D_3 - z^4P^o_2$
4	3917.115*v*	8–II	25,521.79	$a^2P_1 - x^2D^o_1$
4	3915.503*v*	2	25,532.30	$a^2P_1 - x^2D^o_2$
4	3909.933*v*	15–I	25,568.67	$a^4F_4 - z^6G^o_5$
9	3908.57	1	25,577.59	$z^4G^o_5 - e^6H^o_4$
4	3906.287*v*	10–I	25,592.54	$b^4F_4 - z^4G^o_3$
7	3905.540	2–V	25,597.43	
7	3904.790	3–V	25,602.35	$z^4F^o_4 - f^4G_3$
4	3904.058*v*	2–V	25,607.15	$z^4G^o_4 - e^6H^o_4$
7	3902.390	1*n*	25,618.09	$z^4G^o_3 - 5_{1,2}$
10	3899.996	<1	25,633.82	$a^4F_4 - z^6G^o_3$?
4	3898.485*v*	4–III	25,643.75	$b^4P_3 - x^4D^o_3$
4	3894.976*v*	20–II	25,666.85	$b^4F_4 - z^4D^o_3$
4	3894.073*v*	60–II	25,672.81	$a^2F_3 - y^2G^o_4$
5	3893.303	2–V	25,677.88	$z^4G^o_4 - e^6H_4$
7	3893.067	2–III	25,679.44	$a^2P_1 - z^2S^o_1$
7	3892.968	1*n*	25,680.09	$z^4F^o_2 - f^4F_3$
7	3892.210	1	25,685.09	$b^2D_1 - w^2S^o_1$
4	3892.118*v*	3–III	25,685.70	$b^2P_1 - y^2D^o_1$
5	3891.680	2–V	25,688.59	$z^4F^o_3 - i^4F_3$
4	3890.734*v*	1	25,694.84	$c^2D_1 - 23^o_1$
4	3889.978*v*	2–III	25,699.83	$z^4F^o_3 - i^4F_3$
4	3885.275*v*	6–I	25,730.94	$a^2F_3 - y^4G^o_3$
4	3884.601*v*	10–I	25,735.41	$a^2F_3 - y^4F^o_3$
4	3881.869*v*	25–I	25,753.52	$b^4F_3 - z^4D^o_3$
5	3881.006	3	25,759.24	$b^2P_1 - z^4D^o_1$
5	3880.839	8	25,760.35	
12	3880.40	3	25,763.26	
4	3878.750*v*	70*r*	25,774.23	$b^4P_1 - z^4P^o_1$
4	3876.831*v*	20–I	25,786.98	$\begin{cases} b^4F_4 - z^4G^o_4 \\ b^4P_1 - z^4P^o_1 \end{cases}$
4	3873.953*v*	40–II	25,806.14	$b^4F_3 - z^4D^o_2$
4	3873.120*v*	60–II	25,811.69	$b^4F_4 - z^4D^o_3$
4	3870.534*v*	4–III	25,828.93	$b^2P_1 - z^4D^o_2$
4	3866.832*v*	2	25,853.66	$a^4P_2 - x^4D^o_2$
7	3863.966	1	25,872.84	$b^2D_1 - w^2P^o_1$
5	3863.607	2–III	25,875.24	$b^2P_1 - y^2P^o_1$
4	3861.164*v*	20–I	25,891.61	$a^2F_3 - z^2D^o_3$
12	3860.42	4	25,896.60	
4	3856.796*v*	4–III	25,920.93	$b^4P_2 - 2^o_2$
4	3851.848*v*	2–III	25,954.23	$b^2P_1 - w^2D^o_2$
4	3850.945*v*	4–I*A*	25,960.32	$b^4F_3 - z^4G^o_3$
4	3850.097*v*	5–III	25,966.03	$c^2D_2 - 22^o_2$
4	3845.468*v*	60–II	25,997.29	$a^2F_4 - y^2G^o_4$
7	3844.866	1	26,001.36	$b^2P_1 - z^4D^o_2$
4	3843.692*v*	4–III	26,009.30	$a^2G_3 - w^4D^o_2$
4	3842.047*v*	30–II	26,020.44	$a^2F_3 - z^2D^o_2$
4	3841.458*v*	5–I	26,024.43	$a^2F_3 - y^4F^o_3$
5	3835.900	8	26,062.13	$b^2P_1 - y^4S^o_1$
5	3835.689	10	26,063.57	
5	3835.497	3	26,064.87	$a^2P_1 - z^2S^o_1$
4	3832.899*v*	5	26,082.54	$a^2P_1 - y^4P^o_1$
11	3830.096	1*n*	26,101.63	$z^4D^o_1 - g^4F_2$
9	3823.52	1–IV	26,146.52	
4	3819.908*v*	4–II	26,171.24	$b^2P_1 - z^2D^o_2$
4	3817.940*v*	18	26,184.73	$b^2P_1 - y^2P^o_1$
4	3816.876*v*	5–II	26,192.03	$a^2G_3 - x^2F^o_3$
4	3816.458*v*	15–I	26,194.90	$b^4P_1 - z^4P^o_2$
4	3816.318*v*	15–I	26,195.86	$b^4P_1 - z^4P^o_1$
4	3814.457*v*	5–III	26,208.64	$b^4P_1 - z^4P^o_1$
5	3813.925	30*r*	26,212.29	$z^4F^o_3 - e^6G_3$
5	3812.470	4–III	26,222.30	$a^4P_2 - z^4S_1$
4	3811.065*v*	5–I	26,231.97	$a^2F_4 - y^4G^o_3$
4	3808.102*v*	10–I	26,252.38	$b^4F_4 - z^4G^o_3$
4	3805.775*v*	2–III	26,268.43	$a^2P_1 - y^4P^o_1$
7	3801.233	1*n*	26,299.81	$b^2G_4 - 10^o_3$
11	3799.808	1	26,309.68	$a^4P_1 - x^4D^o_2$
4	3797.442*v*	1	26,326.07	$a^2D_3 - x^4F^o_4$
4	3795.856*v*	1	26,337.07	$z^4F^o_4 - e^6G_4$
7	3787.345	1	26,396.25	$b^2P_1 - w^4D^o_1$
4	3783.731*v*	5*h*	26,421.46	$a^2D_3 - x^4G^o_4$
4	3777.543*v*	6–III	26,464.74	$a^2D_3 - w^4D^o_3$
5	3777.078	1–III	26,468.00	$a^2P_1 - y^4P^o_1$
4	3774.599*v*	8–II	26,485.38	$a^2D_3 - w^4D^o_3$
11	3771.851	1	26,504.68	$z^4F^o_3 - 5_{1,2}$
11	3769.703	1	26,519.78	$z^6F^o_3 - e^4D^o_2$?
4	3760.401*v*	4–II	26,585.38	$a^4P_1 - z^4S^o_1$
4	3759.684*v*	3–III	26,590.45	$b^2P_1 - y^2P^o_1$
9	3756.30	1	26,614.40	$a^2G_3 - w^4F^o_3$
4	3755.447*v*	10–II	26,620.45	$a^2D_3 - w^4D^o_3$
4	3754.346*v*	4–III	26,628.26	$b^2P_1 - w^2F^o_2$
4	3752.787*v*	10	26,639.32	$b^2G_4 - 11^o_4$
9	3752.18	1	26,643.63	$z^4F^o_4 - e^6G_4$
11	3751.805	1	26,646.29	$y^4D^o_4 - g^4H_4$
4	3751.625*v*	5–III	26,647.57	$a^2D_3 - x^2F^o_3$
4	3749.930*v*	9–II	26,659.62	$a^2D_3 - z^2P^o_2$
4	3745.491*v*	25–I	26,691.21	$a^2F_4 - y^2G^o_4$
4	3740.186*v*	5–II	26,729.07	$a^2D_3 - x^4G^o_4$
4	3739.441*v*	0	26,734.39	$b^4P_3 - x^4F^o_4$
9	3739.20	1	26,736.12	$a^2G_3 - 4^o_4$
5	3735.928	12–II	26,759.53	$a^2D_2 - z^2P^o_1$
4	3734.139*v*	7–II	26,772.35	$a^2D_3 - w^4D^o_3$
4	3733.483*v*	12–II	26,777.05	$a^2D_3 - x^2F^o_3$
4	3732.390*v*	20–I	26,784.89	$b^4P_3 - z^4P^o_2$
4	3731.268*v*	2–III	26,792.95	$a^2D_3 - w^4D^o_3$
4	3730.476*v*	20–II	26,798.63	$b^4P_3 - z^4P^o_3$
4	3728.840*v*	3–III	26,810.40	$b^2P_1 - x^2S^o_1$
4	3726.653*v*	5–III	26,826.13	$a^4P_2 - z^4S^o_1$
4	3712.177*v*	6–III	26,930.74	$a^2G_4 - w^4D^o_3$
4	3711.646*v*	3–III	26,934.59	$b^4P_1 - z^2P^o_1$
4	3708.823*v*	12–II	26,955.09	$a^2D_3 - x^2F^o_3$

TABLE VIII.—*Continued.*

REF.	λ *IA*	INT.–*TC*	WAVE NO. VAC.	MULTIPLET DESIGNATION
4	3707.465*v*	6–II	26,964.96	$a^3D_{1\frac{1}{2}} - w^4D^0_{\frac{1}{2}}$
10	3707.01	—	26,968.28	$a^3G_{3\frac{1}{2}} - w^4F^0_{2\frac{1}{2}}$
4	3704.060*v*	25–I	26,989.75	$a^3F_{2\frac{1}{2}} - y^3F^0_{2\frac{1}{2}}$
4	3702.237*v*	12–III	27,003.04	$b^3G_{3\frac{1}{2}} - y^3H^0_{4\frac{1}{2}}$
5	3699.017	2*n*–IV	27,026.55	$b^3G_{4\frac{1}{2}} - y^3H^0_{4\frac{1}{2}}$
4	3693.476*v*	8–I	27,067.09	$a^3D_{1\frac{1}{2}} - z^3P^0_{1\frac{1}{2}}$
5	3693.364	2–III	27,067.91	$b^4P_{\frac{1}{2}} - w^4D^0_{1\frac{1}{2}}$
4	3693.106*v*	8–I	27,069.80	$a^3D_{2\frac{1}{2}} - w^4F^0_{2\frac{1}{2}}$
4	3690.715*v*	7–II	27,087.34	$a^3G_{4\frac{1}{2}} - x^3F^0_{3\frac{1}{2}}$
4	3686.477*v*	2–III	27,118.49	$b^3P_{\frac{1}{2}} - x^3P^0_{1\frac{1}{2}}$
4	3684.960*v*	2–III	27,129.64	$a^3P_{\frac{1}{2}} - x^4P^0_{1\frac{1}{2}}$
5	3684.479	10–III	27,133.18	$a^3D_{2\frac{1}{2}} - x^3D^0_{1\frac{1}{2}}$
4	3683.047*v*	20–II	27,143.73	$a^3D_{2\frac{1}{2}} - x^3D^0_{2\frac{1}{2}}$
11	3677.980	1	27,181.13	$b^4P_{2\frac{1}{2}} - z^3F^0_{2\frac{1}{2}}$
10	3677.835	1	27,182.20	$a^3P_{\frac{1}{2}} - x^4P^0_{\frac{1}{2}}$
4	3676.552*v*	12–III	27,191.68	$b^3G_{4\frac{1}{2}} - y^3H^0_{5\frac{1}{2}}$
4	3670.041*v*	3–III	27,239.92	$b^4P_{\frac{1}{2}} - w^4D^0_{\frac{1}{2}}$
4	3669.237*v*	1	27,245.89	$a^4P_{2\frac{1}{2}} - 1^0_{2\frac{1}{2}}$
9	3668.66	1–III	27,250.18	$b^4P_{2\frac{1}{2}} - x^4F^0_{3\frac{1}{2}}$
9	3664.6	1*n*	27,280.37	$z^6D^0_{4\frac{1}{2}} - e^2D_{4\frac{1}{2}}$
4	3662.158*v*	12–II	27,298.56	$a^3P_{1\frac{1}{2}} - w^3D^0_{2\frac{1}{2}}$
4	3660.699*v*	5	27,309.44	$a^4P_{2\frac{1}{2}} - 2^0_{2\frac{1}{2}}$
4	3657.918*v*	2–III	27,330.20	$b^3P_{\frac{1}{2}} - t^4D^0_{1\frac{1}{2}}$
4	3656.962*v*	7–I	27,337.34	$b^4F_{3\frac{1}{2}} - y^4D^0_{3\frac{1}{2}}$
10	3656.33	<1	27,342.07	$b^4P_{\frac{1}{2}} - z^3P^0_{1\frac{1}{2}}$
4	3654.441*v*	5–II	27,356.20	$b^4P_{1\frac{1}{2}} - z^3P^0_{\frac{1}{2}}$
4	3652.541*v*	15–I	27,370.43	$a^4F_{2\frac{1}{2}} - z^4F^0_{3\frac{1}{2}}$
4	3651.254*v*	4–III	27,380.08	$a^3G_{4\frac{1}{2}} - w^4F^0_{3\frac{1}{2}}$
4	3649.329*v*	8–III	27,394.52	$b^3G_{4\frac{1}{2}} - u^3F^0_{3\frac{1}{2}}$
4	3648.140*v*	3–III	27,403.45	$b^3G_{5\frac{1}{2}} - w^3G^0_{5\frac{1}{2}}$
4	3647.658*v*	12–I	27,407.07	$a^4F_{1\frac{1}{2}} - z^4F^0_{2\frac{1}{2}}$
5	3647.388	1–III	27,409.10	$b^3G_{4\frac{1}{2}} - w^3G^0_{4\frac{1}{2}}$
4	3647.081*v*	5–III	27,411.41	$a^3P_{\frac{1}{2}} - y^3D^0_{1\frac{1}{2}}$
7	3645.440	3–III	27,423.75	$a^3D_{2\frac{1}{2}} - w^4F^0_{3\frac{1}{2}}$
4	3645.190*v*	5–III	27,425.63	$b^4P_{1\frac{1}{2}} - x^4G^0_{2\frac{1}{2}}$
11	3645.005	1g?	27,427.02	$b^3G_{4\frac{1}{2}} - w^3G^0_{4\frac{1}{2}}$
4	3643.181*v*	9–II	27,440.75	$a^3D_{1\frac{1}{2}} - x^3D^0_{1\frac{1}{2}}$
4	3641.784*v*	6–II	27,451.28	$a^3D_{1\frac{1}{2}} - x^3D^0_{2\frac{1}{2}}$
7	3641.673	1*n*	27,452.11	$c^3D_{1\frac{1}{2}} - 33^0_{1\frac{1}{2},2\frac{1}{2}}$?
4	3639.443*v*	10–II	27,468.93	$b^4P_{1\frac{1}{2}} - w^4D^0_{2\frac{1}{2}}$
4	3638.346*v*	1–III	27,477.21	$b^3P_{1\frac{1}{2}} - y^3S^0_{1\frac{1}{2}}$
4	3637.45*v*	1	27,483.98	$a^3G_{4\frac{1}{2}} - w^4G^0_{5\frac{1}{2}}$
4	3637.319*v*	4–III	27,484.97	$a^3P_{\frac{1}{2}} - y^4D^0_{1\frac{1}{2}}$
4	3636.713*v*	6–II	27,489.55	$b^4P_{1\frac{1}{2}} - w^4D^0_{1\frac{1}{2}}$
4	3635.06*v*	2	27,502.02	$a^3G_{4\frac{1}{2}} - 4^0_{3\frac{1}{2}}$
4	3634.713*v*	7–III	27,504.68	$b^3G_{3\frac{1}{2}} - w^3F^0_{2\frac{1}{2}}$
4	3633.340*v*	2–III	27,515.07	$a^3P_{1\frac{1}{2}} - x^4P^0_{1\frac{1}{2}}$
4	3632.839*v*	7–III	27,518.87	$b^3G_{4\frac{1}{2}} - x^3H^0_{5\frac{1}{2}}$
5	3631.948	2–III	27,525.61	$b^3P_{1\frac{1}{2}} - x^3S^0_{1\frac{1}{2}}$
4	3631.390*v*	20*r*–I	27,529.85	$a^4F_{3\frac{1}{2}} - z^4F^0_{4\frac{1}{2}}$
7	3628.228	2*n*	27,553.84	$b^3G_{4\frac{1}{2}} - 13^0_{3\frac{1}{2},4\frac{1}{2}}$
4	3627.806*v*	25*r*–I	27,557.04	$b^4F_{4\frac{1}{2}} - z^3G^0_{4\frac{1}{2}}$
4	3626.020*v*	2–III*A*	27,570.62	$a^4P_{\frac{1}{2}} - z^4P^0_{\frac{1}{2}}$
4	3625.56*v*	3	27,574.09	$z^6G^0_{4\frac{1}{2}} - f^4G_{5\frac{1}{2}}$
4	3624.955*v*	8–I	27,578.71	$b^4F_{1\frac{1}{2}} - y^4D^0_{2\frac{1}{2}}$
4	3624.337*v*	5–III	27,583.42	$a^4P_{\frac{1}{2}} - z^4P^0_{1\frac{1}{2}}$
4	3623.02*v*	2	27,593.44	$z^6F^0_{3\frac{1}{2}} - e^4D_{4\frac{1}{2}}$?
4	3622.35*v*	1	27,598.57	$b^3G_{4\frac{1}{2}} - 14^0_{4\frac{1}{2}}$
4	3621.70*v*	15*R*	27,603.49	$z^6D^0_{4\frac{1}{2}} - e^3D_{4\frac{1}{2}}$
4	3620.422*v*	5–III	27,613.25	$a^3P_{1\frac{1}{2}} - x^4P^0_{2\frac{1}{2}}$
4	3620.03*v*	2	27,616.26	$a^3D_{2\frac{1}{2}} - w^4G^0_{3\frac{1}{2}}$
11	3619.285	1	27,621.92	$b^3P_{\frac{1}{2}} - w^3S^0_{1\frac{1}{2}}$
4	3618.010*v*	4–II*A*	27,631.65	$a^3F_{3\frac{1}{2}} - y^3D^0_{2\frac{1}{2}}$
4	3617.48*v*	2	27,635.69	$b^3P_{\frac{1}{2}} - 8^0_{1\frac{1}{2}}$
4	3615.387*v*	6–II	27,651.70	$b^4P_{1\frac{1}{2}} - x^3F^0_{2\frac{1}{2}}$
4	3614.34*v*	1	27,659.74	$b^3P_{1\frac{1}{2}} - x^3P^0_{\frac{1}{2}}$
4	3614.10*v*	0	27,661.51	$b^4P_{1\frac{1}{2}} - w^4D^0_{\frac{1}{2}}$
4	3611.701*v*	10–II	27,679.92	$a^3P_{\frac{1}{2}} - w^3D^0_{1\frac{1}{2}}$
4	3609.752*v*	4–III	27,694.86	$b^3G_{5\frac{1}{2}} - x^3H^0_{4\frac{1}{2}}$
4	3608.82*v*	3	27,702.02	$a^3D_{3\frac{1}{2}} - y^4P^0_{2\frac{1}{2}}$
5	3608.307	3–II*A*	27,705.96	$b^4F_{1\frac{1}{2}} - z^3F^0_{2\frac{1}{2}}$
4	3607.04*v*	0	27,715.72	$b^4P_{\frac{1}{2}} - x^3D^0_{1\frac{1}{2}}$
4	3606.69*v*	7	27,718.39	$b^3G_{4\frac{1}{2}} - x^3H^0_{4\frac{1}{2}}$
4	3605.370*v*	20*r*–I	27,728.52	$b^4F_{3\frac{1}{2}} - z^3F^0_{3\frac{1}{2}}$
5	3605.015	5–III	27,731.25	$a^3D_{1\frac{1}{2}} - w^4F^0_{2\frac{1}{2}}$
4	3604.469*v*	4–II	27,735.45	$a^3H_{4\frac{1}{2}} - y^3H^0_{4\frac{1}{2}}$
4	3602.38*v*	2	27,751.52	$c^3D_{1\frac{1}{2}} - 35^0_{1\frac{1}{2},2\frac{1}{2}}$
4	3602.079*v*	40*R*–II	27,753.86	$a^4F_{1\frac{1}{2}} - z^4F^0_{1\frac{1}{2}}$
4	3600.803*v*	3–III	27,763.69	$b^4P_{1\frac{1}{2}} - z^3P^0_{1\frac{1}{2}}$
4	3596.510*v*	5–III	27,796.83	$a^3P_{1\frac{1}{2}} - y^3D^0_{1\frac{1}{2}}$
4	3595.545	3	27,804.29	$b^4P_{2\frac{1}{2}} - 3^0_{3\frac{1}{2}}$?
4	3594.870*v*	50*R*–II	27,809.51	$\begin{cases} a^4F_{2\frac{1}{2}} - z^4F^0_{2\frac{1}{2}} \\ (b^3P_{\frac{1}{2}} - w^3P^0_{1\frac{1}{2}}) \end{cases}$
4	3592.33*v*	2	27,829.18	$z^6G^0_{5\frac{1}{2}} - h^4F_{4\frac{1}{2}}$?
4	3591.746*v*	4–III	27,833.70	$b^3P_{1\frac{1}{2}} - x^3P^0_{1\frac{1}{2}}$
4	3589.47*v*	2	27,851.31	$\begin{cases} z^6G^0_{4\frac{1}{2}} - i^4F_{4\frac{1}{2}} \\ z^6G^0_{4\frac{1}{2}} - e^6P_{3\frac{1}{2}} \end{cases}$
4	3587.186*v*	70*R*–II	27,869.08	$a^3F_{2\frac{1}{2}} - y^3F^0_{2\frac{1}{2}}$
7	3586.082	3–III	27,877.66	$a^3G_{5\frac{1}{2}} - z^3H^0_{4\frac{1}{2}}$
5	3585.808	4–II	27,879.79	$a^3D_{2\frac{1}{2}} - y^4P^0_{1\frac{1}{2}}$
4	3585.154*v*	25*R*–I	27,884.88	$b^4F_{3\frac{1}{2}} - y^4D^0_{3\frac{1}{2}}$
5	3584.801	15–I	27,887.62	$a^4F_{2\frac{1}{2}} - z^4D^0_{2\frac{1}{2}}$
4	3581.873*v*	4–II	27,910.42	$a^3P_{\frac{1}{2}} - y^3P^0_{1\frac{1}{2}}$
4	3579.15*v*	3	27,931.63	$b^3G_{5\frac{1}{2}} - x^4D^0_{4\frac{1}{2}}$
5	3579.029	6–II	27,932.60	$a^4P_{1\frac{1}{2}} - z^4P^0_{2\frac{1}{2}}$
5	3578.903	6–II	27,933.58	$a^4P_{1\frac{1}{2}} - z^4P^0_{\frac{1}{2}}$
4	3578.076*v*	6–II	27,940.03	$a^3P_{1\frac{1}{2}} - w^4D^0_{2\frac{1}{2}}$
5	3577.688	2–V	27,943.06	$\begin{cases} b^3P_{1\frac{1}{2}} - t^4D^0_{2\frac{1}{2}} \\ z^6G^0_{3\frac{1}{2}} - f^4G_{4\frac{1}{2}} \end{cases}$
4	3577.260*v*	3–II	27,946.41	$a^4P_{1\frac{1}{2}} - z^4P^0_{1\frac{1}{2}}$
4	3575.361*v*	60*r*–II	27,961.25	$a^4F_{2\frac{1}{2}} - z^4F^0_{3\frac{1}{2}}$
4	3574.967*v*	25*r*–I	27,964.33	$b^4F_{3\frac{1}{2}} - y^4D^0_{3\frac{1}{2}}$
4	3573.37*v*	1	27,976.81	$\begin{cases} b^3G_{5\frac{1}{2}} - 15^0_{6\frac{1}{2}} \\ z^6G^0_{5\frac{1}{2}} - h^4F_{6\frac{1}{2}} \end{cases}$
4	3570.35*v*	4*n*–II	28,000.48	$b^3G_{4\frac{1}{2}} - 15^0_{4\frac{1}{2}}$
4	3569.370*v*	80*R*–II	28,008.18	$a^3F_{2\frac{1}{2}} - y^3F^0_{3\frac{1}{2}}$
5	3568.426	2–III	28,015.59	$b^4P_{2\frac{1}{2}} - x^4G^0_{3\frac{1}{2}}$
4	3564.947*v*	25*r*–I	28,042.93	$b^4F_{2\frac{1}{2}} - z^3G^0_{3\frac{1}{2}}$
5	3564.643	2	28,045.32	$b^2P_{1\frac{1}{2}} - t^4D^0_{\frac{1}{2}}$
4	3564.115*v*	4–III	28,049.48	$z^6G^0_{5\frac{1}{2}} - f^4H^0_{4\frac{1}{2}}$
4	3562.912*v*	7–II	28,058.95	$b^4P_{2\frac{1}{2}} - w^4D^0_{1\frac{1}{2}}$
4	3562.097*v*	6–III	28,065.37	$a^3P_{1\frac{1}{2}} - w^3D^0_{1\frac{1}{2}}$
4	3561.38*v*	1	28,070.98	$b^2P_{1\frac{1}{2}} - t^4D^0_{\frac{1}{2}}$
4	3560.891*v*	20*r*–I	28,074.87	$b^4F_{1\frac{1}{2}} - y^4D^0_{\frac{1}{2}}$
5	3560.306	5–III	28,079.48	$b^4P_{2\frac{1}{2}} - w^4D^0_{1\frac{1}{2}}$
7	3559.597	1–IV	28,085.08	$a^2D_{1\frac{1}{2}} - w^4F^0_{\frac{1}{2}}$
4	3558.772*v*	12–I	28,091.59	$\begin{cases} b^4F_{3\frac{1}{2}} - z^3F^0_{3\frac{1}{2}} \\ (z^6G^0_{4\frac{1}{2}} - f^4F_{4\frac{1}{2}}) \end{cases}$
7	3557.980	2	28,097.84	$a^2D_{1\frac{1}{2}} - w^4G^0_{2\frac{1}{2}}$
10	3556.120	1	28,112.54	$a^3P_{1\frac{1}{2}} - t^4D^0_{\frac{1}{2}}$
5	3553.161	2–III	28,135.95	$a^3H_{4\frac{1}{2}} - w^3G^0_{4\frac{1}{2}}$
4	3552.989*v*	8–II	28,137.31	$b^4P_{1\frac{1}{2}} - x^3D^0_{1\frac{1}{2}}$
4	3552.720*v*	8–I	28,139.44	$a^4F_{1\frac{1}{2}} - z^4D^0_{2\frac{1}{2}}$
5	3551.666	2–III	28,147.79	$b^4P_{1\frac{1}{2}} - x^3D^0_{2\frac{1}{2}}$
4	3550.592*v*	20*r*–I	28,156.30	$a^4F_{2\frac{1}{2}} - z^4F^0_{3\frac{1}{2}}$
4	3550.20*v*	5	28,159.38	$z^6G^0_{5\frac{1}{2}} - e^4G_{4\frac{1}{2}}$?
4	3548.438*v*	7–II	28,173.40	$a^4P_{2\frac{1}{2}} - z^4P^0_{2\frac{1}{2}}$
4	3546.88*v*	1	28,185.73	$b^4P_{\frac{1}{2}} - 5^0_{\frac{1}{2}}$
4	3546.707*v*	6–III	28,187.14	$a^4P_{2\frac{1}{2}} - z^4P^0_{1\frac{1}{2}}$
4	3543.256*v*	15–II	28,214.59	$b^4P_{2\frac{1}{2}} - w^4D^0_{3\frac{1}{2}}$
7	3542.976	2–II*A*	28,216.83	$b^4F_{4\frac{1}{2}} - z^3G^0_{4\frac{1}{2}}$
5	3542.508	2*h*	28,220.55	$z^6G^0_{4\frac{1}{2}} - f^4G_{4\frac{1}{2}}$
4	3540.40*v*	3*w*	28,237.33	$z^6F^0_{3\frac{1}{2}} - f^2F_{3\frac{1}{2}}$
4	3539.442*v*	1	28,245.00	$z^6G^0_{5\frac{1}{2}} - i^4F_{4\frac{1}{2}}$
4	3538.44*v*	1	28,253.00	$b^2P_{1\frac{1}{2}} - x^4S^0_{1\frac{1}{2}}$
4	3537.707*v*	1–III	28,258.85	$b^4P_{\frac{1}{2}} - z^2S^0_{\frac{1}{2}}$
4	3534.769*v*	4–III	28,282.34	$\begin{cases} a^2P_{1\frac{1}{2}} - z^2D^0_{2\frac{1}{2}} \\ (z^6G^0_{5\frac{1}{2}} - f^4G_{4\frac{1}{2}}) \end{cases}$
4	3533.356*v*	25*r*–I	28,293.65	$a^4F_{1\frac{1}{2}} - z^4G^0_{2\frac{1}{2}}$
6	3533.081	2	28,295.84	$a^2P_{1\frac{1}{2}} - y^2P^0_{1\frac{1}{2}}$
5	3530.554	1–III	28,316.10	$a^2P_{\frac{1}{2}} - y^2P^0_{\frac{1}{2}}$
4	3529.816*v*	80*R*–II	28,322.03	$b^4F_{2\frac{1}{2}} - y^4G^0_{3\frac{1}{2}}$
4	3529.032*v*	30*r*–I	28,328.31	$a^4F_{2\frac{1}{2}} - z^4G^0_{3\frac{1}{2}}$
5	3527.947	5–III	28,337.02	$b^2P_{1\frac{1}{2}} - w^2S^0_{\frac{1}{2}}$
4	3526.847*v*	100*R*–II	28,345.86	$a^4F_{4\frac{1}{2}} - z^4F^0_{4\frac{1}{2}}$
5	3525.872	3–III	28,353.70	$b^4P_{2\frac{1}{2}} - z^2P^0_{\frac{1}{2}}$
5	3525.089	2*h*	28,360.00	$b^4P_{\frac{1}{2}} - w^4F^0_{\frac{1}{2}}$
5	3523.701	7–II	28,371.17	$b^4P_{2\frac{1}{2}} - z^2F^0_{3\frac{1}{2}}$
4	3523.423*v*	25*r*–I	28,373.41	$b^4F_{1\frac{1}{2}} - y^4D^0_{\frac{1}{2}}$
7	3522.856	4–III	28,377.98	$z^6G^0_{4\frac{1}{2}} - f^4H^0_{5\frac{1}{2}}$
5	3521.731	5–I	28,387.04	$\begin{cases} a^2D_{1\frac{1}{2}} - y^2P^0_{\frac{1}{2}} \\ b^4F_{1\frac{1}{2}} - z^2D^0_{2\frac{1}{2}} \end{cases}$
5	3521.567	30*r*–I	28,388.36	$b^4F_{4\frac{1}{2}} - z^3F^0_{3\frac{1}{2}}$
4	3520.075*v*	15–II	28,400.39	$a^4F_{3\frac{1}{2}} - z^3F^0_{3\frac{1}{2}}$
4	3518.340*v*	50*R*–II	28,414.40	$a^2F_{2\frac{1}{2}} - y^2D^0_{2\frac{1}{2}}$
5	3516.675	1–III	28,427.85	$b^4P_{1\frac{1}{2}} - w^4F^0_{2\frac{1}{2}}$
5	3516.418	2	28,429.93	$z^6G^0_{4\frac{1}{2}} - e^4G_{5\frac{1}{2}}$
4	3516.04*v*	3	28,433.03	$z^4D^0_{3\frac{1}{2}} - f^4D_{4\frac{1}{2}}$
4	3513.82*v*	3?	28,450.92	$z^4G^0_{3\frac{1}{2}} - e^4G_{4\frac{1}{2}}$
4	3513.478*v*	50*R*–II	28,453.72	$a^4F_{4\frac{1}{2}} - z^4G^0_{5\frac{1}{2}}$
4	3512.640*v*	60*R*–II	28,460.51	$b^4F_{3\frac{1}{2}} - y^4D^0_{3\frac{1}{2}}$
4	3512.41*v*	2	28,462.35	$b^4P_{\frac{1}{2}} - y^4P^0_{\frac{1}{2}}$
4	3510.426*v*	30*r*–I	28,478.46	$a^4F_{3\frac{1}{2}} - z^4D^0_{3\frac{1}{2}}$
4	3509.843*v*	50*r*–II	28,483.19	$b^4F_{2\frac{1}{2}} - y^4G^0_{3\frac{1}{2}}$
4	3506.310*v*	80*R*–II	28,511.89	$b^4F_{3\frac{1}{2}} - y^4D^0_{3\frac{1}{2}}$
4	3505.133*v*	3–III	28,521.46	$z^6G^0_{4\frac{1}{2}} - f^4F^0_{3\frac{1}{2}}$
4	3504.728*v*	5–III	28,524.76	$b^2P_{1\frac{1}{2}} - w^2P^0_{\frac{1}{2}}$
5	3503.717	3–III	28,532.98	$a^3G_{3\frac{1}{2}} - x^3G^0_{3\frac{1}{2}}$
7	3502.998	2*d*	28,538.84	$b^2P_{\frac{1}{2}} - w^2P^0_{\frac{1}{2}}$
4	3502.63*v*	20*r*–I	28,541.81	$a^4F_{2\frac{1}{2}} - z^4D^0_{2\frac{1}{2}}$
4	3502.278*v*	100*R*–II	28,544.71	$b^4F_{4\frac{1}{2}} - y^4D^0_{4\frac{1}{2}}$
5	3496.794	6–III	28,589.47	$z^6G^0_{4\frac{1}{2}} - e^4G_{4\frac{1}{2}}$
5	3496.681	15–I	28,590.40	$b^4F_{3\frac{1}{2}} - z^3G^0_{4\frac{1}{2}}$
5	3496.070	3–III	28,595.39	$a^3H_{4\frac{1}{2}} - y^3H^0_{5\frac{1}{2}}$
4	3495.682*v*	50*r*–II	28,598.57	$b^4F_{4\frac{1}{2}} - y^4G^0_{5\frac{1}{2}}$
4	3494.63*v*	2	28,607.17	$b^4P_{1\frac{1}{2}} - 5^0_{2\frac{1}{2}}$
5	3491.987	3–III	28,628.83	$\begin{cases} z^6G^0_{5\frac{1}{2}} - f^4H^0_{6\frac{1}{2}} \\ z^6G^0_{5\frac{1}{2}} - 2^0_{3\frac{1}{2}} \end{cases}$
4	3491.316*v*	15–I	28,634.33	$a^4F_{1\frac{1}{2}} - z^4D^0_{\frac{1}{2}}$
4	3490.736*v*	10–I	28,639.09	$b^4F_{2\frac{1}{2}} - z^3F^0_{2\frac{1}{2}}$
4	3489.399*v*	60*r*–II	28,650.06	$a^3F_{2\frac{1}{2}} - y^3D^0_{2\frac{1}{2}}$
4	3488.73*v*	1	28,655.56	$b^2G_{4\frac{1}{2}} - 16^0_{5\frac{1}{2}}$
7	3487.956	1*n*	28,661.91	$b^4P_{\frac{1}{2}} - y^4P^0_{\frac{1}{2}}$
4	3487.712*v*	8–II	28,663.92	$b^4P_{2\frac{1}{2}} - w^4F^0_{3\frac{1}{2}}$

TABLE VIII.—*Continued.*

Ref.	λ *IA*	Int.–*TC*	Wave No. Vac.	Multiplet Designation
4	3487.29*v*	2	28,667.37	$z^6D^o_{3\frac{1}{2}} - f^6P_{3\frac{1}{2}}$
4	3485.700*v*	4–II	28,680.46	$b^4P_{1\frac{1}{2}} - z^2S^o_{\frac{1}{2}}$
4	3485.368*v*	15–III	28,683.20	$z^6G^o_{5\frac{1}{2}} - e^6H^o_{7\frac{1}{2}}$
4	3483.80*v*	6	28,696.10	$a^4F_{3\frac{1}{2}} - z^4G^o_{2\frac{1}{2}}$
4	3483.410*v*	20*r*–I	28,699.32	$b^4F_{3\frac{1}{2}} - y^4F^o_{4\frac{1}{2}}$
5	3483.141	2–III	28,701.54	$a^2P_{1\frac{1}{2}} - y^2P^o_{\frac{1}{2}}$
7	3482.590	1*n*	28,706.07	$b^4P_{1\frac{1}{2}} - y^4P^o_{2\frac{1}{2}}$
4	3482.07*v*	3	28,710.40	$b^2D_{1\frac{1}{2}} - 16^o_{2\frac{1}{2}}$
4	3481.52*v*	1	28,714.85	$z^6G^o_{3\frac{1}{2}} - e^6D^o_{4\frac{1}{2}}$
4	3481.42*v*	1	28,715.74	$z^6G^o_{2\frac{1}{2}} - f^4G^o_{2\frac{1}{2}}$
4	3480.29*v*	3	28,725.03	$c^2D_{2\frac{1}{2}} - 35^o_{3\frac{1}{2},2\frac{1}{2}}$
4	3480.012*v*	6–II	28,727.34	$b^4P_{2\frac{1}{2}} - x^2D^o_{1\frac{1}{2}}$
11	3479.579	1–III	28,730.92	$a^4P_{\frac{1}{2}} - z^2P^o_{\frac{1}{2}}$
5	3478.744	7–II	28,737.81	$b^4P_{2\frac{1}{2}} - x^2D^o_{2\frac{1}{2}}$
5	3478.555	8–III	28,739.37	$a^2P_{1\frac{1}{2}} - w^2F^o_{2\frac{1}{2}}$
4	3477.836*v*	4–III	28,745.31	$z^6G^o_{4\frac{1}{2}} - e^6G^o_{4\frac{1}{2}}$
4	3477.64*v*	1	28,746.91	$z^6G^o_{3\frac{1}{2}} - f^6H^o_{4\frac{1}{2}}$
5	3476.360#	5*n*–IV	28,757.51	$z^6G^o_{2\frac{1}{2}} - e^6G^o_{3\frac{1}{2}}$
11	3476.002	1	28,760.48	$a^4P_{1\frac{1}{2}} - x^4F^o_{1\frac{1}{2}}$
4	3474.530*v*	6–I	28,772.66	$b^4F_{3\frac{1}{2}} - z^2D^o_{2\frac{1}{2}}$
4	3474.26*v*	6–?	28,774.86	$z^6D^o_{4\frac{1}{2}} - f^6G^o_{5\frac{1}{2}}$
11	3474.018	100*R*–II	28,776.90	$\begin{cases} a^4F_{4\frac{1}{2}} - z^4F^o_{5\frac{1}{2}} \\ b^4F_{3\frac{1}{2}} - y^4F^o_{3\frac{1}{2}} \end{cases}$
7	3473.455	1–III	28,781.57	$b^4P_{1\frac{1}{2}} - w^4F^o_{1\frac{1}{2}}$
5	3472.707	6	28,787.76	$z^6G^o_{5\frac{1}{2}} - f^6F_{4\frac{1}{2}}$
7	3472.196	1–IV	28,792.00	$z^6G^o_{4\frac{1}{2}} - e^6G^o_{5\frac{1}{2}}$
4	3471.382*v*	7–III	28,798.75	$z^6G^o_{3\frac{1}{2}} - e^6G^o_{3\frac{1}{2}}$
7	3469.683	8	28,812.85	$a^2H_{5\frac{1}{2}} - w^2G^o_{4\frac{1}{2}}$
4	3468.973*v*	3–III	28,818.75	$z^6G^o_{2\frac{1}{2}} - f^4H^o_{3\frac{1}{2}}$
5	3468.592	1–IV	28,821.92	$z^6D^o_{2\frac{1}{2}} - 1^o_{2\frac{1}{2}}$
11	3467.262	1–IV	28,832.97	$z^6G^o_{3\frac{1}{2}} - f^6F^o_{2\frac{1}{2}}$
4	3465.792*v*	100*R*–II	28,845.20	$a^4F_{4\frac{1}{2}} - z^4G^o_{5\frac{1}{2}}$
4	3464.95*v*	1	28,852.24	$z^6G^o_{3\frac{1}{2}} - e^6G^o_{3\frac{1}{2}}$
5	3463.499	3–III	28,864.30	$a^4P_{\frac{1}{2}} - w^4D^o_{1\frac{1}{2}}$
4	3462.804*v*	60*r*–II	28,870.09	$b^4F_{1\frac{1}{2}} - y^4F^o_{2\frac{1}{2}}$
4	3461.173*v*	15–III	28,883.70	$z^6G^o_{4\frac{1}{2}} - e^6H^o_{5\frac{1}{2}}$
4	3460.85*v*	1	28,886.43	$b^2D_{2\frac{1}{2}} - 14^o_{2\frac{1}{2}}$
5	3460.719	4–I	28,887.48	$a^2F_{3\frac{1}{2}} - y^2F^o_{2\frac{1}{2}}$
4	3460.58*v*	1	28,888.69	$z^6D^o_{4\frac{1}{2}} - f^4G^o_{4\frac{1}{2}}$?
5	3458.028	3–III	28,909.96	$a^2D_{2\frac{1}{2}} - w^2D^o_{2\frac{1}{2}}$
4	3456.924*v*	9–I	28,919.20	$a^4F_{3\frac{1}{2}} - z^4G^o_{3\frac{1}{2}}$
7	3456.525	1–IV	28,922.53	$a^2H_{5\frac{1}{2}} - x^2H^o_{4\frac{1}{2}}$
5	3456.437	1–IV	28,923.27	$z^6G^o_{4\frac{1}{2}} - f^4H^o_{4\frac{1}{2}}$
4	3455.237*v*	25*r*–I	28,933.32	$a^4F_{1\frac{1}{2}} - z^4D^o_{\frac{1}{2}}$
4	3454.61*v*	2*d*?	28,938.54	$z^6G^o_{5\frac{1}{2}} - g^4H^o_{6\frac{1}{2}}$
4	3454.47*v*	0	28,939.77	$z^6G^o_{2\frac{1}{2}} - e^6G^o_{3\frac{1}{2}}$
4	3453.514*v*	200*R*–II	28,947.75	$b^4F_{4\frac{1}{2}} - y^4G^o_{5\frac{1}{2}}$
4	3452.324*v*	3–III	28,957.73	$z^6G^o_{3\frac{1}{2}} - e^4H^o_{2\frac{1}{2}}$
4	3452.18*v*	2	28,958.98	$z^6G^o_{4\frac{1}{2}} - f^6F^o_{5\frac{1}{2}}$
5	3449.706	5	28,979.70	$z^6G^o_{3\frac{1}{2}} - f^6F^o_{3\frac{1}{2}}$
5	3449.441	60*R*–II	28,981.93	$b^4F_{4\frac{1}{2}} - y^4G^o_{4\frac{1}{2}}$
5	3449.170	60*R*–II	28,984.21	$b^4F_{2\frac{1}{2}} - y^4G^o_{2\frac{1}{2}}$
5	3448.358	4–III	28,991.03	$z^6G^o_{2\frac{1}{2}} - 3^o_{2\frac{1}{2}}$
5	3447.281	3–IV	29,000.09	$z^6G^o_{3\frac{1}{2}} - e^6G^o_{3\frac{1}{2}}$
4	3446.66*v*	1	29,005.33	$b^2D_{2\frac{1}{2}} - g^2P^o_{1\frac{1}{2}}$?
5	3446.088	12–III	29,010.13	$z^6G^o_{4\frac{1}{2}} - e^6H^o_{4\frac{1}{2}}$
4	3445.68*v*	2	29,013.54	$z^6D^o_{3\frac{1}{2}} - f^4D^o_{2\frac{1}{2}}$
7	3445.445	1*n*	29,015.54	$z^6D^o_{4\frac{1}{2}} - 2^o_{3\frac{1}{2}}$
4	3445.17*v*	1–III	29,017.87	$b^4P_{2\frac{1}{2}} - w^4F^o_{2\frac{1}{2}}$
4	3443.644*v*	80*R*–II	29,030.74	$b^4F_{3\frac{1}{2}} - y^4G^o_{3\frac{1}{2}}$
4	3443.42*v*	4	29,032.64	$z^6D^o_{4\frac{1}{2}} - f^6F^o_{4\frac{1}{2}}$
5	3443.203	5–III?	29,034.43	
4	3442.918*v*	40*r*–II	29,036.84	$\begin{cases} a^4F_{3\frac{1}{2}} - z^4D^o_{4\frac{1}{2}} \\ (a^4P_{\frac{1}{2}} - w^4D^o_{\frac{1}{2}}) \end{cases}$
6	3441.255	3	29,050.87	$z^6G^o_{2\frac{1}{2}} - f^6F^o_{2\frac{1}{2}}$
5	3441.140	2–IV	29,051.84	$z^6G^o_{4\frac{1}{2}} - e^6G^o_{4\frac{1}{2}}$
4	3439.39*v*	4	29,066.62	$z^6D^o_{4\frac{1}{2}} - h^4F^o_{4\frac{1}{2}}$?
5	3438.909	5–IV	29,070.69	$z^6G^o_{2\frac{1}{2}} - e^6H^o_{3\frac{1}{2}}$
5	3438.713	4–III	29,072.35	$a^2G_{4\frac{1}{2}} - z^2H^o_{5\frac{1}{2}}$
4	3438.47*v*	2	29,074.43	$z^6D^o_{4\frac{1}{2}} - f^4D^o_{3\frac{1}{2}}$
4	3438.18*v*	3*w*	29,076.81	$z^6G^o_{5\frac{1}{2}} - g^4H^o_{6\frac{1}{2}}$
4	3437.680*v*	6*n*–III	29,081.08	$z^6G^o_{3\frac{1}{2}} - e^6H^o_{4\frac{1}{2}}$
11	3437.453	1	29,083.00	$z^6D^o_{3\frac{1}{2}} - e^6D^o_{2\frac{1}{2}}$
4	3436.955*v*	3–III	29,087.22	$z^6D^o_{4\frac{1}{2}} - f^6F^o_{4\frac{1}{2}}$
10	3436.169	1	29,093.86	$a^4P_{1\frac{1}{2}} - z^2P^o_{\frac{1}{2}}$
4	3435.95*v*	1	29,095.71	$a^2G_{4\frac{1}{2}} - z^4D^o_{3\frac{1}{2}}$
5	3435.753	8	29,097.39	$z^6D^o_{4\frac{1}{2}} - e^6D^o_{4\frac{1}{2}}$
11	3435.149	1	29,102.50	$z^6D^o_{3\frac{1}{2}} - f^6G^o_{4\frac{1}{2}}$
4	3433.045*v*	60*R*–II	29,120.34	$b^4F_{1\frac{1}{2}} - y^4F^o_{2\frac{1}{2}}$
5	3432.845	3	29,122.04	$a^2H_{4\frac{1}{2}} - x^2H^o_{5\frac{1}{2}}$
5	3432.318	3–III	29,126.51	$a^2D_{2\frac{1}{2}} - x^4D^o_{1\frac{1}{2}}$
4	3431.582*v*	50*r*–II	29,132.76	$a^4F_{2\frac{1}{2}} - z^4D^o_{2\frac{1}{2}}$
7	3430.900	1*n*	29,138.55	$a^4P_{\frac{1}{2}} - z^2P^o_{\frac{1}{2}}$
7	3430.810	1*n*	29,139.31	$z^6D^o_{\frac{1}{2}} - e^6G^o_{1\frac{1}{2}}$
5	3429.681	1–IV	29,148.90	$z^6G^o_{2\frac{1}{2}} - 4^o_{2\frac{1}{2}}$
4	3428.763*v*	3–III	29,156.71	$z^6D^o_{2\frac{1}{2}} - f^6F^o_{2\frac{1}{2}}$
4	3428.222*v*	6–III	29,161.31	$\begin{cases} z^6D^o_{4\frac{1}{2}} - e^6P^o_{3\frac{1}{2}} \\ (z^6D^o_{4\frac{1}{2}} - i^4F^o_{4\frac{1}{2}}) \end{cases}$
5	3427.768	2–IV	29,165.17	$z^6D^o_{2\frac{1}{2}} - i^4F^o_{3\frac{1}{2}}$
4	3427.05*v*	1	29,171.29	$z^6G^o_{4\frac{1}{2}} - g^4H^o_{4\frac{1}{2}}$
4	3426.454*v*	3–III	29,176.36	$z^6D^o_{2\frac{1}{2}} - e^6P^o_{2\frac{1}{2}}$
4	3424.500*v*	10–II	29,193.00	$a^2D_{2\frac{1}{2}} - y^4D^o_{2\frac{1}{2}}$
4	3424.00*v*	1	29,197.30	$b^4P_{2\frac{1}{2}} - 5^o_{3\frac{1}{2}}$
4	3423.35*v*	1	29,202.84	$a^2P_{\frac{1}{2}} - y^2S^o_{\frac{1}{2}}$
4	3422.900*v*	4–III	29,206.65	$a^4P_{1\frac{1}{2}} - w^4D^o_{2\frac{1}{2}}$
5	3422.784	7	29,207.64	$z^6D^o_{3\frac{1}{2}} - i^4F^o_{4\frac{1}{2}}$
11	3422.497	1–IV	29,210.09	$z^6D^o_{2\frac{1}{2}} - e^6P^o_{1\frac{1}{2}}$
4	3422.29*v*	2	29,211.84	$z^6G^o_{3\frac{1}{2}} - g^4H^o_{4\frac{1}{2}}$
4	3421.628*v*	3–III	29,217.51	$a^2D_{1\frac{1}{2}} - w^2D^o_{2\frac{1}{2}}$
5	3421.348	3	29,219.90	$z^6D^o_{1\frac{1}{2}} - f^6F^o_{2\frac{1}{2}}$
7	3421.029	1	29,222.62	$a^2P_{1\frac{1}{2}} - u^4D^o_{1\frac{1}{2}}$
4	3420.790*v*	7–III	29,224.66	$a^2D_{2\frac{1}{2}} - x^4P^o_{2\frac{1}{2}}$
4	3420.474*v*	5–II	29,227.36	$a^4P_{\frac{1}{2}} - u^4D^o_{\frac{1}{2}}$
5	3417.795	6–I	29,250.27	$b^4F_{4\frac{1}{2}} - z^2G^o_{4\frac{1}{2}}$
5	3417.673	5–III	29,251.31	$a^2P_{\frac{1}{2}} - x^2S^o_{\frac{1}{2}}$
7	3417.353	1*d*	29,254.05	$b^2P_{1\frac{1}{2}} - w^2F^o_{2\frac{1}{2}}$
4	3417.154*v*	50*r*–II	29,255.76	$b^4F_{3\frac{1}{2}} - y^4F^o_{3\frac{1}{2}}$
4	3415.519*v*	5–I	29,269.76	$a^4F_{4\frac{1}{2}} - z^4G^o_{4\frac{1}{2}}$
5	3414.736	200*W*	29,276.47	$b^4F_{1\frac{1}{2}} - z^2D^o_{1\frac{1}{2}}$
4	3413.52*v*	3Ni?	29,286.94	$a^4F_{3\frac{1}{2}} - z^4G^o_{3\frac{1}{2}}$
4	3413.33*v*	1	29,288.53	$z^6G^o_{4\frac{1}{2}} - e^6H^o_{5\frac{1}{2}}$
4	3412.87*v*	2	29,292.50	$\begin{cases} b^2G_{4\frac{1}{2}} - 18^o_{4\frac{1}{2}} \\ z^6D^o_{4\frac{1}{2}} - 1^o_{3\frac{1}{2}} \end{cases}$
5	3412.633	80*R*–II	29,294.52	$a^4F_{4\frac{1}{2}} - z^4D^o_{3\frac{1}{2}}$
5	3412.339	80*R*–II	29,297.04	$b^4F_{3\frac{1}{2}} - y^2G^o_{4\frac{1}{2}}$
5	3409.646	15	29,320.18	$b^4F_{3\frac{1}{2}} - z^2D^o_{2\frac{1}{2}}$
5	3409.177	60*r*–II	29,324.21	$b^4F_{3\frac{1}{2}} - y^4F^o_{3\frac{1}{2}}$
5	3408.891	2–IV?	29,326.67	$\begin{cases} z^6D^o_{4\frac{1}{2}} - e^6G^o_{5\frac{1}{2}} \\ z^6D^o_{3\frac{1}{2}} - f^6F^o_{4\frac{1}{2}} \end{cases}$
4	3407.467*v*	2	29,338.93	$z^6D^o_{3\frac{1}{2}} - 2^o_{2\frac{1}{2}}$
9	3406.89	1	29,343.89	$z^6D^o_{4\frac{1}{2}} - e^6D^o_{4\frac{1}{2}}$
5	3405.816	30*R*	29,353.15	
5	3405.120	150*R*–II	29,359.15	$b^4F_{4\frac{1}{2}} - y^4F^o_{4\frac{1}{2}}$
4	3404.05*v*	1	29,368.36	$z^6F^o_{5\frac{1}{2}} - h^4F^o_{6\frac{1}{2}}$
11	3403.166	1	29,376.00	$z^6F^o_{4\frac{1}{2}} - f^4D^o_{3\frac{1}{2}}$
4	3402.18*v*	2	29,384.50	$b^4P_{2\frac{1}{2}} - w^4G^o_{3\frac{1}{2}}$
5	3402.064	4–III	29,385.52	$a^2P_{\frac{1}{2}} - x^2P^o_{\frac{1}{2}}$
5	3401.913	20	29,386.82	$z^6D^o_{3\frac{1}{2}} - e^6G^o_{3\frac{1}{2}}$
5	3401.617	2–III	29,389.38	$a^4P_{1\frac{1}{2}} - x^4F^o_{2\frac{1}{2}}$
4	3400.471*v*	1–III	29,399.29	$a^4P_{1\frac{1}{2}} - w^4D^o_{\frac{1}{2}}$
4	3399.93*v*	1*w*	29,403.95	$z^6G^o_{4\frac{1}{2}} - g^4H^o_{4\frac{1}{2}}$
4	3399.44*v*	1–IV	29,408.22	$a^2D_{2\frac{1}{2}} - v^2D^o_{2\frac{1}{2}}$
4	3398.811*v*	3–III	29,413.64	$z^6D^o_{3\frac{1}{2}} - e^6G^o_{4\frac{1}{2}}$
5	3396.457	1–III	29,434.03	$a^2D_{1\frac{1}{2}} - x^4F^o_{1\frac{1}{2}}$
4	3395.370*v*	40*r*–II	29,443.45	$b^4F_{3\frac{1}{2}} - y^2G^o_{3\frac{1}{2}}$
5	3394.916	2–III	29,447.39	$a^4P_{3\frac{1}{2}} - w^4D^o_{2\frac{1}{2}}$
4	3393.16*v*	2	29,462.67	$z^6F^o_{5\frac{1}{2}} - i^4F^o_{4\frac{1}{2}}$
4	3390.94*v*	1	29,481.92	$a^2D_{2\frac{1}{2}} - v^4D^o_{1\frac{1}{2}}$
7	3390.797	3–III	29,483.16	$z^6D^o_{2\frac{1}{2}} - 3^o_{1\frac{1}{2}}$
4	3390.396*v*	5–III	29,486.65	$a^2D_{1\frac{1}{2}} - x^4F^o_{\frac{1}{2}}$
11	3388.677	1–III	29,501.60	$a^4P_{1\frac{1}{2}} - z^2P^o_{1\frac{1}{2}}$
5	3388.494	3	29,503.20	$a^2G_{4\frac{1}{2}} - z^4D^o_{3\frac{1}{2}}$
4	3388.163*v*	30*r*–II	29,506.08	$b^4F_{3\frac{1}{2}} - y^4F^o_{3\frac{1}{2}}$
4	3387.47*v*	1–IV	29,512.09	$a^4P_{\frac{1}{2}} - x^2D^o_{1\frac{1}{2}}$
5	3387.061	1–IV	29,515.68	$a^2P_{1\frac{1}{2}} - u^4D^o_{\frac{1}{2}}$
11	3386.471	1*g*?	29,520.82	$z^6F^o_{3\frac{1}{2}} - 1^o_{2\frac{1}{2}}$
5	3385.559	6	29,528.77	$z^6D^o_{2\frac{1}{2}} - f^4H^o_{3\frac{1}{2}}$
4	3385.219*v*	25*r*–II	29,531.74	$b^4F_{3\frac{1}{2}} - y^4G^o_{3\frac{1}{2}}$
4	3384.78*v*	4	29,535.57	$z^6D^o_{1\frac{1}{2}} - 4^o_{2\frac{1}{2}}$
4	3383.909*v*	4–III	29,543.17	$z^6D^o_{2\frac{1}{2}} - f^6F^o_{2\frac{1}{2}}$
4	3383.18*v*	3	29,549.51	$z^6F^o_{3\frac{1}{2}} - f^4D^o_{2\frac{1}{2}}$
4	3382.96*v*	1	29,551.45	$a^2D_{2\frac{1}{2}} - v^4D^o_{2\frac{1}{2}}$
7	3382.071	2–III	29,559.22	$a^2P_{\frac{1}{2}} - x^2P^o_{\frac{1}{2}}$
5	3381.498	4–III	29,564.23	$a^2G_{4\frac{1}{2}} - x^2G^o_{4\frac{1}{2}}$
4	3379.71*v*	1	29,579.86	$z^4G^o_{5\frac{1}{2}} - g^4H^o_{5\frac{1}{2}}$
4	3378.736*v*	5–III	29,588.40	$a^2P_{1\frac{1}{2}} - y^2S^o_{\frac{1}{2}}$
4	3378.357*v*	3–III	29,591.72	$z^6D^o_{4\frac{1}{2}} - f^4H^o_{4\frac{1}{2}}$
4	3377.90*v*	2	29,595.75	$z^4G^o_{5\frac{1}{2}} - g^4H^o_{6\frac{1}{2}}$
4	3377.060*v*	5–II	29,603.08	$a^4P_{2\frac{1}{2}} - w^4D^o_{2\frac{1}{2}}$
5	3376.934	2	29,604.18	$b^2P_{1\frac{1}{2}} - 12^o_{2\frac{1}{2}}$
4	3376.206*v*	2–III	29,610.57	$z^6F^o_{4\frac{1}{2}} - f^4P^o_{3\frac{1}{2}}$
7	3375.238	1	29,619.06	$z^6F^o_{5\frac{1}{2}} - e^6D^o_{4\frac{1}{2}}$
5	3374.303	5–III	29,627.27	$z^6D^o_{3\frac{1}{2}} - f^6F^o_{3\frac{1}{2}}$
4	3373.969*v*	4–III	29,630.20	$a^4P_{2\frac{1}{2}} - x^4F^o_{2\frac{1}{2}}$
4	3373.33*v*	2	29,635.78	$z^6D^o_{3\frac{1}{2}} - f^4F^o_{2\frac{1}{2}}$
4	3373.226*v*	7–III	29,636.73	$a^2P_{1\frac{1}{2}} - x^2S^o_{\frac{1}{2}}$
4	3372.45*v*	2	29,643.58	$b^2D_{1\frac{1}{2}} - f^2F^o_{2\frac{1}{2}}$
5	3371.015	2	29,656.17	$z^6F^o_{4\frac{1}{2}} - f^4G^o_{5\frac{1}{2}}$
4	3370.80*v*	2	29,658.02	$z^6D^o_{3\frac{1}{2}} - 5^o_{3\frac{1}{2},2\frac{1}{2}}$
4	3370.322*v*	10–I	29,662.27	$b^4F_{3\frac{1}{2}} - z^2D^o_{2\frac{1}{2}}$
10	3368.67	1	29,676.81	$a^2D_{2\frac{1}{2}} - w^2D^o_{2\frac{1}{2}}$
5	3368.570	8	29,677.69	$z^6D^o_{4\frac{1}{2}} - e^6D^o_{3\frac{1}{2}}$
11	3367.411	1	29,687.91	$z^6D^o_{4\frac{1}{2}} - f^4H^o_{5\frac{1}{2}}$
4	3367.111*v*	30*r*–II	29,690.55	$b^4F_{4\frac{1}{2}} - y^4G^o_{5\frac{1}{2}}$
5	3365.014	2–III	29,709.05	$\begin{cases} b^4P_{\frac{1}{2}} - x^4P^o_{1\frac{1}{2}} \\ (b^2P_{\frac{1}{2}} - y^2P^o_{1\frac{1}{2}}) \end{cases}$
7	3364.900	1*n*	29,710.06	$z^6D^o_{2\frac{1}{2}} - e^6G^o_{2\frac{1}{2}}$
4	3364.255*v*	4–III	29,715.76	$a^2D_{1\frac{1}{2}} - y^2D^o_{1\frac{1}{2}}$
5	3363.760	3–IV	29,720.13	$z^6D^o_{3\frac{1}{2}} - e^6G^o_{3\frac{1}{2}}$
5	3363.274	4–III	29,724.42	$z^6D^o_{4\frac{1}{2}} - e^6D^o_{3\frac{1}{2}}$

TABLE VIII.—*Continued.*

REF.	λ *IA*	INT.–*TC*	WAVE NO. VAC.	MULTIPLET DESIGNATION
4	3362.797*v*	6–III	29,728.64	$z^6D^0_{4\frac{1}{2}} - f^6F_{4\frac{1}{2}}$
10	3362.085	1	29,734.93	$a^4F_{4\frac{1}{2}} - z^4G^0_{3\frac{1}{2}}$?
4	3361.553*v*	5?–III	29,739.64	$z^6D^0_{4\frac{1}{2}} - e^6G_{5\frac{1}{2}}$
5	3361.267	18	29,742.17	$a^4P_{2\frac{1}{2}} - z^6P^0_{3\frac{1}{2}}$
5	3361.093	5	29,743.71	$z^6F^0_{2\frac{1}{2}} - i^4F_{3\frac{1}{2}}$
4	3359.284*v*	6–III	29,759.73	$a^4P_{2\frac{1}{2}} - x^2F^0_{3\frac{1}{2}}$
4	3359.066*v*	3–III	29,761.66	$b^4P_{\frac{1}{2}} - x^4P^0_{\frac{1}{2}}$
4	3358.003*v*	3–III	29,771.08	$\begin{cases} a^2P_{1\frac{1}{2}} - x^2P^0_{1\frac{1}{2}} \\ a^2P_{\frac{1}{2}} - i^4D^0_{1\frac{1}{2}} \end{cases}$
4	3356.842*v*	3–III	29,781.38	$z^6F^0_{2\frac{1}{2}} - f^4G_{3\frac{1}{2}}$
4	3356.464*v*	6–III	29,784.73	$a^2D_{2\frac{1}{2}} - y^4S^0_{1\frac{1}{2}}$
4	3355.940*v*	2–III	29,789.38	$a^2D_{1\frac{1}{2}} - y^4D^0_{1\frac{1}{2}}$
5	3355.118	3–III	29,796.68	$a^2P_{\frac{1}{2}} - i^4D^0_{\frac{1}{2}}$
4	3354.374*v*	20–II	29,803.29	$b^4F_{3\frac{1}{2}} - y^4F^0_{3\frac{1}{2}}$
5	3354.213	4–III?	29,804.72	$z^6F^0_{4\frac{1}{2}} - f^6F_{4\frac{1}{2}}$
4	3351.539*v*	3–III	29,828.50	$z^6F^0_{2\frac{1}{2}} - 1_{2\frac{1}{2}}$
4	3351.138*v*	1–IV	29,832.06	$z^6F^0_{3\frac{1}{2}} - f^4G_{4\frac{1}{2}}$
5	3350.376	4*h*	29,838.85	$z^6F^0_{4\frac{1}{2}} - h^4F_{5\frac{1}{2}}$
4	3349.519*v*	7	29,846.49	$z^6F^0_{4\frac{1}{2}} - f^4D_{3\frac{1}{2}}$
4	3349.204*v*	3*h*	29,849.29	$z^6D^0_{4\frac{1}{2}} - i^4F_{5\frac{1}{2}}$
4	3348.112*v*	8–II	29,859.03	$a^2D_{1\frac{1}{2}} - y^4D^0_{2\frac{1}{2}}$
5	3347.574	7	29,863.82	$z^6F^0_{3\frac{1}{2}} - i^4F_{3\frac{1}{2}}$
4	3346.932*v*	8–III	29,869.55	$z^6F^0_{4\frac{1}{2}} - e^6D_{4\frac{1}{2}}$
5	3346.310	1–III*A*	29,875.10	$a^4P_{1\frac{1}{2}} - x^2D^0_{1\frac{1}{2}}$
4	3345.57*v*	2	29,881.69	$b^2G_{4\frac{1}{2}} - 21^0_{3\frac{1}{2},4\frac{1}{2}}$
7	3345.146	1	29,885.50	$a^4P_{1\frac{1}{2}} - x^2D^0_{2\frac{1}{2}}$
4	3345.02*v*	3	29,886.63	$z^6D^0_{4\frac{1}{2}} - f^4G_{5\frac{1}{2}}$?
5	3344.245	2–III	29,893.55	$a^2D_{2\frac{1}{2}} - v^2D^0_{2\frac{1}{2}}$
7	3343.530	1	29,899.94	$z^6F^0_{4\frac{1}{2}} - f^4G_{5\frac{1}{2}}$
5	3342.734	8–III	29,907.07	$a^2D_{2\frac{1}{2}} - y^2P^0_{1\frac{1}{2}}$
5	3342.564	4	29,908.59	
4	3341.947*v*	5–III	29,914.11	$b^4P_{1\frac{1}{2}} - w^2D^0_{2\frac{1}{2}}$
4	3341.341*v*	5–III	29,919.53	$b^2G_{4\frac{1}{2}} - s^2F^0_{3\frac{1}{2}}$
4	3341.04*v*	5	29,922.22	$b^2D_{1\frac{1}{2}} - u^2L^0_{1\frac{1}{2}}$
4	3339.780*v*	8–III	29,933.51	$z^6F^0_{4\frac{1}{2}} - e^6P_{3\frac{1}{2}}$
4	3339.15*v*	4	29,939.15	$b^2G_{3\frac{1}{2}} - s^2F^0_{3\frac{1}{2}}$
4	3338.71*v*	2	29,943.07	$b^2D_{2\frac{1}{2}} - 16^0_{2\frac{1}{2}}$
5	3338.519	1–III	29,944.82	$a^2P_{1\frac{1}{2}} - x^2F^0_{2\frac{1}{2}}$
4	3337.50*v*	3	29,954.00	$z^6D^0_{3\frac{1}{2}} - 3_{3\frac{1}{2}}$
4	3337.171*v*	8–I	29,956.92	$b^4F_{4\frac{1}{2}} - y^2G^0_{4\frac{1}{2}}$
4	3334.45*v*	1	29,981.38	$z^6D^0_{2\frac{1}{2}} - 5_{1\frac{1}{2},2\frac{1}{2}}$
4	3334.146*v*	30*r*–II	29,984.10	$\begin{cases} b^4F_{4\frac{1}{2}} - y^4F^0_{3\frac{1}{2}} \\ (a^2D_{1\frac{1}{2}} - u^2D^0_{1\frac{1}{2}}) \end{cases}$
7	3333.688	1*n*	29,988.22	$b^2G_{4\frac{1}{2}} - u^2D^0_{2\frac{1}{2}}$
4	3333.388*v*	10–I	29,990.91	$\begin{cases} b^4F_{4\frac{1}{2}} - y^2G^0_{4\frac{1}{2}} \\ (b^4P_{\frac{1}{2}} - y^2L^0_{1\frac{1}{2}}) \end{cases}$
4	3331.67*v*	2	30,006.36	$z^6F^0_{5\frac{1}{2}} - f^4H_{6\frac{1}{2}}$
4	3330.81*v*	4*w*	30,014.12	$z^6D^0_{3\frac{1}{2}} - f^6F_{2\frac{1}{2}}$?
4	3329.466*v*	5–III	30,026.24	$z^6F^0_{3\frac{1}{2}} - e^6D_{3\frac{1}{2}}$
4	3329.013*v*	2–III	30,030.33	$z^6F^0_{3\frac{1}{2}} - f^6F_{4\frac{1}{2}}$
4	3328.207*v*	3–III	30,037.60	$z^6F^0_{1\frac{1}{2}} - 2_{1\frac{1}{2}}$
4	3327.50*v*	4*w*	30,043.94	$z^6D^0_{5\frac{1}{2}} - e^6H_{6\frac{1}{2}}$
5	3326.991	8–III	30,048.57	$z^6F^0_{5\frac{1}{2}} - f^6F_{5\frac{1}{2}}$
5	3326.564	2–III*A*	30,052.43	$a^4P_{2\frac{1}{2}} - w^4F^0_{2\frac{1}{2}}$
4	3326.38*v*	0	30,054.10	$a^2P_{1\frac{1}{2}} - i^4D^0_{2\frac{1}{2}}$
4	3326.27*v*	1	30,055.06	$\begin{cases} a^4P_{\frac{1}{2}} - z^2S^0_{\frac{1}{2}} \\ z^6D^0_{4\frac{1}{2}} - e^6G_{4\frac{1}{2}} \end{cases}$
4	3325.43*v*	2	30,062.69	$a^2P_{\frac{1}{2}} - w^2S^0_{\frac{1}{2}}$
4	3325.240*v*	10–II	30,064.40	$b^4P_{\frac{1}{2}} - y^4D^0_{1\frac{1}{2}}$
4	3324.81*v*	2*w*	30,068.26	$b^2G_{4\frac{1}{2}} - y^2G^0_{4\frac{1}{2}}$
4	3324.70*v*	1	30,069.31	$b^2D_{2\frac{1}{2}} - 17^0_{2\frac{1}{2}}$
4	3322.198*v*	8–III	30,091.93	$\begin{cases} a^2D_{1\frac{1}{2}} - y^4S^0_{1\frac{1}{2}} \\ b^2G_{4\frac{1}{2}} - y^2G^0_{4\frac{1}{2}} \end{cases}$
5	3321.912	2–III	30,094.51	$a^2D_{2\frac{1}{2}} - u^4L^0_{2\frac{1}{2}}$
4	3319.822*v*	4–III	30,113.46	$z^6F^0_{4\frac{1}{2}} - e^6D_{4\frac{1}{2}}$
5	3319.561	8	30,115.83	$a^4P_{2\frac{1}{2}} - x^2D^0_{1\frac{1}{2}}$
5	3319.478	8–II	30,116.58	$z^6F^0_{5\frac{1}{2}} - e^6G_{6\frac{1}{2}}$
5	3319.156	4–III	30,119.51	$z^6F^0_{3\frac{1}{2}} - e^6P_{2\frac{1}{2}}$
4	3318.60*v*	1	30,124.60	$z^6F^0_{3\frac{1}{2}} - f^4G_{3\frac{1}{2}}$
4	3318.398*v*	4–II	30,126.38	$a^4P_{2\frac{1}{2}} - x^2D^0_{2\frac{1}{2}}$
4	3317.93*v*	0	30,130.63	$b^4P_{1\frac{1}{2}} - x^4P^0_{1\frac{1}{2}}$
5	3315.035	3–III	30,156.94	$\begin{cases} a^2P_{1\frac{1}{2}} - i^4D^0_{1\frac{1}{2}} \\ z^6F^0_{\frac{1}{2}} - e^6G_{1\frac{1}{2}} \end{cases}$
5	3314.345	2–V	30,163.22	$z^6F^0_{2\frac{1}{2}} - f^6F_{2\frac{1}{2}}$
4	3314.073*v*	8–III	30,165.70	$\begin{cases} a^4P_{1\frac{1}{2}} - w^4F^0_{2\frac{1}{2}} \\ b^2G_{4\frac{1}{2}} - y^2G^0_{3\frac{1}{2}} \end{cases}$
4	3313.38*v*	1	30,171.99	$z^6F^0_{3\frac{1}{2}} - i^4F_{3\frac{1}{2}}$
4	3313.116*v*	2–IV	30,174.41	$\begin{cases} z^6F^0_{\frac{1}{2}} - e^6D_{1\frac{1}{2}} \\ (q^4P_{2\frac{1}{2}} - 4^0_{2\frac{1}{2}}) \\ (z^6F^0_{5\frac{1}{2}} - i^4F_{4\frac{1}{2}}) \end{cases}$
4	3312.825*v*	3–III	30,177.06	$a^2P_{1\frac{1}{2}} - i^4D^0_{\frac{1}{2}}$
5	3312.277	3	30,182.05	$b^4P_{1\frac{1}{2}} - x^4P^0_{\frac{1}{2}}$
5	3312.148	7–II	30,183.23	$b^2G_{4\frac{1}{2}} - y^2G^0_{3\frac{1}{2}}$
4	3311.48*v*	3	30,189.28	$a^2D_{1\frac{1}{2}} - y^2D^0_{2\frac{1}{2}}$
4	3310.16*v*	1	30,201.32	$b^2P_{1\frac{1}{2}} - u^2F^0_{2\frac{1}{2}}$
5	3309.017	2	30,211.79	$z^6F^0_{3\frac{1}{2}} - e^6D_{2\frac{1}{2}}$
4	3308.814*v*	4–III	30,213.64	$a^2D_{1\frac{1}{2}} - y^2P^0_{1\frac{1}{2}}$
7	3308.688	1	30,214.79	$z^6F^0_{3\frac{1}{2}} - e^6P_{1\frac{1}{2}}$
4	3308.482*v*	4–III	30,216.68	$a^2P_{1\frac{1}{2}} - v^2F^0_{2\frac{1}{2}}$
5	3307.473	4	30,225.89	$b^4P_{1\frac{1}{2}} - x^4P^0_{2\frac{1}{2}}$
4	3307.156*v*	7–II	30,228.79	$z^6F^0_{2\frac{1}{2}} - 1_{2\frac{1}{2}}$
4	3306.404*v*	1–IV	30,235.66	$z^6F^0_{\frac{1}{2}} - f^6F_{2\frac{1}{2}}$
4	3305.730*v*	2–III	30,241.83	
4	3305.109*v*	2–IV	30,247.51	
4	3304.791*v*	1–IV	30,250.42	$a^2P_{\frac{1}{2}} - w^2P^0_{1\frac{1}{2}}$
4	3304.119*v*	3–IV	30,256.57	$z^6F^0_{2\frac{1}{2}} - e^6G_{3\frac{1}{2}}$
4	3303.881*v*	4–II	30,258.75	$a^4P_{\frac{1}{2}} - y^4P^0_{\frac{1}{2}}$
7	3302.781	1	30,268.83	$z^6D^0_{4\frac{1}{2}} - f^6F_{5\frac{1}{2}}$
4	3299.11*v*	0	30,302.49	$z^6F^0_{4\frac{1}{2}} - f^6G_{5\frac{1}{2}}$
4	3298.680*v*	6–III	30,306.46	$b^4P_{\frac{1}{2}} - y^4D^0_{\frac{1}{2}}$
4	3297.22*v*	6	30,319.85	$z^6D^0_{4\frac{1}{2}} - e^6H^0_{5\frac{1}{2}}$
4	3296.19*v*	3	30,329.36	$z^6D^0_{3\frac{1}{2}} - 4_{2\frac{1}{2}}$
5	3294.536	2–IV	30,344.58	$z^6F^0_{\frac{1}{2}} - f^6F^0_{1\frac{1}{2}}$
4	3294.48*v*	1	30,345.09	$a^4P_{1\frac{1}{2}} - 5^0_{2\frac{1}{2}}$
5	3294.098	3	30,348.61	$z^6F^0_{1\frac{1}{2}} - e^6G^0_{1\frac{1}{2}}$
5	3293.861	2–III	30,350.80	$a^2D_{2\frac{1}{2}} - w^2F^0_{2\frac{1}{2}}$
4	3293.210*v*	3–III	30,356.80	$z^6F^0_{3\frac{1}{2}} - e^6G_{4\frac{1}{2}}$
4	3292.44*v*	2	30,363.94	$a^2P_{1\frac{1}{2}} - x^4S^0_{1\frac{1}{2}}$
4	3292.22*v*	1	30,365.96	$z^6F^0_{1\frac{1}{2}} - e^6D^0_{1\frac{1}{2}}$
4	3292.081*v*	3–III	30,367.21	$b^4P_{\frac{1}{2}} - y^4S^0_{1\frac{1}{2}}$
5	3287.827	5	30,406.49	$a^4P_{2\frac{1}{2}} - w^4F^0_{3\frac{1}{2}}$
4	3287.575*v*	2–III	30,408.83	$z^6F^0_{3\frac{1}{2}} - e^6G^0_{3\frac{1}{2}}$
4	3287.192*v*	7–II	30,412.37	$b^4P_{1\frac{1}{2}} - y^2D^0_{2\frac{1}{2}}$
5	3286.545	1–III	30,418.35	$a^4P_{1\frac{1}{2}} - z^2S^0_{\frac{1}{2}}$
5	3285.874	5	30,424.57	$b^2P_{1\frac{1}{2}} - y^2P^0_{1\frac{1}{2}}$?
5	3283.777	3–II	30,444.00	$a^4P_{1\frac{1}{2}} - y^4P^0_{2\frac{1}{2}}$
4	3283.466*v*	9–I	30,446.88	$a^2D_{2\frac{1}{2}} - u^2F^0_{3\frac{1}{2}}$
5	3283.329	4–III	30,448.15	$a^2P_{1\frac{1}{2}} - u^2S^0_{\frac{1}{2}}$
5	3282.232	1–III	30,458.32	$a^4P_{\frac{1}{2}} - y^4P^0_{\frac{1}{2}}$
7	3282.041	1–IV	30,460.10	$z^6F^0_{4\frac{1}{2}} - f^4H^0_{5\frac{1}{2}}$
7	3281.820	2	30,462.15	$a^2P_{1\frac{1}{2}} - 8^0_{1\frac{1}{2}}$
4	3281.585*v*	2–I*A*	30,464.34	$a^4F_{3\frac{1}{2}} - z^2F^0_{3\frac{1}{2}}$
4	3279.254*v*	5–II	30,485.99	$b^4P_{1\frac{1}{2}} - y^4D^0_{2\frac{1}{2}}$
4	3278.842*v*	6–III	30,489.82	$b^4P_{\frac{1}{2}} - y^2P^0_{1\frac{1}{2}}$
4	3278.105*v*	2–IV	30,496.67	$z^6F^0_{4\frac{1}{2}} - e^6L^0_{5\frac{1}{2}}$
4	3277.662*v*	3–III	30,500.79	$z^6F^0_{4\frac{1}{2}} - f^6F_{4\frac{1}{2}}$
4	3277.304*v*	4–III	30,504.12	$b^4P_{2\frac{1}{2}} - w^2D^0_{2\frac{1}{2}}$
4	3276.483*v*	4–III	30,511.77	$z^6F^0_{4\frac{1}{2}} - e^6G_{5\frac{1}{2}}$
4	3276.23*v*	2	30,514.08	$z^6F^0_{5\frac{1}{2}} - e^6H^0_{5\frac{1}{2}}$
4	3275.66*v*	1	30,519.40	$a^4P_{1\frac{1}{2}} - w^4F^0_{1\frac{1}{2}}$
5	3273.931	10	30,535.55	
4	3272.76*v*	1	30,546.49	$z^6F^0_{5\frac{1}{2}} - f^6G_{6\frac{1}{2}}$
5	3272.405	3	30,549.79	$z^6F^0_{3\frac{1}{2}} - f^6F_{3\frac{1}{2}}$
4	3271.778*v*	8–II	30,555.64	$b^4P_{1\frac{1}{2}} - y^4D^0_{1\frac{1}{2}}$
5	3270.198	2–IV	30,570.40	$z^6F^0_{5\frac{1}{2}} - f^6F_{6\frac{1}{2}}$
4	3269.30*v*	3	30,578.80	$z^6F^0_{3\frac{1}{2}} - i^4F_{3\frac{1}{2}}$
4	3268.894*v*	1–III	30,582.60	$b^2P_{2\frac{1}{2}} - x^2G^0_{3\frac{1}{2}}$
4	3268.56*v*	2*w*	30,585.77	$a^4P_{2\frac{1}{2}} - 5^0_{3\frac{1}{2}}$
4	3267.998*v*	1–IV	30,590.99	
4	3267.68*v*	2	30,593.98	$z^6P^0_{\frac{1}{2}} - 6^0_{\frac{1}{2}}$
4	3266.47*v*	4	30,605.30	$a^2G_{3\frac{1}{2}} - 6^0_{3\frac{1}{2}}$
4	3265.352*v*	3–III	30,615.77	$a^2D_{2\frac{1}{2}} - u^4D^0_{3\frac{1}{2}}$
4	3264.842*v*	5–I	30,620.56	$\begin{cases} a^2D_{1\frac{1}{2}} - y^2P^0_{\frac{1}{2}} \\ (a^4F_{2\frac{1}{2}} - y^4D^0_{2\frac{1}{2}}) \\ (z^6F^0_{4\frac{1}{2}} - e^6D^0_{3\frac{1}{2}}) \end{cases}$
7	3264.718	7*h*	30,621.72	$a^4P_{1\frac{1}{2}} - y^4P^0_{2\frac{1}{2}}$
4	3263.213*v*	4–II	30,635.84	$a^2P_{\frac{1}{2}} - w^2P^0_{1\frac{1}{2}}$
4	3260.814*v*	9–II	30,658.38	$a^2D_{1\frac{1}{2}} - w^2F^0_{2\frac{1}{2}}$
4	3260.72*v*?	—	30,659.31	$b^2P_{1\frac{1}{2}} - u^4P^0_{2\frac{1}{2}}$
5	3260.286	5	30,663.34	$z^6F^0_{5\frac{1}{2}} - e^6G_{6\frac{1}{2}}$
5	3259.847	3	30,667.48	
4	3259.20*v*	6	30,673.60	$z^6F^0_{3\frac{1}{2}} - e^6D^0_{3\frac{1}{2}}$
4	3258.418*v*	1–III	30,680.92	$b^4P_{1\frac{1}{2}} - w^2D^0_{2\frac{1}{2}}$
4	3258.035*v*	4–III	30,684.53	$a^4P_{\frac{1}{2}} - y^4P^0_{\frac{1}{2}}$
4	3254.63*v*	9	30,716.60	$z^6F^0_{2\frac{1}{2}} - e^6G^0_{2\frac{1}{2}}$
4	3254.202*v*	12–II	30,720.67	$b^4P_{2\frac{1}{2}} - x^4P^0_{2\frac{1}{2}}$
7	3253.416	1–IV	30,728.09	$b^4P_{1\frac{1}{2}} - y^4D^0_{\frac{1}{2}}$
4	3251.656*v*	2	30,744.72	$z^6F^0_{5\frac{1}{2}} - f^6F_{6\frac{1}{2}}$
4	3250.51*v*	5*w*	30,755.57	$z^6F^0_{3\frac{1}{2}} - e^6G^0_{4\frac{1}{2}}$
5	3250.335	4	30,757.22	$a^2G_{4\frac{1}{2}} - w^2F^0_{3\frac{1}{2}}$
4	3249.995*v*	6–II	30,760.44	$b^4F_{3\frac{1}{2}} - y^2F^0_{3\frac{1}{2}}$
4	3247.170*v*	8–II	30,787.20	$\begin{cases} b^4P_{2\frac{1}{2}} - y^4D^0_{2\frac{1}{2}} \\ (z^6F^0_{5\frac{1}{2}} - e^6H^0_{6\frac{1}{2}}) \end{cases}$
5	3246.997	4–III	30,788.83	$b^4P_{1\frac{1}{2}} - y^4S^0_{1\frac{1}{2}}$
4	3245.750*v*	3	30,800.67	$a^2H_{4\frac{1}{2}} - y^2G^0_{4\frac{1}{2}}$
4	3243.840*v*	8–II	30,818.80	$b^4P_{2\frac{1}{2}} - x^4P^0_{2\frac{1}{2}}$
5	3243.579	2–III	30,821.28	$a^4P_{1\frac{1}{2}} - y^4P^0_{\frac{1}{2}}$
4	3241.548*v*	5	30,840.59	$z^6F^0_{5\frac{1}{2}} - e^6H^0_{6\frac{1}{2}}$
4	3241.05*v*	3	30,845.31	$a^4F_{1\frac{1}{2}} - y^4D^0_{2\frac{1}{2}}$
7	3239.256	1	30,862.41	$a^4P_{2\frac{1}{2}} - y^4P^0_{2\frac{1}{2}}$
4	3238.92*v*	5	30,865.59	$z^6F^0_{3\frac{1}{2}} - 4_{3\frac{1}{2}}$
4	3237.80*v*	2	30,876.25	$b^2D_{2\frac{1}{2}} - v^2F^0_{3\frac{1}{2}}$
4	3237.028*v*	8–II	30,883.65	$a^4F_{3\frac{1}{2}} - z^2G^0_{4\frac{1}{2}}$
5	3235.783	5*h*	30,895.53	$b^4P_{\frac{1}{2}} - y^2P^0_{\frac{1}{2}}$
4	3235.532*v*	6–II	30,897.93	$\begin{cases} a^2H_{4\frac{1}{2}} - z^2G^0_{4\frac{1}{2}} \\ b^4P_{1\frac{1}{2}} - y^2D^0_{2\frac{1}{2}} \end{cases}$
5	3234.119	1–IV	30,911.43	$b^4P_{1\frac{1}{2}} - y^2P^0_{1\frac{1}{2}}$
4	3232.874*v*	60	30,923.33	$a^2D_{1\frac{1}{2}} - u^4D^0_{2\frac{1}{2}}$
4	3229.36*v*	3	30,956.93	$z^6F^0_{4\frac{1}{2}} - f^6F_{5\frac{1}{2}}$
4	3227.752*v*	2–II*A*	30,972.40	$a^4F_{1\frac{1}{2}} - z^2F^0_{2\frac{1}{2}}$
4	3226.986*v*	4–III	30,979.75	$a^2P_{\frac{1}{2}} - w^2P^0_{\frac{1}{2}}$
4	3226.25*v*	6	30,986.84	$z^6F^0_{5\frac{1}{2}} - e^6H^0_{5\frac{1}{2}}$
4	3226.15*v*	2	30,987.77	$\begin{cases} a^2H_{4\frac{1}{2}} - 22^0_{4\frac{1}{2}} \\ z^6F^0_{2\frac{1}{2}} - 5_{1\frac{1}{2},2\frac{1}{2}} \end{cases}$
4	3224.632*v*	4–III	31,002.37	$b^4P_{2\frac{1}{2}} - y^2D^0_{3\frac{1}{2}}$

TABLE VIII.—*Continued.*

Ref.	λ *IA*	Int.–*TC*	Wave No. Vac.	Multiplet Designation
5	3223.147	1–III*A*	31,016.65	$b^4F_{1\frac{1}{2}} - y^3D^o_{2\frac{1}{2}}$
4	3220.62*v*	4	31,040.99	$z^5F^o_{4\frac{1}{2}} - f^5F_{3\frac{1}{2}}$
4	3219.150*v*	5–II	31,055.17	$a^4F_{3\frac{1}{2}} - z^5F^o_{3\frac{1}{2}}$
4	3216.996	1–III	31,075.95	$b^4P_{2\frac{1}{2}} - v^4D^o_{1\frac{1}{2}}$
5	3215.332*v*	1–IV	31,092.04	$z^5F^o_{4\frac{1}{2}} - e^6H_{3\frac{1}{2}}$
4	3211.01*v*	4	31,133.87	$z^5F^o_{4\frac{1}{2}} - e^6G_{3\frac{1}{2}}$
4	3210.85*v*	3*n*–IV	31,135.41	
4	3210.219*v*	5–III	31,141.56	$a^2D_{1\frac{1}{2}} - u^4D^o_{1\frac{1}{2}}$
4	3209.80*v*	1	31,145.57	$b^4P_{2\frac{1}{2}} - v^4D^o_{2\frac{1}{2}}$
4	3208.85*v*	1	31,154.84	$b^2D_{2\frac{1}{2}} - u^2D^o_{1\frac{1}{2}}$
4	3205.883*v*	1–IV	31,183.67	$b^2D_{2\frac{1}{2}} - s^3F^o_{3\frac{1}{2}}$
4	3205.40*v*	0	31,188.34	$a^2F_{3\frac{1}{2}} - x^4D^o_{3\frac{1}{2}}$
4	3204.77*v*	1	31,194.54	$z^5F^o_{5\frac{1}{2}} - e^6H_{4\frac{1}{2}}$
4	3203.026*v*	4–I	31,211.49	$a^4F_{4\frac{1}{2}} - y^4D^o_{3\frac{1}{2}}$
4	3199.322*v*	4–I	31,247.62	$a^4F_{3\frac{1}{2}} - y^4D^o_{2\frac{1}{2}}$
4	3198.660*v*	5–II	31,254.09	$b^4F_{1\frac{1}{2}} - y^2F^o_{2\frac{1}{2}}$
4	3196.93*v*	2*w*	31,270.96	$b^4P_{2\frac{1}{2}} - w^2D^o_{1\frac{1}{2}}$
4	3196.74*v*	1	31,272.86	$z^5F^o_{5\frac{1}{2}} - 4_{3\frac{1}{2}}$?
7	3196.423	1	31,275.96	$b^2D_{2\frac{1}{2}} - u^2D^o_{2\frac{1}{2}}$
4	3193.164*v*	5–II	31,307.88	$b^4F_{4\frac{1}{2}} - y^2F^o_{3\frac{1}{2}}$
4	3192.220*v*	3–III	31,317.14	$b^4P_{1\frac{1}{2}} - y^2F^o_{1\frac{1}{2}}$
4	3191.297*v*	4–II	31,326.20	$a^4F_{3\frac{1}{2}} - z^2G^o_{3\frac{1}{2}}$
7	3190.910	1	31,329.99	$a^2P_{\frac{1}{2}} - 12^o_{1\frac{1}{2}}$
4	3189.752*v*	5–I	31,341.37	$a^4F_{1\frac{1}{2}} - y^4D^o_{1\frac{1}{2}}$
4	3188.377*v*	7–III	31,354.88	$b^4P_{1\frac{1}{2}} - w^2F^o_{2\frac{1}{2}}$
4	3187.60*v*	3	31,362.52	$b^2P_{1\frac{1}{2}} - 16^o_{2\frac{1}{2}}$
4	3187.34*v*	4	31,365.13	$a^2P_{1\frac{1}{2}} - w^2D^o_{2\frac{1}{2}}$
4	3186.350*v*	5–I	31,374.83	$a^4F_{2\frac{1}{2}} - z^2F^o_{2\frac{1}{2}}$
4	3185.948*v*	2–III	31,378.79	$b^4P_{2\frac{1}{2}} - y^4S^o_{1\frac{1}{2}}$
4	3182.118*v*	7–III	31,416.55	$b^4P_{\frac{1}{2}} - u^4D^o_{1\frac{1}{2}}$
4	3180.290*v*	2–III	31,434.61	$a^2D_{1\frac{1}{2}} - u^4D^o_{\frac{1}{2}}$
4	3179.828*v*	1–IV	31,439.18	$a^2D_{2\frac{1}{2}} - t^4D^o_{2\frac{1}{2}}$
4	3177.266*v*	8–III	31,464.53	
4	3174.905*v*	4–III	31,487.93	$b^4P_{2\frac{1}{2}} - z^2D^o_{2\frac{1}{2}}$
4	3174.140*v*	2–III	31,495.51	$a^2H_{4\frac{1}{2}} - v^2G^o_{4\frac{1}{2}}$
4	3173.56*v*	1	31,501.30	$b^2P_{2\frac{1}{2}} - y^2F^o_{3\frac{1}{2}}$
4	3173.140*v*	1–III	31,505.44	$a^4P_{\frac{1}{2}} - x^4P^o_{0\frac{1}{2}}$
4	3169.766*v*	9–III	31,538.97	$a^2D_{2\frac{1}{2}} - v^2F^o_{3\frac{1}{2}}$
5	3168.060	6–III	31,555.96	$a^2D_{2\frac{1}{2}} - x^2P^o_{1\frac{1}{2}}$
4	3161.652*v*	5–III	31,619.91	$b^4P_{1\frac{1}{2}} - u^4D^o_{2\frac{1}{2}}$
4	3159.662*v*	10–II	31,639.83	$\begin{cases} a^4F_{1\frac{1}{2}} - y^4D^o_{\frac{1}{2}} \\ b^4F_{2\frac{1}{2}} - y^2F^o_{2\frac{1}{2}} \end{cases}$
4	3158.772*v*	12–II	31,648.74	$a^4F_{2\frac{1}{2}} - y^4G^o_{2\frac{1}{2}}$
7	3158.458	1	31,651.89	$a^4P_{1\frac{1}{2}} - w^2D^o_{2\frac{1}{2}}$
7	3158.293	1	31,653.54	$a^4F_{1\frac{1}{2}} - z^2D^o_{2\frac{1}{2}}$
4	3157.090*v*	1–III	31,665.60	$a^2D_{2\frac{1}{2}} - t^4D^o_{2\frac{1}{2}}$
4	3154.794*v*	10–II	31,688.65	$b^4P_{2\frac{1}{2}} - u^4D^o_{2\frac{1}{2}}$
5	3154.678	5–III	31,689.81	$a^2D_{1\frac{1}{2}} - x^2P^o_{\frac{1}{2}}$
7	3153.692	1	31,699.72	$a^4F_{4\frac{1}{2}} - z^2G^o_{4\frac{1}{2}}$
4	3152.707*v*	6–III	31,709.62	$b^4P_{\frac{1}{2}} - u^4D^o_{\frac{1}{2}}$
7	3152.120	1	31,715.53	$a^2P_{1\frac{1}{2}} - 12^o_{1\frac{1}{2}}$
5	3150.819	2–V	31,728.62	
5	3150.655	2–V	31,730.27	
4	3149.310*v*	10–II	31,743.82	$a^4F_{2\frac{1}{2}} - y^4D^o_{1\frac{1}{2}}$
4	3147.060*v*	15*r*–II	31,766.52	$a^4F_{2\frac{1}{2}} - y^4G^o_{3\frac{1}{2}}$
4	3145.49*v*	15*g*?	31,782.37	$b^4P_{\frac{1}{2}} - y^2S^o_{\frac{1}{2}}$
4	3145.022*v*	3–III	31,787.10	$a^4P_{\frac{1}{2}} - z^2D^o_{1\frac{1}{2}}$
4	3143.814*v*	2	31,799.32	$b^4F_{1\frac{1}{2}} - y^2D^o_{1\frac{1}{2}}$
4	3140.715*v*	2–IV	31,830.69	$b^4P_{\frac{1}{2}} - x^2S^o_{\frac{1}{2}}$
4	3139.947*v*	12–II	31,838.48	$\begin{cases} a^4F_{3\frac{1}{2}} - y^4D^o_{2\frac{1}{2}} \\ (b^4P_{1\frac{1}{2}} - u^4D^o_{1\frac{1}{2}}) \end{cases}$
7	3138.893	1	31,849.17	$a^2G_{4\frac{1}{2}} - z^2F^o_{3\frac{1}{2}}$
4	3138.36*v*	2	31,854.58	$b^2P_{1\frac{1}{2}} - w^4P^o_{\frac{1}{2}}$
4	3137.755*v*	4–III	31,860.72	$a^4P_{\frac{1}{2}} - t^4D^o_{\frac{1}{2}}$
7	3137.454	3–III	31,863.78	$a^2D_{1\frac{1}{2}} - x^2P^o_{1\frac{1}{2}}$
4	3137.328*v*	10–II	31,865.05	$a^4F_{1\frac{1}{2}} - y^4G^o_{2\frac{1}{2}}$
5	3136.999	1–III	31,868.40	$a^4P_{1\frac{1}{2}} - x^4P^o_{1\frac{1}{2}}$
4	3136.726*v*	5–II	31,871.17	$a^4F_{4\frac{1}{2}} - z^2F^o_{3\frac{1}{2}}$
4	3134.62*v*	2	31,892.56	$a^4P_{2\frac{1}{2}} - w^2D^o_{2\frac{1}{2}}$
4	3132.218*v*	4–II	31,917.04	$a^4F_{3\frac{1}{2}} - z^2G^o_{4\frac{1}{2}}$
4	3131.829*v*	1–IV	31,921.00	$a^4P_{1\frac{1}{2}} - x^4P^o_{\frac{1}{2}}$
4	3129.481*v*	3–III	31,944.95	$b^4P_{2\frac{1}{2}} - u^2F^o_{2\frac{1}{2}}$
4	3129.006*v*	3–II	31,949.80	$b^4F_{3\frac{1}{2}} - y^2D^o_{2\frac{1}{2}}$
4	3127.252*v*	7–I	31,967.72	$b^4F_{4\frac{1}{2}} - y^2F^o_{3\frac{1}{2}}$
5	3126.725	4–III	31,973.11	$a^2D_{1\frac{1}{2}} - t^4D^o_{2\frac{1}{2}}$
5	3126.488	1–IV	31,975.53	$a^2D_{2\frac{1}{2}} - x^4S^o_{1\frac{1}{2}}$
5	3121.566	10–II	32,025.95	$a^4F_{4\frac{1}{2}} - y^4F^o_{4\frac{1}{2}}$
5	3121.415	10–II	32,027.50	$a^4F_{4\frac{1}{2}} - y^4D^o_{3\frac{1}{2}}$
4	3120.10*v*	3	32,040.98	$b^4P_{2\frac{1}{2}} - u^2F^o_{3\frac{1}{2}}$
7	3119.154	1	32,050.71	$a^2D_{2\frac{1}{2}} - 7^o_{3\frac{1}{2}}$
4	3118.636*v*	1–II*A*	32,056.04	$a^4F_{3\frac{1}{2}} - z^2D^o_{2\frac{1}{2}}$
4	3118.249*v*	5–II	32,060.01	$a^4F_{3\frac{1}{2}} - y^4F^o_{3\frac{1}{2}}$
4	3116.75*v*	1	32,075.40	$a^2D_{1\frac{1}{2}} - t^4D^o_{1\frac{1}{2}}$
4	3114.118*v*	10Ni?	32,102.54	$a^4P_{\frac{1}{2}} - t^4D^o_{\frac{1}{2}}$
4	3113.473*v*	6–III	32,109.19	$a^4P_{2\frac{1}{2}} - x^4P^o_{1\frac{1}{2}}$
5	3111.339	2–III	32,131.21	$b^4P_{1\frac{1}{2}} - u^4D^o_{\frac{1}{2}}$
4	3110.821*v*	5–I	32,136.56	$a^4F_{1\frac{1}{2}} - y^4F^o_{2\frac{1}{2}}$
4	3110.62*v*	5	32,138.63	$b^4P_{\frac{1}{2}} - x^2P^o_{1\frac{1}{2}}$
5	3110.021	5–III	32,144.83	$a^2D_{1\frac{1}{2}} - v^2F^o_{2\frac{1}{2}}$
4	3109.506*v*	4–III	32,150.15	$\begin{cases} a^4P_{1\frac{1}{2}} - z^2D^o_{1\frac{1}{2}} \\ (a^2P_{\frac{1}{2}} - z^2P^o_{1\frac{1}{2}}) \end{cases}$
4	3108.48*v*	1	32,160.74	$a^2F_{2\frac{1}{2}} - z^4S^o_{1\frac{1}{2}}$
**	3108.223	1	32,163.40	$a^4P_{\frac{1}{2}} - y^4S^o_{1\frac{1}{2}}$
4	3107.540*v*	1–IV	32,170.49	$a^2P_{\frac{1}{2}} - z^2P^o_{\frac{1}{2}}$
5	3107.044	3–III	32,175.62	$a^4P_{2\frac{1}{2}} - v^4D^o_{2\frac{1}{2}}$
4	3106.142*v*	1–III*A*	32,184.97	$b^4F_{3\frac{1}{2}} - y^2D^o_{2\frac{1}{2}}$
4	3105.929*v*	3–II	32,187.18	$b^4F_{3\frac{1}{2}} - y^2F^o_{2\frac{1}{2}}$
5	3103.983	5–III	32,207.35	$a^4P_{2\frac{1}{2}} - x^4P^o_{2\frac{1}{2}}$
4	3103.735*v*	5–III	32,209.93	$b^4P_{2\frac{1}{2}} - u^4D^o_{2\frac{1}{2}}$
4	3102.405*v*	4–III	32,223.74	$a^4P_{1\frac{1}{2}} - v^4D^o_{1\frac{1}{2}}$
4	3100.33*v*	5	32,245.32	$b^2D_{2\frac{1}{2}} - 23^o_{3\frac{1}{2}}$
4	3100.15*v*	6*d*	32,247.22	$a^2D_{2\frac{1}{2}} - w^2P^o_{1\frac{1}{2}}$
4	3099.667*v*	2–III	32,252.20	$b^4P_{1\frac{1}{2}} - x^2S^o_{\frac{1}{2}}$
4	3098.194*v*	10–II	32,267.53	$a^4F_{3\frac{1}{2}} - y^4G^o_{3\frac{1}{2}}$
4	3096.705*v*	2–III	32,283.05	$a^2D_{1\frac{1}{2}} - x^4S^o_{1\frac{1}{2}}$
4	3096.402*v*	3–III	32,286.21	$a^4P_{\frac{1}{2}} - y^2P^o_{1\frac{1}{2}}$
4	3095.716*v*	3–III	32,293.36	$a^4P_{1\frac{1}{2}} - v^4D^o_{2\frac{1}{2}}$
4	3090.251*v*	4–III	32,350.47	$b^4P_{\frac{1}{2}} - t^4D^o_{1\frac{1}{2}}$
4	3089.596*v*	10–II	32,357.33	$a^4F_{4\frac{1}{2}} - y^4G^o_{5\frac{1}{2}}$
4	3088.676*v*	1–III*A*	32,366.97	$\begin{cases} a^2P_{\frac{1}{2}} - x^4D^o_{\frac{1}{2}} \\ (a^2D_{1\frac{1}{2}} - w^2S^o_{\frac{1}{2}}) \end{cases}$
4	3087.806*v*	3–III	32,376.09	$b^4P_{\frac{1}{2}} - t^4D^o_{\frac{1}{2}}$
4	3087.35*v*	2	32,380.91	$a^2D_{1\frac{1}{2}} - 8^o_{1\frac{1}{2}}$
4	3086.83*v*?	1?	32,386.30	$b^4P_{1\frac{1}{2}} - x^2P^o_{\frac{1}{2}}$
4	3086.777*v*	15*r*–II	32,386.88	$a^4F_{1\frac{1}{2}} - y^4F^o_{1\frac{1}{2}}$
4	3086.393*v*	4–III	32,390.90	$a^4P_{2\frac{1}{2}} - v^2D^o_{2\frac{1}{2}}$
4	3085.65*v*	3	32,398.72	$a^2H_{4\frac{1}{2}} - 25^o_{4\frac{1}{2}}$
4	3083.749*v*	1	32,418.68	$a^4P_{1\frac{1}{2}} - w^2D^o_{1\frac{1}{2}}$
5	3082.844	2–III	32,428.19	$b^4P_{2\frac{1}{2}} - u^4D^o_{1\frac{1}{2}}$
4	3082.614*v*	12*r*–II	32,430.61	$a^4F_{4\frac{1}{2}} - y^4G^o_{4\frac{1}{2}}$
4	3079.394*v*	5–II	32,464.52	$\begin{cases} a^4F_{4\frac{1}{2}} - y^4G^o_{4\frac{1}{2}} \\ a^4P_{2\frac{1}{2}} - v^4D^o_{1\frac{1}{2}} \end{cases}$
4	3073.520*v*	3–III	32,526.56	$a^4P_{1\frac{1}{2}} - y^4S^o_{1\frac{1}{2}}$
5	3072.664	20	32,535.62	$a^2P_{\frac{1}{2}} - v^2P^o_{\frac{1}{2}}$
4	3072.341*v*	15*r*–II	32,539.04	$a^4F_{2\frac{1}{2}} - y^4F^o_{2\frac{1}{2}}$
4	3071.957*v*	6–I	32,543.11	$a^4F_{1\frac{1}{2}} - z^2D^o_{1\frac{1}{2}}$
5	3070.857	1–IV	32,554.77	$a^2D_{1\frac{1}{2}} - w^2P^o_{1\frac{1}{2}}$
5	3070.752	5	32,555.88	$a^2P_{1\frac{1}{2}} - x^2P^o_{\frac{1}{2}}$
7	3070.550	1	32,558.02	$b^4P_{\frac{1}{2}} - x^4S^o_{1\frac{1}{2}}$
4	3070.34*v*	1	32,560.26	$b^4P_{1\frac{1}{2}} - x^2P^o_{1\frac{1}{2}}$
7	3069.032	1	32,574.13	$b^2P_{1\frac{1}{2}} - u^2D^o_{1\frac{1}{2}}$
4	3064.370*v*	5–II	32,623.68	$a^4F_{4\frac{1}{2}} - y^2G^o_{4\frac{1}{2}}$
4	3063.25*v*	1	32,635.58	$a^4P_{1\frac{1}{2}} - v^2D^o_{2\frac{1}{2}}$
4	3062.46*v*	1	32,643.97	$a^2F_{3\frac{1}{2}} - 2^o_{2\frac{1}{2}}$?
4	3062.199*v*	5–II	32,646.81	$a^4F_{3\frac{1}{2}} - z^2D^o_{2\frac{1}{2}}$
7	3061.983	1	32,649.11	$a^4P_{1\frac{1}{2}} - y^2P^o_{1\frac{1}{2}}$
4	3061.822*v*	20*r*–II	32,650.83	$a^4F_{4\frac{1}{2}} - y^4F^o_{3\frac{1}{2}}$
4	3061.013*v*	1–III	32,659.46	$a^4P_{2\frac{1}{2}} - w^2D^o_{1\frac{1}{2}}$
4	3060.048*v*	5–III	32,669.76	$b^4P_{1\frac{1}{2}} - t^4D^o_{2\frac{1}{2}}$
4	3056.668*v*	2	32,705.88	$a^2D_{2\frac{1}{2}} - 10^o_{3\frac{1}{2}}$
5	3054.724	4–II	32,726.69	$a^4F_{3\frac{1}{2}} - y^2G^o_{3\frac{1}{2}}$
5	3054.132	18	32,733.04	$a^4F_{4\frac{1}{2}} - z^2G^o_{4\frac{1}{2}}$
5	3050.932	60	32,767.37	$a^4P_{2\frac{1}{2}} - y^4S^o_{1\frac{1}{2}}$
4	3050.496*v*	3–III	32,772.05	$b^4P_{1\frac{1}{2}} - t^4D^o_{1\frac{1}{2}}$
4	3048.888*v*	12*r*–II	32,789.34	$a^4F_{2\frac{1}{2}} - y^4F^o_{2\frac{1}{2}}$
4	3048.108*v*	2–IV	32,797.73	$b^4P_{1\frac{1}{2}} - t^4D^o_{\frac{1}{2}}$
4	3044.004*v*	30*R*–II	32,841.94	$\begin{cases} a^4F_{4\frac{1}{2}} - y^4F^o_{4\frac{1}{2}} \\ (b^4P_{1\frac{1}{2}} - v^2F^o_{2\frac{1}{2}}) \end{cases}$
4	3042.481*v*	8–II	32,858.38	$a^4F_{3\frac{1}{2}} - y^4G^o_{4\frac{1}{2}}$
4	3040.812*v*	1–IV	32,876.42	$a^4P_{2\frac{1}{2}} - v^2D^o_{2\frac{1}{2}}$
4	3039.563*v*	3–III	32,889.93	$a^4P_{2\frac{1}{2}} - y^2P^o_{1\frac{1}{2}}$
4	3038.302*v*	2–III	32,903.57	$a^2F_{3\frac{1}{2}} - x^4D^o_{2\frac{1}{2}}$
4	3034.432*v*	6–II	32,945.53	$a^4F_{3\frac{1}{2}} - z^2D^o_{2\frac{1}{2}}$
4	3034.08*v*	1	32,949.30	$\begin{cases} b^2D_{1\frac{1}{2}} - 34^o_{1\frac{1}{2},2\frac{1}{2}} \\ b^2P_{\frac{1}{2}} - 23^o_{1\frac{1}{2}} \end{cases}$
4	3031.51*v*	0	32,977.28	$a^2G_{4\frac{1}{2}} - y^2H^o_{4\frac{1}{2}}$
4	3031.288*v*	2–III	32,979.70	$b^4P_{1\frac{1}{2}} - x^4S^o_{1\frac{1}{2}}$
4	3028.184*v*	1	33,013.51	
4	3026.373*v*	6–III	33,033.26	$b^4P_{\frac{1}{2}} - t^4D^o_{\frac{1}{2}}$
4	3024.400*v*	1	33,054.81	$\begin{cases} a^4P_{1\frac{1}{2}} - y^2P^o_{\frac{1}{2}} \\ b^4P_{1\frac{1}{2}} - 7^o_{2\frac{1}{2}} \end{cases}$
4	3023.590*v*	1	33,063.67	$b^4P_{1\frac{1}{2}} - w^2S^o_{\frac{1}{2}}$
4	3023.11*v*	0	33,068.88	$a^2D_{2\frac{1}{2}} - 11^o_{3\frac{1}{2}}$
4	3022.355*v*	3–III	33,077.18	$a^4P_{2\frac{1}{2}} - u^4D^o_{2\frac{1}{2}}$
4	3020.96*v*	1	33,092.46	$a^4P_{1\frac{1}{2}} - w^2F^o_{2\frac{1}{2}}$
4	3020.85*v*	2	33,093.65	$a^2H_{4\frac{1}{2}} - 25^o_{4\frac{1}{2}}$
4	3017.548*v*	15*r*–II	33,129.87	$a^4F_{4\frac{1}{2}} - y^4F^o_{4\frac{1}{2}}$
4	3017.254*v*	3–III	33,133.09	$b^4P_{2\frac{1}{2}} - v^2F^o_{2\frac{1}{2}}$
4	3015.686*v*	3–III	33,150.32	$b^4P_{2\frac{1}{2}} - x^2P^o_{1\frac{1}{2}}$
4	3013.592*v*	8–II	33,173.36	$a^4F_{4\frac{1}{2}} - y^4G^o_{5\frac{1}{2}}$
4	3010.01*v*	0	33,212.85	$a^4P_{\frac{1}{2}} - u^4D^o_{1\frac{1}{2}}$
4	3007.59*v*	1	33,239.51	$a^2P_{\frac{1}{2}} - w^4P^o_{1\frac{1}{2}}$
4	3006.523*v*	1	33,251.35	$b^4P_{1\frac{1}{2}} - w^2P^o_{1\frac{1}{2}}$
4	3005.974*v*	2	33,257.43	
4	3005.766*v*	3–III	33,259.72	$b^4P_{2\frac{1}{2}} - t^4D^o_{2\frac{1}{2}}$
4	3000.545*v*	7–II	33,317.59	$a^4F_{4\frac{1}{2}} - y^2G^o_{3\frac{1}{2}}$
7	2999.714	1–IV	33,326.82	$a^2D_{2\frac{1}{2}} - 12^o_{3\frac{1}{2}}$
4	2998.08*v*	3	33,344.99	$a^2G_{4\frac{1}{2}} - u^2F^o_{3\frac{1}{2}}$
7	2996.945	1	33,357.62	$a^4P_{1\frac{1}{2}} - u^4D^o_{2\frac{1}{2}}$

** Measure by R. B. King, communicated by letter, January, 1940.

TABLE VIII.—*Continued.*

Ref.	λ *IA*	Int.–*TC*	Wave No. Vac.	Multiplet Designation
4	2996.76*v*	2	33,359.70	$a^3G_{3\frac{1}{2}} - w^3G^0_{4\frac{1}{2}}$
4	2996.549*v*	1–IV	33,362.02	$b^4P_{2\frac{1}{2}} - t^4D^0_{1\frac{1}{2}}$
7	2995.248	1	33,376.51	$a^2D_{1\frac{1}{2}} - 11^0_{2\frac{1}{2}}$
4	2995.150*v*	50	33,377.60	$a^3G_{4\frac{1}{2}} - w^3G^0_{5\frac{1}{2}}$
4	2990.51*v*	4	33,429.42	$a^4P_{2\frac{1}{2}} - w^2F^0_{3\frac{1}{2}}$
4	2989.590*v*	15*r*–II	33,439.68	$a^4F_{4\frac{1}{2}} - y^3G^0_{4\frac{1}{2}}$
4	2987.166*v*	15*r*–II	33,466.81	$a^4F_{4\frac{1}{2}} - y^4F^0_{3\frac{1}{2}}$
4	2986.10*v*	0	33,478.74	$a^2G_{3\frac{1}{2}} - u^2F^0_{3\frac{1}{2}}$
4	2983.68*v*	0	33,505.88	$a^4P_{1\frac{1}{2}} - u^4D^0_{1\frac{1}{2}}$
4	2983.50*v*	2	33,507.96	$a^2F_{2\frac{1}{2}} - z^4P^0_{2\frac{1}{2}}$
4	2982.262*v*	1–III	33,521.84	$a^2F_{2\frac{1}{2}} - z^4P^0_{1\frac{1}{2}}$
7	2978.950	1*n*	33,559.11	$b^4P_{1\frac{1}{2}} - w^2P^0_{1\frac{1}{2}}$
4	2978.010*v*	30	33,569.70	$b^4P_{2\frac{1}{2}} - x^4S^0_{1\frac{1}{2}}$
4	2977.462*v*	1	33,575.88	$a^4P_{1\frac{1}{2}} - u^4D^0_{1\frac{1}{2}}$
4	2975.464*v*	4	33,598.43	$a^4P_{2\frac{1}{2}} - u^4D^0_{2\frac{1}{2}}$
4	2975.35*v*	1	33,599.68	$a^2P_{1\frac{1}{2}} - 17^0_{2\frac{1}{2}}$
4	2973.123*v*	1	33,624.88	$a^2P_{1\frac{1}{2}} - w^4P^0_{1\frac{1}{2}}$
4	2972.93*v*	1	33,627.05	$a^4P_{\frac{1}{2}} - x^4S^0_{\frac{1}{2}}$
4	2972.30*v*	0	33,634.23	$a^2D_{1\frac{1}{2}} - 12^0_{1\frac{1}{2}}$
4	2971.363*v*	1	33,644.78	$b^4P_{2\frac{1}{2}} - 7^0_{2\frac{1}{2}}$
4	2969.79*v*	1	33,662.60	$a^2F_{3\frac{1}{2}} - 2^0_{2\frac{1}{2}}$
7	2969.617	1*w*	33,664.58	$b^2P_{1\frac{1}{2}} - 23^0_{1\frac{1}{2}}$
4	2969.24*v*	2	33,668.84	$a^2G_{3\frac{1}{2}} - x^2H^0_{4\frac{1}{2}}$
4	2959.16*v*	1	33,783.52	$a^2F_{3\frac{1}{2}} - x^4F^0_{4\frac{1}{2}}$
4	2957.672*v*	50	33,800.53	$a^2D_{2\frac{1}{2}} - u^2F^0_{2\frac{1}{2}}$
4	2955.382*v*	30	33,826.72	
4	2954.83*v*	1?	33,833.01	$a^2D_{2\frac{1}{2}} - w^2G^0_{3\frac{1}{2}}$
4	2951.69*v*	1	33,868.99	$a^4P_{1\frac{1}{2}} - u^4D^0_{\frac{1}{2}}$
4	2948.49*v*	1	33,905.74	$a^2G_{3\frac{1}{2}} - s^4D^0_{2\frac{1}{2}}$
4	2948.30*v*	2	33,907.94	$a^2G_{4\frac{1}{2}} - y^2H^0_{5\frac{1}{2}}$
4	2946.01*v*	0	33,934.36	$a^2D_{2\frac{1}{2}} - u^2F^0_{2\frac{1}{2}}$
4	2944.58*v*	2	33,950.79	$a^2G_{3\frac{1}{2}} - 15^0_{3\frac{1}{2}}$?
4	2943.479*v*	30	33,963.50	$a^2D_{2\frac{1}{2}} - s^4D^0_{2\frac{1}{2}}$
4	2942.624*v*	1	33,973.37	$a^2F_{2\frac{1}{2}} - x^4F^0_{2\frac{1}{2}}$
4	2941.993*v*	1	33,980.66	$b^4P_{1\frac{1}{2}} - w^2P^0_{\frac{1}{2}}$
4	2941.182*v*	1	33,990.03	$a^4P_{1\frac{1}{2}} - x^2S^0_{\frac{1}{2}}$
4	2936.546*v*	1	34,043.68	$\begin{cases} a^4F_{3\frac{1}{2}} - y^2F^0_{2\frac{1}{2}} \\ a^4P_{2\frac{1}{2}} - 6^0_{2\frac{1}{2}} \end{cases}$
4	2934.014*v*	5	34,073.06	$b^4P_{1\frac{1}{2}} - 11^0_{2\frac{1}{2}}$
4	2929.505*v*	75	34,125.50	$a^2G_{4\frac{1}{2}} - w^2G^0_{4\frac{1}{2}}$
4	2928.812*v*	50	34,133.58	$a^4F_{4\frac{1}{2}} - y^2G^0_{3\frac{1}{2}}$
4	2927.970*v*	4	34,143.39	$a^2G_{4\frac{1}{2}} - w^2G^0_{5\frac{1}{2}}$
4	2927.667*v*	50	34,146.92	$a^2D_{2\frac{1}{2}} - v^2P^0_{1\frac{1}{2}}$
4	2919.552*v*	30	34,241.83	$a^2D_{1\frac{1}{2}} - u^2F^0_{2\frac{1}{2}}$
4	2917.12*v*	1	34,270.38	$a^2G_{4\frac{1}{2}} - 13^0_{3\frac{1}{2}}$,4
7	2916.041	1	34,283.06	$a^4F_{1\frac{1}{2}} - y^2D^0_{2\frac{1}{2}}$
4	2914.608*v*	7	34,299.91	$a^2P_{\frac{1}{2}} - u^2D^0_{1\frac{1}{2}}$
4	2911.970*v*	5	34,330.99	$b^4P_{1\frac{1}{2}} - 12^0_{1\frac{1}{2}}$
4	2911.560*v*	5	34,335.82	$a^2F_{2\frac{1}{2}} - x^4F^0_{1\frac{1}{2}}$
4	2910.31*v*	1	34,350.61	$a^2F_{2\frac{1}{2}} - x^4G^0_{2\frac{1}{2}}$
4	2909.984*v*	4	34,354.42	$a^4P_{\frac{1}{2}} - x^4S^0_{1\frac{1}{2}}$
7	2907.670	1	34,381.75	$a^2D_{2\frac{1}{2}} - w^4P^0_{2\frac{1}{2}}$
7	2905.576	1	34,406.53	$\begin{cases} a^2P_{1\frac{1}{2}} - t^2F^0_{2\frac{1}{2}} \\ a^2D_{2\frac{1}{2}} - 15^0_{2\frac{1}{2}} \end{cases}$
7	2905.496	1	34,407.48	$a^4P_{1\frac{1}{2}} - t^4D^0_{2\frac{1}{2}}$
4	2905.132*v*	3	34,411.79	
4	2904.290*v*	2	34,421.76	$a^4P_{2\frac{1}{2}} - t^4D^0_{3\frac{1}{2}}$
4	2903.197*v*	25	34,434.72	$a^2G_{4\frac{1}{2}} - x^2H^0_{4\frac{1}{2}}$
4	2901.53*v*	1	34,454.48	$a^2D_{1\frac{1}{2}} - v^2P^0_{1\frac{1}{2}}$
4	2899.819*v*	25	34,474.83	$a^2D_{1\frac{1}{2}} - v^2P^0_{\frac{1}{2}}$
4	2899.73*v*	4	34,475.90	$a^2F_{2\frac{1}{2}} - x^4F^0_{2\frac{1}{2}}$
5	2895.891	3	34,521.59	$a^4P_{2\frac{1}{2}} - v^2F^0_{2\frac{1}{2}}$
5	2895.485	20	34,526.44	$a^2F_{2\frac{1}{2}} - z^4P^0_{2\frac{1}{2}}$
5	2895.335	4	34,528.23	
4	2892.242*v*	25	34,565.15	
4	2889.845*v*	3	34,593.81	
4	2887.14*v*	1	34,626.16	$a^4P_{\frac{1}{2}} - w^2P^0_{1\frac{1}{2}}$
4	2886.86*v*	2	34,629.61	$a^2G_{4\frac{1}{2}} - 16^0_{5\frac{1}{2}}$
4	2886.444*v*	50	34,634.57	$a^4F_{3\frac{1}{2}} - y^2F^0_{2\frac{1}{2}}$
7	2885.307	3	34,648.22	$a^4P_{2\frac{1}{2}} - t^4D^0_{2\frac{1}{2}}$
7	2884.074	1	34,663.03	$\begin{cases} a^2G_{3\frac{1}{2}} - t^2F^0_{3\frac{1}{2}} \\ b^4P_{2\frac{1}{2}} - 11^0_{2\frac{1}{2}} \end{cases}$
4	2883.602*v*	15	34,668.71	$a^2D_{1\frac{1}{2}} - s^4D^0_{2\frac{1}{2}}$
4	2882.219*v*	30	34,685.34	$\begin{cases} a^2P_{1\frac{1}{2}} - u^2D^0_{1\frac{1}{2}} \\ (a^4F_{3\frac{1}{2}} - y^2D^0_{2\frac{1}{2}}) \end{cases}$
4	2881.876*v*	5	34,689.47	$a^2D_{1\frac{1}{2}} - w^4P^0_{2\frac{1}{2}}$
4	2879.612*v*	25	34,716.74	$a^2G_{4\frac{1}{2}} - 15^0_{5\frac{1}{2}}$
4	2878.558*v*	12	34,729.45	$b^4P_{\frac{1}{2}} - v^2P^0_{1\frac{1}{2}}$
4	2876.86*v*	2	34,749.91	$b^4P_{\frac{1}{2}} - v^2P^0_{\frac{1}{2}}$
4	2876.82*v*	2	34,750.47	$a^4P_{2\frac{1}{2}} - t^4D^0_{1\frac{1}{2}}$
4	2876.383*v*	3	34,755.71	$a^2G_{3\frac{1}{2}} - 17^0_{2\frac{1}{2}}$
4	2875.438*v*	2	34,767.13	
4	2874.196*v*	4	34,782.16	$a^2F_{2\frac{1}{2}} - w^4D^0_{2\frac{1}{2}}$
4	2873.32*v*	5	34,792.77	$a^4P_{1\frac{1}{2}} - 7^0_{2\frac{1}{2}}$
4	2872.497*v*	15	34,802.73	$a^2F_{2\frac{1}{2}} - w^4D^0_{1\frac{1}{2}}$
4	2871.06*v*	1*g*?	34,820.16	$a^4P_{2\frac{1}{2}} - v^2F^0_{3\frac{1}{2}}$
4	2870.506*v*	3	34,826.87	$a^2F_{3\frac{1}{2}} - x^4G^0_{4\frac{1}{2}}$
4	2867.463*v*	4	34,863.82	
5	2863.538	3	34,911.61	
7	2862.768	9*h*	34,921.00	$b^4P_{2\frac{1}{2}} - 12^0_{3\frac{1}{2}}$
4	2862.602*v*	50	34,923.02	$a^4F_{2\frac{1}{2}} - y^2F^0_{2\frac{1}{2}}$
4	2861.351*v*	15*r*	34,938.29	$b^4P_{1\frac{1}{2}} - u^2F^0_{2\frac{1}{2}}$
4	2859.654*v*	40	34,959.02	$b^4F_{2\frac{1}{2}} - x^4D^0_{2\frac{1}{2}}$
4	2857.98*v*	0	34,979.48	$b^2G_{3\frac{1}{2}} - 36^0_{3\frac{1}{2}}$,4
4	2857.21*v*	1	34,988.97	$a^4P_{1\frac{1}{2}} - w^2P^0_{1\frac{1}{2}}$
4	2856.98*v*	0	34,991.72	$a^2F_{2\frac{1}{2}} - x^4F^0_{2\frac{1}{2}}$
4	2856.04*v*	1	35,003.20	$b^2G_{4\frac{1}{2}} - 36^0_{4\frac{1}{2}}$,4
4	2851.74*v*	2	35,056.03	$a^4P_{2\frac{1}{2}} - 8^0_{3\frac{1}{2}}$
4	2850.947*v*	30	35,065.79	$a^4F_{1\frac{1}{2}} - y^2D^0_{1\frac{1}{2}}$
4	2850.047*v*	75	35,076.86	$a^2F_{2\frac{1}{2}} - z^2P^0_{1\frac{1}{2}}$
4	2849.38*v*	2	35,085.03	$a^2D_{2\frac{1}{2}} - 16^0_{3\frac{1}{2}}$
4	2848.61*v*	0	35,094.59	$a^2F_{3\frac{1}{2}} - x^2F^0_{3\frac{1}{2}}$?
4	2842.382*v*	30	35,171.44	$b^4P_{1\frac{1}{2}} - v^2P^0_{\frac{1}{2}}$
4	2837.154*v*	75*r*	35,236.25	$a^2D_{2\frac{1}{2}} - w^4P^0_{1\frac{1}{2}}$
4	2836.64*v*	0	35,242.68	$a^2G_{3\frac{1}{2}} - 18^0_{3\frac{1}{2}}$
4	2834.428*v*	50	35,270.14	$b^4F_{1\frac{1}{2}} - x^4D^0_{1\frac{1}{2}}$
4	2833.922*v*	40	35,276.43	$a^4F_{2\frac{1}{2}} - y^2D^0_{2\frac{1}{2}}$
4	2828.466*v*	15	35,344.48	
4	2826.797*v*	50*W*	35,365.34	$b^4P_{1\frac{1}{2}} - s^4D^0_{2\frac{1}{2}}$
4	2825.89*v*	0	35,376.66	$a^2D_{1\frac{1}{2}} - s^4D^0_{1\frac{1}{2}}$
5	2825.151	75*w*	35,385.95	$b^4P_{1\frac{1}{2}} - w^4P^0_{2\frac{1}{2}}$
4	2824.62*v*	1	35,392.58	$a^2D_{1\frac{1}{2}} - 16^0_{2\frac{1}{2}}$
4	2824.45*v*	1	35,394.68	$b^4P_{2\frac{1}{2}} - u^2F^0_{2\frac{1}{2}}$
5	2823.647	5*h*	35,404.80	
5	2821.745	30*h*	35,428.66	$a^2G_{4\frac{1}{2}} - t^2F^0_{3\frac{1}{2}}$?
4	2820.002*v*	50	35,450.55	$\begin{cases} a^2F_{2\frac{1}{2}} - x^2D^0_{1\frac{1}{2}} \\ a^4F_{4\frac{1}{2}} - y^2F^0_{3\frac{1}{2}} \end{cases}$
5	2819.174	10	35,460.97	$a^2F_{2\frac{1}{2}} - x^2D^0_{2\frac{1}{2}}$
4	2818.592*v*	30	35,468.29	$a^4F_{2\frac{1}{2}} - y^2D^0_{1\frac{1}{2}}$
4	2815.555*v*	50*r*	35,506.54	$b^4F_{2\frac{1}{2}} - x^4D^0_{2\frac{1}{2}}$
4	2814.976*v*	25	35,513.85	$a^4F_{2\frac{1}{2}} - y^2F^0_{2\frac{1}{2}}$
5	2812.449	3	35,545.75	$b^4F_{1\frac{1}{2}} - z^4S^0_{1\frac{1}{2}}$
4	2811.508*v*	50*w*	35,557.65	$b^4P_{2\frac{1}{2}} - s^4D^0_{2\frac{1}{2}}$
4	2811.126*v*	50	35,562.48	$a^2G_{4\frac{1}{2}} - t^2F^0_{3\frac{1}{2}}$
4	2804.098*v*	5	35,651.61	$b^4P_{\frac{1}{2}} - s^4D^0_{1\frac{1}{2}}$
4	2803.770*v*	100	35,655.78	$b^4F_{2\frac{1}{2}} - x^4D^0_{1\frac{1}{2}}$
4	2800.42*v*	00	35,698.48	$a^2D_{2\frac{1}{2}} - 18^0_{3\frac{1}{2}}$
4	2799.37*v*	0	35,711.83	$a^2H_{4\frac{1}{2}} - 36^0_{5\frac{1}{2}}$,4
4	2797.081*v*	50	35,741.04	$\begin{cases} a^2F_{2\frac{1}{2}} - w^4F^0_{2\frac{1}{2}} \\ b^4P_{2\frac{1}{2}} - v^2P^0_{1\frac{1}{2}} \end{cases}$
4	2796.228*v*	50	35,751.94	$b^4F_{1\frac{1}{2}} - x^4D^0_{\frac{1}{2}}$
5	2795.819	15	35,757.17	$a^2F_{2\frac{1}{2}} - x^4G^0_{3\frac{1}{2}}$
4	2792.436*v*	40	35,800.49	$a^2F_{2\frac{1}{2}} - w^4D^0_{2\frac{1}{2}}$
4	2791.430*v*	2	35,813.39	
4	2791.009*v*	50	35,818.80	$b^4P_{\frac{1}{2}} - w^4P^0_{1\frac{1}{2}}$
4	2790.284*v*	30*h*	35,828.10	
4	2787.016*v*	5	35,870.11	$a^2G_{4\frac{1}{2}} - z^2F^0_{3\frac{1}{2}}$
4	2785.899*v*	50	35,884.49	$a^2D_{1\frac{1}{2}} - w^4P^0_{\frac{1}{2}}$
4	2782.258*v*	3	35,931.45	$b^4F_{2\frac{1}{2}} - z^4S^0_{1\frac{1}{2}}$
4	2782.11*v*	0	35,933.40	$a^2F_{2\frac{1}{2}} - w^4G^0_{4\frac{1}{2}}$?
5	2781.032	8	35,947.28	
4	2778.813*v*	75	35,975.99	$b^4P_{2\frac{1}{2}} - w^4P^0_{2\frac{1}{2}}$
4	2775.578*v*	50	36,017.92	$a^2D_{2\frac{1}{2}} - t^2F^0_{3\frac{1}{2}}$
4	2774.960*v*	50	36,025.94	$b^4F_{1\frac{1}{2}} - x^4D^0_{\frac{1}{2}}$
4	2773.68*v*	3	36,042.56	$a^2G_{3\frac{1}{2}} - v^2G^0_{4\frac{1}{2}}$?
4	2772.692*v*	30*h*	36,055.41	$a^2D_{1\frac{1}{2}} - 20^0_{1\frac{1}{2}}$,4
4	2772.541*v*	15*h*	36,057.37	
4	2771.697*v*	9*h*	36,068.35	$b^4P_{\frac{1}{2}} - s^4D^0_{\frac{1}{2}}$
4	2771.324*v*	1	36,073.21	$b^4P_{1\frac{1}{2}} - s^4D^0_{1\frac{1}{2}}$
4	2770.10*v*	0	36,089.13	$b^4P_{1\frac{1}{2}} - 16^0_{2\frac{1}{2}}$
4	2769.659*v*	10	36,094.89	$a^2F_{2\frac{1}{2}} - w^4F^0_{1\frac{1}{2}}$
4	2768.686*v*	20	36,107.58	$a^2F_{2\frac{1}{2}} - w^4G^0_{3\frac{1}{2}}$
5	2768.294	9	36,112.69	$a^2F_{2\frac{1}{2}} - z^2F^0_{2\frac{1}{2}}$
4	2766.382*v*	50	36,137.65	$b^4F_{2\frac{1}{2}} - x^4D^0_{2\frac{1}{2}}$
4	2766.215*v*	50	36,139.83	$a^2G_{3\frac{1}{2}} - t^2G^0_{3\frac{1}{2}}$
4	2764.188*v*	100*r*	36,166.33	$b^4F_{4\frac{1}{2}} - x^4D^0_{3\frac{1}{2}}$
4	2763.062*v*	1	36,181.07	$b^2G_{4\frac{1}{2}} - 37^0_{4\frac{1}{2}}$,4
4	2761.366*v*	75	36,203.29	$b^4F_{2\frac{1}{2}} - x^4D^0_{2\frac{1}{2}}$
4	2758.538*v*	30	36,240.40	$b^4P_{1\frac{1}{2}} - w^4P^0_{\frac{1}{2}}$
4	2754.26*v*	1	36,296.64	$a^2D_{2\frac{1}{2}} - u^2D^0_{1\frac{1}{2}}$
4	2752.070*v*	40	36,325.57	$\begin{cases} a^2D_{1\frac{1}{2}} - t^2F^0_{2\frac{1}{2}} \\ (a^2D_{2\frac{1}{2}} - z^2F^0_{2\frac{1}{2}}) \end{cases}$
5	2750.141	15	36,351.05	$b^4F_{2\frac{1}{2}} - 15^0_{3\frac{1}{2}}$
4	2746.028*v*	50	36,405.49	$a^2F_{2\frac{1}{2}} - w^4F^0_{2\frac{1}{2}}$
4	2745.098*v*	50	36,417.82	$a^2D_{2\frac{1}{2}} - u^2D^0_{2\frac{1}{2}}$
4	2740.457*v*	50	36,479.49	$a^2F_{2\frac{1}{2}} - x^2D^0_{2\frac{1}{2}}$
4	2732.848*v*	2 Co II?	36,581.05	$b^4P_{1\frac{1}{2}} - w^4P^0_{\frac{1}{2}}$
4	2731.112*v*	50*W*	36,604.31	$a^2D_{1\frac{1}{2}} - u^2D^0_{\frac{1}{2}}$
4	2728.754*v*	3	36,635.94	$a^2G_{4\frac{1}{2}} - z^2F^0_{3\frac{1}{2}}$
4	2723.05*v*	0	36,712.71	$b^4P_{2\frac{1}{2}} - t^2F^0_{2\frac{1}{2}}$
4	2722.106*v*	50*w*	36,725.40	$a^2D_{1\frac{1}{2}} - u^2D^0_{1\frac{1}{2}}$
4	2719.581*v*	25	36,759.50	$a^2F_{2\frac{1}{2}} - w^4F^0_{2\frac{1}{2}}$
4	2715.987*v*	75*w*	36,808.14	$a^2G_{4\frac{1}{2}} - v^2G^0_{4\frac{1}{2}}$
4	2709.29*v*	0	36,899.10	$b^4F_{2\frac{1}{2}} - 18^0_{3\frac{1}{2}}$?
4	2708.810*v*	30	36,905.66	$a^2G_{4\frac{1}{2}} - v^2G^0_{5\frac{1}{2}}$
4	2707.99*v*	1 Co II?	36,916.86	$a^4P_{2\frac{1}{2}} - u^2F^0_{2\frac{1}{2}}$
4	2705.843*v*	15*w* Co II?	36,946.12	$a^4P_{2\frac{1}{2}} - s^4D^0_{2\frac{1}{2}}$
4	2705.412*v*	3	36,952.01	$a^2F_{3\frac{1}{2}} - w^4G^0_{4\frac{1}{2}}$
7	2700.298	1	37,021.98	$b^4P_{\frac{1}{2}} - t^2F^0_{1\frac{1}{2}}$
4	2695.846*v*	50*w*	37,083.12	$b^4F_{3\frac{1}{2}} - x^4F^0_{3\frac{1}{2}}$
4	2694.392*v*	25	37,103.13	$a^4P_{1\frac{1}{2}} - s^4D^0_{2\frac{1}{2}}$
7	2692.479	1	37,129.49	$a^4P_{2\frac{1}{2}} - z^2P^0_{2\frac{1}{2}}$
4	2685.336*v*	75*w*	37,228.25	$b^4F_{2\frac{1}{2}} - x^4F^0_{2\frac{1}{2}}$
4	2680.104*v*	25	37,300.92	$b^4P_{1\frac{1}{2}} - u^2D^0_{1\frac{1}{2}}$

TABLE VIII.—*Continued.*

Ref.	λ *IA*	Int.–*TC*	Wave No. Vac.	Multiplet Designation
4	2679.751*v*	75*W*	37,305.83	$a^3F_{3\frac{1}{2}}-x^3G^0_{3\frac{1}{2}}$
4	2677.021*v*	0	37,343.88	$a^4F_{3\frac{1}{2}}-z^4D^0_{3\frac{1}{2}}$
4	2675.980*v*	10*W* Co II?	37,358.40	$b^4F_{1\frac{1}{2}}-x^4F^0_{2\frac{1}{2}}$
4	2675.546*v*	1	37,364.46	$a^4P_{2\frac{1}{2}}-w^4P^0_{2\frac{1}{2}}$
4	2673.918*v*	25	37,387.21	$a^2D_{2\frac{1}{2}}-23^0_{3\frac{1}{2}}$
4	2669.575*v*	2	37,448.03	$a^4P_{\frac{1}{2}}-s^4D^0_{1\frac{1}{2}}$
4	2668.08*v*	1	37,468.97	$b^2D_{2\frac{1}{2}}-37^0_{2\frac{1}{2}}.^3_4$
4	2661.714*v*	2 Co II?	37,558.62	$b^4F_{\frac{1}{2}}-1^0_{\frac{1}{2}}$
4	2657.340*v*	0	37,620.44	$a^2D_{2\frac{1}{2}}-24^0_{3\frac{1}{2}}$
4	2650.266*v*	50*w*	37,720.85	$b^4F_{1\frac{1}{2}}-x^4F^0_{1\frac{1}{2}}$
4	2649.931*v*	50*w*	37,725.61	$a^2F_{2\frac{1}{2}}-v^2D^0_{3\frac{1}{2}}$
5	2648.635	5 Co II?	37,744.07	$\{b^4F_{2\frac{1}{2}}-x^4F^0_{2\frac{1}{2}}$ $b^4F_{4\frac{1}{2}}-x^4F^0_{4\frac{1}{2}}$
4	2646.413*v*	10*w*	37,775.76	$b^4F_{2\frac{1}{2}}-x^4F^0_{2\frac{1}{2}}$
4	2644.772*v*	10*w*	37,799.20	$a^2F_{2\frac{1}{2}}-y^4D^0_{1\frac{1}{2}}$
4	2642.884*v*	10*r*	37,826.20	$b^4F_{4\frac{1}{2}}-z^4F^0_{3\frac{1}{2}}$
5	2636.365	5 Co II?	37,919.72	$b^4P_{2\frac{1}{2}}-z^2F^0_{2\frac{1}{2}}$
4	2632.89*v*	3	37,969.73	$b^4P_{\frac{1}{2}}-23^0_{1\frac{1}{2}}$
7	2631.215	1*n*	37,993.94	$a^2F_{2\frac{1}{2}}-w^2D^0_{1\frac{1}{2}}$
4	2629.970*v*	30	38,011.93	$b^4P_{2\frac{1}{2}}-u^2D^0_{2\frac{1}{2}}$
4	2628.761	3	38,029.41	
5	2627.638*v*	50*W*	38,045.66	$b^4F_{4\frac{1}{2}}-x^4G^0_{5\frac{1}{2}}$
4	2627.031*v*	2	38,054.45	$b^4F_{1\frac{1}{2}}-z^2F^0_{\frac{1}{2}}$
7	2626.122	1	38,067.62	$a^4P_{2\frac{1}{2}}-16^0_{2\frac{1}{2}}$
4	2624.795*v*	1	38,086.86	
4	2623.96*v*	5	38,098.95	$a^4P_{\frac{1}{2}}-19^0_{1\frac{1}{2}}$
4	2623.755*v*	40	38,101.97	$a^2F_{2\frac{1}{2}}-y^4S^0_{1\frac{1}{2}}$
4	2623.440*v*	2	38,106.54	$b^4F_{2\frac{1}{2}}-x^4F^0_{1\frac{1}{2}}$
4	2622.430*v*	30*r*	38,121.21	$b^4F_{3\frac{1}{2}}-x^4G^0_{3\frac{1}{2}}$
4	2622.250*v*	3	38,123.83	$b^4F_{1\frac{1}{2}}-x^4G^0_{2\frac{1}{2}}$
4	2622.059*v*	40*w* Co I+II	38,126.61	$b^4F_{3\frac{1}{2}}-x^4G^0_{4\frac{1}{2}}$
4	2619.276*v*	50*w*	38,167.11	$b^4F_{1\frac{1}{2}}-w^4D^0_{2\frac{1}{2}}$
4	2617.859*v*	50*w*	38,187.77	$b^4F_{1\frac{1}{2}}-w^4D^0_{1\frac{1}{2}}$
4	2616.260*v*	40*w*	38,211.11	$a^2F_{2\frac{1}{2}}-v^2D^0_{2\frac{1}{2}}$
4	2615.336*v*	10	38,224.61	$a^2F_{2\frac{1}{2}}-y^2F^0_{2\frac{1}{2}}$
4	2614.124*v*	30	38,242.33	$a^4F_{3\frac{1}{2}}-x^4D^0_{2\frac{1}{2}}$
4	2613.894*v*	4	38,245.69	$a^2F_{2\frac{1}{2}}-w^2D^0_{2\frac{1}{2}}$
4	2613.492*v*	25 Co I+II	38,251.58	
4	2610.762*v*	40*w*	38,291.57	$b^4F_{3\frac{1}{2}}-x^4F^0_{2\frac{1}{2}}$
4	2608.900*v*	1*g*?	38,318.90	$a^4P_{1\frac{1}{2}}-w^4P^0_{\frac{1}{2}}$
4	2606.120*v*	40	38,359.77	$b^4F_{1\frac{1}{2}}-w^4D^0_{\frac{1}{2}}$
4	2602.581*v*	1	38,411.93	$a^2F_{2\frac{1}{2}}-u^4D^0_{3\frac{1}{2}}$
4	2600.977*v*	10*w*	38,435.62	$b^4F_{4\frac{1}{2}}-x^4F^0_{3\frac{1}{2}}$
4	2599.200*v*	5	38,461.89	$\{b^4F_{1\frac{1}{2}}-z^2F^0_{1\frac{1}{2}}$ $a^4P_{1\frac{1}{2}}-19^0_{1\frac{1}{2}}$
4	2595.986*v*	0	38,509.51	$b^4F_{3\frac{1}{2}}-x^4G^0_{3\frac{1}{2}}$
4	2595.214*v*	1	38,520.97	
4	2594.161*v*	10*w*	38,536.60	$a^4F_{4\frac{1}{2}}-x^4D^0_{3\frac{1}{2}}$
4	2593.070*v*	1	38,552.81	$b^4F_{3\frac{1}{2}}-w^4D^0_{3\frac{1}{2}}$
4	2592.563*v*	0	38,560.35	$a^2F_{2\frac{1}{2}}-x^4P^0_{2\frac{1}{2}}$
4	2591.686*v*	10*r*	38,573.40	$b^4F_{2\frac{1}{2}}-w^4D^0_{1\frac{1}{2}}$
5	2590.594	75*W*	38,589.65	$a^2F_{3\frac{1}{2}}-x^2G^0_{4\frac{1}{2}}$
4	2589.30*v*	00	38,608.95	$a^2D_{2\frac{1}{2}}-29^0_{2\frac{1}{2}}$
4	2585.335*v*	50*W*	38,668.15	$a^2F_{3\frac{1}{2}}-u^2F^0_{2\frac{1}{2}}$
4	2583.03*v*	3	38,702.59	$a^4P_{2\frac{1}{2}}-19^0_{1\frac{1}{2}}$
4	2580.838*v*	50*W*	38,735.52	$b^4F_{3\frac{1}{2}}-x^2F^0_{2\frac{1}{2}}$
4	2578.924*v*	30	38,764.26	$a^2F_{2\frac{1}{2}}-w^2F^0_{3\frac{1}{2}}$
4	2577.446*v*	1	38,786.49	$b^4F_{4\frac{1}{2}}-x^4G^0_{4\frac{1}{2}}$
4	2575.733*v*	2	38,812.29	$a^4F_{1\frac{1}{2}}-z^4S^0_{1\frac{1}{2}}$
4	2574.351*v*	6*r*	38,833.12	$a^4F_{3\frac{1}{2}}-x^4D^0_{2\frac{1}{2}}$
4	2573.538*v*	30*r*	38,845.39	$b^4F_{4\frac{1}{2}}-3^0_{3\frac{1}{2}}$
4	2573.395*v*	40	38,847.55	$b^4F_{2\frac{1}{2}}-z^2F^0_{1\frac{1}{2}}$
4	2572.234*v*	50*w*	38,865.08	$b^4F_{3\frac{1}{2}}-x^2F^0_{2\frac{1}{2}}$
10	2570.762	<1	38,887.33	$a^2F_{3\frac{1}{2}}-v^4D^0_{2\frac{1}{2}}$
11	2567.742	1	38,933.06	$a^2F_{2\frac{1}{2}}-u^4D^0_{2\frac{1}{2}}$
4	2567.344*v*	50*r*	38,939.10	$a^4F_{2\frac{1}{2}}-x^4D^0_{2\frac{1}{2}}$
4	2565.985*v*	1	38,959.72	$a^2D_{2\frac{1}{2}}-31^0_{1\frac{1}{2}}$
4	2564.566*v*	0	38,981.28	$b^4P_{\frac{1}{2}}-23^0_{1\frac{1}{2}}$
4	2562.124*v*	10*r*	39,018.42	$a^4F_{1\frac{1}{2}}-x^4D^0_{1\frac{1}{2}}$
4	2561.280*v*	25	39,031.28	
4	2560.027*v*	1*d* Co II?	39,050.39	
4	2559.595*v*	0	39,056.98	$b^4F_{3\frac{1}{2}}-x^4G^0_{3\frac{1}{2}}$
4	2556.762*v*	50*w* Co II?	39,100.25	$b^4F_{4\frac{1}{2}}-w^4D^0_{3\frac{1}{2}}$
4	2555.074*v*	6	39,126.08	$b^4F_{1\frac{1}{2}}-w^4F^0_{2\frac{1}{2}}$
4	2553.337*v*	10*r*	39,152.69	$b^4F_{3\frac{1}{2}}-w^4F^0_{4\frac{1}{2}}$
4	2553.004*v*	40*r*	39,157.80	$b^4F_{3\frac{1}{2}}-w^4F^0_{3\frac{1}{2}}$
4	2551.230*v*	0	39,185.03	
4	2549.296*v*	4	39,214.75	$a^4F_{2\frac{1}{2}}-z^4S^0_{1\frac{1}{2}}$
4	2548.875*v*	3	39,221.23	$b^4F_{2\frac{1}{2}}-x^2D^0_{1\frac{1}{2}}$
4	2548.333*v*	20 Co II?	39,229.57	$a^2F_{2\frac{1}{2}}-z^2D^0_{2\frac{1}{2}}$
4	2548.194*v*	0	39,231.71	$b^4F_{2\frac{1}{2}}-x^2D^0_{2\frac{1}{2}}$
4	2544.862*v*	4	39,283.07	$b^4F_{3\frac{1}{2}}-z^2F^0_{3\frac{1}{2}}$
4	2544.252*v*	50*r* Co II?	39,292.49	$a^4F_{1\frac{1}{2}}-x^4D^0_{\frac{1}{2}}$
4	2543.232*v*	1	39,308.25	$a^4P_{2\frac{1}{2}}-z^2F^0_{2\frac{1}{2}}$
10	2538.70	<1	39,378.41	$\{a^2F_{2\frac{1}{2}}-6^0_{2\frac{1}{2}}$ $b^4F_{1\frac{1}{2}}-z^2S^0_{\frac{1}{2}}$?
4	2538.339*v*	6	39,384.02	
4	2536.503*v*	1	39,412.52	$b^4F_{3\frac{1}{2}}-x^2F^0_{3\frac{1}{2}}$
4	2535.961*v*	10*r* Co II?	39,420.94	$a^4F_{2\frac{1}{2}}-x^4D^0_{1\frac{1}{2}}$
4	2535.359*v*	5	39,430.30	$a^2F_{2\frac{1}{2}}-u^4D^0_{2\frac{1}{2}}$
4	2532.176*v*	10 Co II?	39,479.86	$b^4F_{1\frac{1}{2}}-w^4F^0_{2\frac{1}{2}}$
4	2531.354*v*	5	39,492.68	$b^4F_{1\frac{1}{2}}-w^4G^0_{2\frac{1}{2}}$
4	2530.546*v*	5	39,505.29	$b^4F_{4\frac{1}{2}}-3^0_{3\frac{1}{2}}$
4	2530.134*v*	40*w* Co II?	39,511.72	$b^4F_{3\frac{1}{2}}-w^4F^0_{2\frac{1}{2}}$
5	2528.967	50*R*	39,529.96	$a^4F_{3\frac{1}{2}}-x^4D^0_{3\frac{1}{2}}$
4	2528.186*v*	3 Co II?	39,542.16	$b^4P_{\frac{1}{2}}-31^0_{1\frac{1}{2}}$?
4	2525.626*v*	4	39,582.24	$b^4F_{1\frac{1}{2}}-y^4F^0_{2\frac{1}{2}}$
4	2523.00*v*	4 Co II?	39,623.45	$b^4P_{\frac{1}{2}}-32^0_{1\frac{1}{2}}$?
5	2521.363	75*R* Co II?	39,649.16	$a^4F_{4\frac{1}{2}}-x^4D^0_{3\frac{1}{2}}$
4	2520.908*v*	3	39,656.31	
4	2518.988*v*	3	39,686.54	$a^2F_{2\frac{1}{2}}-u^2F^0_{2\frac{1}{2}}$
5	2517.869	10*w*	39,704.17	$b^4F_{2\frac{1}{2}}-w^4G^0_{3\frac{1}{2}}$
4	2517.792*v*	6	39,705.39	$b^4F_{2\frac{1}{2}}-w^4F^0_{2\frac{1}{2}}$
4	2515.075*v*	1	39,748.28	$b^4P_{2\frac{1}{2}}-26^0_{2\frac{1}{2}}$
4	2513.119*v*	4	39,779.22	$b^4F_{2\frac{1}{2}}-x^2D^0_{2\frac{1}{2}}$
4	2512.900*v*	5	39,782.68	$a^2F_{2\frac{1}{2}}-w^2F^0_{2\frac{1}{2}}$
4	2511.019*v*	10*r* Co II?	39,812.48	$b^4F_{4\frac{1}{2}}-w^4F^0_{4\frac{1}{2}}$
4	2510.10*v*	0 Co II?	39,827.01	$b^4F_{2\frac{1}{2}}-4^0_{3\frac{1}{2}}$
4	2509.234*v*	2	39,840.80	
4	2508.730*v*	1	39,848.80	$b^4P_{1\frac{1}{2}}-v^4F^0_{1\frac{1}{2}}$
4	2507.678*v*	40*w*	39,865.52	$b^4F_{2\frac{1}{2}}-w^4F^0_{1\frac{1}{2}}$
4	2507.169*v*	2	39,873.62	$a^2F_{2\frac{1}{2}}-z^2P^0_{1\frac{1}{2}}$
4	2506.873*v*	10*w*	39,878.32	$b^4F_{2\frac{1}{2}}-w^4G^0_{2\frac{1}{2}}$
4	2505.107*v*	3	39,906.43	
4	2504.518*v*	4 Co II?	39,915.82	$b^4F_{4\frac{1}{2}}-w^4D^0_{3\frac{1}{2}}$
4	2503.860*v*	1	39,926.30	
4	2503.24*v*	1	39,936.26	$b^4P_{2\frac{1}{2}}-28^0_{2\frac{1}{2}}$
4	2502.284*v*	5	39,951.45	$a^2F_{2\frac{1}{2}}-u^4D^0_{2\frac{1}{2}}$
4	2501.508*v*	2	39,963.84	$b^4P_{1\frac{1}{2}}-31^0_{1\frac{1}{2}}$
4	2501.257*v*	2	39,967.85	$b^4F_{2\frac{1}{2}}-y^4F^0_{3\frac{1}{2}}$
4	2500.494*v*	10*h*	39,980.05	
4	2496.713*v*	12	40,040.59	$b^4F_{2\frac{1}{2}}-w^4G^0_{4\frac{1}{2}}$
4	2496.45*v*	1	40,044.86	$b^4P_{1\frac{1}{2}}-32^0_{2\frac{1}{2}}$
4	2495.551*v*	10	40,059.23	$b^4F_{3\frac{1}{2}}-w^4F^0_{2\frac{1}{2}}$
4	2494.730*v*	9	40,072.42	$b^4F_{4\frac{1}{2}}-z^2F^0_{3\frac{1}{2}}$
4	2493.930*v*	30*w*	40,085.27	$a^2F_{2\frac{1}{2}}-t^4D^0_{1\frac{1}{2}}$
4	2491.15*v*	1	40,130.00	$b^4P_{2\frac{1}{2}}-y^4F^0_{3\frac{1}{2}}$
4	2490.02*v*	0	40,148.2	$b^4P_{1\frac{1}{2}}-33^0_{1\frac{1}{2}}.^3_4$
4	2489.62*v*	3	40,154.6	$a^2F_{2\frac{1}{2}}-z^2F^0_{2\frac{1}{2}}$
4	2489.507*v*	1	40,156.48	
4	2489.249*v*	4	40,160.64	$a^4F_{1\frac{1}{2}}-z^4P^0_{\frac{1}{2}}$
4	2488.461*v*	4	40,173.36	$a^4F_{1\frac{1}{2}}-z^4P^0_{1\frac{1}{2}}$
4	2485.952*v*	1	40,213.90	
4	2483.613*v*	12 Co II?	40,251.77	$b^4F_{2\frac{1}{2}}-w^4G^0_{3\frac{1}{2}}$
4	2481.09*v*	0	40,292.7	$a^2F_{2\frac{1}{2}}-x^4S^0_{1\frac{1}{2}}$
4	2478.293*v*	2	40,338.17	
4	2476.640*v*	40*w*	40,365.09	$b^4F_{4\frac{1}{2}}-w^4F^0_{3\frac{1}{2}}$
9	2476.43	1 Co II?	40,368.5	$a^2F_{2\frac{1}{2}}-7^0_{3\frac{1}{2}}$?
4	2474.702*v*	5	40,396.70	$a^2F_{2\frac{1}{2}}-6^0_{2\frac{1}{2}}$
4	2473.901*v*	8	40,409.77	$a^4F_{3\frac{1}{2}}-x^4F^0_{4\frac{1}{2}}$
4	2472.922*v*	7	40,425.77	$b^4F_{3\frac{1}{2}}-w^4G^0_{2\frac{1}{2}}$
4	2472.066*v*	3	40,439.77	
4	2470.270*v*	20*w*	40,469.17	$b^4F_{4\frac{1}{2}}-w^4G^0_{5\frac{1}{2}}$
4	2467.685*v*	20*w*	40,511.55	$a^4F_{2\frac{1}{2}}-x^4F^0_{2\frac{1}{2}}$
4	2465.111*v*	3	40,553.86	$b^4P_{2\frac{1}{2}}-31^0_{3\frac{1}{2}}$
4	2464.615*v*	3	40,562.02	$a^4F_{2\frac{1}{2}}-z^4P^0_{2\frac{1}{2}}$
4	2464.459*v*	2	40,564.59	$a^2F_{2\frac{1}{2}}-w^2P^0_{1\frac{1}{2}}$
4	2463.776*v*	4	40,575.84	$a^4F_{3\frac{1}{2}}-z^4P^0_{2\frac{1}{2}}$
4	2462.122*v*	20	40,603.09	$a^4P_{2\frac{1}{2}}-24^0_{2\frac{1}{2}}$
4	2461.562*v*	2	40,612.32	$b^4F_{1\frac{1}{2}}-w^2D^0_{2\frac{1}{2}}$
4	2460.800*v*	20	40,624.90	$a^4F_{1\frac{1}{2}}-x^4F^0_{2\frac{1}{2}}$
4	2460.195*v*	20	40,634.89	$b^4P_{2\frac{1}{2}}-32^0_{2\frac{1}{2}}$
5	2456.237	20*w*	40,700.36	$b^4F_{4\frac{1}{2}}-w^4G^0_{4\frac{1}{2}}$
4	2453.382*v*	4	40,747.72	
4	2451.747*v*	3	40,774.89	$a^2F_{2\frac{1}{2}}-t^4D^0_{2\frac{1}{2}}$
4	2451.237*v*	1	40,783.37	
4	2448.505*v*	2	40,828.87	$b^4F_{1\frac{1}{2}}-x^4P^0_{1\frac{1}{2}}$
4	2445.756*v*	3	40,874.76	$a^2F_{2\frac{1}{2}}-v^2F^0_{2\frac{1}{2}}$
4	2445.353*v*	2	40,881.50	$b^4F_{1\frac{1}{2}}-x^4P^0_{\frac{1}{2}}$
4	2443.548*v*	5	40,911.70	$b^4F_{4\frac{1}{2}}-w^4G^0_{5\frac{1}{2}}$
4	2443.18*v*	0	40,917.8	$b^4P_{2\frac{1}{2}}-34^0_{1\frac{1}{2}}.^3_4$
4	2442.888*v*	4	40,922.75	
4	2442.62*v*	2 Co II?	40,927.2	$b^4F_{1\frac{1}{2}}-x^4P^0_{2\frac{1}{2}}$
4	2441.040*v*	20	40,953.73	$a^2G_{4\frac{1}{2}}-36^0_{3\frac{1}{2}}.^4_5$
4	2440.141*v*	4*w*	40,968.81	$b^4F_{3\frac{1}{2}}-z^2H^0_{4\frac{1}{2}}$
4	2439.495*v*	8*h*	40,979.66	
4	2439.038*v*	20*R*	40,987.34	$a^4F_{1\frac{1}{2}}-x^4F^0_{1\frac{1}{2}}$
5	2438.411	2	40,997.87	$b^4F_{3\frac{1}{2}}-u^2D^0_{2\frac{1}{2}}$
4	2438.201*v*	1	41,001.41	$a^2F_{2\frac{1}{2}}-t^4D^0_{2\frac{1}{2}}$
4	2436.786*v*	3	41,025.21	$a^4P_{1\frac{1}{2}}-27^0_{2\frac{1}{2}}$
5	2436.657	50*R*	41,027.38	$a^4F_{3\frac{1}{2}}-x^4F^0_{2\frac{1}{2}}$
4	2435.823*v*	10	41,041.43	$a^4F_{4\frac{1}{2}}-1^0_{3\frac{1}{2}}$
4	2435.094*v*	20*w*	41,053.71	
4	2433.75*v*	0	41,076.4	$b^4F_{2\frac{1}{2}}-z^2G^0_{3\frac{1}{2}}$
4	2432.213*v*	40*R*	41,102.34	$a^4F_{3\frac{1}{2}}-x^4F^0_{3\frac{1}{2}}$
4	2431.74*v*	1	41,110.3	$b^4F_{1\frac{1}{2}}-v^2D^0_{1\frac{1}{2}}$
4	2430.176*v*	10	41,136.79	$a^4P_{2\frac{1}{2}}-26^0_{3\frac{1}{2}}$
4	2429.226*v*	25	41,152.88	$a^4F_{3\frac{1}{2}}-z^4P^0_{2\frac{1}{2}}$
4	2428.596*v*	10	41,163.55	
4	2426.997*v*	12	41,190.67	
4	2425.593*v*	8	41,214.51	$b^4F_{3\frac{1}{2}}-x^4P^0_{1\frac{1}{2}}$
4	2424.932*v*	250*R*	41,225.74	$a^4F_{4\frac{1}{2}}-x^4F^0_{4\frac{1}{2}}$
4	2422.568*v*	30*w*	41,265.97	$a^4P_{2\frac{1}{2}}-27^0_{2\frac{1}{2}}$
4	2421.688*v*	8	41,280.96	$b^4F_{2\frac{1}{2}}-v^4D^0_{3\frac{1}{2}}$

TABLE VIII.—*Continued.*

Ref.	λ *IA*	Int.–*TC*	Wave No. Vac.	Multiplet Designation
4	2419.828*v*	6	41,312.69	$b^4F_{2\frac{1}{2}} - x^4P^o_{2\frac{1}{2}}$
4	2419.324*v*	10*d*‡	41,321.30	
4	2419.122*v*	20*w*	41,324.75	
4	2418.580*v*	1	41,334.01	
4	2418.476*v*	1 Co II?	41,335.78	
4	2417.329*v*	25	41,355.40	
4	2417.045*v*	10	41,360.25	
4	2415.516*v*	3	41,386.43	$a^2F_{2\frac{1}{2}} - 7^o_{2\frac{1}{2}}$
4	2415.32*v*	2*w*	41,389.8	$a^4F_{2\frac{1}{2}} - x^4F^o_{3\frac{1}{2}}$
4	2415.29*v*	4	41,390.3	$a^4F_{1\frac{1}{2}} - x^4G^o_{2\frac{1}{2}}$
4	2414.458*v*	40*R*	41,404.56	$a^4F_{2\frac{1}{2}} - x^4G^o_{3\frac{1}{2}}$
4	2413.580*v*	15	41,419.63	$a^4P_{\frac{1}{2}} - 32^o_{1\frac{1}{2}}$
4	2413.187*v*	15	41,426.37	$b^4F_{1\frac{1}{2}} - y^4D^o_{\frac{1}{2}}$
4	2412.896*v*	6	41,431.37	
4	2412.762*v*	12*r*	41,433.67	$a^4F_{1\frac{1}{2}} - w^4D^o_{2\frac{1}{2}}$
4	2411.618*v*	250*R*	41,453.32	$\begin{cases} a^4F_{2\frac{1}{2}} - x^4G^o_{3\frac{1}{2}} \\ (a^4F_{1\frac{1}{2}} - w^4D^o_{1\frac{1}{2}}) \end{cases}$
4	2410.504*v*	40*w*	41,472.48	$a^4P_{1\frac{1}{2}} - 30^o_{2\frac{1}{2}}$
4	2409.654*v*	8	41,487.11	$b^4F_{1\frac{1}{2}} - y^4S^o_{1\frac{1}{2}}$
4	2409.123*v*	20	41,496.25	$b^4F_{2\frac{1}{2}} - y^2D^o_{1\frac{1}{2}}$
4	2407.249*v*	100	41,528.58	$a^4F_{4\frac{1}{2}} - x^4G^o_{5\frac{1}{2}}$
4	2406.266*v*	25	41,545.52	$b^4F_{2\frac{1}{2}} - w^2D^o_{2\frac{1}{2}}$
4	2404.84*v*	10	41,570.1	$b^4F_{2\frac{1}{2}} - y^2D^o_{1\frac{1}{2}}$
4	2403.637*v*	15	41,590.95	
4	2403.337*v*	15	41,596.14	$b^4F_{1\frac{1}{2}} - y^2D^o_{2\frac{1}{2}}$
4	2402.559*v*	15	41,609.61	$b^4F_{1\frac{1}{2}} - y^2P^o_{1\frac{1}{2}}$
4	2402.164*v*	30*r*	41,616.46	$a^4F_{1\frac{1}{2}} - x^2F^o_{2\frac{1}{2}}$
4	2402.058*v*	10*r*	41,618.29	$a^4F_{3\frac{1}{2}} - x^4F^o_{4\frac{1}{2}}$
4	2401.595*v*	30	41,626.31	$a^4F_{1\frac{1}{2}} - w^4D^o_{\frac{1}{2}}$
4	2401.102*v*	30	41,634.86	
4	2400.833*v*	30	41,639.52	$b^4F_{2\frac{1}{2}} - y^4D^o_{2\frac{1}{2}}$
4	2400.558*v*	30	41,644.29	$a^2F_{2\frac{1}{2}} - 12^o_{1\frac{1}{2}}$
4	2398.554*v*	4	41,679.08	
4	2397.25*v*	4	41,701.7	$a^4P_{1\frac{1}{2}} - 31^o_{1\frac{1}{2}}$
5	2397.03	6	41,705.6	
4	2396.779*v*	90	41,709.95	
4	2396.588*v*	5	41,713.27	$a^4P_{2\frac{1}{2}} - 30^o_{2\frac{1}{2}}$
4	2396.232*v*	10	41,719.47	$a^2G_{4\frac{1}{2}} - 36^o_{3\frac{1}{2}.4\frac{1}{2}}$
4	2395.300*v*	6	41,734.13	
5	2394.227	4	41,754.40	
10	2393.635	1	41,764.73	$b^4F_{2\frac{1}{2}} - w^2D^o_{1\frac{1}{2}}$
4	2392.029*v*	2	41,792.76	$a^4F_{2\frac{1}{2}} - x^4G^o_{3\frac{1}{2}}$
4	2391.369*v*	9	41,804.30	
4	2390.426*v*	4	41,820.79	
4	2389.984*v*	8	41,828.52	$b^4F_{3\frac{1}{2}} - y^4D^o_{3\frac{1}{2}}$
5	2389.540	12 Co II	41,836.29	$(a^4F_{3\frac{1}{2}} - w^4D^o_{4\frac{1}{2}})$
4	2388.374*v*	3	41,856.72	$a^4F_{3\frac{1}{2}} - w^4D^o_{4\frac{1}{2}}$
4	2388.175*v*	5	41,860.21	$b^4F_{4\frac{1}{2}} - x^4P^o_{3\frac{1}{2}}$
4	2387.460*v*	10	41,872.74	$b^4F_{2\frac{1}{2}} - y^4S^o_{1\frac{1}{2}}$
5	2386.509	3	41,889.42	$b^4F_{2\frac{1}{2}} - x^2G^o_{4\frac{1}{2}}$
4	2385.813*v*	9	41,901.65	
4	2384.858*v*	10*R*	41,918.42	$a^4F_{4\frac{1}{2}} - x^4F^o_{3\frac{1}{2}}$
4	2381.26*v*	4	41,981.8	$b^4F_{2\frac{1}{2}} - y^2D^o_{2\frac{1}{2}}$
4	2380.696*v*	4	41,991.70	$a^4F_{2\frac{1}{2}} - w^4D^o_{2\frac{1}{2}}$
4	2380.483*v*	20*d*	41,995.46	$\begin{cases} a^4F_{3\frac{1}{2}} - x^4G^o_{3\frac{1}{2}} \\ b^4F_{2\frac{1}{2}} - y^2P^o_{1\frac{1}{2}} \end{cases}$
4	2379.357*v*	4	42,015.33	$b^4F_{1\frac{1}{2}} - y^2P^o_{\frac{1}{2}}$
4	2379.160*v*	4	42,018.81	$a^4F_{2\frac{1}{2}} - x^2F^o_{2\frac{1}{2}}$
4	2378.905*v*	5	42,023.31	$a^4P_{2\frac{1}{2}} - 32^o_{1\frac{1}{2}}$
4	2377.215*v*	12	42,053.18	$b^4F_{1\frac{1}{2}} - w^2F^o_{2\frac{1}{2}}$
4	2376.975*v*	6	42,057.43	$b^4F_{4\frac{1}{2}} - z^2H^o_{5\frac{1}{2}}$
5	2374.456	4	42,102.04	$a^4F_{1\frac{1}{2}} - x^2D^o_{1\frac{1}{2}}$
4	2373.862*v*	9	42,112.58	$a^4F_{1\frac{1}{2}} - x^2D^o_{2\frac{1}{2}}$
4	2373.56*v*	0	42,117.9	$a^2F_{2\frac{1}{2}} - w^2F^o_{3\frac{1}{2}}$
4	2373.370*v*	20	42,121.30	
4	2372.832*v*	15	42,130.86	$a^4F_{2\frac{1}{2}} - z^2I^o_{3\frac{1}{2}}$
4	2371.845*v*	6 Co II?	42,148.38	$a^4F_{2\frac{1}{2}} - x^2F^o_{3\frac{1}{2}}$
4	2371.458*v*	15	42,155.26	$a^2G_{4\frac{1}{2}} - 37^o_{3\frac{1}{2}.4\frac{1}{2}}$
4	2370.514*v*	10	42,172.05	$a^4F_{4\frac{1}{2}} - 3^o_{3\frac{1}{2}}$
4	2369.924*v*	9	42,182.54	$b^4F_{3\frac{1}{2}} - w^4D^o_{3\frac{1}{2}}$
4	2369.674*v*	15	42,187.00	$b^4F_{2\frac{1}{2}} - y^4D^o_{2\frac{1}{2}}$
4	2366.046*v*	5	42,251.68	$a^2F_{2\frac{1}{2}} - w^2F^o_{2\frac{1}{2}}$
4	2365.057*v*	18*d*	42,269.34	$a^4F_{4\frac{1}{2}} - x^4G^o_{4\frac{1}{2}}$
5	2364.251	3	42,283.76	$b^4F_{4\frac{1}{2}} - x^2G^o_{3\frac{1}{2}}$
4	2362.327*v*	8	42,318.19	$b^4F_{1\frac{1}{2}} - w^4D^o_{2\frac{1}{2}}$
4	2360.789*v*	9	42,345.76	$a^2F_{3\frac{1}{2}} - 14^o_{2\frac{1}{2}}$
4	2358.676*v*	10	42,383.69	$a^4F_{3\frac{1}{2}} - x^4G^o_{4\frac{1}{2}}$
4	2358.177*v*	20	42,392.65	$a^4F_{1\frac{1}{2}} - w^4F^o_{2\frac{1}{2}}$
4	2357.507*v*	10	42,404.70	$a^2F_{2\frac{1}{2}} - 11^o_{2\frac{1}{2}}$
4	2356.267*v*	10	42,427.02	$a^4F_{3\frac{1}{2}} - w^4F^o_{2\frac{1}{2}}$
4	2355.611*v*	7	42,438.83	$b^4F_{2\frac{1}{2}} - w^2F^o_{2\frac{1}{2}}$
4	2355.480*v*	30	42,441.19	$a^4F_{3\frac{1}{2}} - w^4F^o_{4\frac{1}{2}}$
5	2354.41	5	42,460.5	
4	2354.18*v*	2	42,464.6	$a^2F_{2\frac{1}{2}} - y^2P^o_{1\frac{1}{2}}$
4	2353.36*v*	10	42,479.4	$a^4F_{3\frac{1}{2}} - w^4F^o_{4\frac{1}{2}}$
4	2352.864*v*	15*d*	42,488.37	$b^4F_{4\frac{1}{2}} - y^4L^o_{5\frac{1}{2}}$
4	2351.98*v*	4	42,504.4	$a^4F_{2\frac{1}{2}} - x^2L^o_{3\frac{1}{2}}$
4	2351.385*v*	10	42,515.10	$a^4F_{3\frac{1}{2}} - x^2D^o_{2\frac{1}{2}}$
4	2350.596*v*	6	42,529.36	$b^4F_{3\frac{1}{2}} - y^2D^o_{2\frac{1}{2}}$
4	2350.284*v*	12	42,535.01	$b^4F_{2\frac{1}{2}} - w^2F^o_{3\frac{1}{2}}$
4	2347.657*v*	4	42,582.60	$a^4F_{3\frac{1}{2}} - w^4D^o_{3\frac{1}{2}}$
4	2346.161*v*	7	42,609.75	$a^4F_{3\frac{1}{2}} - x^2F^o_{3\frac{1}{2}}$
5	2342.793	2	42,671.00	$a^4F_{1\frac{1}{2}} - y^4P^o_{2\frac{1}{2}}$
4	2341.784*v*	4	42,689.38	
4	2340.99*v*	5	42,703.8	$b^4F_{2\frac{1}{2}} - w^4D^o_{2\frac{1}{2}}$
4	2339.92*v*	?	42,723.5	$a^2F_{2\frac{1}{2}} - 15^o_{2\frac{1}{2}}$
4	2339.550*v*	5	42,730.15	$b^4F_{3\frac{1}{2}} - w^4D^o_{3\frac{1}{2}}$
4	2339.048*v*	4 Co II?	42,739.32	$a^4F_{3\frac{1}{2}} - x^2F^o_{3\frac{1}{2}}$
4	2338.656*v*	10*d*	42,746.48	$a^4F_{1\frac{1}{2}} - w^4F^o_{1\frac{1}{2}}$
4	2337.95*v*	3*w* Co II?	42,759.4	$a^4F_{1\frac{1}{2}} - w^4G^o_{2\frac{1}{2}}$
4	2337.477*v*	4	42,768.04	
4	2336.00*v*	10*d*	42,795.1	$a^4F_{2\frac{1}{2}} - w^4F^o_{2\frac{1}{2}}$
4	2335.102*v*	15	42,811.53	$a^4F_{4\frac{1}{2}} - x^4G^o_{5\frac{1}{2}}$
4	2334.12*v*	5 Co II?	42,829.6	$b^4F_{1\frac{1}{2}} - w^4D^o_{\frac{1}{2}}$
4	2333.980*v*	3	42,832.11	
4	2333.071*v*	6	42,848.79	$a^4F_{1\frac{1}{2}} - y^4P^o_{1\frac{1}{2}}$
4	2332.087*v*	10	42,866.88	
4	2329.089*v*	6 Co II?	42,922.05	$b^4F_{2\frac{1}{2}} - w^4D^o_{1\frac{1}{2}}$
4	2328.861*v*	10	42,926.25	
4	2328.298*v*	6	42,936.63	
4	2327.539*v*	5	42,950.63	$b^4F_{1\frac{1}{2}} - x^2S^o_{\frac{1}{2}}$
5	2325.80	6	42,982.7	
5	2325.615	50*w*	42,986.16	$b^4F_{3\frac{1}{2}} - w^2F^o_{2\frac{1}{2}}$
4	2325.530*v*	12	42,987.73	$a^4F_{2\frac{1}{2}} - w^4G^o_{3\frac{1}{2}}$
4	2323.131*v*	15*d*	43,032.12	$a^4F_{3\frac{1}{2}} - w^4F^o_{3\frac{1}{2}}$
4	2322.260*v*	4	43,048.26	$a^4F_{1\frac{1}{2}} - y^4P^o_{\frac{1}{2}}$
4	2320.906*v*	4	43,073.37	$a^4F_{2\frac{1}{2}} - y^4F^o_{2\frac{1}{2}}$
4	2320.41*v*	1	43,082.5	$b^4F_{3\frac{1}{2}} - w^2F^o_{3\frac{1}{2}}$
4	2319.152*v*	4	43,105.94	$a^4F_{3\frac{1}{2}} - x^2D^o_{2\frac{1}{2}}$
4	2317.516*v*	5	43,136.37	$a^2F_{2\frac{1}{2}} - w^2F^o_{2\frac{1}{2}}$
4	2316.843*v*	5	43,148.90	$\begin{cases} a^4F_{3\frac{1}{2}} - w^4F^o_{4\frac{1}{2}} \\ b^4F_{2\frac{1}{2}} - 6^o_{3\frac{1}{2}} \end{cases}$
4	2316.733*v*	5	43,150.95	$a^2F_{3\frac{1}{2}} - w^2G^o_{4\frac{1}{2}}$
4	2316.157*v*	10*w*	43,161.68	$a^4F_{2\frac{1}{2}} - w^4G^o_{3\frac{1}{2}}$
4	2311.35*v*	10	43,251.4	$\begin{cases} a^4F_{2\frac{1}{2}} - y^4P^o_{2\frac{1}{2}} \\ b^4F_{3\frac{1}{2}} - w^4D^o_{3\frac{1}{2}} \end{cases}$
5	2310.962	12	43,258.69	$b^4F_{1\frac{1}{2}} - x^2P^o_{1\frac{1}{2}}$
4	2310.36*v*	1	43,270.0	$a^2F_{3\frac{1}{2}} - w^2F^o_{3\frac{1}{2}}$
5	2309.020	10*R*	43,295.09	$a^4F_{4\frac{1}{2}} - w^4F^o_{4\frac{1}{2}}$
4	2308.98*v*	?	43,295.9	$a^2F_{3\frac{1}{2}} - 13^o_{3\frac{1}{2}.4\frac{1}{2}}$
4	2305.169*v*	15	43,367.40	$a^4F_{3\frac{1}{2}} - w^4G^o_{4\frac{1}{2}}$
4	2304.182*v*	10	43,385.97	$a^4F_{3\frac{1}{2}} - w^4F^o_{3\frac{1}{2}}$
4	2303.966*v*	12	43,390.04	$b^4F_{4\frac{1}{2}} - w^4D^o_{3\frac{1}{2}}$
4	2303.504*v*	9	43,398.74	$a^4F_{4\frac{1}{2}} - w^4D^o_{4\frac{1}{2}}$
4	2303.31*v*	?	43,402.3	$a^2F_{2\frac{1}{2}} - 16^o_{2\frac{1}{2}}$
4	2298.356*v*	15	43,495.93	$b^4F_{1\frac{1}{2}} - t^4D^o_{\frac{1}{2}}$
4	2296.704*v*	18	43,527.22	$b^4F_{2\frac{1}{2}} - t^4D^o_{1\frac{1}{2}}$
4	2296.038*v*	18	43,539.84	$b^4F_{1\frac{1}{2}} - y^2F^o_{2\frac{1}{2}}$
4	2295.223*v*	15	43,555.30	$a^4F_{4\frac{1}{2}} - x^2F^o_{3\frac{1}{2}}$
4	2294.003*v*	10	43,578.46	$a^4F_{3\frac{1}{2}} - w^4G^o_{3\frac{1}{2}}$
4	2291.450*v*	12	43,627.01	$b^4F_{3\frac{1}{2}} - y^2F^o_{3\frac{1}{2}}$
4	2290.541*v*	10	43,644.32	$b^4F_{3\frac{1}{2}} - x^2P^o_{2\frac{1}{2}}$
4	2289.495*v*	9	43,664.26	$a^4F_{3\frac{1}{2}} - y^4P^o_{2\frac{1}{2}}$
4	2288.774*v*	15	43,678.01	$b^4F_{1\frac{1}{2}} - x^4S^o_{1\frac{1}{2}}$
4	2287.804*v*	12*d*	43,696.53	$b^4F_{4\frac{1}{2}} - 6^o_{3\frac{1}{2}}$
4	2285.408*v*	12	43,742.34	$b^4F_{4\frac{1}{2}} - w^2I^o_{5\frac{1}{2}}$
4	2284.86*v*	30	43,752.8	$a^4F_{4\frac{1}{2}} - w^4G^o_{4\frac{1}{2}}$?
4	2284.81*v*	3	43,753.8	$b^4F_{2\frac{1}{2}} - t^4D^o_{2\frac{1}{2}}$
4	2284.375*v*	8	43,762.25	$b^4F_{1\frac{1}{2}} - w^2S^o_{\frac{1}{2}}$
5	2281.34	5	43,820.3	
4	2279.927*v*	10Fe	43,847.48	$(a^4F_{4\frac{1}{2}} - w^4F^o_{4\frac{1}{2}})$
4	2279.480*v*	15	43,856.08	$b^4F_{3\frac{1}{2}} - t^4D^o_{3\frac{1}{2}}$
5	2278.298	9	43,878.83	$a^4F_{1\frac{1}{2}} - w^2D^o_{2\frac{1}{2}}$
4	2276.523*v*	20*r*	43,913.04	
4	2275.884*v*	9	43,925.37	$b^4F_{2\frac{1}{2}} - y^2F^o_{2\frac{1}{2}}$
4	2274.617*v*	8	43,949.83	$b^4F_{1\frac{1}{2}} - w^2F^o_{1\frac{1}{2}}$
4	2274.495*v*	9	43,952.19	$a^4F_{4\frac{1}{2}} - w^4G^o_{5\frac{1}{2}}$
4	2273.58*v*	2	43,969.9	$a^4F_{4\frac{1}{2}} - 4^o_{3\frac{1}{2}}$
4	2268.742*v*	12	44,063.63	$b^4F_{2\frac{1}{2}} - x^4S^o_{1\frac{1}{2}}$
4	2268.163*v*	15	44,074.88	$b^4F_{3\frac{1}{2}} - t^4D^o_{3\frac{1}{2}}$
4	2267.113*v*	12	44,095.29	$a^4F_{1\frac{1}{2}} - x^4P^o_{1\frac{1}{2}}$
4	2264.880*v*	15	44,138.76	$b^4F_{2\frac{1}{2}} - 7^o_{3\frac{1}{2}}$
4	2264.41*v*	10	44,148.0	$a^4F_{1\frac{1}{2}} - x^4P^o_{\frac{1}{2}}$
4	2262.592*v*	10	44,183.39	$a^4F_{4\frac{1}{2}} - w^4G^o_{4\frac{1}{2}}$
10	2262.07	0 Co II?	44,193.6	$a^4F_{1\frac{1}{2}} - x^4P^o_{2\frac{1}{2}}$
5	2258.328	9	44,266.81	
4	2257.582*v*	10	44,281.43	$a^4F_{2\frac{1}{2}} - w^2I^o_{3\frac{1}{2}}$
4	2256.565*v*	10	44,301.39	$b^4F_{3\frac{1}{2}} - t^4D^o_{3\frac{1}{2}}$
4	2254.82*v*	10	44,335.6	$a^2F_{2\frac{1}{2}} - t^2F^o_{3\frac{1}{2}}$
5	2253.776	10	44,356.20	$b^4F_{4\frac{1}{2}} - 6^o_{3\frac{1}{2}}$
10	2253.587	3	44,359.92	$a^4F_{3\frac{1}{2}} - x^2G^o_{3\frac{1}{2}}$
4	2252.712*v*	10	44,377.15	$a^4F_{1\frac{1}{2}} - w^2D^o_{1\frac{1}{2}}$
4	2251.83*v*	8	44,394.5	$a^4F_{4\frac{1}{2}} - w^4G^o_{4\frac{1}{2}}$
4	2250.496*v*	10	44,420.84	$a^2F_{3\frac{1}{2}} - 16^o_{3\frac{1}{2}}$
4	2248.981*v*	5	44,450.78	$a^4F_{1\frac{1}{2}} - w^4D^o_{\frac{1}{2}}$
4	2248.80*v*	1	44,454.3	$a^2F_{2\frac{1}{2}} - t^2F^o_{2\frac{1}{2}}$
4	2247.86*v*	4	44,472.8	$b^4F_{2\frac{1}{2}} - y^2F^o_{2\frac{1}{2}}$
4	2246.599*v*	25	44,497.91	$a^4F_{2\frac{1}{2}} - x^4P^o_{1\frac{1}{2}}$
5	2245.600	10	44,517.68	
4	2245.463*v*	5	44,520.42	$a^4F_{1\frac{1}{2}} - y^4D^o_{\frac{1}{2}}$

‡ Partly Ni—Burns.

TABLE VIII.—*Continued.*

Ref.	λ *IA*	Int.–*TC*	Wave No. Vac.	Multiplet Designation
4	2244.12*v*	?	44,547.0	$a^3F_3 - 17^0_2$
4	2243.254*v*	10	44,564.26	$a^4F_3 - v^4D^0_3$
4	2241.65*v*	9	44,596.1	$a^4F_3 - x^4F^0_4$
4	2240.74*v*	6	44,614.1	$a^3F_3 - u^3D^0_3$
4	2239.30*v*	1	44,643.0	$a^3F_3 - s^3F^0_3$
4	2237.125*v*	10	44,686.31	$a^3F_3 - s^3F^0_2$; $b^4F_3 - 7^0_3$
4	2236.796*v*	15	44,692.88	$a^4F_4 - v^4D^0_4$
4	2234.710*v*	12	44,734.60	$b^4F_4 - t^4D^0_4$
4	2233.759*v*	10	44,753.64	$a^4F_4 - y^4S^0_4$
4	2233.099	9	44,766.87	
5	2232.88*v*	4	44,771.4	$b^4F_4 - 11^0_3$
4	2232.460*v*	8 Co II?	44,779.68	$a^4F_3 - v^4D^0_4$
4	2231.749	6	44,793.95	$b^4F_3 - 10^0_4$
5	2230.07	8	44,827.7	
13	2229.734*v*	10	44,834.42	$b^4F_4 - v^4F^0_5$
4	2228.806	12	44,853.09	$a^4F_3 - v^4D^0_4$
5	2228.334	4	44,862.59	$a^4F_4 - v^3D^0_3$
5	2227.853*v*	10	44,872.27	$a^4F_3 - w^3D^0_3$
4	2227.666*v*	12	44,876.04	$a^4F_4 - y^3F^0_4$
4	2225.848	5	44,912.69	$a^3F_3 - v^2G^0_3$
5	2225.350	12	44,922.74	$a^4F_3 - v^4D^0_3$
5	2223.97*v*	0	44,950.5	$a^4F_3 - x^2G^0_3$
4	2219.154	9	45,048.15	$a^4F_3 - w^3D^0_4$
5	2218.813	10	45,055.08	$b^4F_3 - 9^0_3.4_4$
5	2213.86	4 Co II?	45,155.9	$a^4F_3 - y^4S^0_4$; $(a^4F_3 - v^4D^0_3)$
5	2213.819	7	45,156.70	$b^4F_3 - 11^0_3$
5	2212.354	9	45,186.60	$a^4F_3 - x^4F^0_3$
13	2212.23	15	45,189.1	
13	2210.89	2	45,216.5	$a^4F_4 - x^2G^0_4$
4	2208.508*v*	12	45,265.28	$a^4F_3 - v^3D^0_3$
4	2207.853*v*	9	45,278.70	$a^4F_3 - y^3F^0_4$
5	2207.697	10	45,281.90	$a^4F_4 - y^3F^0_4$
4	2204.796*v*	18	45,341.48	$b^4F_3 - 10^0_3$
13	2203.96	3*N*	45,358.7	
13	2203.53	4	45,367.5	
13	2202.59	3	45,386.9	
13	2201.79	4	45,403.4	
13	2201.55	6	45,408.3	
13	2201.41	6	45,411.2	
5	2201.235	4	45,414.82	$b^4F_3 - 12^0_4$
5	2198.764	2	45,465.85	$a^4F_3 - u^4D^0_3$
13	2197.98	3	45,482.1	
5	2197.633	5	45,489.25	
13	2197.34	8	45,495.3	
5	2196.904	3	45,504.34	
4	2196.458*v*	15	45,513.58	$a^4F_3 - v^4D^0_3$
13	2196.02	3	45,522.7	
13	2195.17	2	45,540.3	$a^4F_4 - z^3H^0_4$
13	2191.16	3	45,623.6	$a^3F_3 - 21^0_3.4_4$
5	2189.350	3	45,661.34	$a^3F_3 - s^3F^0_3$
5	2187.284	5	45,704.45	$a^3F_3 - 23^0_4$; $b^4F_3 - 11^0_2$; $(a^3F_4 - s^3F^0_4)$
4	2186.777*v*	12	45,715.1	$b^4F_4 - 9^0_3.4_4$
13	2186.45	8	45,721.9	$a^4F_3 - w^3F^0_3$
5	2186.030	3	45,730.67	$b^4F_3 - 14^0_3$
5	2184.950	10	45,753.28	$a^3F_3 - u^3D^0_3$
5	2184.314	8	45,766.59	$a^4F_4 - x^2G^0_3$
13	2183.33	3*N*	45,787.2	
5	2182.587	15	45,802.80	$a^4F_4 - u^4D^0_4$
5	2181.121	12	45,833.58	$a^3F_3 - v^2G^0_4$
13	2180.23	7	45,852.3	
4	2180.060*v*	10	45,855.88	$a^4F_3 - v^2D^0_2$
13	2178.59	25*w*	45,886.8	
13	2178.06	8Fe?	45,898.0	
5	2176.968	2	45,921.00	$b^4F_3 - w^2G^0_3$
5	2176.494	4	45,931.01	$a^2F_3 - v^2G^0_4$
13	2176.03	3	45,940.8	
13	2174.90	8	45,964.7	
4	2174.589*v*	30*r*	45,971.24	$a^4F_4 - v^4D^0_4$
5	2173.845	10	45,986.98	$a^4F_3 - u^4D^0_3$
5	2173.173	10	46,001.19	$b^4F_4 - 10^0_4$
5	2172.175	4	46,022.33	$b^4F_3 - u^2F^0_3$
13	2171.68	0*N*	46,032.8	$a^4F_4 - x^2G^0_4$
5	2170.565	10	46,056.45	$a^4F_3 - u^4D^0_3$
5	2168.711	18	46,095.83	$a^4F_4 - u^4D^0_4$
13	2167.75	3	46,116.3	$b^4F_3 - 14^0_3$
13	2164.36	6	46,188.5	
13	2163.96	5*NN*	46,197.0	
13	2163.78	3?	46,200.9	
5	2163.574	12	46,205.26	$a^4F_3 - u^4D^0_4$
5	2163.034	15	46,216.79	$a^4F_4 - x^4S^0_4$
5	2162.196	6	46,234.70	$b^4F_3 - v^2F^0_4$
13	2161.58	3*N*	46,247.9	
13	2158.87	4	46,305.9	
5	2158.542	10	46,312.96	$a^4F_3 - u^2F^0_3$
13	2158.30	8	46,318.2	
13	2157.20	5*N*	46,341.8	
13	2156.33	5*NN*	46,360.5	
13	2155.29	12	46,382.8	
13	2154.24	3	46,405.4	
5	2154.074	10	46,409.01	$a^4F_3 - w^2F^0_3$
13	2153.50	12	46,421.4	
13	2152.83	2	46,435.8	$b^4F_3 - u^2F^0_3$
5	2152.148	10	46,450.54	$b^4F_3 - w^2G^0_4$
13	2151.69	3*N*	46,460.4	
13	2151.26	2 Co II?	46,469.7	$b^4F_3 - w^4F^0_3$
13	2150.11	5	46,494.6	$b^4F_3 - 15^0_3$
5	2148.708	6	46,524.90	$a^4F_4 - x^2F^0_4$
13	2147.77	5*N*	46,545.2	
13	2146.65	0	46,569.5	$b^4F_3 - u^2F^0_3$
5	2146.264	12	46,577.87	$a^4F_3 - u^4D^0_3$
5	2145.45	12	46,595.5	$b^4F_3 - 13^0_3.4_4$
5	2143.679	3	46,634.03	$a^4F_4 - t^4D^0_3$
13	2142.34	2*N*	46,663.2	$b^4F_3 - 14^0_3$
5	2138.971	15	46,736.67	$a^4F_4 - t^4D^0_4$
5	2137.780	15	46,762.70	$a^4F_4 - t^4D^0_3$
13	2137.38	0	46,771.4	$b^4F_4 - s^4D^0_4$
5	2135.798	4	46,806.09	$a^4F_4 - v^3F^0_3$
5	2135.59	3	46,810.64	$a^4F_3 - t^4D^0_2$
13	2134.92	6	46,825.3	
13	2134.10	8*N*	46,843.3	
5	2132.767	10	46,872.60	$a^4F_4 - u^4D^0_4$
13	2131.84	0	46,893.0	$b^4F_4 - y^2H^0_4$
5	2131.052	3	46,910.32	$a^4F_3 - v^3F^0_2$
13	2130.91	tr	46,913.4	$b^4F_4 - 17^0_3$
5	2130.276	8	46,927.40	$a^4F_3 - x^2F^0_4$
5	2129.508	5	46,944.32	$a^4F_4 - x^4S^0_4$
5	2127.147	10	46,996.42	$b^4F_3 - s^4D^0_2$
5	2126.199	5	47,017.37	$b^4F_3 - u^4F^0_3$
5	2125.949	5	47,022.90	$a^4F_3 - 6^0_3$
5	2125.322	5	47,036.77	$a^4F_3 - t^4D^0_2$
5	2125.116	10	47,041.33	$b^4F_3 - 15^0_3$
13	2124.80	0	47,048.3	$a^2F_3 - 30^0_3$
13	2124.13	8	47,063.2	
13	2122.64	10	47,096.2	$b^4F_4 - u^2F^0_3$
13	2121.99	6*N*	47,110.6	$b^4F_4 - u^2G^0_4$
5	2121.391	3	47,123.92	
5	2120.705	10	47,139.16	$a^4F_3 - t^4D^0_4$
5	2119.904	10	47,156.97	$b^4F_3 - s^4D^0_3$
5	2119.192	5	47,172.82	$b^4F_3 - 16^0_3$
5	2118.505	6	47,188.11	$b^4F_4 - s^4D^0_3$
13	2117.68	15*s*	47,206.5	$b^4F_3 - t^2F^0_3$
5	2116.842	10	47,225.17	$a^4F_4 - w^2F^0_3$
13	2116.29	8	47,237.5	
13	2115.49	2?	47,255.4	$b^4F_4 - 13^0_3.4_4$
5	2115.338	12	47,258.74	$b^4F_4 - s^4D^0_3$
5	2114.41	4	47,279.5	$b^4F_4 - w^4F^0_4$
5	2113.536	12	47,299.03	$b^4F_3 - 17^0_3$
13	2113.20	3	47,306.6	
13	2112.40	12	47,324.5	$b^4F_3 - w^4F^0_4$
5	2111.416	10	47,346.52	$a^4F_3 - x^4S^0_4$?
13	2111.08	5*N*	47,354.1	
13	2110.89	tr	47,358.3	$a^2F_3 - 32^0_4$
5	2109.206	5	47,396.12	
5	2108.980	15	47,401.20	$a^4F_3 - t^4D^0_3$
13	2108.16	0	47,419.6	$b^4F_4 - x^2H^0_4$
13	2108.05	0	47,422.1	$a^4F_3 - 7^0_3$; $b^4F_3 - 19^0_3$
5	2106.798	25 Co II?	47,450.29	$b^4F_3 - 20^0_4.2_3$
13	2105.02?	?*NN*	47,490.4	$a^2F_3 - 26^0_3$?
5	2104.730	25	47,496.90	
13	2104.50	12*Nd*?	47,502.1	
13	2103.85	5	47,516.8	
13	2103.10	4*N*	47,533.7	
13	2102.62	10	47,544.6	
13	2101.70	3	47,565.4	
13	2100.66	6	47,588.9	
5	2099.35	10	47,618.6	$a^4F_3 - w^2F^0_3$
5	2098.942	12	47,627.87	$a^4F_3 - t^4D^0_2$
5	2097.511	20	47,660.35	
5	2095.77	15	47,699.9	
13	2094.86	15	47,720.7	$b^4F_4 - t^2F^0_3$; $b^4F_3 - 16^0_2$
5	2093.40	15	47,753.9	$b^4F_3 - t^2F^0_2$
13	2091.98	12	47,786.3	$b^4F_3 - 18^0_3$
13	2091.40	10	47,799.6	$a^4F_3 - v^3F^0_2$
13	2091.05	15	47,807.6	$b^4F_3 - 19^0_3$
13	2089.83	10	47,835.5	$b^4F_3 - 20^0_4.2_3$
13	2089.67	10	47,839.2	$a^4F_4 - 6^0_3$
13	2089.35	15	47,846.5	$b^4F_3 - 17^0_2$
13	2087.55	15	47,887.7	
13	2085.67	15*N*	47,930.9	
13	2085.04	9	47,945.4	$a^4F_4 - w^2F^0_4$
13	2084.09	10	47,967.2	
13	2082.11	12	48,012.8	$a^4F_3 - 7^0_3$
13	2081.04	10	48,037.5	$a^4F_4 - 11^0_3$
13	2079.55	tr	48,071.9	$b^4F_4 - s^2F^0_3$?
13	2079.32	12	48,077.3	$a^4F_2 - 10^0_3$
13	2078.06	2	48,106.4	$b^4F_3 - t^2F^0_3$
13	2077.76	25*NN*	48,113.3	
13	2077.44	1*N*	48,120.8	$b^4F_4 - u^2D^0_3$?

TABLE VIII.—*Continued.*

REF.	λ *IA*	INT.–*TC*	WAVE NO. VAC.	MULTIPLET DESIGNATION
5	2073.27	10	48,217.5	$a^4F_{4\frac{1}{2}} - t^6D^o_{3\frac{1}{2}}$
13	2071.95	4*N*	48,248.3	
13	2069.91	12	48,295.8	$a^4F_{1\frac{1}{2}} - 12^6_{1\frac{1}{2}}$
5	2068.99	10	48,317.3	$a^4F_{4\frac{1}{2}} - v^2F^o_{3\frac{1}{2}}$
13	2067.58	5	48,350.2	
13	2067.42	6*NN*	48,354.0	
13	2066.22	12	48,382.0	$a^4F_{3\frac{1}{2}} - 9^6_{3\frac{1}{2},4\frac{1}{2}}$
13	2066.12	0 Co II?	48,384.4	$b^4F_{2\frac{1}{2}} - u^2D^o_{1\frac{1}{2}}$
5	2064.86	4	48,413.9	$b^4F_{4\frac{1}{2}} - t^2F^o_{3\frac{1}{2}}$ $b^4F_{2\frac{1}{2}} - s^2F^o_{2\frac{1}{2}}$
13	2062.92	6	48,459.4	
13	2061.39	6	48,495.4	
13	2059.90	3	48,530.5	
13	2058.51	3*NN*	48,563.2	
13	2055.46	4*N*	48,635.3	
5	2054.07	10	48,668.2	$a^4F_{2\frac{1}{2}} - 10^6_{2\frac{1}{2}}$
13	2053.46	5*N*	48,682.6	
13	2053.27	6	48,687.1	
13	2052.82	6	48,697.8	$a^4F_{2\frac{1}{2}} - 12^6_{1\frac{1}{2}}$
13	2048.59	5	48,798.3	
13	2043.70	8?	48,915.1	
13	2043.37	8	48,923.0	$b^4F_{3\frac{1}{2}} - 21^6_{3\frac{1}{2},4\frac{1}{2}}$
5	2043.00	8	48,931.8	
13	2042.72	8*N*	48,938.6	
13	2041.76	3	48,961.6	$b^4F_{3\frac{1}{2}} - s^2F^o_{3\frac{1}{2}}$
13	2041.11	20	48,977.1	
13	2039.95?	25 Co II?	49,005.0	$b^4F_{2\frac{1}{2}} - s^2F^o_{2\frac{1}{2}}$?
13	2038.86	0 Co II?	49,031.2	$a^4F_{3\frac{1}{2}} - 11^6_{2\frac{1}{2}}$
13	2037.92	2 Co II?	49,053.8	$b^4F_{3\frac{1}{2}} - u^2D^o_{2\frac{1}{2}}$
13	2035.35	5	49,115.7	$a^4F_{1\frac{1}{2}} - b^2P^o_{1\frac{1}{2}}$
13	2035.05	7*N*	49,123.0	
13	2034.49	8*N*	49,136.5	$a^4F_{1\frac{1}{2}} - v^2P^o_{\frac{1}{2}}$
13	2031.96	15	49,197.7	$a^4F_{4\frac{1}{2}} - 9^6_{3\frac{1}{2},4\frac{1}{2}}$
13	2029.99	8	49,245.4	
13	2029.78	8	49,250.5	
13	2027.77	3	49,299.3	
10	2026.794	—	49,323.0	$a^4F_{3\frac{1}{2}} - s^4D^o_{3\frac{1}{2}}$
13	2026.51	6	49,330.0	$a^4F_{1\frac{1}{2}} - s^4D^o_{2\frac{1}{2}}$
13	2026.35	8*d*?	49,333.8	
13	2024.68	10	49,374.5	
13	2023.17	4	49,411.4	
13	2020.56	tr*N*	49,475.2	$b^4F_{2\frac{1}{2}} - 23^6_{1\frac{1}{2}}$
13	2020.18	2	49,484.5	$a^4F_{4\frac{1}{2}} - 10^6_{3\frac{1}{2}}$
5	2017.26	4	49,556.1	
13	2016.17	15 Co II?	49,582.9	$b^4F_{4\frac{1}{2}} - 21^6_{3\frac{1}{2},4\frac{1}{2}}$
5	2015.99	4	49,587.3	
5	2014.58	20*w*	49,622.03	
13	2011.77	8*N*?	49,691.3	
5	2011.07	5 Co II?	49,708.6	$b^4F_{2\frac{1}{2}} - 24^6_{2\frac{1}{2}}$
5	2010.10	8	49,732.6	$a^4F_{2\frac{1}{2}} - s^4D^o_{2\frac{1}{2}}$
13	2009.24	9	49,753.9	$a^4F_{2\frac{1}{2}} - w^4P^o_{2\frac{1}{2}}$?
13	2008.85	8	49,763.6	
5	2008.28	5	49,777.7	$a^4F_{2\frac{1}{2}} - 15^6_{2\frac{1}{2}}$
13	2008.04	15	49,783.6	
13	2004.00	10*N*	49,884.0	
13	2002.44	6?	49,922.8	$a^4F_{2\frac{1}{2}} - 13^6_{2\frac{1}{2},4\frac{1}{2}}$
13	2002.32	25 Co II?	49,925.8	$a^4F_{3\frac{1}{2}} - s^4D^o_{3\frac{1}{2}}$
13	2002.01	3	49,933.6	
13	2000.12	12*N*	49,980.7	$b^4F_{4\frac{1}{2}} - 22^6_{3\frac{1}{2}}$
13	1999.89	8	49,986.5	
	λ Vac.			
13	1998.49	25*l*	50,037.8	$a^4F_{1\frac{1}{2}} - s^4D^o_{1\frac{1}{2}}$
13	1994.98	15*N*	50,125.8	
13	1993.25	10*N*	50,169.3	
13	1992.79	20	50,180.9	
13	1991.80	3	50,205.8	$a^4F_{1\frac{1}{2}} - w^4P^o_{1\frac{1}{2}}$?
13	1990.34	30 Co II?	50,242.7	$b^4F_{3\frac{1}{2}} - 26^6_{3\frac{1}{2}}$?
13	1989.80	25 Co II?	50,256.3	$b^4F_{3\frac{1}{2}} - 24^6_{2\frac{1}{2}}$
13	1989.28	10	50,269.4	
13	1987.65	20	50,310.7	$b^4F_{1\frac{1}{2}} - 29^6_{2\frac{1}{2}}$
13	1987.24	10?	50,321.0	
13	1987.15	12?	50,323.3	
13	1987.03	15	50,326.4	
13	1986.31	6	50,344.6	$a^4F_{3\frac{1}{2}} - w^4P^o_{2\frac{1}{2}}$
13	1985.88	4	50,355.5	
13	1985.36	10	50,368.7	$a^4F_{3\frac{1}{2}} - 15^6_{3\frac{1}{2}}$
13	1985.25	10	50,371.5	$b^4F_{2\frac{1}{2}} - 27^6_{2\frac{1}{2}}$
13	1982.81	8	50,433.5	$b^4F_{1\frac{1}{2}} - 30^6_{2\frac{1}{2}}$
13	1982.52	20	50,440.8	$a^4F_{3\frac{1}{2}} - s^4D^o_{3\frac{1}{2}}$
13	1981.97	20	50,454.9	$a^4F_{1\frac{1}{2}} - s^4D^o_{\frac{1}{2}}$
13	1980.89	40*N*	50,482.4	
13	1980.59	15	50,490.0	$a^4F_{3\frac{1}{2}} - t^2F^o_{2\frac{1}{2}}$
13	1978.53	12	50,542.6	
13	1978.36	10	50,546.9	$b^4F_{1\frac{1}{2}} - v^4F^o_{1\frac{1}{2}}$
13	1976.97	30	50,582.5	$a^4F_{3\frac{1}{2}} - 17^6_{2\frac{1}{2}}$
13	1975.94	6	50,608.8	$b^4F_{1\frac{1}{2}} - v^4F^o_{2\frac{1}{2}}$
13	1975.67	20	50,615.7	
13	1975.36	6*N*	50,623.7	$b^4F_{2\frac{1}{2}} - v^4F^o_{2\frac{1}{2}}$
13	1974.39	15	50,648.6	$b^4F_{3\frac{1}{2}} - v^4F^o_{4\frac{1}{2}}$
13	1973.85	25	50,662.4	$b^4F_{1\frac{1}{2}} - 31^6_{1\frac{1}{2}}$
13	1973.62	5	50,668.3	

REF.	λ *IA*	INT.–*TC*	WAVE NO. VAC.	MULTIPLET DESIGNATION
13	1972.82	tr?	50,688.9	$a^4F_{1\frac{1}{2}} - 19^6_{1\frac{1}{2}}$
13	1972.52	30*N*	50,696.6	$b^4F_{3\frac{1}{2}} - 29^6_{3\frac{1}{2}}$
13	1971.75	15	50,716.4	$a^4F_{1\frac{1}{2}} - 20^6_{1\frac{1}{2},2\frac{1}{2}}$
13	1971.16	30*N*	50,731.6	$b^4F_{2\frac{1}{2}} - 25^6_{2\frac{1}{2}}$
13	1970.71	50	50,743.1	$b^4F_{1\frac{1}{2}} - 32^6_{2\frac{1}{2}}$ $(a^4F_{4\frac{1}{2}} - s^4D^o_{3\frac{1}{2}})$
13	1969.68	3	50,769.7	
13	1968.93	25*N*	50,789.0	$b^4F_{3\frac{1}{2}} - 26^6_{3\frac{1}{2}}$
13	1968.69	25*N*	50,795.2	
13	1967.78	10	50,818.7	$b^4F_{2\frac{1}{2}} - 30^6_{2\frac{1}{2}}$
13	1966.96	10	50,839.9	
13	1966.68	9	50,847.1	$b^4F_{1\frac{1}{2}} - 33^6_{1\frac{1}{2},2\frac{1}{2}}$
13	1964.03	20	50,915.7	$b^4F_{4\frac{1}{2}} - 24^6_{3\frac{1}{2}}$
13	1963.92	8?	50,918.6	$b^4F_{2\frac{1}{2}} - 27^6_{2\frac{1}{2}}$
13	1963.55	20	50,928.2	$a^2F_{2\frac{1}{2}} - 37^6_{2\frac{1}{2},3\frac{1}{2}}$
13	1963.38	12	50,932.6	$b^4F_{2\frac{1}{2}} - v^4F^o_{3\frac{1}{2}}$
13	1961.59	25	50,979.0	
13	1961.26	8	50,987.6	$a^4F_{1\frac{1}{2}} - t^2F^o_{2\frac{1}{2}}$?
13	1961.00	15	50,994.4	$b^4F_{2\frac{1}{2}} - v^4F^o_{3\frac{1}{2}}$
13	1958.94	15	51,048.0	$b^4F_{2\frac{1}{2}} - 31^6_{2\frac{1}{2}}$ $(a^4F_{4\frac{1}{2}} - 16^6_{3\frac{1}{2}})$
13	1958.55	25	51,058.2	
13	1958.10	8	51,069.9	$a^4F_{2\frac{1}{2}} - 18^6_{2\frac{1}{2}}$
13	1957.69	12*N*	51,080.6	$a^4F_{3\frac{1}{2}} - t^2F^o_{2\frac{1}{2}}$
13	1956.22	15	51,119.0	$a^4F_{2\frac{1}{2}} - 20^6_{2\frac{1}{2},3\frac{1}{2}}$
13	1955.17	30	51,146.4	$b^4F_{1\frac{1}{2}} - 35^6_{2\frac{1}{2},3\frac{1}{2}}$
13	1954.22	30	51,171.3	$b^4F_{3\frac{1}{2}} - v^4F^o_{4\frac{1}{2}}$
13	1953.71	8	51,184.7	$a^4F_{4\frac{1}{2}} - 15^6_{3\frac{1}{2}}$
13	1953.50	4	51,190.2	
13	1951.90	25	51,232.1	$b^4F_{2\frac{1}{2}} - 33^6_{2\frac{1}{2},3\frac{1}{2}}$
13	1951.44	12	51,244.2	$b^4F_{3\frac{1}{2}} - 29^6_{3\frac{1}{2}}$
13	1949.00	15	51,308.4	$b^4F_{4\frac{1}{2}} - v^4F^o_{4\frac{1}{2}}$
13	1948.09	10	51,332.3	
13	1947.58	5	51,345.8	
13	1946.79	25	51,366.6	$b^4F_{3\frac{1}{2}} - 30^6_{3\frac{1}{2}}$
13	1945.86	0	51,391.2	$b^4F_{4\frac{1}{2}} - 25^6_{3\frac{1}{2}}$
13	1945.09	12	51,411.5	$b^4F_{2\frac{1}{2}} - 34^6_{2\frac{1}{2},3\frac{1}{2}}$
13	1943.64	12	51,449.9	$b^4F_{4\frac{1}{2}} - 26^6_{3\frac{1}{2}}$
13	1940.16	15 Co II?	51,542.1	$b^4F_{3\frac{1}{2}} - v^4F^o_{3\frac{1}{2}}$
13	1939.75	3	51,553.0	
13	1938.94	10	51,574.6	
13	1936.58	30 Co II?	51,637.4	$b^4F_{4\frac{1}{2}} - 28^6_{3\frac{1}{2}}$
13	1935.72	0*N*	51,660.4	$a^4F_{3\frac{1}{2}} - 18^6_{2\frac{1}{2}}$
13	1935.46	0*N*	51,667.3	$a^4F_{2\frac{1}{2}} - u^2D^o_{1\frac{1}{2}}$
13	1934.34	12	51,697.2	$a^4F_{2\frac{1}{2}} - s^2F^o_{2\frac{1}{2}}$
13	1933.03	3	51,732.3	
13	1931.89	8	51,762.8	
13	1931.00	10*N*	51,786.6	
13	1930.90	6?	51,789.3	$a^4F_{2\frac{1}{2}} - u^2D^o_{2\frac{1}{2}}$
13	1930.38	10	51,803.3	
13	1929.34	15	51,831.2	$b^4F_{4\frac{1}{2}} - v^4F^o_{3\frac{1}{2}}$
13	1926.90	10	51,896.8	$a^4F_{4\frac{1}{2}} - t^2F^o_{3\frac{1}{2}}$
13	1925.05	12	51,946.7	$a^2F_{2\frac{1}{2}} - 37^6_{2\frac{1}{2},3\frac{1}{2}}$
13	1924.46	15	51,962.6	
13	1911.86	8	52,305.1	
13	1906.72	5	52,446.1	
13	1905.87	20	52,469.5	
13	1905.41	6	52,482.2	
13	1904.75	5	52,500.3	
13	1902.15	10	52,572.1	
13	1901.75	20	52,583.1	
13	1897.73	8	52,694.6	
13	1897.48	10	52,701.5	
13	1895.78	4	52,748.7	
13	1894.07	3	52,796.4	
13	1893.43	3	52,814.2	
13	1889.87	10	52,913.7	
13	1889.60	6	52,921.2	
13	1887.89	12	52,969.2	
13	1884.56	10*N*	53,062.8	
13	1884.45	10	53,065.9	$a^4F_{4\frac{1}{2}} - 21^6_{3\frac{1}{2},4\frac{1}{2}}$
13	1881.09	5	53,160.7	
13	1880.82	15	53,168.3	
13	1880.34	4	53,181.9	
13	1878.28	25	53,240.2	
13	1877.40	15	53,265.1	
13	1876.88	8	53,279.9	
13	1876.48	7	53,291.2	
13	1876.01	10	53,304.6	
13	1875.22	4	53,327.1	
13	1872.37	8	53,408.3	
13	1870.45	5	53,463.1	
13	1869.16	5	53,500.0	
13	1866.45	3	53,577.7	$a^4F_{1\frac{1}{2}} - 29^6_{2\frac{1}{2}}$
13	1866.27	6	53,582.8	$a^4F_{4\frac{1}{2}} - 24^6_{3\frac{1}{2}}$
13	1864.92	4	53,621.6	
13	1862.31	25	53,696.8	
13	1858.26	3	53,813.8	$a^4F_{4\frac{1}{2}} - v^4F^o_{4\frac{1}{2}}$
13	1856.13	15 Co II?	53,875.5	$a^4F_{1\frac{1}{2}} - v^4F^o_{2\frac{1}{2}}$
13	1855.05	40 Co II?	53,906.9	$a^4F_{2\frac{1}{2}} - v^4F^o_{3\frac{1}{2}}$
13	1854.28	8	53,929.3	$a^4F_{1\frac{1}{2}} - 31^6_{1\frac{1}{2}}$

TABLE VIII.—*Concluded.*

Ref.	λ *IA*	Int.–*TC*	Wave No. Vac.	Multiplet Designation
13	1852.71	30 Co II?	53,975.0	$a^4F_{3\frac{1}{2}} - v^4F^0_{4\frac{1}{2}}$
13	1852.52	15?	53,980.5	$a^4F_{2\frac{1}{2}} - 29^0_{2\frac{1}{2}}$
13	1851.49	8	54,010.6	
13	1850.80	4	54,030.7	
13	1847.89	30	54,115.8	$a^4F_{3\frac{1}{2}} - 26^0_{3\frac{1}{2}}$
13	1846.94	4	54,143.6	
13	1843.45	8	54,246.1	$a^4F_{3\frac{1}{2}} - 27^0_{2\frac{1}{2}}$
13	1842.34	25 Co II?	54,278.8	$a^4F_{2\frac{1}{2}} - v^4F^0_{3\frac{1}{2}}$?
13	1841.88	3	54,292.4	$a^4F_{1\frac{1}{2}} - 34^0_{1\frac{1}{2},2\frac{1}{2}}$
13	1841.47	10	54,304.5	$a^4F_{2\frac{1}{2}} - 28^0_{3\frac{1}{2}}$
13	1840.79	10	54,324.5	
13	1840.55	10	54,331.6	$a^4F_{2\frac{1}{2}} - 31^0_{3\frac{1}{2}}$
13	1838.28	15	54,398.7	$a^4F_{4\frac{1}{2}} - 24^0_{3\frac{1}{2}}$
13	1837.82	8	54,412.3	$\begin{cases} a^4F_{1\frac{1}{2}} - 35^0_{1\frac{1}{2},2\frac{1}{2}} \\ a^4F_{2\frac{1}{2}} - 32^0_{1\frac{1}{2}} \end{cases}$
13	1837.13	3	54,432.7	
13	1836.97	3	54,437.5	
13	1834.99	10 Co II?	54,496.2	$a^4F_{3\frac{1}{2}} - v^4F^0_{3\frac{1}{2}}$?
13	1834.34	10	54,515.5	$a^4F_{2\frac{1}{2}} - 33^0_{1\frac{1}{2},2\frac{1}{2}}$
13	1832.47	15	54,571.2	$a^4F_{3\frac{1}{2}} - 29^0_{2\frac{1}{2}}$
13	1828.35	12	54,694.2	$a^4F_{3\frac{1}{2}} - 34^0_{1\frac{1}{2},2\frac{1}{2}}$
13	1825.17	1 Co II?	54,789.4	$a^4F_{4\frac{1}{2}} - v^4F^0_{4\frac{1}{2}}$?
13	1822.03	3	54,883.8	
13	1820.42	12	54,932.4	$a^4F_{4\frac{1}{2}} - 26^0_{4\frac{1}{2}}$
13	1814.20	12	55,120.7	$a^4F_{4\frac{1}{2}} - 28^0_{4\frac{1}{2}}$

Notes in intensity column: *d*, double; *g*, ghost; *h*, hazy; *l*, shaded to longer wave-length (asymmetrical); *n*, diffuse; *N*, very diffuse; *r*, narrow self-reversal; *R*, wide self-reversal; *s*, shaded to shorter wave-length (asymmetrical); *w*, wide or complex; *W*, very wide or complex.

1 Meggers, unpublished material, 1935.
2 Meggers and Kiess, J. Research Nat. Bur. Stand. **9**, 319 (1932), (RP 473).
3 Meggers and Kiess, Sci. Pap. Bur. Stand. **14**, 645 (1918); (No. 324).
4 Burns, unpublished material. Three-place measures in heavy type are interferometer measures; "v" denotes vacuum source.
5 *M. I. T. Wave-Length Tables* (The Technology Press; John Wiley and Sons, New York, 1939).
6 Russell, unpublished material.
7 Dhein, Zeits. f. Wiss. Ptg. **19**, 289 (1920).
8 Stüting, Zeits. f. Wiss. Ptg. **7**, 73 (1909).
9 Exner and Haschek, see Kayser, *Handbuch der Spectroscopie*, Vol. **5** (1910), p. 310; also reference 10 below; also King, Mt. Wilson Contr. No. 108; Astrophys. J. **42**, 347 (1915).
10 Catalan and Antunes, Anal. Soc. Española de Fisica y Quimica **34**, 207 (1936).
11 Krebs, Zeits. f. Wiss. Ptg. **16**, 292 (1917).
12 Hasselberg, see Kayser, *Handbuch der Spectroscopie*, Vol. **5** (1910), p. 310.
13 C. E. Moore, unpublished material.

There are a few conspicuous cases of sharing of *g* values between neighboring terms, as shown in Table VII. The most remarkable group is $y^4S_{1\frac{1}{2}}{}^0$, $v^4D_{1\frac{1}{2}}{}^0$, $v^2D_{1\frac{1}{2}}{}^0$. The designations of the first two might almost as well be interchanged. Those here given depend on the intensities in the multiplets with a^4P, b^4P; but these also indicate such an extensive sharing of properties by the three levels that it is hardly more than a formality to give them definite names. The intermixture of $b^4P_{1\frac{1}{2}}$ and $a^2D_{1\frac{1}{2}}$ is less complete, and they may be definitely labeled. A somewhat better agreement with the theoretical *g* values could also be obtained by interchanging the designations $e^4P_{\frac{1}{2}}$ and $e^4D_{\frac{1}{2}}$, and also $e^6P_{1\frac{1}{2}}$ and $e^6D_{1\frac{1}{2}}$, without much disturbing the energy levels or intensities.

9. Line List

Table VIII includes all the classified lines, and all unclassified lines of intensity exceeding 5 on the M.I.T. scale or 2 on that of other observers. Fainter unclassified lines are included for which King gives a temperature class or Burns has an interferometer measure. Lines which are very probably due to impurities, or to Co II, are also omitted.

The wave-lengths in column 2 have been collected from many sources, as described in the notes, and indexed in column 1. The values printed in heavy type are Burns' interferometer measures. They greatly exceed the rest in accuracy. For other lines, we have entered what appears to us to be the best available wave-length, but it has been impracticable to secure a strictly homogeneous system. The intensities in the third column are King's estimates for all lines to which he has assigned a temperature class (column 4). For the other lines the values of the M.I.T. catalog are entered, when available, except in the red (λ8648–11,894) where the values of Meggers and Kiess were adopted. For the remaining lines the intensity assigned by the measurer is given.

All these intensities are estimates of the strength of the lines on the negatives, and different observers have used extremely different scales—the older lists going usually from 1 to 10 and some recent ones from 1 to 3000, so that great caution is necessary in comparing them.

King's estimates are much more nearly homogeneous, but fall off at both ends with the sensitivity of his plates. His temperature classes show the usual close correlation with the energy levels, and have been of great aid in the analysis. The wave number and the adopted designation are given in the last two columns.

Of the 3007 lines in this table 282 have not been classified. Only one, λ3177.266, is of any considerable strength. This, and some other low-temperature lines between λ3500 and λ3150 are probably the principal components of the missing

combinations of a^2G and a^2H (§4); but, since the faint components of the multiplets have not been found, they cannot be classified.

This spectrum may now be regarded as pretty well analyzed. Between λ11,900 and λ2500 there are 90 unclassified lines out of 2388; between λ2500 and λ2200, 52 out of 279; and between λ2200 and λ1810, 140 out of 340.

The classification is therefore fairly complete except in the remoter ultraviolet. Here many of the lines we list may belong to Co II, a spectrum still very incompletely analyzed. Some of these are noted by "Co II?" following the intensity in Table VIII.

It is a pleasure to express our gratitude to Dr. M. T. Antunes for making the important work of Catalan and himself accessible to us; to Dr. Keivin Burns for the communication of his extensive and accurate measures,—especially with the interferometer—; to Dr. A. S. King for the loan of a set of plates of the spectrum, and for Zeeman data; and to Dr. A. G. Shenstone for taking the spectrogram which permitted the extension of our work beyond λ2230.

SEPTEMBER 1, 1940 PHYSICAL REVIEW VOLUME 58

The Effect of an Activator on the Absorption Spectrum of Zinc Sulphide Powders

CHARLES J. BRASEFIELD
U. S. Coast Guard Academy, New London, Connecticut
(Received May 24, 1940)

The absorption of zinc sulphide powders, both pure and with various concentrations of activator, was measured in the region 3200–4800A by the diffuse reflection method. It was found that the long wave-length limit of the absorption band for a pure ZnS powder was at 3800A and that this limit moved to longer wave-lengths with increasing concentration of Ag activator. No evidence could be found of a secondary absorption peak characteristic of the activator.

IF pure zinc sulphide is to luminesce under ultraviolet light, it must be activated. This is usually done by heating the powder with a trace of the salt of a foreign atom, such as silver or copper. In order to get a clearer picture of the nature of this activating process, it seems desirable to find out what effect the heat treatment and the presence of foreign atoms have on the absorption spectrum of the pure powder. Gisolf,[1] studying the transmission of thin layers of ZnS powder, has reported that, within an accuracy of 10 angstrom units, no difference is found between the wave-lengths of the absorption edge for both pure ZnS and for ZnS activated with traces of Cu or Ag. He also claims to have found a secondary absorption peak, characteristic of the impurity, on the long wave-length side of the principal absorption edge.[2] These results were not confirmed, however, in the experiments about to be described.

The absorption spectra of the ZnS powders were obtained by the diffuse reflection method. The source of radiation was a 120-watt tungsten lamp with a quartz window.[3] The ZnS powder[4] was sprinkled in a thin layer over the corrugated end of a black wooden rod, held at an angle of approximately 45° in front of the slit of a small Littrow quartz spectrograph. During preliminary experiments a quartz mercury arc was used as a source of radiation. The appearance on the photographic plate, with small but uniformly diminished intensity, of the mercury lines in the region 3342 to 2537A was interpreted as indicating that a little light enters the spectrograph after one surface reflection from the crystals. Most of the reflected light, however, is apparently totally reflected internally, perhaps several times, so that it arrives at the slit of the

[1] J. H. Gisolf, Physica **6**, 87 (1939).
[2] See reference 1, Fig. 2 on page 87, and remarks on page 88.
[3] Kindly loaned by Professor George Winchester of Rutgers University.
[4] Thanks are due to Dr. G. R. Shaw, Dr. L. B. Headrick and Mr. H. W. Leverenz of the RCA Manufacturing Company, for supplying the samples of ZnS used in these experiments.

spectrograph after having passed through an unknown thickness of ZnS.

The spectrum of the light reflected from ZnS was photographed on an Eastman Spectroscopic Plate, Type IV–O; exposure times were around 20 minutes. On the same plate was photographed the spectrum of the source as reflected from an aluminum mirror which is known[5] to have a uniform reflectivity of approximately 90 percent over the range 3000–5000A. The exposure time was adjusted so as to duplicate the blackening of the ZnS spectrum in the region 4500–5000A; usually this required an exposure of about one second.

The density of blackening of the plate was determined by using a crude densitometer.[6] The absorption spectrum of ZnS was obtained by plotting the difference between the densitometer readings in the spectrum of the light reflected from ZnS and the densitometer readings in the spectrum of the light reflected from the aluminum mirror. Curves obtained in this way for a sample of pure ZnS, precipitated and dried, and for another sample of ZnS containing 0.128 percent Ag, which had been fired with NaCl flux at 940°C for two hours, are shown in Fig. 1. Measurements are less reliable at high absorption but for all the samples which were studied, absorption was complete for wave-lengths less than 3500A. There is no evidence, either in the curves of Fig. 1, or in similar curves obtained with different concentrations of Ag activator, of a secondary absorption peak on the long wave-length side of the main absorption edge—at least as far as 4800A. These curves are in fair agreement with similar curves obtained by Kitchener[7] and by Kroger,[8] but, as previously mentioned, differ from the curve shown by Gisolf.[2]

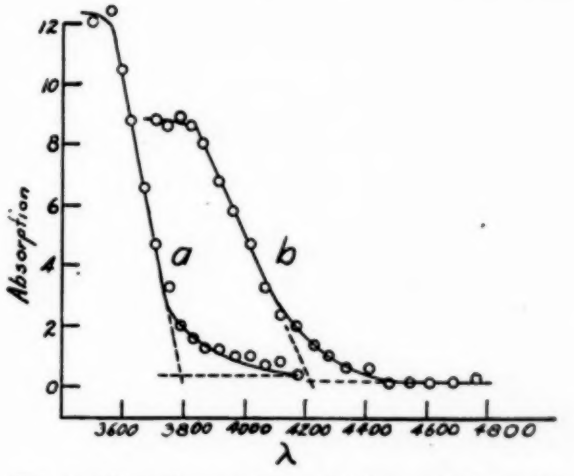

FIG. 1. Absorption spectrum of (*a*) pure ZnS, precipitated and dried; (*b*) ZnS containing 0.128 percent Ag which had been fired with NaCl flux at 940° C for two hours.

TABLE I. *Absorption limits under various conditions.*

SAMPLE	LONG WAVE-LENGTH LIMIT OF ABSORPTION
1. Pure ZnS, precipitated and dried	3800A
2. Pure ZnS, heated at 940° C; no flux	4220A
3. Pure ZnS, heated at 940° C for 2 hours with NaCl	3980A
4. ZnS+0.005% Ag, heated at 940° C for 2 hours with NaCl	4120A
5. ZnS+0.032% Ag, heated at 940° C for 2 hours with NaCl	4180A
6. ZnS+0.128% Ag, heated at 940° C for 2 hours with NaCl	4220A
7. ZnS+0.512% Ag, heated at 940° C for 2 hours with NaCl	4280A
8. ZnS+0.001% Cu, heated at 1200° C with 2% NaCl	4120A

The long wave-length limit of the absorption edge was determined, as indicated in Fig. 1, by extrapolating the steep portion of the curve. Values for this long wave-length limit for various samples of ZnS are shown in Table I. For the first and third samples, values should be accurate within 20A; for the other samples, within 50A. It is apparent from this table that, contrary to Gisolf's findings, previously mentioned, the long wave-length limit of the absorption band of a ZnS powder in general moves toward longer wave-lengths with increasing activation. Moreover, the long wave-length limit even for pure powdered ZnS is considerably greater than re-

[5] See for example M. Auwarter, J. App. Phys. **10**, 706 (1939). The mirror was kindly supplied by Dr. A. B. Focke of Brown University.

[6] The densitometer was constructed by focusing the filament of a straight-filament incandescent lamp, suitably masked, on the spectroscopic plate. The plate was clamped to the carriage of an old Michelson interferometer, and could thus be moved across the beam of light. Behind the plate was mounted a Weston Photronic Cell connected to a L. & N. model 2420-C galvanometer (sensitivity 0.02 microampere per mm) whose deflection was a measure of the quantity of light transmitted by the spectroscopic plate.

[7] Kitchener, Trans. Faraday Soc. **35**, 98 (1939).

[8] F. A. Kroger, Physica **7**, 1 (1940). Note, however, that Kroger defines the long wave limit of absorption as the longest wave-length at which absorption is complete.

ported by Gisolf[1] (*viz.* 3350A); Kroger's curve,[8] on the other hand, indicates an "extrapolated" long wave-length limit around 3800A, in good agreement with the value in Table I. Dr. Headrick has suggested that since sample No. 2 oxidized considerably on firing, the unusually high value for its long wave-length limit may be characteristic of ZnO rather than ZnS. The long wave-length limit for sample No. 8 is not very different from a value of 4250A found for a ZnS single crystal containing about 0.004 percent Cu.[9]

The emission spectrum of samples 3, 4, 5 and 6 is of appreciable intensity over the range 4200 to 5000A, with a peak around 4600A.[10] Since a tungsten filament emits little ultraviolet light, the intensity of the fluorescent light from the ZnS powders was small; however, some of the blackening of the plates was undoubtedly due to fluorescent light. To correct for this, densitometer readings for wave-lengths greater than 4200A should be increased. This would mean that, in curves similar to those of Fig. 1, all points on the long wave-length side of 4200A might be raised as high as, but no higher than, the point at 4200A. If this correction is made, it turns out that the long wave-length limit of the absorption edge for samples 3, 4, 5 and 6 would be shifted an average of 20A toward shorter wave-lengths; this correction is within the limit of error (50A) claimed for these measurements.

In conclusion, it has been found that the long wave-length limit of the absorption band for a pure ZnS powder was at 3800A and that this limit moved to longer wave-lengths with increasing concentration of Ag activator. No evidence could be found of a secondary absorption peak characteristic of the activator. An interpretation of these results cannot be given at this time.

[9] C. J. Brasefield, Phys. Rev. **57**, 162 (1940).
[10] See H. W. Leverenz and F. Seitz, J. App. Phys. **10**, 487 (1939). Samples 1, 3, 5, 6 and 7 described in Fig. 15 of this article are identical with samples 3, 4, 5, 6 and 7 of Table I.

SEPTEMBER 1, 1940 PHYSICAL REVIEW VOLUME 58

On the Radiofrequency Spectra of Sodium, Rubidium and Caesium*

S. MILLMAN,
Columbia University and City College, New York, New York
AND
P. KUSCH,
Columbia University, New York, New York

(Received June 24, 1940)

The hyperfine structures of the ground state of Na^{23}, Rb^{85}, Rb^{87} and Cs^{133} were measured by observing radiofrequency spectra of these atoms. In each case the particular lines chosen for study and the magnetic fields at which they were observed were such as to yield the greatest precision for the hyperfine structure measurements, consistent with frequencies conveniently obtainable in our laboratory (up to 700 megacycles). The measured h.f.s. separations are given both in absolute frequency units and in wave numbers.

	sec.$^{-1}\times10^{-6}$	cm^{-1}
Na^{23}	1771.75	0.059103
Rb^{85}	3035.7	0.10127
Rb^{87}	6834.1	0.22797
Cs^{133}	9191.4	0.30661

INTRODUCTION

IN a previous paper[1] methods were described for the study of the radiofrequency spectra of atoms and in particular for the accurate determination of the hyperfine structure of the ground states of atoms. These methods were applied to the measurement of the h.f.s. separation of the normal states of Li^6, Li^7, K^{39} and K^{41}. In the present paper we present the results of the

* Publication assisted by the Ernest Kempton Adams Fund for Physical Research of Columbia University.
[1] P. Kusch, S. Millman and I. I. Rabi, Phys. Rev. **57**, 765 (1940).

application of these methods to the measurement of the h.f.s. of the ground states of Na^{23}, Rb^{85}, Rb^{87} and Cs^{133}.

We shall first present a brief resumé of these methods. A beam of atoms is projected through two inhomogeneous magnetic fields so arranged that the deflection of the beam at the detector produced by the first magnet is equal and opposite to that produced by the second magnet when the gradients and fields in both magnets are the same. The net deflection produced by the two magnets is zero, however, only when the component of the magnetic moment of the atom in the direction of the field, is the same in the two deflecting fields. If any changes affecting the value of this component take place in the space between the two deflecting magnets, they will be recognized by a drop of beam intensity at the detector set at zero deflection position. Between the two inhomogeneous fields is placed a homogeneous field which can be set at any desired value, while at right angles to this field is superimposed a weak radiofrequency oscillating field. If the oscillating frequency corresponds to the energy difference between two levels of the atom, transitions, consistent with selection rules, will occur. These reorientations will, in general, produce a change in the magnetic moment of the atom and, therefore, a drop in the intensity of the beam at the detector. To observe the radiofrequency spectrum of an atom in a given magnetic field, one merely observes the intensity of the beam as a function of the applied frequency.

Two procedures were outlined in the earlier paper[1] for measuring the h.f.s. of the ground state of an atom in a $^2S_{\frac{1}{2}}$ state. One was to observe the frequencies of lines associated with transitions between the two F levels of the hyperfine structure doublet in very weak magnetic fields. Since each F level is split up into $2F+1$ magnetic levels, a Zeeman pattern is observed. For sufficiently low magnetic fields the center of gravity of this pattern determines the $\Delta\nu$ of the ground state. The other procedure involved the measurement of the frequencies of the lines associated with a change in nuclear magnetic quantum number, m_i, in strong magnetic fields. Not only did the latter method yield results which were just as precise as those obtained by use of the first method, but it also had the additional

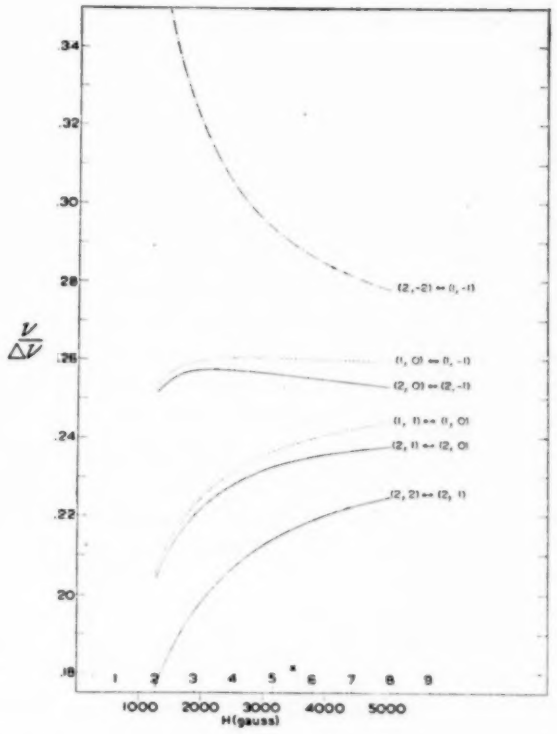

FIG. 1. The field dependence of the frequencies of the lines of Na^{23} associated with the transitions $\Delta m_i = \pm 1$, $\Delta m_J = 0$.

advantage of requiring lower working frequencies. The reduction factor in frequency of the lines was shown to be of the order of $(2i+1)$. The $\Delta\nu$ of Li^7 and that of K^{39} were determined by both methods. In each case the results obtained with the two methods were in complete agreement, indicating that the expressions for the variation of the energies of the magnetic levels of h.f.s. multiplets in external fields, varying from the weak Zeeman region to the strong Paschen-Back region, are accurate to at least one part in 10^4.

In view of the large h.f.s. splittings associated with the atoms under discussion in this paper, the weak field method could not be used with the range of frequencies available in this laboratory. Our present measurements are based on observations of frequencies of lines resulting from atomic transitions in intermediate and in strong magnetic fields.

The apparatus used and the general technique followed in this work is the same as that used in earlier experiments.

RESULTS

Na^{23}

The $\Delta\nu$ of the ground state of Na^{23} is[2] about 0.059 cm^{-1} or 1770×10^6 $sec.^{-1}$. Since the nuclear spin of Na^{23} is $\frac{3}{2}$, frequencies of the order of $\Delta\nu/4$ or of 450 megacycles are required to induce the transitions $\Delta m_i=\pm1$, $\Delta m_J=0$ at high magnetic fields. Because of the convenience of this frequency range we have, accordingly, determined the $\Delta\nu$ of Na^{23} from measurements of the frequencies of the lines resulting from these transitions. The spectrum is similar to that already described[1] for the cases of Li^7 and K^{39}.

Figure 1 gives a graphical representation of the frequencies of the lines associated with these transitions, in units of $\Delta\nu$, as a function of the field parameter x. This parameter is defined by the equation,

$$x=\frac{g_J-g_i}{h\Delta\nu}\mu_0H, \qquad (1)$$

where $\Delta\nu$ is expressed in $sec.^{-1}$ and μ_0 is the Bohr magneton.

In the first column of Table I are listed the transitions which give rise to the lines. The notation is the same as that previously employed; the first symbol in the parenthesis gives the F value and the second the m value which characterizes the state. The second column gives the expressions for the frequencies of the lines. The value $-1.476/1837$ was used for the nuclear gyromagnetic ratio[3] of Na^{23}. Since the term $g_i\mu_0H/h$ contributes only slightly to the value of $\nu/\Delta\nu$ an uncertainty of 0.5 percent in g_i does not affect the precision of the results. It may be seen from Fig. 1 that the frequencies of certain lines, notably that of the line $(1,0)\leftrightarrow(1,1)$, are practically independent of the field in an experimentally convenient range of field. $\Delta\nu$ may then be determined from the frequency of such a line and an approximate knowledge of the field by use of the expressions in Table I. On the other hand the lines $(2,-2)\leftrightarrow(1,-1)$ and $(2,2)\leftrightarrow(2,1)$ show considerable dependence on field, even in fields as high as 5000 gauss. If the frequencies of these two lines are observed at some fixed field, the value of x may be determined by use of the proper expressions in Table I. In this way it was found that the x value appropriate to the lines listed in this table is 7.724. The observed frequencies of all the lines are given in the third column. The corresponding values of $\nu/\Delta\nu$ are tabulated in the fourth column and the value of $\Delta\nu$ in the fifth.

It has been pointed out in an earlier paper[1] that the $\Delta\nu$ of an atom in a $^2S_{\frac{1}{2}}$ state with nuclear spin $\frac{3}{2}$ may also be determined by adding the frequency of the line $(2,2)\leftrightarrow(2,1)$, that of the line $(2,-2)\leftrightarrow(1,-1)$, the mean frequency of the lines $(1,0)\leftrightarrow(1,-1)$ and $(2,0)\leftrightarrow(2,-1)$, and the mean frequency of the lines $(1,1)\leftrightarrow(1,0)$ and $(2,1)\leftrightarrow(2,0)$. Such a determination is inde-

[2] M. Fox and I. I. Rabi, Phys. Rev. **48**, 746 (1935).

[3] P. Kusch, S. Millman and I. I. Rabi, Phys. Rev. **55**, 1176 (1939).

TABLE I. *The lines in the spectrum of* Na^{23} *resulting from the transitions* $\Delta m_i=\pm1$, $\Delta m_J=0$. *All lines were observed at a value of the field parameter, x, of 7.724. This corresponds to a field of 4886 gauss.*

TRANSITIONS	EXPRESSIONS FOR FREQUENCIES	OBS. (ν MC)	$\nu/\Delta\nu$	$\Delta\nu$ (MC)	ν' (MC)
$(2,2)\leftrightarrow(2,1)$	$\frac{\Delta\nu}{2}[(1+x)-(1+x+x^2)^{\frac{1}{2}}]+\frac{g_i\mu_0H}{h}$	397.16	0.224167	1771.74	397.16
$(2,1)\leftrightarrow(2,0)$	$\frac{\Delta\nu}{2}[(1+x+x^2)^{\frac{1}{2}}-(1+x^2)^{\frac{1}{2}}]+\frac{g_i\mu_0H}{h}$	420.62	0.237406	1771.80	
$(1,1)\leftrightarrow(1,0)$	$\frac{\Delta\nu}{2}[(1+x+x^2)^{\frac{1}{2}}-(1+x^2)^{\frac{1}{2}}]-\frac{g_i\mu_0H}{h}$	431.60	0.243600	1771.70	426.11
$(2,0)\leftrightarrow(2,-1)$	$\frac{\Delta\nu}{2}[(1+x^2)^{\frac{1}{2}}-(1-x+x^2)^{\frac{1}{2}}]+\frac{g_i\mu_0H}{h}$	448.72	0.253274	1771.74	
$(1,0)\leftrightarrow(1,-1)$	$\frac{\Delta\nu}{2}[(1+x^2)^{\frac{1}{2}}-(1-x+x^2)^{\frac{1}{2}}]-\frac{g_i\mu_0H}{h}$	459.74	0.259468	1771.74	454.23
$(2,-2)\leftrightarrow(1,-1)$	$\frac{\Delta\nu}{2}[(1-x+x^2)^{\frac{1}{2}}+(1-x)]-\frac{g_i\mu_0H}{h}$	494.24	0.278960	1771.74	494.24
				1771.74	1771.74

pendent of any assumption as to the value of the magnetic field or the nuclear magnetic moment. It is only necessary that all lines be observed at the same magnetic field. Column 6 in Table I lists the appropriate frequencies to be used in the summation and the resulting sum. From a number of sets of observations similar to that presented in the table, the $\Delta\nu$ of the ground state of Na^{23} is found to be $(1771.75\pm0.07)\times10^6$ sec.$^{-1}$ or 0.059103 cm^{-1} if we take as the velocity of light the value 2.99776×10^{10} cm/sec.

The frequency difference between the two lines $(1,0)\leftrightarrow(1,-1)$ and $(2,0)\leftrightarrow(2,-1)$ and between the two lines $(1,1)\leftrightarrow(1,0)$ and $(2,1)\leftrightarrow(2,0)$ is given by the expression $2g_i\mu_0H/h$ or by the equivalent expression $(2g_ix\Delta\nu)/(g_J-g_i)$. The value of x at which the observations in Table I were made is 7.724. The mean value of the frequency difference is 11.00 megacycles per second. This leads to a value of $-1.477/1837$ as the g_i of Na^{23}. The excellent agreement with the value of $-1.476/1837$ found by the molecular beam magnetic resonance method is fortuitous since the frequency difference of 11.00 megacycles cannot be determined with a precision better than about 0.4 percent in the present case.

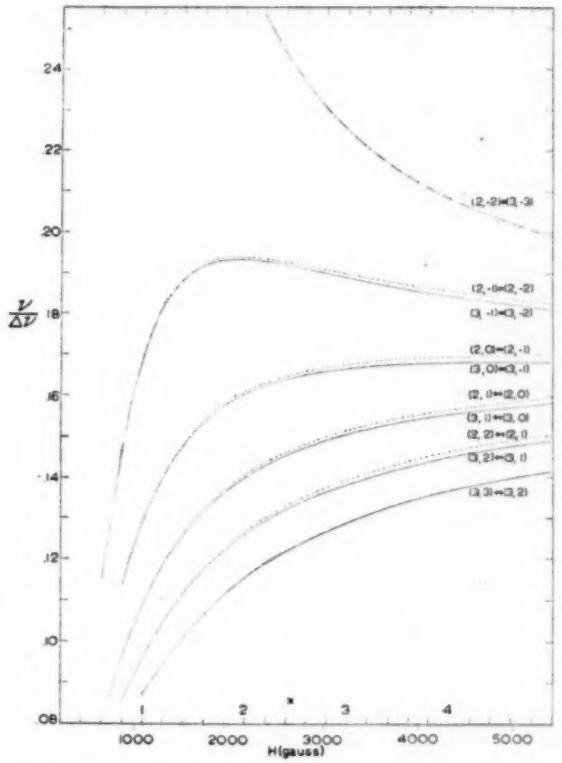

FIG. 2. The field dependence of the frequencies of the lines of Rb^{85} associated with the transitions $\Delta m_i=\pm1$, $\Delta m_J=0$.

Rb^{85}

The $\Delta\nu$ of the ground state of this atom is[4] about 0.1 cm^{-1} or 3000×10^6 sec.$^{-1}$. Since the nuclear spin is 5/2 the frequency required to induce the transitions $\Delta m_i=\pm1$, $\Delta m_J=0$, in strong magnetic fields will be in the neighborhood of 500 megacycles per second, again in a very convenient frequency range. Figure 2 shows graphically the expected transition frequencies, in units of $\Delta\nu$, as a function of the field parameter x. The number of lines to be expected in this region of frequencies is ten. Eight of the lines comprise four doublets; one member of a given doublet arises for transitions between magnetic levels in the state $F=3$ and the other from transitions between the same magnetic levels in the state $F=2$. Since the magnetic levels $m=\pm3$ occur only for $F=3$, lines arising from transitions to these m levels are single. The first column in Table II lists the transitions in the usual notation. The second column lists the expressions for the frequencies associated with the transitions. As in the case of Na^{23} these expressions are obtained from the expressions 9–12 of the previous paper.[1] The observed frequencies of the lines, ν, are tabulated in the third column of the table. To simplify the calculation we have used the mean frequencies of the double lines for the calculation of $\Delta\nu$; this procedure eliminates the use of the term in g_i. The mean frequencies are listed in the fourth column. It may be seen by reference to Fig. 2 that the frequencies of some of the lines vary quite rapidly in the region of field at which we have made our observations, about 5000 gauss. The lines recorded in Table I were not all observed at the same magnetic field. The drift in field occurred because of the rather long time required to shift the frequency of the oscillator from one range to another. The relative values of the field at which lines were observed could be determined to within one gauss, but the absolute field values were not known to better than ten gauss. To find this absolute value of the field we have calculated several sets of values of $\Delta\nu$, each

[4] S. Millman and M. Fox, Phys. Rev. **50**, 220 (1936); H. Kopfermann, Zeits. f. Physik **83**, 417 (1933).

TABLE II. *The lines in the spectrum of* Rb^{85} *resulting from the transitions* $\Delta m_i = \pm 1$, $\Delta m_J = 0$.

TRANSITIONS	EXPRESSIONS FOR FREQUENCIES	ν (MC)	ν' (MC)	H (GAUSS)	$\nu/\Delta\nu$	$\Delta\nu$ (MC)
(3, 3) ↔ (3, 2)	$\frac{\Delta\nu}{2}[(1+x)-(1+\frac{4}{3}x+x^2)^{\frac{1}{2}}]+\frac{g_i\mu_0 H}{h}$	426.53	426.53	5163	0.140509	3035.6
(3, 2) ↔ (3, 1)	$\frac{\Delta\nu}{2}[(1+\frac{4}{3}x+x^2)^{\frac{1}{2}}-(1+\frac{2}{3}x+x^2)^{\frac{1}{2}}]+\frac{g_i\mu_0 H}{h}$	449.90	452.03	5170	0.148913	3035.6
(2, 2) ↔ (2, 1)	$\frac{\Delta\nu}{2}[(1+\frac{4}{3}x+x^2)^{\frac{1}{2}}-(1+\frac{2}{3}x+x^2)^{\frac{1}{2}}]-\frac{g_i\mu_0 H}{h}$	454.15				
(3, 1) ↔ (3, 0)	$\frac{\Delta\nu}{2}[(1+\frac{2}{3}x+x^2)^{\frac{1}{2}}-(1+x^2)^{\frac{1}{2}}]+\frac{g_i\mu_0 H}{h}$	477.55	479.67	5178	0.158014	3035.6
(2, 1) ↔ (2, 0)	$\frac{\Delta\nu}{2}[(1+\frac{2}{3}x+x^2)^{\frac{1}{2}}-(1+x^2)^{\frac{1}{2}}]-\frac{g_i\mu_0 H}{h}$	481.79				
(3, 0) ↔ (3, −1)	$\frac{\Delta\nu}{2}[(1+x^2)^{\frac{1}{2}}-(1-\frac{2}{3}x+x^2)^{\frac{1}{2}}]+\frac{g_i\mu_0 H}{h}$	510.89	513.01	5182	0.168982	3035.9
(2, 0) ↔ (2, −1)	$\frac{\Delta\nu}{2}[(1+x^2)^{\frac{1}{2}}-(1-\frac{2}{3}x+x^2)^{\frac{1}{2}}]-\frac{g_i\mu_0 H}{h}$	515.13				
(3, −1) ↔ (3, −2)	$\frac{\Delta\nu}{2}[(1-\frac{2}{3}x+x^2)^{\frac{1}{2}}-(1-\frac{4}{3}x+x^2)^{\frac{1}{2}}]+\frac{g_i\mu_0 H}{h}$	552.09	554.23	5192	0.182574	3035.6
(2, −1) ↔ (2, −2)	$\frac{\Delta\nu}{2}[(1-\frac{2}{3}x+x^2)^{\frac{1}{2}}-(1-\frac{4}{3}x+x^2)^{\frac{1}{2}}]-\frac{g_i\mu_0 H}{h}$	556.37				
(3, −3) ↔ (2, −2)	$\frac{\Delta\nu}{2}[(1-\frac{4}{3}x+x^2)^{\frac{1}{2}}+(1-x)]-\frac{g_i\mu_0 H}{h}$	609.44	609.44	5195	0.200766	3035.6
						3035.7

set corresponding to an assumed value of the absolute field. The relative field values at which the lines were observed were kept unaltered. We have chosen as the correct absolute field that which corresponds to the set of values of $\Delta\nu$ of best internal consistency. The apparent value of $\Delta\nu$ was altered by only about 0.25×10^6 sec.$^{-1}$ when the absolute field values used in the calculation were changed by ten gauss. The values of the field which were finally chosen are given in the fifth column of the table, the appropriate values of $\nu/\Delta\nu$ in the sixth column and the values of the calculated $\Delta\nu$ in the last column. We have used in these calculations the value $-0.536/1837$ as the gyromagnetic ratio[5] of Rb^{85}.

It is also possible to find the value of $\Delta\nu$ by application of the summation method used for Na^{23}, even though the field is not quite constant throughout the series of observations. The observed frequencies may be corrected to a common field by use of the known slopes of the curves in Fig. 2 and an accurate knowledge of the relative fields if the approximate value of the field is known. In the present case the difference between the apparent and the corrected sum is only 0.75×10^6 sec.$^{-1}$. A considerable error in the correction affects the value of $\Delta\nu$ but slightly. The value of $\Delta\nu$ so calculated is 3035.7×10^6 sec.$^{-1}$. Our measurements yield the value $(3035.7\pm0.2)\times10^6$ sec.$^{-1}$ or 0.10127 cm^{-1} as the $\Delta\nu$ of Rb^{85}.

From the separations of the components of the double lines we have calculated the g_i as $-0.539/1837$. This value is to be compared to the value of $-0.536/1837$ obtained with the molecular beam magnetic resonance method. The frequency difference between the two lines which comprise a doublet cannot be determined to better than 0.7 percent, and hence the present value may be in error by this amount. The older value was not known to better than 0.8 percent. The agreement between the two values is therefore satisfactory.

Rb^{87}

The nuclear spin[4] of Rb^{87} is $\frac{3}{2}$ and the $\Delta\nu$ is about 0.23 cm^{-1} or about 6900×10^6 sec.$^{-1}$. The transitions $\Delta m_i = \pm1$, $\Delta m_J = 0$ could not, there-

[5] P. Kusch and S. Millman, Phys. Rev. **56**, 527 (1939).

fore, be observed at magnetic fields where the line frequencies do not vary rapidly with field, since the reduction factor of $(2i+1)$ is insufficient to bring these frequencies within the range conveniently obtainable in this laboratory. In order to measure the $\Delta\nu$ of Rb^{87} with the use of available radiofrequencies we have observed transitions at intermediate magnetic fields. These transitions can be characterized by the selection rules $\Delta F=0$, $\Delta m=\pm 1$. It must not be inferred, however, that F and m are good quantum numbers; the applied magnetic field in the case under consideration is of the same order of magnitude as the field at the valence electron arising from the nuclear magnetic moment. The symbols F and m merely refer to the weak field quantum numbers of the states from which those under consideration are derived. These symbols are used in the same sense in the expressions which give a complete description of the energy levels of an alkali atom in the ground state as a function of the magnetic field. In Fig. 3 are plotted the frequencies, in units of $\Delta\nu$, of the lines to be expected in the field region chosen for this experiment. Each of these lines was observed. It will be noted that the line frequencies vary rapidly with field and that the rate of variation is different for the various lines and depends on the field. For example, the slope of the curve representing the $(2, 2)\leftrightarrow(2, 1)$ transition decreases with field while the slope of the $(2, -1)\leftrightarrow(2, -2)$ curve increases with field. This difference in behavior is clearly indicated graphically in Fig. 3 by the dashed curve which represents the ratio $(B-A)/A$, where B denotes the frequency of the line $(2, -1)\leftrightarrow(2, -2)$ and A that of the line $(2, 2)\leftrightarrow(2, 1)$. Hence if both A and B are determined at the same field the value of x appropriate to the observed frequencies may be determined. A knowledge of x, of course, enables one to determine $\Delta\nu$. Any pair of lines in the spectrum might be used for such a determination of $\Delta\nu$; the lines here chosen are most satisfactory because their frequencies differ most widely in their dependence on field. In Table III are listed the observed frequencies of the lines B and A, the ratio $(B-A)/A$, the value of x obtained from this ratio, the values of $\nu/\Delta\nu$ appropriate to this value of x for both lines and finally the $\Delta\nu$ calculated from $\nu/\Delta\nu$ and the observed frequencies. We have used the value[5] $-1.820/1837$ as the g_i of Rb^{87}. The equality of the values of $\Delta\nu$ as calculated from two lines observed at the same magnetic field merely verifies the accuracy of the calculations. From the observations listed in Table III and from other similar observations we find for the $\Delta\nu$ of Rb^{87} the value $(6833.8\pm 1.5)\times 10^6$ sec.$^{-1}$.

TABLE III. *The determination of the $\Delta\nu$ of Rb^{87} from the frequencies of the lines $(2, 2)\leftrightarrow(2, 1)$ and $(2, -1)\leftrightarrow(2, -2)$. A represents the frequency of the first of these lines and B that of the second.*

ν (obs.) (Megacycles)							
B	A	$(B-A)/A$	x	$\nu/\Delta\nu$ (B)	$\nu/\Delta\nu$ (A)	$\Delta\nu$ (mc) (B)	$\Delta\nu$ (mc) (A)
432.27	313.45	0.37907	0.21511	0.063288	0.045891	6830.2	6830.3
650.67	415.16	0.56728	0.30247	0.095218	0.060753	6833.5	6833.6
656.63	417.64	0.57224	0.30465	0.096066	0.061102	6835.2	6835.1
						6833.0	

We may also determine the $\Delta\nu$ of Rb^{87} by making use of the known value of the $\Delta\nu$ of Rb^{85}. For magnetic fields in the neighborhood of 750 gauss the frequency of the line $(3, -2)\leftrightarrow(3, -3)$ of Rb^{85} lies close to that of the line $(2, -1)\leftrightarrow(2, -2)$

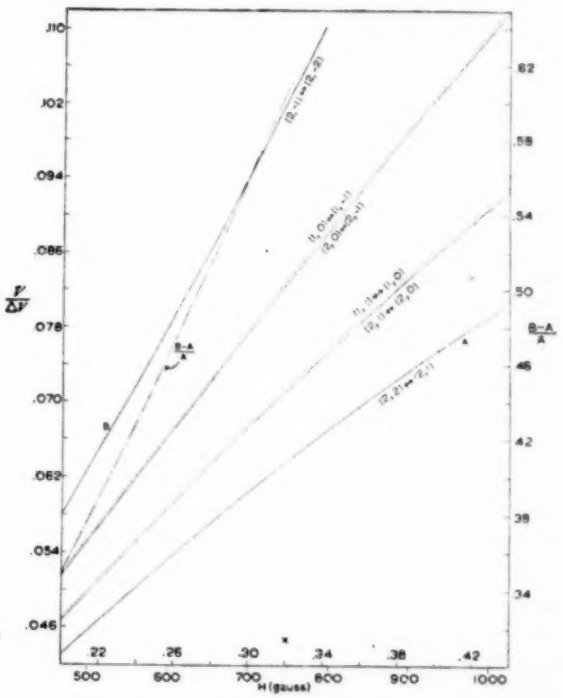

FIG. 3. The field dependence of the frequencies of the lines of Rb^{87} for which $\Delta F=0$, $\Delta m=\pm 1$ in intermediate magnetic fields.

of Rb^{87}. The frequency of the Rb^{85} line can be used to determine the field, and this together with the frequency of the Rb^{87} line can, in turn, be used for the determination of the $\Delta\nu$ of Rb^{87}. It is not essential in this determination that the frequencies of the two lines lie in the same range; in practice, however, it is convenient to measure the frequencies of lines which are close together. By use of the Eqs. (9)–(12) of the previous paper,[1] the expression,

$$\Delta\nu=\frac{4(\nu-g_i k)(g_J k-\nu)}{4\nu-(g_J+3g_i)k}, \qquad (2)$$

may be written for the calculation of $\Delta\nu$ from the observed frequency, ν, of the line $(2,-1)\leftrightarrow(2,-2)$ of Rb^{87} and the quantity k. The value of g_i is known[5] to be $-1.820/1837$ and that of g_J is 2. The quantity k is determined by use of the relationship,

$$k=\frac{\mu_0 H}{h}=\frac{(\Delta\nu)_{85}}{(g_J-g_i)_{85}}x_{85}=1517.63x_{85}, \qquad (3)$$

where x_{85} may be found from a knowledge of the ratio $\nu/\Delta\nu$ for the line $(3,-2)\leftrightarrow(3,-3)$ of Rb^{85}.

TABLE IV. *The determination of the $\Delta\nu$ of Rb^{87} from the observation of the frequencies of the line $(3,-2)\leftrightarrow(3,-3)$ of Rb^{85} and of the line $(2,-1)\leftrightarrow(2,-2)$ of Rb^{87}.*

ν (obs.) (mc)					
Rb^{85}	Rb^{87}	$\nu/\Delta\nu$ Rb^{85}	x_{85}	k	$\Delta\nu$ (mc) Rb^{87}
659.73	660.75	0.217324	0.689153	1045.88	6833.2
653.95	656.33	0.215420	0.685447	1040.25	6834.6
654.25	656.63	0.215519	0.685640	1040.55	6831.5
646.59	650.67	0.212995	0.680699	1033.05	6837.0
659.30	660.38	0.217182	0.688877	1045.46	6835.0
657.74	659.24	0.216668	0.687879	1043.95	6833.2
669.71	668.26	0.220611	0.695510	1055.53	6835.0
					6834.2

In Table IV are listed the observed frequencies of the two lines, the value of $\nu/\Delta\nu$ of Rb^{85}, x_{85}, the values of k and the calculated values of the $\Delta\nu$ of Rb^{87}. The precision of the determination is affected not only by the precision of the frequency measurements, which is best estimated from the internal consistency of the results, but also by the precision with which the $\Delta\nu$ of Rb^{85} is known. An error of 0.01 percent in the latter quantity will introduce an error of about 0.02

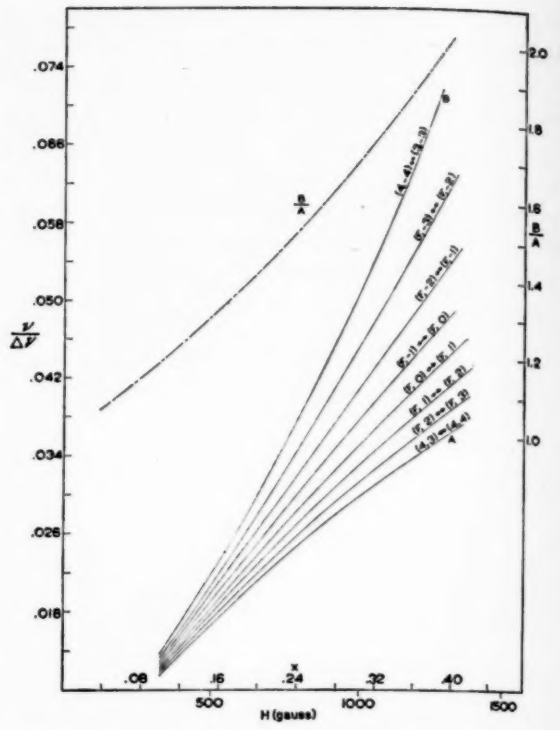

FIG. 4. The field dependence of the frequencies of the lines of Cs^{133} for which $\Delta F=0$, $\Delta m=\pm1$ in intermediate magnetic fields. All lines except those arising from the transitions $(F,4)\leftrightarrow(F,3)$ and $(F,-4)\leftrightarrow(F,-3)$ are double; to simplify the plotting we have used the mean frequency of the two lines which constitute a given doublet.

percent in the $\Delta\nu$ of Rb^{87}. We find with this method the value $(6834.2\pm1.2)\times10^6$ sec.$^{-1}$ for the $\Delta\nu$ of Rb^{87}. This result is in excellent agreement with that determined from observations of Rb^{87} lines alone. The weighted mean of the results of the two methods yields for the $\Delta\nu$ of Rb^{87} the value $(6834.1\pm1.0)\times10^6$ sec.$^{-1}$ or 0.22797 cm^{-1}.

The value of g_i cannot be accurately determined from our present data. This arises from the fact that the observations are made at rather low values of the magnetic field. In consequence the term, $2g_i\mu_0 H$, which gives the separation of the components of the double lines, is small and cannot be determined with great precision since this frequency must be measured as the difference between two very large frequencies. We obtain as the g_i of Rb^{87} the value $-1.79/1837$, in satisfactory agreement with the much more precise value of $-1.820/1837$ obtained by the molecular beam magnetic resonance method.[5]

The ratio $(\Delta\nu)_{87}/(\Delta\nu)_{85}$ should yield the ratio of

the nuclear magnetic moments of the two isotopes of rubidium on the assumption that h.f.s. is due solely to the electromagnetic interaction between nuclear and electronic spins. We obtain for the ratio μ_{87}/μ_{85} the value 2.0261 ± 0.0003. This is to be compared to the value 2.026 ± 0.004 determined by Millman and Fox[4] by the atomic beam method of zero moments. The ratio of moments as measured directly by the molecular beam magnetic resonance method[5] is 2.038 ± 0.010. The discrepancy of 0.6 percent lies somewhat outside the limits of experimental error, but in view of the difficulties encountered in the direct measurement, it does not give conclusive indication of the existence of a non-electromagnetic interaction between nucleus and electron.

TABLE V. *The determination of the $\Delta\nu$ of Cs^{133} from the frequencies of the lines $(4, 4) \leftrightarrow (4, 3)$ and $(4, -4) \leftrightarrow (4, -3)$. A represents the frequency of the first of these lines and B that of the second.*

ν (obs.) (Mega-cycles)							
B	A	B/A	x	$\nu/\Delta\nu$ (B)	$\nu/\Delta\nu$ (A)	$\Delta\nu$ (mc) (B)	$\Delta\nu$ (mc) (A)
645.62	327.32	1.97244	0.385337	0.070243	0.035612	9191.2	9191.3
650.52	328.62	1.97955	0.387365	0.070768	0.035749	9192.3	9192.4
654.17	329.54	1.98510	0.388945	0.071178	0.035856	9190.6	9190.7
						9191.4	

Cs^{133}

The nuclear spin[6] of Cs^{133} is 7/2. The $\Delta\nu$[4,7] of its ground state is 0.31 cm^{-1} or about 9300×10^6 $sec.^{-1}$. This large $\Delta\nu$ can be determined by the same procedure as the first of the two employed in the determination of the $\Delta\nu$ of Rb^{87}. Figure 4 indicates the field dependence of the frequencies of the lines for which $\Delta F=0$, $\Delta m=\pm1$, in the region of field chosen for this experiment. We have observed the frequency of the line $(4, 4) \leftrightarrow (4, 3)$, which we shall call A, and that of the line $(4, -4) \leftrightarrow (4, -3)$, which we shall call B, at the same magnetic field and have determined the value of the parameter x from the ratio of the frequencies of the two lines. In Table V are tabulated the observed frequencies of the two lines, the observed value of B/A, the corresponding value of x, the value of $\nu/\Delta\nu$ for each of the two observed lines and the calculated value of $\Delta\nu$. We have used the value[3] $-0.730/1837$ as the g_i of Cs^{133}. For the value of the field corresponding to the third series of observations listed in the table we have also observed the frequencies of the remaining lines in the spectrum. In the determination of $\Delta\nu$ from the observed frequencies of these lines we have used the value of x determined by the values of B and A. We obtain as the $\Delta\nu$ of Cs^{133} the value $(9191.4\pm0.9)\times10^6$ $sec.^{-1}$ or 0.30661 cm^{-1}.

From the splitting of the double lines we find the g_i of Cs^{133} to be $-0.734/1837$. In view of the poor precision involved in the measurement of the small frequency, $2g_i\mu_0H$, which is obtained as a difference between two large frequencies, the agreement between this result and that of $-0.730/1837$ obtained by the molecular beam magnetic resonance method[3] is to be considered as fortuitous.

This research has been aided by a grant from the Research Corporation.

[6] V. W. Cohen, Phys. Rev. **46**, 707 (1934).
[7] L. P. Granath and R. K. Stranathan, Phys. Rev. **48**, 725 (1935).

The Characteristics and Function of Anode Spots in Glow Discharges*

SIDNEY M. RUBENS† AND J. E. HENDERSON
University of Washington, Seattle, Washington

(Received January 5, 1940)

Brilliant hemispherical anode spots appeared on a small disk or spherical anode mounted at the center of a large copper spherical discharge chamber which served as cathode during an investigation of nitrogen glows. Such an arrangement permits large anode current densities with a normal cathode fall in potential. At a critical current density at the anode, the spots form and arrange themselves in beautiful geometrical patterns. In nitrogen the spots appeared only in the pressure range of 0.15 to 1.50 mm Hg. Space potentials, electron temperatures, electron and ion densities determined by a Langmuir probe analysis revealed that the spots are regions of intense ionization, and that the region just above them contains a net positive space charge. The potential fall through a spot is nearly equal to the first ionization potential of nitrogen. A method was developed for growing anode spots at will on a small disk probe mounted flush with the anode surface but insulated from it. The current-voltage characteristics for this probe, or auxiliary anode, exhibit peaks which account for the stability and size of the spots. An investigation of the current-voltage relationships of the entire discharge showed that anode spots occur chiefly in the region in which the current increases with small change in voltage. At sufficiently great current densities the spots move about because of the magnetic field accompanying the discharge. The function of the spots is to furnish the positive ions necessary for the maintenance of a stable discharge in the plasma extending from anode to negative glow and to aid in the collection of electrons at the anode. A mechanism for the formation of the spots as a combined space charge and bipolar current phenomenon is proposed.

INTRODUCTION

IN the course of some investigations of the general characteristics of glow discharges maintained between concentric spherical electrodes, an unexpected phenomenon appeared when the inner electrode was small and was made the anode. In a limited pressure range, and for the relatively large current densities available near the anode in this type of discharge chamber, the anode surface, instead of being coated with a uniform glow, became overlaid with a number of brilliant hemispherical spots. At times these were arranged in beautiful geometrical patterns of remarkable stability, while at other times they were in rapid motion. Their velocity could be accelerated or retarded by the application of an external magnetic field.

The appearance of these anode spots in a nitrogen glow at various pressures and current densities is shown in Fig. 1. In this gas the spots consist of two bright layers. The inner portion of the spots is salmon pink, while the outer layer is of a yellow-orange color. A faint luminous membrane of glow covers the region between the spots. A thin dark space exists between the spot and the anode itself. So long as the nitrogen was fairly pure, the spots were all of the same size at a given pressure. If the discharge was contaminated with air, the spots were always fewer in number, and not all of uniform size.

The pattern formed by the spots depends on the shape and size of the anode. The number of spots present increases, in general, with the current and pressure, but is influenced somewhat by the surface conditions of the anode. The size of individual spots increases as the gas pressure is reduced.

Although the observation of this phenomenon at first appeared to be a new discovery, a search of the literature revealed that it had been reported previously by other investigators. Apparently anode spots were first described by Lehmann[1] who found their occurrence in an air glow discharge, and were later reported by other workers[2–5] for several other gases. Thomas and Duffendack found the spots present in pure H_2, N_2, CO, and mixtures of these diatomic gases with various noble gases, but could not produce

* Presented at the meeting of the American Physical Society, San Diego, California, June 22–24, 1938; Palo Alto, California, June 28–July 1, 1939.

† Now at the University of California at Los Angeles.

[1] O. Lehmann, Ann. d. Physik **7**, 1 (1902).
[2] G. M. J. MacKaye, Phys. Rev. **15**, 309 (1920).
[3] C. H. Thomas and O. S. Duffendack, Phys. Rev. **35**, 72 (1930).
[4] E. Kiessling, Zeits. f. Physik **96**, 365 (1935).
[5] A. Guntherschultze, W. Bär and H. Betz, Zeits. f. Physik **109**, 293 (1938).

them either in O_2 or in pure noble gases in a discharge tube which had been carefully cleaned and outgassed.

In all these investigations only those characteristics of anode spots which could be observed visually were studied. Specifically, the influence of the nature of the gas and the electrodes, current density, pressure, and duration of the discharge on the pattern, number, size, motion and permanence of the spots were investigated. No attempt was made either to correlate the occurrence of the spots with the general circuit characteristics of the discharge or to study the electrical properties of the individual spots.

The researches described in the present paper were performed in order to acquire quantitative information about the physical conditions associated with anode spots which might possibly lead to a better understanding of the processes which occur in their formation as well as their function in the maintenance of a stable discharge.

Method of Investigation

The Langmuir dynamic method of probe analysis permits the determination of the space potentials, electron temperatures, and densities of electrons and positive ions in those regions of a discharge known as a plasma.[3–8] Since a map of these quantities provides the most information at present obtainable about the electrical structure of gaseous discharges, it was determined to make such an analysis of anode spots.

A preliminary attempt to investigate an anode spot occurring at the edge of a disk electrode in this way resulted in failure as the spot was repelled by the probe. A method was developed for growing and anchoring a spot on a small auxiliary electrode mounted flush with the surface of the anode but insulated from it. This permitted a probe analysis of the region surrounding a spot so formed and anchored.

A study was made of the current-voltage characteristics of the auxiliary electrode during the growth of spots upon it. The information so obtained provides a possible explanation of the remarkable stability of the anode spots and their function in maintaining a stable discharge.

Finally, the external circuit characteristics of nitrogen glows maintained in the spherical discharge chamber were studied. This was done to reveal any relationship existing between these circuit characteristics and the occurrence of anode spots.

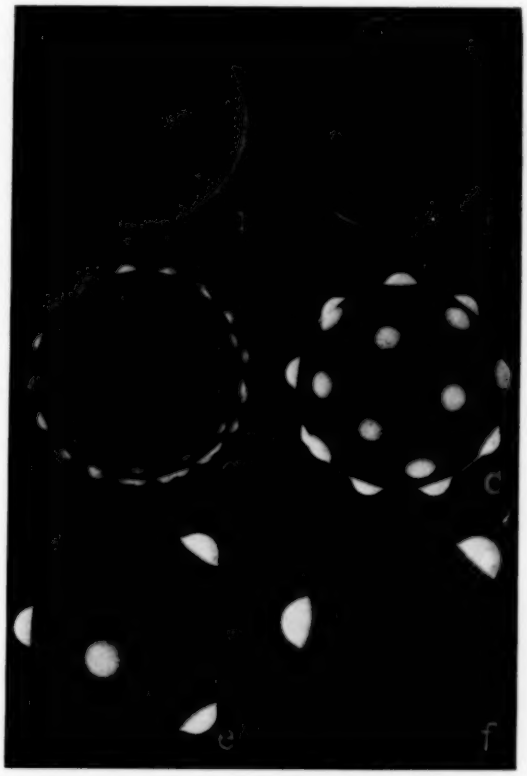

Fig. 1. Anode spots on a spherical anode. (a) Pressure 1.25 mm Hg, current 420 ma; (b) 1.20 mm Hg, 420 ma; (c) 0.79 mm Hg, 425 ma; (d) 0.41 mm Hg, 465 ma; (e) 0.36 mm Hg, 390 ma; (f) 0.26 mm Hg, 400 ma.

Apparatus

The discharge chamber in which these investigations were made was primarily designed for the purpose of studying glow discharges between spherical electrodes. It was admirably suited to these researches, since it provided a very large cathode area (708 sq. cm) which permitted the attainment of very large values of drift current for a normal cathode fall of potential. This permitted far greater current densities at the anode than were attainable in former investigations. The parasitic charging of insulating

[6] I. Langmuir and H. Mott-Smith, Jr., Gen. Elec. Rev. **27**, 449 (1924).
[7] H. Mott-Smith, Jr., and I. Langmuir, Phys. Rev. **28**, 727 (1926).
[8] I. Langmuir and H. Mott-Smith, Jr., Gen. Elec. Rev. **27**, 767 (1924)

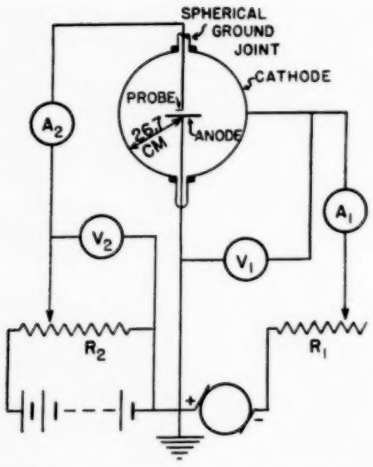

FIG. 2. Discharge chamber and circuit diagram.

surfaces due to the diffusion of ions and electrons to them was practically eliminated by the nature of the apparatus itself. This feature made the discharge currents which are ordinarily considered to be unsteady, very steady, and contributed greatly to the reliability and success of the experiments.

The discharge chamber and the circuit are shown schematically in Fig. 2. The chamber consists of two spun flanged copper hemispheres clamped together between steel rings with "*C*" clamps. A ring of fuse wire, clamped between the flanges, effected an airtight seal. The anode which was a copper sphere, 5.1 cm in diameter, or a circular disk mounted concentrically with the outer sphere was supported by a rod or tube of copper insulated from the discharge with a sheath of Pyrex tubing.

The circuit is shown diagrammatically in this figure. The potential difference for maintaining the discharge was supplied by a 1500-volt d.c. generator. The series ballast resistance, R_1, a rheostat having a maximum value of 21,400 ohms, was always kept in the circuit to assure stability.

The probe used to study the spots was a cylinder of tungsten wire 0.5 cm long, and 0.013 cm in diameter. This probe was fastened with a braid of fine copper wire to a windlass which was turned through a conical ground glass joint at the top of the probe tower. The probe tower was mounted on the spherical or "ball and socket" ground glass joint which permitted an angular displacement from the axis of the probe tower as well as a rotation of the probe about it.[9] With this arrangement any of the region above the anode or to the side of it contained within the frustrum of a limiting cone could be explored with great facility and precision of adjustment. This probe was used to investigate the plasma which surrounds the spots.

These experiments were performed in fairly pure, dry nitrogen which was used for several reasons. Brilliant spots of great stability formed in it quite readily in a very convenient pressure range and with good reproducibility of results. If air should leak into the chamber or be released from the walls the purity is not changed greatly since the oxygen cleans up and combines with the cathode surface after a few hours of running. The gas was obtained from a tank of commercially pure nitrogen and was slowly passed through a liquid-oxygen trap into a reservoir which had previously been evacuated with a 2-stage mercury diffusion pump and flushed several times. It was released from this into the discharge chamber as needed through another trap which was kept at all times in a slush of dry ice and acetone.

ANODE SPOTS ON A SPHERICAL ELECTRODE

When the anode was a copper sphere, it was coated with a uniform glow at all pressures exceeding 1.50 mm Hg and for drift current values not greater than 500 ma. If the pressure was increased or the current decreased so that the anode was not saturated with glow, the luminous region adjoining the anode grew thicker and more diffuse. For nitrogen discharges, anode spots never occurred at pressures exceeding 1.50 mm Hg for the current densities available.

At a pressure of 1.25 mm Hg and a drift current of 420 ma some spots appeared on the part of the anode facing the cathode glow as shown in Fig. 1a. At this pressure, if the current is increased, the spots move about so rapidly that the glow appears to be uniform once more. With the current constant and the pressure reduced to 1.20 mm Hg, some of the spots had an oscillatory motion, while others remained at rest as shown in Fig. 1b. As the pressure was further reduced the

[9] S. M. Rubens and J. E. Henderson, Rev. Sci. Inst. **10**, 49 (1939).

spots increased in size and diminished in number until at 0.15 mm Hg only one large spot was present. These effects are illustrated in Fig. 1c, d, e, and f. Since the spots were more or less uniformly distributed over the surface of the sphere, somewhat more than half the total number of spots are visible in the photographs. The single spot occurring at 0.15 mm Hg was not in a convenient position for photography. At a given pressure, the spacing of the spots changes only slightly with the current regardless of the number present.

On a disk anode, the spots are evenly spaced in a ring about the edge of the disk. Even though the ring is not completely filled, the spacing seems to be fixed for spots of a given size. If both faces of the disk are exposed to the discharge so that there is a ring of spots on each face of the anode, the positions of the spots on one face are between those on the other.

Probe Analysis of an Anchored Spot

When the cylindrical probe was used for exploring the discharge in the vicinity of a spot formed at the edge of the disk anode, data were obtained which were valid for determining the space potentials, electron temperatures and ion densities. However, when it was attempted to penetrate the spot with the probe, the spot was repelled so long as the probe potential was sufficiently negative for it to collect positive ions. In fact, it was not possible to penetrate the surface of a spot with the probe unless its potential was 15 volts or more positive with respect to the anode. If the probe was placed between two spots, and if its potential was raised to a positive value in excess of 15 volts, a spot formed which enveloped the probe wire and rested on the anode. This occurred so long as the probe was not more than a few millimeters distant from the anode regardless of its position relative to the center of the anode. In appearance and behavior a spot so formed resembled those which occurred spontaneously at the edge of the anode. If the probe was moved, this glowing spot moved with it, and when it approached one of the spots already present at the rim of the anode, the spots repelled one another. Evidently there is a repulsive interaction between the positive ion sheath surrounding the probe and the anode spots. Anode spots, therefore, must possess an intrinsically positive charge. All these effects suggested that a spot might be formed and anchored on a small auxiliary disk electrode mounted flush with the anode surface but insulated from it.

The construction of an anode having at its center an auxiliary anode or plane circular probe at the center is shown in Fig. 3. The auxiliary anode is a copper disk 0.60 cm in diameter and is insulated from the anode proper with a thin mica washer. The anode is a circular copper disk 8.00 cm in diameter and 0.275 cm thick.

When the disk probe was made sufficiently positive with respect to the anode, as expected, a spot, which exhibited all the characteristics of those which appeared spontaneously at the edge of the anode, formed on it. When this took place, the current to the plane probe increased discontinuously to several times its former value. In a nitrogen discharge, the potential to which the disk probe had to be raised in order to form a spot ranged from 0 to 10 volts depending on the pressure, total drift current, and the anode surface conditions. The manner in which the probe potential necessary to form the spot depended on the drift current when the pressure was held constant at 0.50 millimeter is shown in Fig. 4. If the current density was sufficiently great the spot occurred when the probe potential was zero, and if the current was further increased, the probe potential had to be made negative in order to remove the spot. This fact shows that for a given pressure of nitrogen a spot forms when the current density reaches a critical value.

Once the probe was made sufficiently positive to form a spot, reversing the potential of the

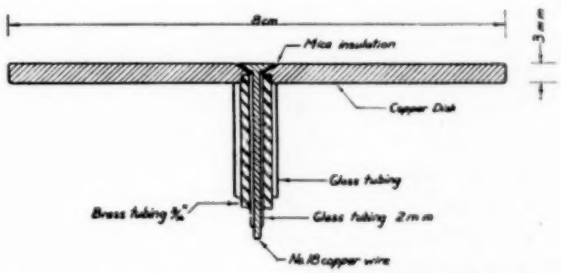

FIG. 3. Diagram showing construction of the anode having at its center an insulated circular disk probe or auxiliary anode upon which anode spots were grown.

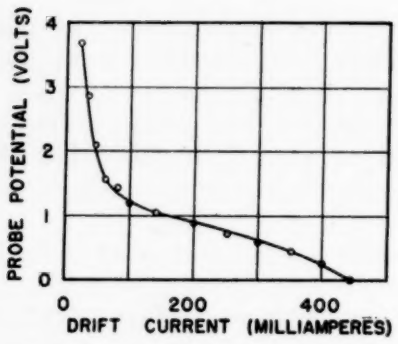

FIG. 4. Curve showing the variation with the drift current of the disk probe potential at which a spot forms in N_2 at 50 mm Hg pressure.

probe did not cause the spot to fade out if the drift current was greater than 100 milliamperes. Instead, the spot moved away from the plane probe as soon as the probe began to collect positive ions and came to rest between the plane probe and the edge of the anode where spots were already present. If the flat probe was again made positive, this spot did not return to the probe, but another spot formed which again moved away upon reversal of the probe potential. At drift currents of 300 ma or more, a continued repetition of this procedure resulted in the formation of a ring of spots between the center and the edge of the anode. As many as six equally spaced spots could be placed in this inner ring. As the spots moved away from the center toward the edge of the anode, they became more brilliant and more sharply defined. Simultaneous with this increase in number of spots an increase in the total drift current occurred.

At a pressure of 0.48 mm Hg and a drift current of 200 ma there was a very symmetrical distribution of spots around the edge of the disk anode. Ten spots rested on the upper surface and ten on the lower one in alternating positions. Under these conditions a spot which had a radius of about 0.5 cm was formed and anchored on the plane probe when its potential was 1.70 volts positive with respect to the anode.

After this spot was formed on the flat disk probe, the movable cylindrical probe was used to explore the region surrounding it. The axis of the probe wire was kept parallel to the anode surface in all the measurements which were along two lines normal to the anode surface, one passing through the center of the flat probe and the other displaced one centimeter from the center. Thus the first line passed through the upper surface of the spot, and the other was about 0.5 cm removed from the base of the spot.

The probe current-voltage characteristics were obtained in the usual manner by plotting the current collected by the probe against the probe potential. These plots were typical of cylindrical probe characteristic curves, and the Langmuir type of analysis permitted the electron temperature, T_e, the space potential, V_s, the positive ion density, N_p, and electron density, N_e, to be computed from them. Logarithmic plots of the electron currents against the probe potential were inear except in the vicinity of the space potential so that a Maxwellian distribution of electron velocities could be assumed.

The results listed in Table I were computed from the probe measurements made directly above the central spot while those in Table II resulted from the measurements taken to one side of it. In Fig. 5 the space potentials and electron temperatures are plotted for these two sets of data. The solid lines are for the measurements directly over the spot, whereas the broken lines represent points which are 1 cm displaced from the center of the anode; that is, to one side of the spot. The diagram below the graph indicates on the same scale the position of the points where the probe measurements were made. The dotted semicircle represents the observed boundary of the spot, and the numbers are the values measured from the anode of the space potential at each point. The shape of the full line curve marked V_s clearly indicates that the spot is a sheath, since the space potential rises rapidly as the boundary of the spot is approached. The

TABLE I. *Results of the probe analysis of the region directly above an anchored anode spot.*

DISTANCE FROM ANODE CM	T_e °K	V_s VOLTS	N_e ELECTRONS/CM³	N_p +IONS/CM³
0.40	26,600	11.2	6.64×10^{7}	7.3×10^{9}
0.53	23,200	12.0	8.90×10^{7}	5.3×10^{9}
0.70	11,600	15.5	1.10×10^{8}	4.0×10^{9}
0.80	11,600	16.0	1.17×10^{8}	4.0×10^{9}
1.00	11,500	17.0	1.52×10^{8}	3.8×10^{9}
1.50	12,100	17.6	1.66×10^{8}	2.8×10^{9}
2.40	12,100	18.0	1.59×10^{8}	2.5×10^{9}
3.50	11,000	18.5	1.46×10^{8}	2.2×10^{9}
4.50	11,100	18.7	1.52×10^{8}	1.7×10^{9}
5.50	10,100	18.8	1.46×10^{8}	1.6×10^{9}

closeness of the two V_s curves at points more than 1 cm from the anode as well as the small slope in this region shows that the potential gradients are low. Tables I and II show that there are about ten times as many positive ions per cm³ as electrons. As the spot is approached from directly above the positive ion density increases quite rapidly while the electron density decreases. On the other hand, the positive ion density decreases as the anode is approached to one side of the spot. These facts imply that the uppermost part of the spot and the region just above it contain a considerable net positive ion space charge. An examination of N_e and T_e in Table I shows that electrons are drawn from the plasma surrounding a spot by the spot itself. Evidently the spot serves as an efficient collector of electrons for the anode.

Further evidence of the existence of positive ion space charge in the outer layer of the spot comes from the examination of the probe characteristic representing measurements taken when the probe is 0.40 cm above the center of the anode. At this distance the probe actually caused severe distortion of the spot when its potential was sufficiently negative so that an extensive positive ion sheath surrounded it. The current-voltage characteristic taken 0.40 cm above the anode together with the one at 1 cm above the anode are shown in Fig. 6. Emeleus and Brown[10] have shown that presence of concave downward curvature in the positive ion branch of the characteristic near the floating potential is always indicative of the presence of positive space charge. This anomaly is clearly exhibited in the curve for 0.4 cm while the one taken at 1.0 cm above the anode is a normal characteristic. Thus,

TABLE II. *Results of the probe analysis of the region 1 cm from the center and to the side of an anchored anode spot.*

DISTANCE FROM ANODE CM	T_e °K	V_s VOLTS	N_e ELECTRONS/CM³	N_p +IONS/CM³
0.50	11,700	16.5	1.15×10^{8}	1.34×10^{9}
1.00	12,100	17.4	1.74×10^{8}	2.08×10^{9}
2.00	10,600	18.7	1.74×10^{8}	2.55×10^{9}
3.00	10,600	18.8	1.58×10^{8}	2.38×10^{9}
4.00	11,600	19.2	1.58×10^{8}	2.19×10^{9}
5.00	10,800	19.3	1.58×10^{8}	1.76×10^{9}

[10] K. G. Emeleus and W. L. Brown. Phil. Mag. **27**, 898 (1936).

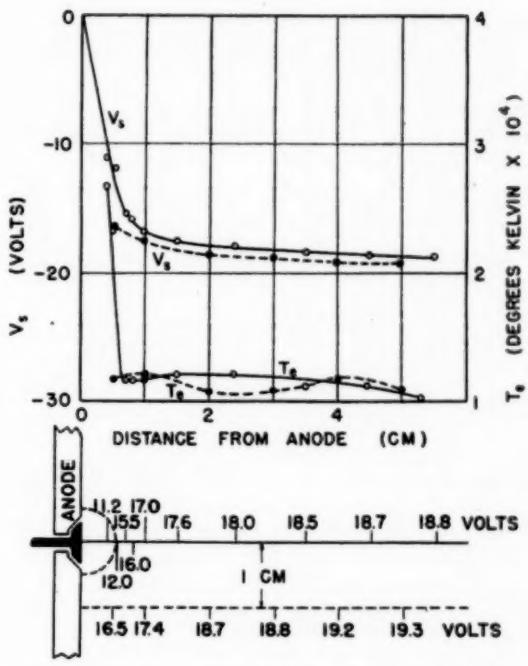

FIG. 5. Space potential and electron temperature distributions directly above and to one side of an anode spot formed on the disk probe or auxiliary anode.

there is a small region near the upper surface of the spot which is densely populated with positive ions. This fact explains two things. First, it shows that the spots are an efficient region of positive ion generation. Second, it provides a plausible explanation for the symmetrical patterns formed by the spots, since the spots represent a net positive charge. The probe measurements indicate that the ionized gas in between the spots is a plasma, where the net space charge and potential gradients are small. Since the motion of the spots was influenced by external magnetic fields, and since the electron temperature increases markedly as the spot is approached, it may be assumed in agreement with Thomas and Duffendack that the spots consist of localized bipolar current beams. Two neighboring spots would then constitute portions of two localized parallel currents, and would attract each other if it were not for their associated positive space charge which repels electrostatically. A balance exists between the electrostatic repulsion of the localized space charge regions and the magnetic forces arising from the interaction of the current beams producing a stable pattern.

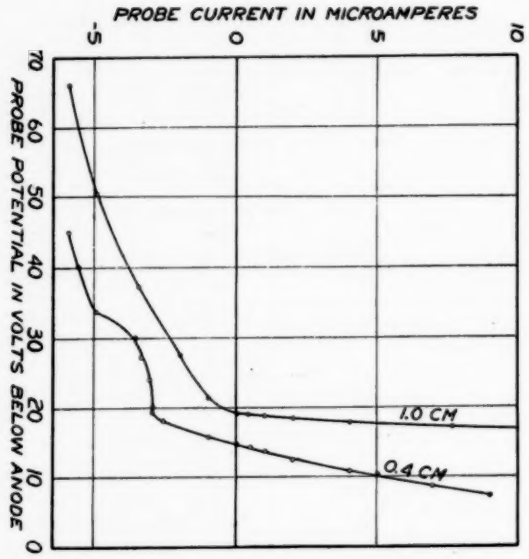

FIG. 6. Normal and anomalous cylindrical probe characteristics showing the effect of positive space charge as observed directly above an anode spot.

From the map of the space potentials, Fig. 5, the anode fall through the spot can be determined. The surface of the spot is an equipotential which is 14.0 volts negative with respect to the anode. The flat probe, on which the spot was anchored during these investigations, was 1.70 volts positive with respect to the anode. Thus the total potential fall through the spot is 15.7 volts. The normal anode fall should be at least equal to the first ionization potential of the gas.[11] The most recently accepted value of the first ionization potential of N_2 is 15.50 volts[12,13] so that the agreement is excellent. The plasma just outside the surface of the spot contains electrons which have a Maxwellian velocity distribution associated with a temperature of about 23,000°K. Therefore, the average energy of the electrons at this point is $\frac{3}{2}KT_e$ or about 3.0 electron volts.

SPOT GROWTH CHARACTERISTICS

The auxiliary anode upon which the spots were formed and anchored was also used as a probe for investigating the current-voltage relationships for the discharge within the spot itself. If the potential of the plane probe is increased beyond the amount necessary to form a spot upon it, the spot at first increases in brilliance as the current to the probe increases. At a critical value of the probe potential the current reaches a sharp maximum from which it rapidly falls. The potential at which the current maximum occurs is definite and reproducible for a given drift current and pressure so long as the surface conditions of the probe do not change appreciably. At pressures of 0.15 mm Hg and less no maximum is present and the current increases continuously with the probe potential. This is the pressure at which only one spot forms on the anode for all current densities up to the maximum value allowed by the power supply. This effect is illustrated in Fig. 7 and Fig. 8.

In each case the spot forms at the discontinuity, increases in brilliance until the current maximum has been reached, and then rapidly dims and shrinks in size as the current decreases with increasing probe potential. After the current minimum has been reached, the spot again grows in size, exceeding the dimensions of the spots occurring at the edge, and becomes far more

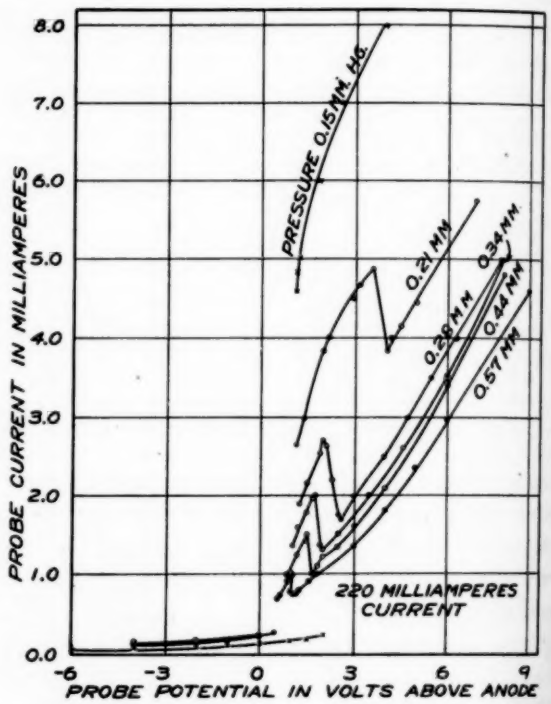

FIG. 7. Disk probe current-potential curves for the formation of a spot in N_2 at various pressures and constant drift current (220 ma).

[11] A. von Engel and M. Steenbeck, *Electrische Gasentladungen*, Vol. 2, p. 93.
[12] R. E. Worley and F. A. Jenkins, Phys. Rev. **54**, 305 (1938).
[13] J. Kaplan, Phys. Rev. **55**, 111 (1939).

brilliant. At the current density corresponding to the maximum, the artificially grown spot is indistinguishable from those occurring naturally. Evidently the spots develop until this condition is reached. Since further development entails a smaller current to the spot as the maximum is passed and the general circuit conditions demand an increase in current, new spots form to meet this current increase rather than the continued growth of any one spot.

Circuit Characteristics for Discharges Which Include Anode Spots

Current-voltage characteristics of the spherical discharge chamber curves were obtained in a nitrogen glow for several different pressures. Figure 9 shows a set of curves obtained when the disk anode illustrated in Fig. 3 was employed at various pressures. Almost identical curves were obtained when a spherical anode 5.1 cm in diameter was used. In each case there is a portion where the currents are low and the voltage falls steeply with increasing current. Along this part of the curve the anode was not yet covered with glow, and what appeared to be a short positive column or possibly an extended sheath protruded from the anode. At two- or three-tenths of a mm Hg pressure, and at currents below 10 milliamperes, the positive column became stri-

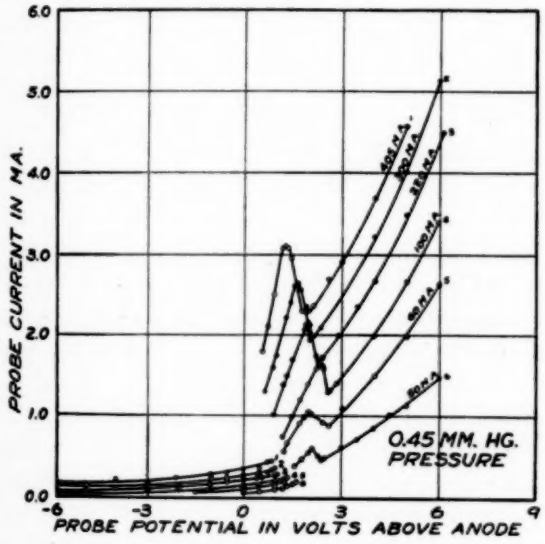

Fig. 8. Disk probe current-potential curves for the formation of a spot in N_2 at various drift currents and constant pressure (0.45 mm Hg).

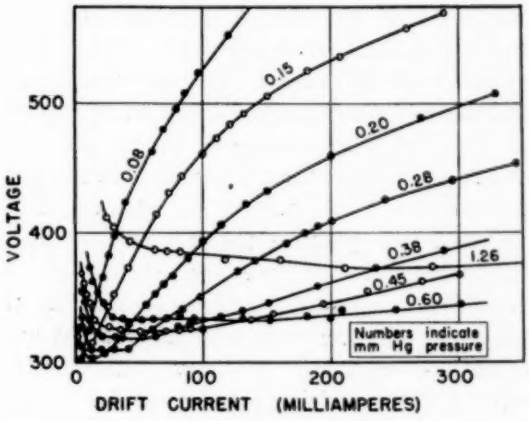

Fig. 9. Characteristic current-voltage curves at various pressures for an N_2 glow discharge with a large circular disk as anode.

ated, the number of striations decreasing as the current was increased. At higher pressure values the positive column was uniform. In any case, whenever a positive column was present, the cathode glow appeared as a small circular patch of light, no larger than the anode so that the discharge path was a narrow tubular region connecting the anode to the cathode glow. When the current density was enhanced, the glow at the cathode was spread over a greater area, and at a critical current density a well-defined anode glow replaced the positive column. This critical current density occurs where the steeply falling portion of the characteristic breaks into the flat portion.

In each case the voltage fell to a small but rather sharp minimum just as the anode became covered with glow and then leveled off to a rather long flat or gently rising portion. The shape of these curves is quite reproducible, but their position along the voltage axis depends to a large extent on the surface conditions of the anode as well as the position of the cathode glow on the outer sphere. At the higher pressures the cathode was never saturated and the small irregular patch of cathode glow appeared at different positions depending upon the discharge path during ignition. The size of the generator limited the current to 500 milliamperes.

The spots first appear at the beginning of the transition from the steeply falling to the flat branch of the curve, and increase in number until a complete ring of evenly spaced spots has

formed around the edge of the disk. It is seen that the length of the flat portion of the curves increases with the pressure, and this flat portion of the characteristic curve is also directly related to the number of spots present. In fact, the spots undoubtedly furnish the mechanism for increasing the current with practically no change in the total voltage drop across the chamber.

At a given pressure the number of spots increased with increasing current so long as the pressure was greater than 0.15 mm Hg. At pressures of 0.40 mm Hg and above, this occurred along the flat and rising portions of the current-voltage curves, but at pressures below 0.40 mm only along the rising portion. For large current values the spots were usually in rapid motion and the voltage increased but very little. Sometimes the pattern of spots as a whole rotated with a constant velocity, while at other times some of the spots remained at rest while others moved about. If an external magnetic field was applied, this motion could be increased, stopped, or even reversed. From these observations, it may be concluded in agreement with Thomas and Duffendack that the spots consist of individual current beams and that their motion is due to the interaction of the magnetic field which accompanies these beams with other magnetic fields that may be present.

At 0.15 mm of mercury pressure there is a fairly narrow minimum but no flat portion for the curve. It is at this pressure that only one large spot occurs. This single spot increased in size as the current was increased and suddenly changed over into a uniform whitish glow on the rising portion of the curve. A further increase in current caused the glow to become thinner and brighter. At a critical current value, the glow disappeared entirely, the entire chamber being filled with a faint luminosity. At about 0.10 mm Hg pressure, the spot having grown in size, suddenly collapsed and a uniform glow enveloped the anode. A further decrease in pressure or increase in current causes this glow to shrink in thickness and increase in brilliance. As the pressure is still further reduced, the minimum becomes more narrow, and the falling branch becomes shorter until at a pressure of 0.05 mm Hg there is only a rising curve. This type of characteristic does not accompany the formation of anode spots at all.

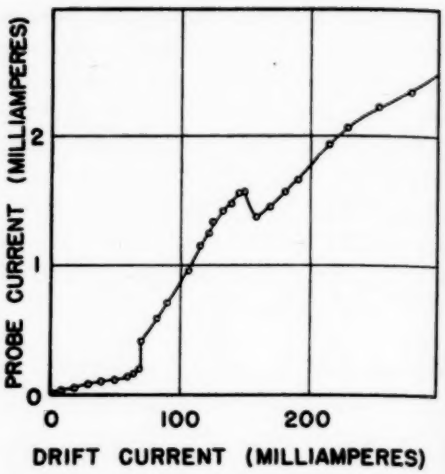

FIG. 10. Curve showing the variation of the disk-probe current with the total drift current at 0.44 mm Hg pressure when the probe is maintained at the anode potential so that a spot forms spontaneously upon it.

In order to see if the current peaks which are so clearly exhibited in the probe current-potential curves have any counterpart in the spots which appear on the anode spontaneously, the probe potential was maintained at that of the anode, and the probe current was recorded as the drift current in the discharge was varied. The results are shown in Fig. 10.

Two peaks are clearly present when the drift current is varied rapidly, but when its value is changed slowly enough so that the data could be recorded, the first peak was reduced to a short plateau. The rapid rise in probe current at about 70 ma drift current was accompanied by the appearance of a diffuse spot which covered the probe. As the drift current was increased, the spot grew brighter and became more sharply defined. When the peak at 150 ma was passed, the spot became less bright and its size was lessened just as was the case of the spots which were formed by altering the probe potential. Simultaneously, another spot appeared at the edge of the anode just as the current peak was passed.

The fact that a spot appears when the flat probe collects a definite current, and that as the total drift current is increased, the probe current passes through a peak even though the surface of the probe is at the anode potential, is further evidence that the spots formed by altering the probe potential are of the same nature as those which are formed spontaneously.

Summary of the Experimental Results

The following are the more important conclusions that may be drawn from these investigations regarding anode spots: Anode spots occur in glow discharges when the current density at the anode becomes sufficiently great. They are regions of intense ionization, consisting of electron beams flowing into the region, toward the anode, and positive ions flowing out, toward the cathode. The spots are regions which possess a net positive charge and are bounded by a plasma. The mutual repulsion of these positive space charges combined with the magnetic attraction of parallel ion beams gives rise to the stable spot patterns. Their size is determined by the pressure, and is larger the lower the pressure. The electrons from the plasma gain energy rapidly as they approach the spot.

The current-voltage characteristic curves are almost flat in the region in which spots occur, there being a slight increase in voltage for a large change in current. The potential drop through a spot is approximately the first ionization potential of the gas in the tube and corresponds well with the normal anode fall. The spots serve to furnish the additional positive ions necessary to keep the discharge stable as the current increases, and to collect electrons from this plasma which surrounds them. The current-voltage characteristic of an individual spot possesses a sharp maximum. The normal condition of a spot is the current density corresponding to this maximum. Since a further increase in voltage results in a current decrease, a new spot tends to form resulting in many spots instead of one large one.

The Mechanism of Anode Spots

The data accumulated in these researches are adequate for postulating a mechanism which explains the stability of anode spots as a combined space charge and bipolar current beam phenomenon. As the gradients are low in the discharge except for the anode and cathode fall, the only place where positive ions can be generated and still serve their function in the plasma is in the anode fall. From the flat characteristics found for this type of discharge, an increase of current with a small increase in voltage must result in both an increased positive ion production at the anode as well as an increase in electron collection from the plasma. The ions are necessary to maintain the plasma between the anode and negative glow with the increased electron current and perhaps even play an additional important role in the electron production at the cathode corresponding to the current increase. Ordinarily the anode glow supplies sufficient positive ions for this purpose. When the anode is made small and the cathode large, resulting in a large current density at the anode, the normal anode glow cannot produce the necessary ions, and the anode spots develop to provide these ions. The results of the Langmuir probe analysis show that the space potential in the vicinity of the anode spot reaches a value close to the normal anode fall at a comparatively large distance from the anode. As a result, the electrons acquire sufficient energy to ionize while their remaining path to the anode is yet long enough to permit a high probability of ionization. The anode fall region should be related to the production of positive ions in a manner somewhat analogous to the way in which the cathode fall is related to the release of electrons from the cathode under positive ion bombardment. In addition to producing positive ions, the spots effectively increase the anode area and provide an efficient means of collecting electrons from the plasma.

The mechanism involved in the case of the disk anode may be explained as follows. When the current density at the anode is small, a thin glow surrounds the anode. This glow in turn is surrounded by a plasma where the net space charge is very low but which contains of the order of 10^8 particles of each sign per cm^3. The equipotentials surrounding the anode probably differ only slightly from the electrostatic case. The drop through this glow is about the same as the first ionization potential of the gas. Although the distance traveled by the electrons which acquire this energy is small, they produce sufficient positive ions for the requirements of the discharge. As soon as the current reaches such a value that this normal glow cannot supply sufficient positive ions, this glow or sheath thickens, with the drop through it remaining about the same. The increase in current to the disk anode is not uniform. As is shown in Fig. 11, the lines of force converge toward the edge providing a lens or focusing

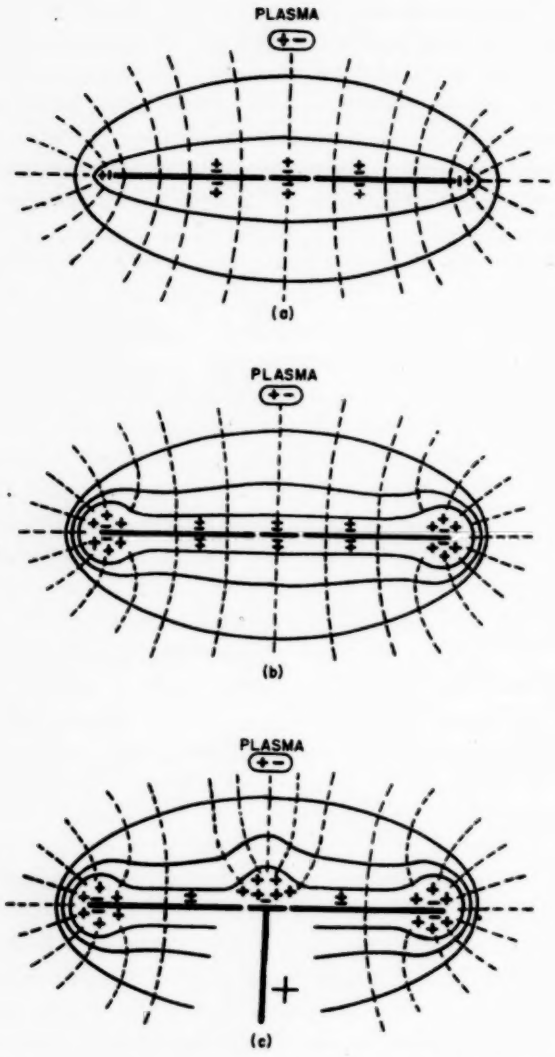

FIG. 11. Possible charge, field and potential distribution about the disk anode. (a) When the current is small. The auxiliary anode is at the same potential as the anode proper. A thin electron sheath surrounded by a positive ion sheath exists near the anode. In the outer regions a plasma exists when the net space charge is nearly zero. (b) The same except that the current is large. (The field converges electrons towards the edge producing intense ionization.) The increased positive space charge near the edge attracts still more electrons to this region. (c) The same as (b) except that the auxiliary anode is maintained positive with respect to the anode proper. Under these conditions a spot forms on this auxiliary anode for the same reason as at the edge.

effect which concentrates the electrons on the edge where they produce a corresponding intense ionization. The presence of these groups of positive ions with their low mobility results in a net positive space charge in this vicinity which in turn tends to further concentrate electrons upon this region. The space potential within the spot may rise above the anode due to this space charge, as occurs in the low voltage arc. The net result is the formation of the spot at the edge. The lower diagram in Fig. 11 shows how this same mechanism operates in the case of the artificially grown spot on the auxiliary anode. Here the distortion of the equipotential resulting in the "lens effect" is produced at will by raising the potential of the auxiliary anode above the anode proper. A spot, once produced, should be stable and persist as a spontaneously formed spot. This was observed experimentally. In the case of the spherical electrode, the same process occurs except that some mechanism must operate to initiate the spots. Any localized thickening of the sheath due to surface irregularities or other causes will serve this purpose.

Electrons must converge toward these spots and from them positive ions must diverge into the plasma. These beams have magnetic fields associated with them which together with the intrinsic positive charge possessed by each spot produces the even spacing around the edge of the disk and the regularity over the sphere. Such a beam of positive ions collects electrons from all around it and tends to converge them to the boundary of the spot, furthering the process detailed above.

Such a mechanism does not require a greatly enhanced drop across the discharge as a whole to produce a large increase in current. The change in space charge distribution merely results in an extended positive ion beam which in turn collects more electrons from the plasma.

The maximum in the individual spot characteristics is evidently responsible for the formation of many spots rather than the continued growth of one spot. The reason for this maximum is not immediately apparent. Possibly below and near the peak the electrons have sufficient energy to excite and not ionize except by cumulative action. Beyond the peak, ionization may occur directly resulting in a dimming of the spot and less electrons reaching the probe since the slower electrons produce a thicker electron space charge sheath near the anode. A spectroscopic examination should reveal the energy changes occurring on collision within the spot. It must be remembered that although the current to the

auxiliary anode decreases, the current as a whole increases as another spot is forming elsewhere. At high pressures, because of frequent collisions, the spot can extract electrons from a relatively small region of the plasma resulting in many spots close together while at low pressure this region from which electrons are drawn is large and the spot correspondingly large.

Anode spots will play an important role in those devices in which the currents are large and the anode areas small. They should occur at the anode when the transition from glow to arc is approached and in gaseous discharge devices employing thermionic emitters or cathode spot emitters where the discharge current may become large.

SEPTEMBER 1, 1940 PHYSICAL REVIEW VOLUME 58

A Complete Isometric Consistency Chart for the Natural Constants e, m and h

JESSE W. M. DUMOND
California Institute of Technology, Pasadena, California
(Received December 12, 1939)

The purpose of this paper is to show in greater detail the construction and use of a certain type of consistency chart already briefly described by the author in a previous paper, and by means of it to exhibit, with a few minor changes and some important new additional data, the present status of the dilemma regarding the values of e, m and h which grows out of the discrepancy between various results of careful measurements of functions of these variables. The discrepancy itself remains practically as glaring and just as unexplained as ever. Scales have been added permitting the values of e, m and h corresponding to any intersection point to be read off directly.

THREE-DIMENSIONAL REPRESENTATION

VERY few experiments have been performed which measure any one of the three atomic constants alone without involving one or both of the others. Thus the values of e, m and h are usually obtained by combining the results of several types of experiment and solving a system of simultaneous equations. There are, however, a great number of ways in which this can be done and these lead to different results so that it becomes desirable to find some graphic representation to exhibit as impartially as possible the inconsistency situation.

In a recent article[1] on the natural constants which will here be referred to as I NC the question of the interconsistency of measurements of functions of the atomic constants e, m and h was discussed by means of a graphic chart which was essentially an isometric[2] projection of a three-dimensional plot of the situation. If one thinks of the values of e, m and h as plotted along the three axes of a three-dimensional rectangular Cartesian coordinate system, then each function of e, m and h for which some physical experiment yields a numerical value is represented by a surface in this three-dimensional space. Since the functions of e, m and h determined by experiment are essentially product functions the general equation for such a surface is

$$e^p h^q m^r = A, \tag{1}$$

in which certain of the exponents may, of course, be zero; e.g. the case of the direct determination of e independent of h and m ($q=0$, $r=0$). At least three of these surfaces are required to determine a point (e, m, h) in this three-dimensional space. With more than three surfaces over-determination may exist and this may be coupled with inconsistency so that various dif-

[1] J. W. M. DuMond, Phys. Rev. **56**, 153 (1939).

[2] Since several different methods of plotting the interconsistency of determinations of functions of e, m and h have been proposed and R. T. Birge (Phys. Rev. **57**, 250A (1940)) has recently even discussed "an indefinitely large number of variations of such types of chart" it seems advisable to adopt suitable descriptive names for some of the outstandingly interesting ones. The present author wishes to take such a responsibility only in the case of the type of chart which he originated and he suggests for it the name isometric chart.

ferent points may be determined by the mutual intersection of different triplets of surfaces. The pattern of variously tilted intersecting surfaces in the small region in three-dimensional space in the vicinity of these intersections therefore tells the entire story as to the consistency of the determinations. If all determinations are completely consistent, all the surfaces will intersect in a common point whose coordinates are the values of e, m and h.

We have said that at least three surfaces are *necessary* to determine a point in this three-dimensional space. *It is important to realize, however, that three such independent surfaces may not be sufficient to determine a point of intersection*, for these surfaces may intersect in a common line rather than in a common point. It is of primary importance therefore to classify the equations corresponding to each type of experiment *into groups having common lines of intersection* for two reasons: first, in order to get a clear picture of what various combinations of the experiments do or do not determine and second, to select, if possible, a most advantageous direction in which to project the entire situation on a plane for the purpose of constructing a two-dimensional chart. It is evident that the way in which a system of equations permits of classification into such groups is a very fundamental absolute property of the system quite independent of any particular geometrical method of representation. The importance of these considerations in connection with the atomic constants seems to have been overlooked in published work up to its recognition in I NC.

The orientation of each surface in space depends on the nature of the function $e^p h^q m^r$ which it represents, while the numerical value A_i determined by an experiment fixes the *position* or *location* of the surface (its origin distance if it is a plane). To give symmetry of treatment and freedom from an arbitrary choice of the scales of e, m and h the author has plotted along the three Cartesian axes not e, m and h directly but $(e-e_0)/e_0$, $(m-m_0)/m_0$, $(h-h_0)/h_0$, where e_0, m_0, h_0 are values of e, m and h chosen as an arbitrary reference or origin point for the new chart. So long as this choice of e_0, m_0, h_0 is judicious so that for the entire region of interest where intersections occur none of the three variables, $x_e=(e-e_0)/e_0$, $x_m=(m-m_0)/m_0$, $x_h=(h-h_0)/h_0$ ever exceeds, say, 0.5 percent it is obviously possible, by dropping higher order terms, to replace each of the curved surfaces by a plane which will nowhere in the region of interest deviate from the curved surface by an amount appreciable for our purposes.[3] The numerical constants A_i determined by some particular experiment, i, are replaced by pure numbers $a_i=(A_i-A_{i0})/A_{i0}$ where $A_{i0}=e_0{}^p h_0{}^q m_0{}^r$ and it is then easy to show that Eq. (1) becomes, with neglect of higher order terms

$$px_e+qx_h+rx_m=a_i. \tag{2}$$

Nine such equations which cover all the functions of e, m and h which to date have been determined by experiments are listed in Table I of I NC.

In I NC experiments 8 ($A_8=e/h^3$) and 9 ($A_9=e^2/h$) (the Stefan-Boltzmann radiation constant σ and the fine structure constant α) were left out of the discussion because they are much less reliable and accurate than the rest. One of the purposes of this paper, however, is to show a chart provided with scales for including also these determinations if at some later date it should become desirable to do so. Figure 1 of I NC is a perspective view of a three-dimensional model showing six of the nine planes corresponding to determinations 1 to 6 inclusive of Table I of I NC (determination 1 is represented in Fig. 1 of I NC by the base plane). In this model the planes have all been made to pass through the origin to simplify the figure since the purpose at this stage is to discuss merely the *orientations* of the planes. In reality each experimental determination yields a different numerical value a_i

[3] R. A. Beth, Phys. Rev. **54**, 865 (1938) and C. G. Darwin (reference 8) have each proposed plotting logarithms of e, m and h instead of their natural values, the advantage in doing so being that then the product functions become not approximately but exactly linear functions represented by plane surfaces. I have refrained from following this more elegant procedure for practical reasons. The percent or relative deviations of e, m and h from the arbitrary values $e_0 m_0 h_0$ are easily understood at a glance. Scales identical to relative deviation could indeed be obtained by the use of natural logarithms but the great convenience of denary logarithms would then be sacrificed. In practice the relative deviations $(e-e_0)/e_0$ are very easy to transform into the numerical values e and vice versa. This can be done very rapidly with ample accuracy on a slide rule, for $(e-e_0)/e_0$, of the order 0.5 percent or less, need itself only be known to 0.5 percent accuracy to give an accuracy of 1/40,000 in e.

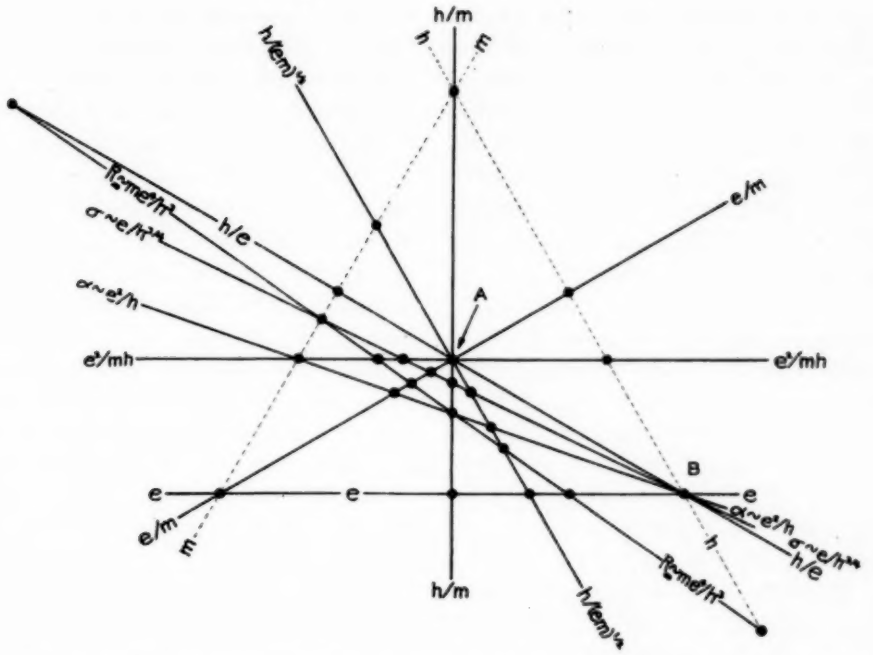

FIG. 1. Graphical representations of cozonal groups. Imagine a three-dimensional rectangular Cartesian coordinate system in which relative deviations of e, m and h from nearly correct conventional values are plotted to the same scale on the three axes. There are eleven variously orientated planes in this three-dimensional space, nine of which represent the nine functions of e, m and h which have been determined experimentally, including e itself. The other two planes (which do not correspond to experimental determinations) are those of m and h themselves. For our purpose here only the orientations of the planes concern us, hence they are plotted through a common origin point. This diagram is a *cross section* taken at some arbitrary origin distance through this complex of planes by an "isometric" cutting plane (one making equal angles with the axes of e, m and h). Every line on this diagram is the trace of some plane which cuts the isometric plane and the intersection points are the points at which axes common to two or more planes cut the isometric plane. All possible intersection points are shown and this diagram gives, therefore, an exhaustive enumeration of all possible cozonal groups of planes. This diagram is obviously not a consistency diagram.

and its plane must pass not through the origin but at a distance proportional to a_i therefrom. A scale of a_i, the percent or relative deviation of the particular experimental result, A_i, from the origin value, A_{i0}, may be thought of as provided on the three-dimensional model to facilitate plotting planes representing the individual experimental results.

In the three-dimensional model all planes which pass through a common point represent consistent determinations of functions of e, m and h and the coordinates of this common point fix the values (e, m, h) upon which these determinations agree.

COZONAL GROUPS ENUMERATED

A striking fact, brought out for the first time in I NC, is that *five* out of the seven most important and accurate types of determinations have planes which are all *parallel to a common line* (the space diagonal making equal angles with the axes x_e, x_h and x_m) and which are all, therefore, seen on edge in an isometric projection (projection on a plane normal to the line just referred to, the plane of the hexagon in the prespective view of Fig. 1 of I NC). Any group of planes parallel to a common line we shall call a cozonal group. Planes corresponding to experiments 7, 8 and 9 have not been shown in Fig. 1 of I NC, to avoid complication. In the present article, Fig. 1, we wish however, in order to effect an exhaustive enumeration of cozonal groups, to show the traces of all nine planes[4] *where these would inter-*

[4] Here also since we are only interested at this point of the discussion in the *orientations* of the planes they are all plotted as though they passed through the origin of the three-dimensional coordinate system.

sect the plane of the hexagon of Fig. 1 of I NC. In the same diagram we also show (with dotted lines because they do not stand for experimental determinations) the traces of the planes $x_h=0$ and $x_m=0$ where they intersect the plane of the hexagon. We thus obtain a diagram with eleven intersecting lines presenting twenty-five points of intersection. Each of these points of intersection is the point where an axis common to two or more planes in three-space pierces the plane of the hexagon. One sees immediately from Fig. 1 that most of the axes in three-space (intersection points in Fig. 1) have only two or three planes passing through them (lines in Fig. 1). There are two exceptional axes, however, indicated by points marked A and B, respectively. Five planes pass through each of these. In the case of axis A these five planes correspond to experiments 2 to 6, inclusive, all of which are capable of excellent precision[5] and many of which have already received extensive and careful attention from many experimenters. In the case of axis B, one of the five planes (h) does not represent an experiment at all and two others are very inaccurate experiments corresponding, respectively, to the determination of the Stefan-Boltzmann radiation constant, σ, and to the fine structure[6] constant, α. Thus for practical purposes axis B has only two interesting planes passing through it, the plane of h/e and the plane of e. It is evident that Fig. 1 enumerates exhaustively all possible cozonal groups of planes and these are seen to be twenty-five in number, most of which, however, consist of more or less trivial groups of two or three members each. The group A is outstatnding in that it has five interesting members. While the cross section Fig. 1 is of no use as a chart for indicating the consistency of the determinations, the classification of the equations into cozonal groups is of great value in indicating the exact properties of the system of equations with which we must deal. For example, this chart tells us at a glance that a combination of the measurements of R, e^2/mh and $h/(em)^{\frac{1}{2}}$ can be solved simultaneously for e, m and h, while a combination of the measurements of R, α, and h/m cannot be used to obtain these constants. The determinant formed of the exponents of e, m and h vanishes for the second case but not for the first. The lines on the diagram corresponding to the first three functions named have no common intersection point, therefore the planes they stand for are not cozonal and hence they determine a point in space whose coordinates are e, m and h. The lines standing for the last three functions named are seen to be cozonal since they pass through a common intersection point on the diagram and hence they cannot determine a point in space, but on the contrary they determine only a line. In particular the system of five equations represented by the five lines e/m, h/e, h/m, e^2/mh, $h/(em)^{\frac{1}{2}}$, which pass through the common point A, is insufficient to determine the constants e, m and h. Only *ratios* between these constants can be determined by this system. Obviously the properties of any set of equations expressed by the cozonal groups into which they fall are absolute properties of the system independent of any choice of geometrical representation.

Method of Projecting the Three-Dimensional Situation on a Plane to Exhibit Consistency

Each axis represented by the points of Fig. 1 may be considered as a candidate for the direction along which to project the three-dimensional plot for two-dimensional representation. For reasons which will soon be clear, I choose the axis A of Fig. 1 for this purpose. Whichever axis is so chosen it is evident that the planes which intersect in, or are parallel to, that axis when projected on a picture plane normal to that axis will be seen on edge and will appear as lines, the traces of the plane in question on the picture plane. From here on for brevity let us call the axis selected for projection simply "the cozonal axis." Now the planes not parallel to this axis (which for brevity we shall call simply the noncozonal planes) must be treated differently since they are not seen on edge. It so happens with the projection we have just selected that the R_∞ plane is a noncozonal plane. The author has adopted the procedure of selecting the R_∞ plane (partly because of the very superior accuracy of

[5] This statement is somewhat less true of experiments 4(*a*) and (*b*) than of the rest but these experiments are capable of improvement with further work.

[6] There is some hope through recent theoretical work of J. R. Oppenheimer and his students that the accuracy of the experimental determination of α may be improved.

this determination) as a standard plane to serve the following very special purpose. *Other noncozonal planes are represented on our consistency diagram by plotting the projection on the picture plane of the line of intersection in space of each noncozonal plane with the R_∞ plane.* If we assume an axis in space fixed as to position by a consistent set of cozonal planes, obviously the question of consistency or inconsistency of noncozonal planes with the cozonal set cannot arise *unless there are two or more* noncozonal planes which may or may not intersect this axis in the same point. The necessary and sufficient condition that any two noncozonal planes shall be consistent with any group of two or more consistent cozonal planes is that the line of intersection of the first two shall pass through the line of intersection of the second set. From this it follows that, *on our consistency chart*, the necessary and sufficient condition that any two noncozonal planes shall be consistent with any self-consistent group of cozonal planes is simply that the projection of the line of intersection of the two noncozonal planes shall pass through the intersection of the traces of the consistent cozonal group.

Our chart thus has two kinds of traces on it. (I) Projections of *lines* in three-space on the plane of the chart. These lines in three-space are the intersections of the R_∞ plane with any other noncozonal plane. The *position* of such lines on the chart depends on two variables, the numerical value of R_∞ and the numerical value of the other noncozonal function which is involved. Such lines on the chart should therefore be provided with double scales showing the displacements they suffer for changes in either of the two variables while the other is held constant. (II) Lines which are simply the projections of cozonal planes seen on edge but which may, if we wish, also be regarded in the same way as class I, namely as the projections of the line of intersection in space of each cozonal plane with the R_∞ plane. It is because the cozonal planes are seen on edge that their traces may be regarded as belonging either to class I or II. The position on the chart of such traces of cozonal planes does not vary, however, with variations in R_∞ and hence only single scales need be attached to represent the displacement which each such line will suffer when the numerical value associated with its determination is changed. It is well worth noting that the chart of I NC which represented all seven of the most interesting types of determinations only needed to have one of these provided with a double scale because of the judicious choice of A as the axis of projection.

By adhering to *one* standard noncozonal plane (the R_∞ plane) as the common cutting plane for the remaining noncozonal planes a necessary and sufficient criterion for consistency of a group of noncozonal planes *among themselves* is obtained directly on the two-dimensional chart. If the projections on the picture plane of the respective lines of intersection in space of each member of a group of noncozonal planes with the R_∞ plane all pass through some cozonal axis (seen projected as a point in the diagram) then these lines in space must not only intersect that axis *but must intersect it at the same point in space*, namely the point where that axis pierces the R_∞ plane.

It is to be noted that the R_∞ plane could not serve as the standard cutting plane for the above described purpose if it were parallel to our chosen axis of projection A.

It may also be added, of course, that only practical considerations of simplicity dictate the choice of the axis A or indeed of any axis represented by any intersection point in Fig. 1 at all, as the axis of our projection. In principle, any arbitrary direction could have been chosen for the axis of projection but then obviously all planes might be noncozonal and all of them should be supplied with double scales on the chart.[7] The great simplification obtained by the choice of axis A is thus clear.

C. G. Darwin[8] plots a diagram similar to the author's in which, however, e, h/e and e/m are selected as the three-dimensional rectangular coordinates, and logarithms are used rather than relative deviations. The axis of projection is normal to the e plane and on account of the choice of variables this is also the axis cozonal to the principal group of five members which we

[7] The chart devised by R. A. Beth (Phys. Rev. **53**, 681 (1938)) is such a projection, the axis of projection being normal to the R_∞ plane. No planes are cozonal with this axis. Beth's chart, however, was not provided with double scales so that the effect of the change in R_∞ could not readily be seen.

[8] C. G. Darwin, Proc. Phys. Soc. London **52**, 202 (1940).

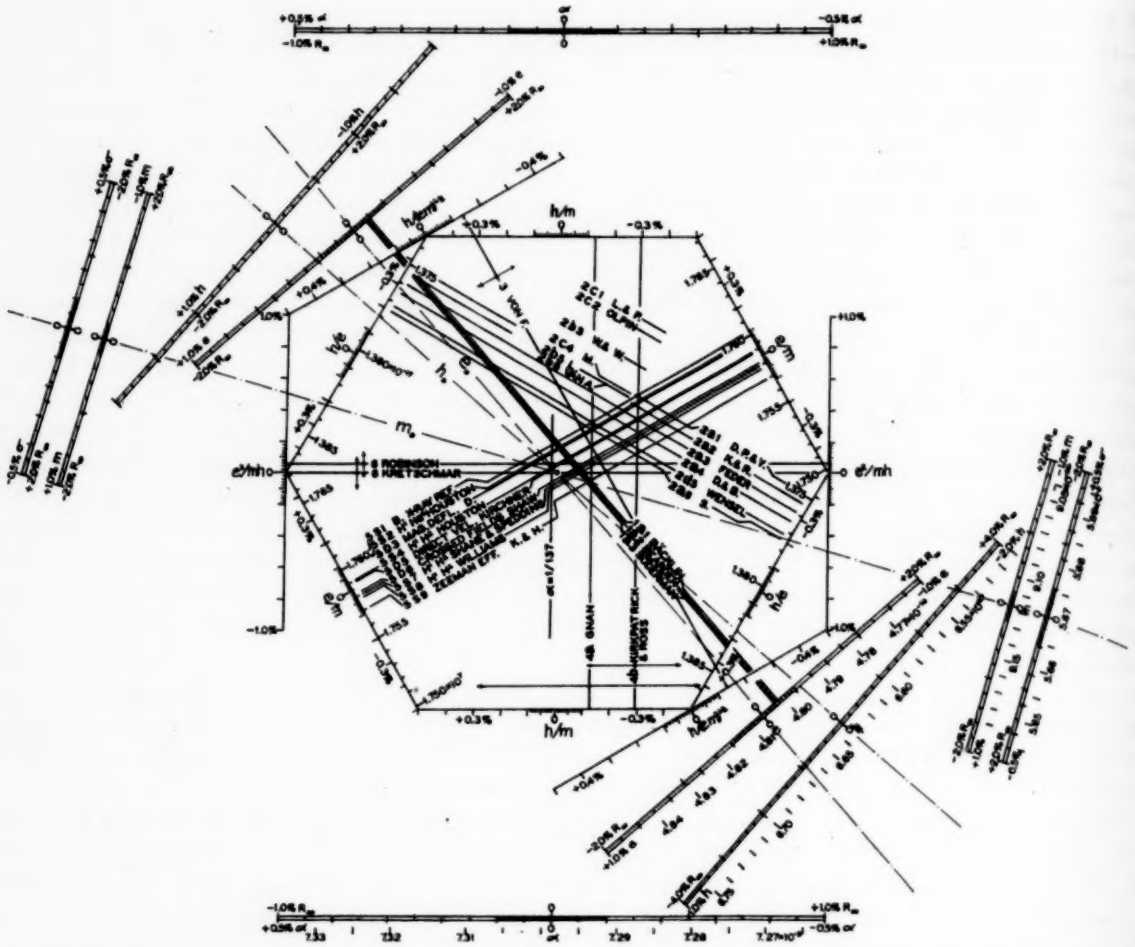

FIG. 2. Complete isometric consistency chart for the nine functions of e, m and h determined by experiment. The scales for displacement of the lines are expressed in percent deviation from the standard conventional values adopted for the construction of the chart, an intersection in the exact center of the chart indicating that the conventional values $e_0 m_0 h_0$ are the true ones. In the more interesting cases scales reading directly in terms of these quantities are also attached. Certain of the scales are "double scales," that is, the position of the trace depends on two variables one of which is R_∞. Each member of the pair in a double scale shows the displacement that the projected line of intersection of the e and R_∞ planes would suffer if the variable of the one scale alone is changed while the other variable is held at its conventional value. A change in *both* variables then calls for the algebraic sum of the displacements indicated on each scale.

The conventional or "origin" values of this chart as well as the experimental values with reference numbers corresponding to those on the chart are listed in Table I.

have here called the cozonal group. Darwin claims that a simplification is obtained by this procedure though it would seem that no greater number of planes are seen on edge by this method than by the more symmetrical isometric projection of the author. Thus if scales of variation were attached to the various lines on Darwin's diagram the same number of double scales would be required as in the isometric chart.

Darwin, in plotting his chart, has followed the procedure of Birge, Dunnington and others of presenting weighted average values for the various plotted functions of e, m and h. The author much prefers to exhibit the situation graphically in order *to show separately all the reliable independent determinations of each function*. Admittedly, this introduces more lines on the graph but it also conveys much more information and permits the reader to use his own judgment more freely. The fact that a point of intersection is the thing to be selected by the reader rather than a line through a number of points (as in the case of the nomographic diagrams of Birge and Bond for example) seems to

the author a distinct advantage if the reader is to be permitted this freedom of choice.

The Complete Isometric Chart and Some of Its Advantages and Uses

Figure 2 shows such a diagram. On it are given scales for all nine classes of functions of e, m and h so far determined by experiment. The double scales are easily recognized. They have been drawn with two parallel lines running lengthwise along them to attract the eye. Direct reading scales for each of the variables and functions have been provided as well as the scales of relative or percent deviation from the standard or origin values. In Table I the origin values are given as well as the numerical values for the different determinations. To use such a chart it is not even necessary to remember the principle of its construction. Each trace is merely to be plotted between its two parallel scales at the percent deviation (plus or minus) from the origin value called for by the experimental value obtained. (Or it may be plotted directly by means of the direct reading scales.) Those traces which intersect in the same point represent mutually consistent determinations. The values of e, m and h upon which such mutually consistent traces agree can be read off immediately on the scales of e, m and h either directly or in terms of percent deviation from the origin values $e_0 m_0 h_0$. This operation is slightly facilitated by drawing the origin traces through the zeros of the percent

Table I. *Conventional or origin values used in isometric chart.*

$e_0 = 4.80650 \times 10^{-10}$ e.s.u., $m_0 = 9.11780 \times 10^{-28}$ gram, $h_0 = 6.63428 \times 10^{-27}$ erg sec. and in consequence:
$e_0/m_0 = 1.75850 \times 10^{7}$ e.m.u./gram, $h_0/e_0 = 1.38028 \times 10^{-17}$ e.s.u., $h_0/m_0 = 7.27621$
$e_0^2/(h_0 m_0) = 3.81921 \times 10^{14}$, $h_0/(e_0 m_0)^{\frac{1}{2}} = 1.00216 \times 10^{-6}$, $R_\infty = 2\pi^2 e^5 c^{-2} (h/e)^{-3} (e/m) = 109{,}737$ cm^{-1}
$c = 2.99776 \times 10^{10}$ cm/sec., $\alpha_0 = 7.29870 \times 10^{-3}$, $\sigma_0 = 5.67122 \times 10^{-5}$ erg cm^{-2} deg.$^{-4}$ sec.$^{-1}$

Experimental values used in isometric chart

Quantity Determined	Value	Symbols on Chart	Method	Observer	Reference	Recomputed by
e	4.8016×10^{-10}	1 *a* 1	Ruled grating and crystal x-ray diffraction	E. Bäcklin	Zeits. f. Physik **93**, 450 (1935)	Birge (1939 letter)
	4.8022	1 *a* 2		J. Bearden	Phys. Rev. **37**, 1210 (1931); **47**, 883; **48**, 385 (1935)	Birge (1939 letter)
	4.8026	1 *a* 3		M. Söderman	Nature **135**, 67 (1935)	Birge (1939 letter)
h/e	1.37494×10^{-17}	2 *a* 1	Continuous x-ray spectrum limit	Duane, Palmer and Yeh	J. Opt. Soc. Am. **5**, 376 (1921)	DuMond
	1.37541	2 *a* 2		P. Kirkpatrick and P. A. Ross	Phys. Rev. **45**, 454 (1934)	"
	1.37588	2 *a* 3		H. Feder	Ann. d. Physik **51**, 497 (1929)	"
	1.37646	2 *a* 4	Continuous x-ray spectrum limit	J. W. M. DuMond and V. Bollman	Phys. Rev. **51**, 400 (1937)	"
	1.3772	2 *a* 5	ϵ_3 optical pyrometry	H. T. Wensel	J. Research Nat. Bur. Stand. **22**, 386, 387 (1939)	Wensel
	1.3775	2 *a* 6		G. Schaitberger	Ann. d. Physik **24**, 84 (1935)	DuMond
	1.3715	2 *c* 1	Photoelectric effect	P. Lukirsky and S. Prilezaev	Zeits. f. Physik **49**, 238 (1928)	"
	1.372	2 *c* 2	Photoelectric effect	A. R. Olpin	Phys. Rev. **36**, 251 (1930)	"
	1.3736	2 *b* 3	Critical potentials	R. Whiddington and E. G. Woodroofe	Phil. Mag. **20**, 1109 (1935)	"
	1.375	2 *c* 4	Photoelectric effect	R. A. Millikan	*Electrons* (+ and −), *Protons, Photons, Neutrons, and Cosmic Rays* (U. of Chicago), p. 242 (1934)	"
	1.3752	2 *b* 5	Critical potentials	E. O. Lawrence	Phys. Rev. **28**, 947 (1926)	"
	1.3752	2 *b* 6	Critical potentials	L. C. Van Atta	Phys. Rev. **38**, 876 (1931); **39**, 1012 (1932)	"
$h/(em)^{\frac{1}{2}}$	1.00079×10^{-6}	3	Electron λ and voltage	S. von Friesen	Proc. Roy. Soc. **A160**, 424 (1937) also Inaugural Diss. Uppsala 1936	"
h/m	7.267	4 *a*	Electron λ and velocity	J. Gnan	Ann. d. Physik [5] **20**, 361 (1934)	Kirchner
	7.255	4 *b*	Compton shift	P. Kirkpatrick and P. A. Ross	Phys. Rev. **45**, 223 (1934)	"
e/m	1.7602×10^{7}	5 *s* 1	X-ray refraction in diamond	J. A. Bearden	Phys. Rev. **54**, 698 (1938)	Birge (1939 letter)
	1.7600	5 *s* 2	Spectroscopic H^1 He^4	W. Houston	Phys. Rev. **30**, 608 (1927)	"
	1.7598	5 *d* 3	Magnetic deflection	F. Dunnington	Phys. Rev. **52**, 498 (1937)	"
	1.7590	5 *s* 4	Spectroscopic H^1 H^2	W. Houston	Phys. Rev. **51**, 446 (1937); **55**, 423 (1939)	"
	1.7590	5 *d* 5	Direct velocity	F. Kirchner	Ann. d. Physik **8**, 975 (1931); **12**, 503 (1932)	"
	1.7582	5 *d* 6	Crossed fields	A. E. Shaw	Phys. Rev. **54**, 193 (1938)	"
	1.7580	5 *s* 7	Spectroscopic H^1 H^2	C. D. Shane and F. H. Spedding	Phys. Rev. **47**, 33 (1935)	"
	1.7578	5 *s* 8	Spectroscopic H^1 H^2	R. C. Williams	Phys. Rev. **54**, 568 (1938)	"
	1.7570	5 *s* 9	Zeeman effect	L. E. Kinsler and W. V. Houston	Phys. Rev. **45**, 104; **46**, 533 (1934)	"
$e^2/(mh)$	3.82155×10^{14}	6	Magnetic deflection of x-ray photoelectrons	H. R. Robinson	Phil. Mag. **22**, 1129 (1936)	Robinson
	3.8194	6		G. G. Kretschmar	Phys. Rev. **43**, 417 (1933)	Kretschmar

scales of e, m and h with a dot and dash line as in Fig. 2 to avoid confusion. For any desired point in the diagram about which two or more traces are consistent one may quickly read off the values of e_0, m_0 and h_0 by scaling with dividers the distance from the point in question to each of the three dot-and-dash origin traces. The distance so scaled is then transferred with the dividers to its appropriate scale and read off immediately.

The *relationships* between different types of determination can be seen at a glance. For example note that the directions of the scales of e, m and h do not differ greatly on the chart, and that the class of determination that comes nearest to this same general direction (other than the direct determination of e itself) is the class h/e. Next to h/e the class $h/(em)^{\frac{1}{2}}$ (so far studied only by von Friesen) comes nearest to having this general direction, while e/m possesses this property perhaps least of all. This means that if we accept the Bohr-Rydberg relationship and the numerical value of the Rydberg as part of our data to be used simultaneously along with other experiments then the best or most crucial type to choose for determining e, h and m is one which measures h/e. Next to this comes $h/(em)^{\frac{1}{2}}$ while e/m need be known with very little precision if it is to be used for this purpose in conjunction with either of the two previous experiments.

The above statement is only a rough way of perceiving these relationships of course. In any precise consideration of the degree of dependence of e, m and h on the various types of determination the size of the scale units (relative variation) for each function naturally plays a role as well as the slopes of the lines.

An advantage of the isometric chart here described is the relatively good independence of the different traces from each other and the resulting facility with which one can see the effect of a change in any single measurement or assumption including the value of R_∞. The choice of the projection is such that even if the functional form of the Bohr-Rydberg formula were modified, only one really significant set of traces (Bäcklin, Bearden and Söderman) would have to be reorientated (for at the present the experimental values of α and σ cannot be regarded as having much meaning).[9]

The values themselves depicted in Fig. 2 have been modified and extended since the charts published in I NC as follows: The values of e/m from the different sources have been taken from a letter dated August, 1939, privately circulated by R. T. Birge who recomputed these values with the latest auxiliary constants.[10] The general aspect of the e/m band remains, however, about as before. The x-ray values of e (Bäcklin, Bearden and Söderman) are also modified very slightly from Birge's recomputation with the new auxiliary constants. No value of σ has been plotted since it would fall in a region very far off the chart.[11] The h/e values have been recom-

[9] The author is indebted to Professor Birge for pointing out to him a misleading statement on page 155 of I NC. It is stated that "the well-known Birge-Bond diagram has two disadvantages" . . . ,'(1) The data are treated in an arbitrary asymmetrical way (certain of the determinations are mixed with Eq. (7) while others are not) so that it becomes difficult to foresee (without replotting) the result of certain changes either from theory or experiment; (2) Relative variations of the same magnitude appear to very different scales on different ordinates." In an effort at brevity two ideas were rather carelessly confused in one sentence here. The arbitrary asymmetry referred to in the B-B diagram is really that one singles out one of the three variables to plot as ordinate (e.g., e) while another one (e.g., h) appears as the slope of a line on the graph and the third variable (e.g., m) does not appear at all because in all the determinations involving that variable the Bohr-Rydberg formula has been used to eliminate it. The present isometric chart lays no especial emphasis on any one of the three variables e, m or h and they can all be made to appear explicitly on scales in a precisely similar way. So much for the "arbitrary asymmetry." The fact that certain of the determinations are mixed with the Bohr-Rydberg equation while others are not is indeed strictly true on both types of chart with the practical difference, however, that many more points on the B-B chart (in its present familiar form) than lines on the isometric chart are so mixed in the present state of what constitutes the interesting determinations. The quoted sentence from I NC implies that the mixture of certain determinations with Eq. (7) is a consequence of the arbitrary asymmetrical treatment when in fact it is a consequence of the effort to represent three variables in two dimensions. The author regrets and wishes to retract this incorrect implication.

[10] The principal change is in the value of q, the ratio of the size of international and absolute units of current as explained by Birge in his August, 1939, letter. This has been changed from $q=0.99993$ to $q=0.99986$ (J. Research Nat. Bur. Stand. **22**, 485 (1939)). This affects the value of the faraday, the value of pq (factor to change from international to absolute volts) and, of course, consequently many other constants. The new value of q ends a discrepancy of long standing with the Nat. Phys. Lab. (England) and is very satisfactory, Birge reports.

[11] For a critical review of determinations of σ see F. G. Dunnington's excellent article, Rev. Mod. Phys. **11**, 72 (1939). That author obtains an average value 5.775×10^{-5} from six sources, a value which, as can easily be seen from the scale of our Fig. 2, falls far off the diagram.

puted by the author to take account of these same slight changes and to correct a slight error on the previous chart all of which, however, makes no essential difference in the general aspect of the h/e band. To this band has also been added information from H. T. Wensel of the National Bureau of Standards who has kindly supplied the author in a private letter with a most interesting computation of h/e based on measurements of the constant c_2 by optical pyrometric methods.[12] Professor F. Kirchner of Cologne, who has adopted the isometric chart to depict the consistency situation in his recent survey of the atomic constants,[13] has been so kind as to point out to the author the necessity for two modifications, one in each of the h/m determinations. The value of $h/(em)^{\frac{1}{2}}$ recomputed by the author from von Friesen's data given in his dissertation remains practically as in I NC save for slight modifications occasioned by the changed auxiliary constants. The same is true of Robinson's results on $e^2/(mh)$. To this function has also been added the results of Kretschmar who has reexamined his plates and recomputed his results which he kindly supplied in a recent letter to the author. It is interesting to note the good agreement between these two workers on this last mentioned precision experiment. The much less accurate work on h/e from the optical photoelectric effect[14] and from ionization potentials[15] is merely added to the continuous x-ray limit work to show how it supports the general trend of the h/e results to be lower than one expects for consistency with the remainder of the diagram. Wensel's computed result which should have very considerable reliability and which is obtained by a method quite radically different from the short wave-length limit of the continuous x-ray spectrum also supports the latter work in giving h/e too low. The discrepancy thus remains as baffling as ever. The conclusions in I NC remain unchanged.

Practical Methods of Construction

The actual construction of the isometric chart is very simple.[16] From the symmetry of the space diagram (Fig. 1, I NC) the scales of percent variation of e/m, h/e and h/m forming the sides of the hexagon are evidently of identical size. The range of ± 0.5 percent for each side of the hexagon seems to work out well in the present state of precision. For the mere mechanics of drafting alone it is, from this point on, unnecessary to think of the three-dimensional origin. The remaining two cozonal scales are laid out as follows. We may choose for example e/m and h/e (or more conveniently the relative deviations of these variables) as two independent variables whose specification fixes the position of any point on the chart. Now since $h/(em)^{\frac{1}{2}} = (h/e)(e/m)^{\frac{1}{2}}$ it is evident that an *increase* of 0.5 percent in h/e and a *decrease* of 1.0 percent in e/m leaves $h/(em)^{\frac{1}{2}}$ unchanged and such a variation therefore defines the direction of the trace $h/(em)^{\frac{1}{2}} = h_0/(e_0 m_0)^{\frac{1}{2}}$ which passes through the zeros of the percent scales for this function. But starting from the origin in the center of the chart an *increase* of 0.5 percent in h/e and a *decrease* of

[12] Wensel's computations are essentially those described in his paper "International temperature scale and some related physical constants," (H. T. Wensel, J. Research Nat. Bur. Stand. **22**, 386–387 (1939)) save that a knowledge of c_2 (see his Table 4) is used to compute h/e by his Eq. (14). In his communication to the author Wensel has computed a weighted mean c_2 with the same numerical result as the unweighted mean of his Table 4. The procedure here of plotting an average value is admittedly inconsistent with the author's policy of showing independent determinations. It is necessitated in this case by the already large number of lines in the h/e band.

[13] F. Kirchner, *Die Atomaren Konstanten, Ergebnisse der Exakten Naturwissenschaften* (Julius Springer, 1939), Vol. 18.

[14] R. A. Millikan, *Electrons (+ and −), Protons, Photons, Neutrons and Cosmic Rays* (University of Chicago Press, 1935), p. 242, also Phys. Rev. **7**, 362 (1916); P. Lukirsky and S. Prilezaev, Zeits. f. Physik **49**, 248 (1928); A. R. Olpin, Phys. Rev. **36**, 284 (1930). From Fig. 34 it is certain that Millikan used the conversion factor 300 instead of 299.776 to obtain the voltage in e.s.u. and it is highly likely that the same was true of the other two authors, hence I have taken the liberty of correcting all three of the above results for this. Each of these authors gives a value of h rather than h/e and from the dates of each work I have therefore, in recomputing back to find h/e, used, respectively, $e = 4.774$, 4.774 and 4.770.

[15] E. O. Lawrence, Phys. Rev. **28**, 947 (1926). L. C. van Atta, Phys. Rev. **38**, 876 (1931); **39**, 1012 (1932). R. Whiddington and E. G. Woodroofe, Phil. Mag. **20**, 1109 (1935). Here I have adopted Dunnington's recomputed values Rev. Mod. Phys. **11**, 72 (1939).

[16] Since the appearance of the work of Beth and of DuMond, R. T. Birge has developed, very elaborately, tables giving analytic expressions for the relative sizes of scale units and angles, etc., etc., which amount, as he points out, to precise directions for constructing a variety of charts both of the type here described and of the Birge-Bond type. These analytic expressions, while interesting, give the impression that such charts are rather tedious and difficult to construct and that extensive computations may be involved. In practice, however, the construction of a chart can be done very simply and accurately by graphical means as here explained.

1.0 percent in e/m corresponds to a displacement to the lower right-hand corner of the hexagon. Thus the zero axis or trace for the percent scale of $h/(em)^{\frac{1}{2}}$ must pass through the upper left and lower right corners of the hexagon and the scale of $h/(em)^{\frac{1}{2}}$ is most conveniently laid out normal to this direction. Suppose we wish to have this scale cover a range of ± 0.5 percent. Evidently a displacement of the percent deviation of h/e from zero to $+0.5$ percent, with e/m maintained at its origin value, will increase $h/(em)^{\frac{1}{2}}$ just $+0.5$ percent. On the chart the point where the percent variations of e/m and h/e have the respective values 0 and 0.5 percent fixes the distance of the $+0.5$ percent trace for $h/(em)^{\frac{1}{2}}$ from the zero percent trace for that function. It is elementary drafting procedure to construct the point in question and project it on the scales of $h/(em)^{\frac{1}{2}}$ which can then be divided and subdivided into the appropriate number of parts. The procedure for e^2/mh follows exactly the same outline.

Now, however, for the noncozonal scales the procedure differs only very slightly from the preceding as was very briefly indicated in a footnote in I NC (page 158). Each noncozonal function F can always be made to satisfy an identity of the form

$$(h/e)^i(e/m)^j \equiv (c/2\pi^2)R_\infty F^k.$$

Upon substituting the Bohr expression for R_∞ into this identity it is possible to solve for i, j and k. An example is $F=h$

$$(h/e)^{-\frac{1}{2}}(e/m)^{-1} = (c/2\pi^2)R_\infty h^{-2}.$$

This calls for a double scale on which variations of R_∞ with h constant and of h with R_∞ constant are to appear. Evidently the zero axis for percent variations of $R_\infty h^{-2}$ corresponds to percent variations of h/e one-fifth as great and of opposite sign as the variations in e/m. Thus the zero axis can be graphically constructed just as explained before and the axis of the $R_\infty h^{-2}$ scale is laid out normal to this direction. Here, evidently, we see from the exponents in the above equation that holding the percent value of e/m at zero a decrease of 0.8 percent in h/e will produce an increase of 4.0 percent in R_∞ (h constant) or a decrease of 2.0 percent in h (R_∞ constant). Thus the displacement and sense for the ranges $R_\infty = \pm 4.0$ percent, $h = \pm 2.0$ percent on this scale are graphically constructed and the scale is divided up accordingly. These procedures suffice to construct scales for any type of function of e, m and h desired.

The origin values should of course be computed for all the functions with considerably greater accuracy than any of the data of experiment. These on the present chart differ slightly from those in I NC. They have been computed to be consistent with $R_\infty = 109{,}737$ cm^{-1}. Once the origin value is known for any function it is a simple matter to construct a direct-reading scale for that function from the existing scale of relative deviation. A slide rule is amply accurate for computing the percent deviations corresponding to the decimal figures of the direct scale. The easiest procedure is to pick out two decimal figures each occurring near one of the ends of the direct-reading scale to be plotted, compute their corresponding percent deviations and plot them. Then by ordinary drafting technique carefully divide up the intermediate interval into the appropriate number of equal parts.[17]

[17] The author has prepared a master blank chart, to large scale, with considerable care, on tracing paper. This carries all the scales shown in Fig. 2 of this article but has no experimental results traced upon it. At a small charge (50¢ each) for the cost of black line contact printing and postage this chart will be supplied to anyone desiring it. The dimensions are approximately 30×35 inches. The contact printing and developing process fortunately introduces quite negligible distortion. All the prints are carefully checked as regards this point.

Note on Interaction Energies in Radiation Theory

H. HURWITZ, JR.
Harvard University, Cambridge, Massachusetts
(Received June 6, 1940)

Radiation interaction energies are calculated for a photon and electron, a photon and scalar or vector mesotron, two electrons, and two scalar mesotrons. For a charged particle and photon the interaction energy is inversely proportional to the frequency of the photon and does not transform like the time component of a four-vector. For two charged particles the interaction energy is closely related to the Møller matrix element.

I. INTRODUCTION

THE procedure in calculating the energy eigenvalues of a system consisting of material particles and a radiation field is to solve the problem exactly with the matter and radiation considered as independent and then treat the interaction as a perturbation. But the change in energy levels due to the perturbation turns out to be infinite so that it is not possible to obtain a satisfactory theory of the self-energy of a single particle by this method. As is well known, however, those results of quantum electrodynamics which are concerned with the interaction of two or more particles are found to be in good agreement with experiment. It is therefore of interest to see whether the ordinary technique of self-energy calculations can be made to give sensible results when applied to the interaction energy of several particles. To obtain this interaction energy it is necessary to calculate the energy when all the particles are present together and subtract from this the energy of each of the particles when it is present by itself. All these energies are infinite, but if the subtractions are made in the most natural manner the answers are definite. Actually, in a theory in which pair production is possible a subtraction of this kind is necessary even to obtain the self-energy of a single particle since the perturbed energy is infinite even for a vacuum.

In this paper interaction energies are calculated for a photon interacting with an electron, scalar mesotron, or vector mesotron; two electrons, and two scalar mesotrons. In all cases the results are finite in the order e^2 and may be given simple physical interpretations. The interaction energy of a photon and electron or mesotron is inversely proportional to the frequency of the photon, and does not transform like the time component of a four-vector. The reason for the latter is that it is not possible to define an energy-momentum four-vector for a system consisting of charged particles and a radiation field without taking adequate account of the forces holding the charges together. The divergent self-energy results show that this is not done adequately in the present quantum theory.

In finding the energy level perturbations due to the interaction between matter and radiation field either of two procedures may be used. One is to apply the ordinary methods of perturbation theory directly.[1] The other, developed by Weisskopf, is to express the change in energy levels as the average value of certain operators over the perturbed state.[2,3] The latter method gives more insight into the physical significance of the various terms. In this paper both procedures will be described.

II. INTERACTION OF A PHOTON AND ELECTRON

The Hamiltonian of the system consisting of electrons and radiation field may be written

$$\mathcal{H}=\frac{1}{8\pi}\int(E^2+H^2)d\tau-\frac{1}{4\pi}\int\varphi\cdot\operatorname{div}E d\tau$$

$$+\int\left(\rho\varphi-\frac{\mathbf{i}\cdot\mathbf{A}}{c}\right)d\tau+c\int\psi^*(\boldsymbol{\alpha}\cdot\mathbf{p}+\beta mc)\psi d\tau, \quad (1)$$

where the third integral constitutes the interaction since it contains variables of both matter

[1] I. Waller, Zeits. f. Physik **62**, 673 (1930).
[2] V. Weisskopf, Zeits. f. Physik **89**, 27 (1934); **90**, 817 (1934).
[3] V. Weisskopf, Phys. Rev. **56**, 72 (1939).

and field. Here

$$\rho = e\psi^*\psi - \sigma, \quad \mathbf{i}/c = e\psi^*\boldsymbol{\alpha}\psi, \tag{2}$$

where e is the algebraic value of the electron charge, and σ is the charge density of electrons in negative energy states. Using second quantization we write

$$\psi = \sum a_q \varphi_q,$$

$$\varphi_q = (u_q/V^{\frac{1}{2}}) \exp[i(\mathbf{p}_q \cdot \mathbf{r})/h],$$

where u_q is a normalized spinor. The a_q's are the Fermi-Dirac operators satisfying the relations

$$a_q a_{q'}^* + a_{q'}^* a_q = \delta_{qq'},$$

$$a_q a_{q'} + a_{q'} a_q = 0,$$

$$a_q^* a_{q'}^* + a_{q'}^* a_q = 0.$$

By eliminating the longitudinal field components the Hamiltonian may be put in the form

$$\mathfrak{H} = H_r + H_m + H',$$

$$H' = W_{st} - \int \frac{\mathbf{i}\cdot\mathbf{A}_t}{c} d\mathbf{r},$$

$$W_{st} = \frac{1}{2}\int \frac{\rho(\mathbf{r}_1)\rho(\mathbf{r}_2)}{|\mathbf{r}_1 - \mathbf{r}_2|} d\mathbf{r}_1 d\mathbf{r}_2,$$

$$H_m = c\int \psi^*(\boldsymbol{\alpha}\cdot\mathbf{p} + \beta mc)\psi d\mathbf{r} = \sum N_q E_q,$$

$$H_r = \sum M_s h\nu_s.$$

$\mathbf{A}_t$ is the transverse part of the vector potential and is given by

$$\mathbf{A}_t = \sum_s \mathbf{e}_s \frac{ch^{\frac{1}{2}}}{(V\nu_s)^{\frac{1}{2}}}\left\{A_s^* \exp\left[-\frac{i\mathbf{k}_s\cdot\mathbf{r}}{h}\right] + A_s \exp\left[\frac{i\mathbf{k}_s\cdot\mathbf{r}}{h}\right]\right\}.$$

$\mathbf{k}_s$ is the momentum of the photon s which is polarized in the direction $\mathbf{e}_s$ and has frequency $\nu_s = ck_s/h$. The A_s's are the Einstein-Bose operators of the radiation field and are defined as follows:

$$(M_s|A_s|M_s+1) = (M_{s+1}|A^*|M_s) = (M_s+1)^{\frac{1}{2}} \tag{3}$$

and all other elements are zero. We have taken a gauge in which the scalar potential of the radiation field vanishes.

If $\Phi(\cdots M_s \cdots; \cdots N_q \cdots)$ is the probability amplitude for the state in which M_s photons are present in state s, and N_q electrons are present in state q, we have

$$ih\partial\Phi/\partial t = (H_m + H_r + H')\Phi.$$

We try to obtain solutions of this equation in the form

$$\Phi = e^{-iWt/h}(\Phi_0 + \lambda\Phi_1 + \cdots),$$

where λ is proportional to the electron charge, and

$$\Phi_0(\cdots M_s \cdots; \cdots N_q \cdots) = \cdots \overset{M_s}{\delta_{M_s 0}} \cdots \overset{N_s}{\delta_{N_s 0}} \cdots$$

so that

$$(H_m + H_r)\Phi_0 = W_0\Phi_0.$$

Then

$$W = W_0 + (o|H'|o) + \sum_j \frac{|(j|H'|o)|^2}{W_0 - W_j} \tag{4}$$

where o and j are abbreviations for complete sets of quantum numbers. The only part of H' which has diagonal elements is W_{st} and this does not contribute to the interaction of a photon and electron. Therefore to compare the energy of two states we simply compare terms in the sum over j. We then have for the interaction energy of a photon and electron

$$\Delta W = (W_{\text{vac+el+phot}} - W_{\text{vac}}) - (W_{\text{vac+el}} - W_{\text{vac}}) - (W_{\text{vac+phot}} - W_{\text{vac}}).$$

The calculations are slightly different depending on whether or not the negative energy electron states are assumed occupied. If we assume them empty we have

$$\Delta W = (A) + (B) + (C) + (D),$$

where (A), (B), (C), and (D) are the terms appearing in the sum over j for the following virtual transitions:

(A): Absorption of the photon; the electron goes to a positive energy state.

(B): Stimulated emission of a second photon similar to the one already present; the electron goes to a positive energy state.

(C) and (D): Same as (A) and (B) with the electron going to a negative energy state. For the

negative energy states assumed filled we have

$$\Delta W=(A)+(B)-(C')-(D'),$$

where (A) and (B) are the same as before, and (C') and (D') are described as follows:

(C'): In calculating $W_{\text{vac+el+phot}}$ the transition in which a vacuum electron absorbs the photon and goes to the state occupied by the positive energy electron does not appear because of the exclusion principle.

(D'): Similarly a vacuum electron cannot make a transition to the state occupied by the positive energy electron with stimulated emission of the photon.

Writing out the matrix elements and energy denominators explicitly and remembering that in all cases the spins of either the initial or final states of the virtual transitions are arbitrary we find, whether the negative energy states are occupied or not,

$$\Delta W=\frac{2\pi e^2ch^2}{kV}\sum_{l=1}^{4}\left\{\frac{|\{u_l^*(\mathbf{p}_0-\mathbf{k})\alpha_s u_{l_0}(\mathbf{p}_0)\}|^2}{E_{l_0}(\mathbf{p}_0)-E_l(\mathbf{p}_0-\mathbf{k})-ck}+\frac{|\{u_l^*(\mathbf{p}_0+\mathbf{k})\alpha_s u_{l_0}(\mathbf{p}_0)\}|^2}{E_{l_0}(\mathbf{p}_0)-E_l(\mathbf{p}_0+\mathbf{k})+ck}\right\}.$$

Here α_s is the component of $\boldsymbol{\alpha}$ parallel to the polarization of the photon $\mathbf{k}$ and

$$E_{1,2}(p)=+(c^2p^2+m^2c^4)^{\frac{1}{2}},$$

$$E_{3,4}(p)=-(c^2p^2+m^2c^4)^{\frac{1}{2}}.$$

To evaluate the above expression it is necessary to consider the sums over $l=1, 2$ and $l=3, 4$ separately because the energy denominators are different in the two cases. These summations may be performed by means of selection operators in the usual way. It is then seen that the expression is independent of the spin state of the electron so that it is permissible to average over any two independent states by further selection operators. Straightforward computations give

$$\Delta W=\frac{2\pi e^2ch^2}{VkE(p_0)}=\frac{e^2}{2VE(p_0)}\left\langle\int\mathbf{A}_s^2d\mathbf{r}\right\rangle_{\text{Av}}, \quad (5)$$

where $\mathbf{A}_s$ is the vector potential due to the photon. If more than one photon is present the interaction energy is just the sum of the interaction energies between the electron and each photon. This follows because from (3) the squares of the matrix elements depend on the number of photons present in the state. (The photons interact with each other only in higher orders than we are considering here.) Therefore if there are M photons of frequency ν per unit volume,

$$\Delta W=\frac{MV2\pi e^2ch^2}{VkE(p_0)}=\frac{1}{2\pi}\frac{e^2c^2}{\nu^2}\frac{G_r}{E(p_0)},$$

where G_r is the radiation energy density.

To obtain this result by the alternative method of Weisskopf we proceed in the following way. It has been shown that the change in energy eigenvalues due to the perturbing Hamiltonian may be obtained by dividing those terms in the perturbation which are explicitly proportional to e by two, leaving the terms explicitly proportional to e^2 unchanged, and then averaging the result over the perturbed state.[4] Therefore

$$W-W_0=\left\langle W_{sl}-\frac{1}{2}\int\frac{\mathbf{i}\cdot\mathbf{A}_l}{c}d\mathbf{r}\right\rangle_{\text{Av}}.$$

As before W_{sl} does not contribute for a photon and electron. It suffices to replace $\mathbf{A}_l$ by $\mathbf{A}_s$, the vector potential of the photon, and $\mathbf{i}$ by $\mathbf{i}'$, the perturbed current, since the scalar product of the unperturbed current and $\mathbf{A}_s$ averages to zero. Therefore

$$\Delta W=-\left\langle\int\frac{\mathbf{i}'\cdot\mathbf{A}_s}{2c}d\mathbf{r}\right\rangle_{\text{Av}}. \quad (6)$$

We do not include the perturbed current due to the vacuum electrons in $\mathbf{i}'$. The perturbed current may be calculated by considering the radiation field as an externally applied time dependent perturbation. Weisskopf has shown that for a stationary electron

$$\mathbf{i}'=-ce^2\mathbf{A}_s/mc^2V. \quad (7)$$

This is true in either one electron theory or hole theory. To obtain the value of $\mathbf{i}'\cdot\mathbf{A}$ for an electron with arbitrary velocity we make a Lorentz transformation. To carry this through we make use of some simple relations. First it may be shown that for a plane light wave

[4] Reference 3, p. 80.

G_r/ν^2 is an invariant. It then follows that if we always use a gauge in which the scalar potential is zero, $\mathbf{A}^2$ is an invariant. From this result, together with (7) we can prove that $\mathbf{i}'\cdot\mathbf{A}$ is also an invariant. Therefore we have

$$\mathbf{i}'\cdot\mathbf{A}=\mathbf{i}_0'\cdot\mathbf{A}_0=-\frac{ce^2}{V_0}\frac{\mathbf{A}_0^2}{mc^2}=-\frac{ce^2\mathbf{A}^2}{V_0mc^2},$$

where the subscript zero indicates the rest system of the electron. But $V=V_0(1-\beta^2)^{\frac{1}{2}}$ where V and V_0 are the volumes ascribed to the electron in the two systems by the quantization procedure, and $\beta=v/c$. Therefore

$$\mathbf{i}'\cdot\mathbf{A}_s=\frac{-ce^2\mathbf{A}_s^2}{Vmc^2}(1-\beta^2)^{\frac{1}{2}}=-\frac{ce^2A_s^2}{VE(p_0)}. \quad (8)^5$$

This expression may also be obtained by carrying through the original calculations for general velocity of the electron. Inserting (8) into (6) we obtain (5) again. Since G_r/ν^2 is an invariant, ΔW transforms as $1/E(p_0)$ and is not the time component of a four-vector.

III. Mesotron and Photon

The calculations for mesotrons are essentially the same as for the Dirac electron. But here the interaction Hamiltonians have terms proportional to $e^2\mathbf{A}^2$ which give rise to diagonal elements that contribute to the expression (4).[6] The off-diagonal elements of the part of the interaction proportional to $e\mathbf{A}$ again give contributions proportional to e^2A^2 through the last term in (4). The virtual transitions occurring are of the same sort as before with transitions involving pair production replacing those described as involving negative energy states. Calculations show that the contributions of the various transitions to the interaction energy always just cancel for a scalar mesotron so that only the diagonal elements remain. For a moving vector mesotron this is in general not so. If we use Weisskopf's alternative method we find that (6) again holds.[4,7] This is because the interaction Hamiltonian for a scalar or vector mesotron is of the form

$$-\int\left(\frac{\mathbf{i}_1\cdot\mathbf{A}}{c}+\frac{\mathbf{i}_2\cdot\mathbf{A}}{2c}\right)d\mathbf{r},$$

where $\mathbf{i}_1$ is the part of the current explicitly independent of $\mathbf{A}$ and proportional to e while $\mathbf{i}_2$ is explicitly proportional to $e^2\mathbf{A}$. To calculate $\mathbf{i}'\cdot\mathbf{A}$ we may again apply a relativity transformation to (7) which holds also for mesotrons.[3,7] By (6) and (8) we see that the interaction energy is again given by (5). It is easy to check the expression (5) by direct calculation for a scalar mesotron with arbitrary velocity, and for a few of the simpler cases for a vector mesotron. For a scalar mesotron the calculations were also carried through with the unquantized Gordon-Klein equation. Equation (5) was again obtained.

IV. Two Charged Particles

To calculate the interaction energy of two electrons it is convenient to start with the Hamiltonian in the form (1). Then, using Weisskopf's method, we have

$$W-W_0=\left\langle\frac{1}{2}\int\left(\rho\varphi-\frac{\mathbf{i}\cdot\mathbf{A}}{c}\right)d\mathbf{r}\right\rangle_{Av}.$$

We may take

$$\mathbf{A}(\mathbf{r},t)=\int\frac{\mathbf{i}(\mathbf{r}',t-|\mathbf{r}-\mathbf{r}'|/c)}{c|\mathbf{r}-\mathbf{r}'|}d\mathbf{r}',$$

$$\varphi(\mathbf{r},t)=\int\frac{\rho(\mathbf{r}',t-|\mathbf{r}-\mathbf{r}'|/c)}{|\mathbf{r}-\mathbf{r}'|}d\mathbf{r}',$$

where $\mathbf{i}(\mathbf{r},t)$ and $\varphi(\mathbf{r},t)$ are given by (2). These expressions may be evaluated and we find

$$\Delta W=(W_{1+2}-W_{\text{vac}})-(W_1-W_{\text{vac}})-(W_2-W_{\text{vac}})$$

$$=\int\frac{\rho(\mathbf{r}_1)\rho(\mathbf{r}_2)}{|\mathbf{r}_1-\mathbf{r}_2|}d\mathbf{r}_1d\mathbf{r}_2-\int\frac{\mathbf{i}(\mathbf{r}_1)\cdot\mathbf{i}(\mathbf{r}_2)}{c^2|\mathbf{r}_1-\mathbf{r}_2|}d\mathbf{r}_1d\mathbf{r}_2$$

$$-\frac{4\pi e^2h^2c^2}{V}\left[\frac{|\{u_{q_1}^*u_{q_2}\}|^2-\{u_{q_1}^*\boldsymbol{\alpha}u_{q_2}\}\{u_{q_2}^*\boldsymbol{\alpha}u_{q_1}\}}{c^2(\mathbf{p}_1-\mathbf{p}_2)^2-(E_1-E_2)^2}\right].$$

[5] This result is not quite the same as for a classical point charge under the influence of a radiation field. There if the point charge is moving parallel to the electric field we obtain, because of the longitudinal mass,

$$\mathbf{i}'\cdot\mathbf{A}_s=-e^2\mathbf{A}_s^2(1-\beta^2)^{\frac{1}{2}}/mc.$$

But if in the rest system there are N_0 charges per unit volume we obtain for the perturbed current per unit volume

$$\mathbf{i}'\cdot\mathbf{A}_s=-e^2N\mathbf{A}_s^2(1-\beta^2)^{\frac{1}{2}}/mc.$$

which is analogous to (8). Here N is the number of charges per unit volume in the system in which the charges are moving, and $N=N_0/(1-\beta^2)^{\frac{1}{2}}$. The difference between the two results is caused by fluctuations in N due to the small oscillations of the charges. This causes the term $Ne\mathbf{v}$ in the current density to fluctuate ($\mathbf{v}$ is the unperturbed velocity).

[6] W. Pauli and V. Weisskopf, Helv. Phys. Acta **7**, 709; H. Yukawa, Proc. Phys. Math. Soc. Japan **20**, 319 (1938); N. Kemmer, Proc. Roy. Soc. **A166**, 127 (1938).

[7] R. Richtmyer, Phys. Rev. **57**, 413 (1940).

where $\rho(r_i)$ and $\mathbf{i}(r_i)$ are the average charge and current densities of the two electrons. The first two terms correspond to the interaction of two uniform charge and current distributions over the volume V. The other term comprises the correction to this due to the antisymmetrical character of the wave functions, and the spin motion of the electrons. It has the form of the Møller matrix element of a transition in which the electrons just change places.[8] Of course such a transition has no physical significance. Formally it is forbidden by the exclusion principle and so appears in the interaction energy with a minus sign. If we eliminate the longitudinal field components and use ordinary perturbation theory we obtain the same expression for ΔW with the exception of the second term. This does not appear since in the expansion of the radiation field which is used there is no photon of zero wave-length to enable the constant current distributions to interact.

For two scalar mesotrons the situation is the same except insofar as it is modified by the Einstein-Bose statistics of the particles. In calculating $\mathbf{A}(\mathbf{r})$ and $\varphi(\mathbf{r})$ care must be taken to give the operators appearing in the Fourier expansion of the wave functions their correct time dependence. We find

$$\Delta W=\int\frac{\rho(\mathbf{r}_1)\rho(\mathbf{r}_2)}{|\mathbf{r}_1-\mathbf{r}_2|}d\mathbf{r}_1d\mathbf{r}_2 -\int\frac{\mathbf{i}(\mathbf{r}_1)\cdot\mathbf{i}(\mathbf{r}_2)}{c^2|\mathbf{r}_1-\mathbf{r}_2|}d\mathbf{r}_1d\mathbf{r}_2+M,$$

where[9]

$$M=\frac{\pi e^2h^2c^2[(E(p_1)+E(p_2))^2-c^2(\mathbf{p}_1+\mathbf{p}_2)^2]}{VE(p_1)E(p_2)[c^2(\mathbf{p}_1-\mathbf{p}_2)^2-(E(p_1)-E(p_2))^2]}$$

for like particles, and

$$M=\frac{\pi e^2h^2c^2[(E(p_1)-E(p_2))^2-c^2(\mathbf{p}_1-\mathbf{p}_2)^2]}{VE(p_1)E(p_2)[c^2(\mathbf{p}_1-\mathbf{p}_2)^2-(E(p_1)-E(p_2))^2]}$$

for unlike particles. $\mathbf{p}_i$ is the momentum of the particle.

The author wishes to thank Professor W. H. Furry for suggesting this problem, and for many helpful discussions and suggestions during the course of its investigation.

[8] C. Møller, Zeits. f. Physik **70**, 790 (1931).

[9] The expression M is analogous to the Møller matrix element for two scalar mesotrons. It has the same transformation properties as the formula obtained for the Dirac electron. (For the Dirac electron

$$|\{u^*_{q_1}u_{q_2}\}|^2-\{u^*_{q_1}\boldsymbol{\alpha}u_{q_2}\}\{u^*_{q_2}\boldsymbol{\alpha}u_{q_1}\}$$

is not an invariant since the u_q's must be taken as normalized in each system and so do not transform in the usual way.)

Internal Friction of Aluminum*

R. H. RANDALL AND CLARENCE ZENER†
College of the City of New York, New York, New York

(Received July 15, 1940)

It has previously been pointed out that the nearly elastic isotropy of aluminum necessitates a very small internal friction. By making measurements over a range of grain size and of frequency, it is established that the internal friction of aluminum is less than a tenth of that of α-brass under corresponding conditions.

IN a polycrystalline metal a macroscopically uniform stress is rendered microscopically inhomogeneous by the elastic anisotropy of the individual crystallites. The thermal currents generated by these stress inhomogeneities in a vibrating specimen are, under appropriate conditions, the dominant source of internal friction.[1–4] One thus expects a correlation between the internal friction of a polycrystalline metal and the elastic anisotropy of the individual crystallites.

The only cubic metal thus far investigated is 70–30 α-brass, whose elastic anisotropy factor

$$\left(\frac{E_{111}-E_{100}}{E_{111}+E_{100}}\right)^2$$

is 0.3. Of the common metals aluminum has the lowest elastic anisotropy factor, namely 0.008. One thus expects that under corresponding conditions the internal friction of aluminum will have an order of magnitude less than that of brass. The present experiment was undertaken to test this expected correlation between elastic anisotropy and internal friction.

Specimens ($\frac{1}{8}\times\frac{1}{2}\times 12$ inches^3) of aluminum with 2 percent magnesium in solid solution were prepared by the Aluminum Company of America through the courtesy of Dr. William L. Fink. The magnesium was added to minimize the effect of creep. The method of preparation has been described elsewhere.[5] The grain size was determined by counting the number of grains along a line 1 mm in length in a number of areas, and the average taken for each of the principal directions. These data, furnished by Dr. Fink, are given in Table I. An arbitrary measure of grain size is the reciprocal of the geometrical mean of the number of grains per mm along the three principal directions. This grain size is given in the last column of Table I.

The internal friction was measured with longitudinal vibrations, by a method previously described.[3] Our observations, given in Fig. 1, may best be interpreted in terms of the dimensionless adiabaticity parameter

$$\frac{\text{frequency}\times(\text{grain size})^2}{\text{thermal diffusion constant}}.$$

The value of this parameter in the middle of the frequency range used is given in Fig. 1 for each specimen. The internal friction has a maximum when this parameter lies between 2 and 3, and decreases steadily as this parameter increases, either due to an increase in frequency or to an increase in grain size. Since the internal friction due to intercrystalline thermal currents has a maximum when this parameter has the order of magnitude of unity, and decreases steadily as

TABLE I. *Grain size of specimens.*

Reduction %	Grains/mm Long	Cross	Thick	Grain Size (in mm)
5	3	1.5	3	0.4
10	5	4	4	0.22
30	9	9	10	0.11
75	12	10	13	0.09

* This research was supported by a grant from the Penrose Fund of the American Philosophical Society, and by a grant from the Rumford Fund of the American Academy of Arts and Sciences.

† Now at The State College of Washington, Pullman, Washington.

[1] C. Zener, Phys. Rev. **53**, 90 (1938).

[2] R. H. Randall, F. C. Rose and C. Zener, Phys. Rev. **56**, 343 (1939).

[3] C. Zener and R. H. Randall, Metals Technology **7**, Jan. (1940).

[4] C. Zener, Proc. Phys. Soc. **52**, 152 (1940).

[5] L. W. Eastwood, R. W. James and R. F. Bell, Trans. Am. Inst. Mining and Metallurgical Eng. **133**, 124 (1939).

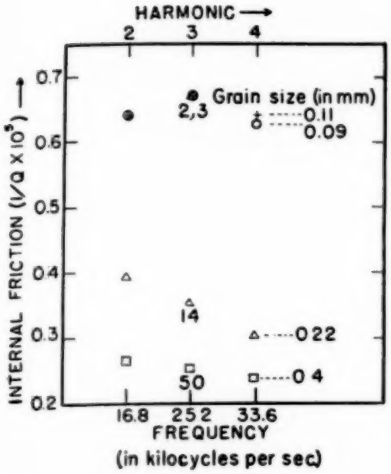

FIG. 1. Internal friction of aluminum (2 percent magnesium) ○, +, △, □ refer to specimens of grain size 0.09, 0.11, 0.22, 0.4 mm, respectively. The numbers beneath each measurement at 25.2 kilocycles/sec. refer to the adiabaticity parameter at that frequency.

this parameter increases to large values,[1] we conclude that the dominant part of the internal friction here measured is due to this cause. Our observed maximum of 0.67×10^{-5} is an upper limit to the maximum internal friction which intercrystalline thermal currents can cause in aluminum. This is an order of magnitude less than the maximum of 9×10^{-5} in 70–30 α-brass.[2]

The maximum of the internal friction of brass occurred at a value of the adiabaticity parameter of about 5, while here we find a maximum in aluminum where this parameter lies between 2 and 3. This discrepancy is removed when we consider that the grain size was determined by different methods in the two cases, in the former by counting the number of grains in a unit area, in the latter by counting the number of grains crossed by a line of unit length. An approximate calculation shows that the grain size defined by the intercept method is smaller by the factor of $4/\pi^{\frac{1}{2}}\backsimeq0.72$ than that obtained by the area method. This factor is just sufficient to remove the apparent discrepancy.

The maximum internal friction here obtained is considerably less than the lowest values heretofore found for aluminum, 1.1×10^{-5} by Wegel and Walther,[6] 1.5×10^{-5} by Förster and Köster.[7]

[6] R. L. Wegel and H. Walther, Physics **6**, 141 (1935).
[7] F. Förster and W. Köster, Zeits. f. Metallkunde **29**, 116 (1937).

LETTERS TO THE EDITOR

Prompt publication of brief reports of important discoveries in physics may be secured by addressing them to this department. Closing dates for this department are, for the first issue of the month, the eighteenth of the preceding month, for the second issue, the third of the month. Because of the late closing dates for the section no proof can be shown to authors. The Board of Editors does not hold itself responsible for the opinions expressed by the correspondents.

Communications should not in general exceed 600 words in length.

The Simultaneous Emission of Three Particles from an Excited Nucleus

In an attempt to observe the half-life of the radioactive isotope of sulphur of mass 31, which is of the type discussed by Wigner,[1] having one more proton than neutron, sulphur was bombarded by very energetic neutrons. When the neutrons from lithium, with energies up to 24 Mev, were allowed to fall on either pure sulphur or carbon disulphide, radioactivities of half-life 12.7 sec. and 2 min. 17 sec. were observed. When neutrons from beryllium, with energies up to 13 Mev are employed only the shorter period of 12.7 sec. is found and there is no indication of the longer-lived activity. This 12.7-sec. activity was shown by the cloud chamber to emit electrons while the 2-min. 17-sec. emitter gives only positrons.

In order to identify the activity chemically a quantity of carbon disulphide with free sulphur in solution was given short bombardments. The activated atoms were extracted by shaking with dilute sulphuric and nitric acids and then separately precipitated as either a phosphate or a sulphate. The strong positron emitter of 2-min. 17-sec. half-life was shown to be an activity in phosphorus and hence undoubtedly the well-known previously reported[2] activity attributed to phosphorus of mass 30. It could be made from the abundant sulphur isotope of mass 32 only by an $(n, 2nP)$ reaction or an $(n, 3n)$ reaction followed by the emission of a positron. This is thus the first well-established case of the simultaneous emission of three heavy particles from a nucleus, a process not unexpected at the high energy of the incident neutrons.

The activity of 12.7-sec. half-life being a negative emitter cannot be due to sulphur of mass 31 but is undoubtedly attributable to a phosphorus isotope of mass greater than 31. The activity due to sulphur 31 as predicted must have a half-life exceedingly short since it could not be detected with the technique here employed.

The rapid chemical separations were very kindly made by Mr. W. H. Sullivan and Mr. A. F. Voigt of the Department of Chemistry. This investigation was made possible by a grant from the Horace H. Rackham Fund.

J. M. Cork
W. Middleton

University of Michigan,
Ann Arbor, Michigan,
August 11, 1940.

[1] E. P. Wigner, Phys. Rev. **56**, 519 (1939).
[2] I. Curie and F. Joliot, Comptes rendus **198**, 254 (1934), *et sub.*

Photon Production of Mesotrons

The photographs of Fig. 1 show two views of a large Wilson cloud chamber containing five horizontal lead plates each one cm thick. The photograph to the left is taken at 30° to the left of normal while that on the right is taken at 30° to the right of normal. Because both tracks penetrate several lead plates without producing shower particles they cannot be electrons. Since it is very unlikely that a photon would have sufficient energy to produce two protons, the conclusion is that the two penetrating particles are mesotrons, and that we have evidence of the production of a pair of mesotrons by a photon.

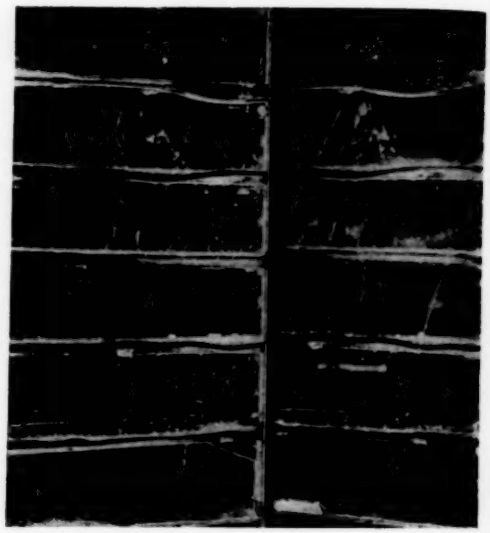

Fig. 1.

This picture was made in the Mt. Evans laboratory at an altitude of 14,170 feet. The dimensions of the chamber are 18×12×5 inches deep, and the chamber was counter-controlled though the picture obtained could not have been controlled by the counters. A rough estimate indicates that heavily ionized tracks were obtained in about one picture out of 80. These could be identified as protons or mesotrons in many cases.

Wilson M. Powell

Department of Physics,
Kenyon College,
Gambier, Ohio,
August 14, 1940.

Nuclear Spin of Cl^{37}

Elliott[1] in his study of the absorption spectrum of Cl_2 was able to identify the spectra of the two species of molecules, $Cl^{35}Cl^{35}$ and $Cl^{35}Cl^{37}$, but, due to their low intensity, was not able to identify lines belonging to the third species, namely $Cl^{37}Cl^{37}$. From the alternating intensity ratio in the lines due to $Cl^{35}Cl^{35}$ he was able to assign the value of 5/2 as the nuclear spin of Cl^{35}. With the view in mind of obtaining the alternating intensity ratio in the spectrum of $Cl^{37}Cl^{37}$ a sufficient amount of chlorine gas enriched in the heavy isotope was obtained for the purpose.

The enriched chlorine was obtained by the use of a multistage thermal diffusion column similar to that first developed by Clusius and Dickel.[2] The column employs hydrogen chloride gas at atmospheric pressure. The column consists of four sections each 3 meters long connected together by convective coupling to give a total effective length of 12 meters. To avail oneself of all the possible separation factor of the column in producing "heavy" HCl, a stream of fresh HCl is passed through the top of the column at a rate of 500 cc an hour.

After allowing the column to approach equilibrium for ten days a withdrawal of approximately 33 cm^3 of HCl daily was begun. Ten days falls short of the time needed to reach equilibrium with zero withdrawal but with a withdrawal of 33 cm^3 a day one will be operating at a considerable distance from equilibrium concentrations; hence, there is no need to reach equilibrium.

After 500 cm^3 of HCl was collected in this way it was converted into Cl_2. The Cl_2 was then placed in a specially constructed absorption tube designed for the longest possible light path with the smallest possible volume. A path length of 5 meters at a gas pressure of 41 cm was sufficient to obtain the 1→11, 1→12, 1→13 vibration bands of the $^1\Sigma^+ \rightarrow 0^+$ system of Cl_2 in the region 5100–5200A. The intensity ratio of lines due to $Cl^{35}Cl^{35}$ and $Cl^{37}Cl^{37}$ in the 1→12 band was 1.76, giving 43 percent Cl^{37} in this sample as against 24.2 percent Cl^{37} in normal Cl_2. The complexity of the 1→11 and 1→13 bands prevented the identification of lines due to $Cl^{37}Cl^{37}$. The alternating intensity ratio of 24 available lines in the 1→12 band for $Cl^{37}Cl^{37}$ was 1.28.

A determination from normal Cl_2 of the alternating intensity ratio of $Cl^{35}Cl^{35}$ for these three bands gave 1.30 as against Elliott's value of 1.34. As Elliott pointed out these values must be taken as lower limits of the intensity ratio since any overlying lines would lower the observed value of any actual intensity ratio. Thus these ratios most nearly correspond to a spin of 5/2 for which the ratio is 1.40. We may conclude that Cl^{35} and Cl^{37} have the same nuclear spin and its most probable value is 5/2.

E. F. SHRADER

Sloane Physics Laboratory,
Yale University,
New Haven, Connecticut,
August 15, 1940.

[1] A. Elliott, Proc. Roy. Soc. **127**, 638–657 (1930).
[2] K. Clusius and G. Dickel, Zeits. f. physik. Chemie **B44**, 397–473 (1939).

Neutron Capture by Uranium (238)*

In continuation of our work on separated uranium isotopes,[1] it was thought worth while to find out experimentally which isotope is responsible for the well-known 24-minute neutron capture product.

A sample of uranium (238) containing between 5 and 10 percent of the natural U^{235} content was prepared by one of us (A. O. N.) by means of a mass spectrometer. From the average value of the current and the time of deposit it was estimated that the weight of the sample was 19 micrograms. The uranium (238), deposited on a thin platinum foil, was placed in a cadmium box and irradiated with neutrons in a paraffin wax geometry near the Columbia cyclotron. A monitor of UX-free ordinary U_3O_8 was irradiated simultaneously in the cadmium box. After 1-hour exposure to neutrons, the uranium (238) oxide was quantitatively dissolved off the platinum foil with nitric acid and redeposited in the form of U_3O_8 upon a fresh platinum sheet. This was necessary in order to get rid of the induced beta-activity in the original platinum foil.

Ten minutes after the end of the neutron irradiation, the second platinum foil was placed around a thin-walled Geiger-Müller counter, and its activity observed. The decay curve, corrected for a natural background of 18 counts per minute, is shown in Fig. 1. The initial activity was 56 counts per minute, and the decay half-life about 24 minutes. After the beta-activity had decayed the alpha-particles from the U^{235} were counted by means of a linear amplifier and found to be given off at an average rate of 5.1±0.3 counts per minute. This corresponds to a weight of $U^{238}{}_3O_8$ of 17±1 micrograms. This weight was further checked by direct differential weighing on a Sartorius microbalance, and found to be 15±3 micrograms—all in reasonable agreement with the originally estimated amounts. Under the assumption that the alpha-value is the most reliable, an initial specific beta-activity of 3290 counts per minute per milligram of $U^{238}{}_3O_8$ follows.

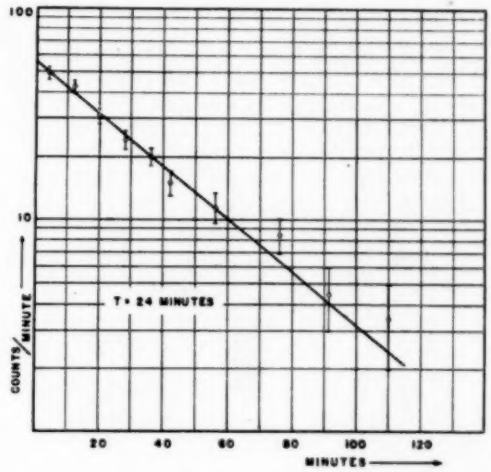

FIG. 1. Decay of resonance capture product of uranium (238).

In order to compare with unseparated uranium under identical geometrical conditions, 40 mg of U_3O_8 were deposited on a platinum surface of 3 square centimeters area, and were irradiated under the same conditions as in the preceding experiment. After irradiation an ether separation of fission products was made. From this sample 8.564 mg of U_3O_8 were deposited on a fresh platinum foil and the initial specific beta-activity determined as before. This gave a value of 3240 counts per minute per milligram of U_3O_8, in good agreement with the value 3290 obtained from the separated isotope.

Substantially the same results were obtained from another sample of 30 micrograms of $U^{238}{}_3O_8$.

The decay period and the specific activity of the neutron induced beta-activity in separated samples of U^{238} are in good agreement with those obtained from the capture in ordinary uranium and leave no doubt that the 24-minute resonance capture in uranium is due to U^{238}. This result was previously anticipated on theoretical grounds by N. Bohr and others.

E. T. Booth
J. R. Dunning
A. V. Grosse

Columbia University,
New York, New York,

A. O. Nier

University of Minnesota,
Minneapolis, Minnesota,
August 13, 1940.

* Publication assisted by the Ernest Kempton Adams Fund for Physical Research of Columbia University.

[1] A. O. Nier, E. T. Booth, J. R. Dunning and A. V. Grosse, Phys. Rev. **57**, 748 (1940).

Period of Photon Emission in a Counter Discharge

That the ionization in a Geiger-Mueller counter takes place in a very early stage of the discharge and before the wire has changed appreciably in potential is an essential element in the mechanism proposed by C. G. Montgomery and D. D. Montgomery.[1] The investigation to be described here leaves no doubt that photon emission in a counter takes place during a short time interval following the initiation of the discharge, and that few, if any, photons are emitted during the greater part of the time required by the wire to reach its maximum negative potential.

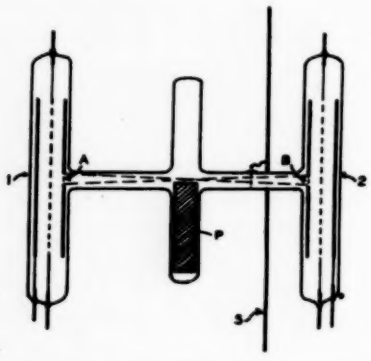

Fig. 1. Arrangement of Geiger-Mueller counters.

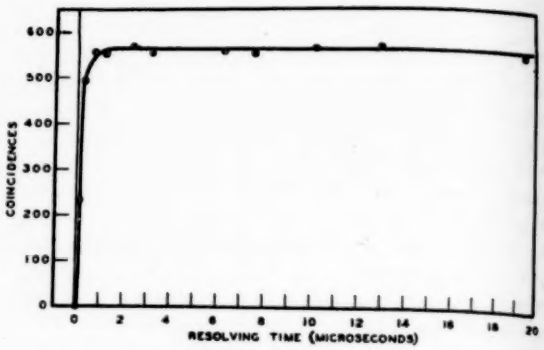

Fig. 2. Relation between coincidence rate and resolving time in experiment A.

Two counters, 1 and 2, Fig. 1, share a common glass envelope. Although the counter wires are carefully shielded electrostatically from each other by S, photons emitted by one may pass to the other through holes A and B in the counter cylinders. This photon transmission is controlled by the plunger P which may be moved to expose any desired portion of the transmitting and receiving areas A and B. The voltage pulses from these counters are applied to a coincidence circuit. The resolving time of this circuit may be varied from $<10^{-7}$ second to 10^{-3} second and special care is exercised to prevent this variation from influencing in any way the discharge phenomena in the counters themselves. These resolving times were determined experimentally employing a pulse generator previously described.[2] With P in such a position as to screen the openings A and B from each other, no coincidences are observed. As A and B are exposed to each other by moving P, coincidences appear, and a point is reached where all discharges in one counter are accompanied by discharges in the other.

In Fig. 2, representing an experiment to be called A, the coincident rate is plotted as a function of resolving time for the case where P was so placed that 90 percent of the discharges in one counter were accompanied by discharges in the other (resolving time 2.0×10^{-4} second). There is no observable increase in the number of coincidences between one and twenty microseconds. In another experiment (experiment B) where P was in such a position that the probability of one counter setting off the other in a time of 2.0×10^{-4} second was 0.42, there was an increase in the number of coincidences between one and twenty microseconds of only (3.1 ± 3.6) percent.

Measurements by the author[3] on a counter of the diameter and pressure used in these experiments indicate that the counter wire experiences one-half of its potential change in the interval between one and twenty microseconds. If the number of photons emitted by a counter in a given time interval were proportional to the change of potential of the wire during the interval, we should expect an increase of the coincidence rate between one and twenty microseconds which amounts to 20 percent for the case A, and 60 percent (or 20 times that found) for the case B. It is safe to assume that any condition, such as

has been formerly assumed in counter discharge theory, in which measurable changes of wire potential were assumed to be accompanied by measurable photon emission, is at variance with the present observations. These experiments are, however, in agreement with the discharge mechanism formulated by C. G. Montgomery and D. D. Montgomery. The lags which actually occur are to be expected, and can be accounted for by electron capture in the gas. This phenomena has been reported elsewhere.[2,4]

W. E. RAMSEY

Bartol Research Foundation of the Franklin Institute,
Swarthmore, Pennsylvania,
July 24, 1940.

[1] C. S. Montgomery and D. D. Montgomery, Phys. Rev. **57**, 1030 (1940).
[2] C. S. Montgomery, W. E. Ramsey, D. B. Cowie and D. D. Montgomery, Phys. Rev. **56**, 635 (1939).
[3] W. E. Ramsey, Phys. Rev. **57**, 1022 (1940).
[4] J. V. Dunworth, Nature **144**, 152 (1939).

The Secondary Peak in the Rossi Curve for Tin

The apparatus, already described[1] comprised primarily five separate horizontal counter areas each containing 18 counters 20 cm long and giving a sensitive area (analyzing tray) 20 cm by 20 cm. The areas were arranged in a vertical array and tin was inserted between the top tray (the first) and the next tray (the second). One-centimeter slabs of lead were placed over trays 3, 4 and 5 for subsidiary reasons. Each counter was connected to an individual electroscope. In addition, above the second tray, but below the tin, there was another counter tray (master tray), without electroscopes. The arrangements were such that the electroscopes were only allowed to operate when at least one ray passed through the whole apparatus including the master tray which, by a side lead shield, guarded against electron showers from the side. The electroscopes recorded photographically the shower history of every *event* associated with the passage of a ray through the whole apparatus.

Figure 1, curve A, shows, plotted against thickness of tin, the number of doubles recorded by the second analyzing tray (below the tin) per 1000 events. It will be observed that the curve shows two maxima, the second one being at 29 cm.

Each point for curve A corresponds in actuality to 1000 observations of events except in the case of the points for 20 cm and 30 cm, which correspond to 2000 observations each. The standard deviations are indicated by the vertical lines. At first sight it is surprising that their magnitude permits the degree of regularity exhibited by the curve. The statistics of this matter will be discussed in greater detail in a more complete publication later to be presented. For the present, it will perhaps cement confidence in the reality of the minimum at 20 cm in the case of curve A by replotting, as in Fig. 1, curve B, the results obtained by utilizing, for each point, just half of the observations utilized in drawing curve A. The statistical errors for curve B are, of course, considerably greater, proportionally, than for curve A. However, the minimum is still well marked. It may be added that in order to avoid systematic changes with time, the curve A was not obtained by taking all the observations for the individual points in succession. A smaller number of observations was taken for the whole set of points and repeated backwards and forwards so as to ensure that as far as possible the observations for each point extended over the same period of operation of the apparatus.

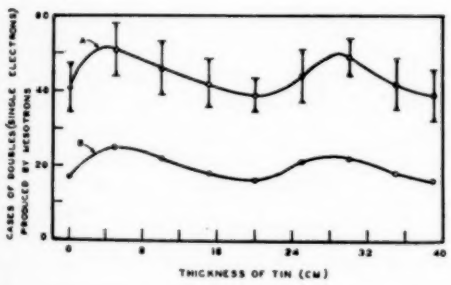

FIG. 1. Number of double coincidences recorded by the analyzing tray (below the tin) as a function of the thickness of the tin.

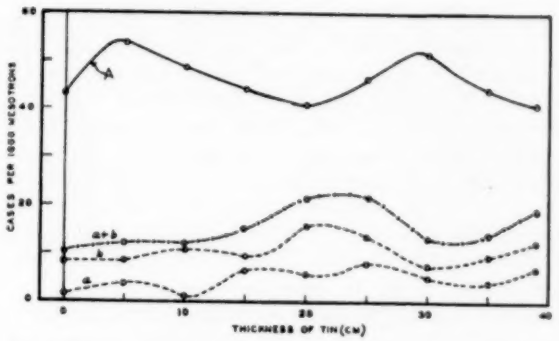

FIG. 2. Curve A, number of double coincidences; curve a, number of quadruple coincidences; curve b, number of triple coincidences at function of the thickness of tin.

It was found that, in 75 percent of the cases, at least one member of each of the two-ray showers disappeared in the lead plate above the third analyzing tray, thus guaranteeing that the shower electrons were in the relatively low energy class.

Figure 2 indicates, in addition to curve A corresponding to Fig. 1, the curve a for quadruple rays, curve b for triple rays, and $a+b$ for the sum of triples and quadruples. In these cases all the curves have been corrected for inefficiency of counter trays, which correction is more important in the case of large showers. Of course, the statistical errors in the large showers are very large, but it is interesting to note that the minimum for doubles is approximately compensated as regards total number of showers by the triples and quadruples.

W. F. G. SWANN
W. E. RAMSEY

Bartol Research Foundation of the Franklin Institute,
Swarthmore, Pennsylvania,
August 2, 1940.

[1] W. F. G. Swann, Rev. Mod. Phys. 11, 242 (1939).

Hydrodynamics and the Morphology of Nebulae

Extragalactic nebulae, in the first approximation, may be regarded as gravitating continuous "viscous fluids," most of them endowed with total angular momenta different from zero.[1] In every nebula two coexisting partial systems must be considered: (1) a *stellar system* and (2) a system formed by *interstellar gases* and dust particles. Hydrodynamically, the two partial systems have radically different characteristics inasmuch as the gaseous systems are characterized by much larger *Reynolds numbers* than the stellar systems. In most cases the motions of the gaseous systems will be turbulent. The Reynolds numbers of the stellar systems lie in the approximate range $0<R<10{,}000$. The flow of stars in some nebulae therefore is "*laminar*," whereas in others it may be "*turbulent*." Nebulae in which the two types of flow coexist show interesting structural subdivisions.

Briefly, some of the results of the hydrodynamical analysis of nebulae are as follows. In an undisturbed nebula of constant total angular momentum, the viscous shearing stresses tend to make the average angular velocity $\bar{\omega}(r)$ independent of the distance r from the center as long as r is smaller than that critical distance r_s at which the mean free path Λ of the particles (or stars) is so great that the difference in gravitational potential $\Phi(r_s+\Lambda)-\Phi(r_s)$ becomes comparable with $\langle w^2\rangle_{Av}$, where w is the velocity of the particles. For $r>r_s$ the angular momenta of the individual particles, rather than $\bar{\omega}$, tend to be constant. In a rotating nebula which has reached a stationary state the average velocity distribution $\bar{v}(r)$ is of the type shown in Fig. 1. Calculations based on the actions of shearing stresses in a laminar flow show that the relaxation time T which is needed to establish the solid body rotation is of the order $Rr_s/\bar{v}_{max}$ if the original motion deviates from the state $\bar{\omega}=$const. by maximum velocity differences $\bar{v}_{max}$. For an originally turbulent flow, it is $T\ll Rr_s/\bar{v}_{max}$. The interstellar gas system therefore reaches the state $\bar{\omega}=$const. long before the stellar system.

In the transition stages of a *stellar system* from $\bar{\omega}\neq$const. to $\bar{\omega}=$const. velocity distributions of the type shown in Fig. 2 may be expected. Region I was originally *turbulent* with large shearing stresses which make T small. Region IIa is characterized by smaller values of R and the smaller shearing stresses of the resulting *laminar* flow result in relatively large values of the time T in which a distribution $\bar{\omega}=$const. can be achieved. Region IIb, because of still smaller R, is a *laminar* flow subject to small values of T. Regions I and IIb consequently reach the stationary state $\bar{\omega}=$const. earlier than the region IIa. While the transition from I to IIa is abrupt, the transitions from IIa to IIb

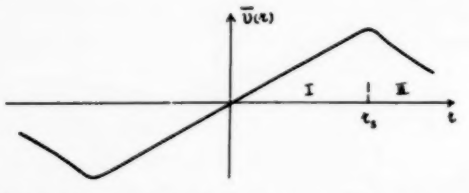

FIG. 1. Velocity distribution in the transition stage of a rotating nebula. The constant angular velocity in the region I and IIb.

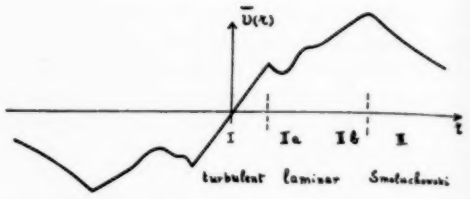

FIG. 2. Velocity distribution in the transition stage of a rotating nebula. The constant angular velocity in the regions I and IIb and the character of $\bar{v}(r)$ in region IIa depend on the original distribution of velocities.

and from IIb to III are more gradual. Region III may be called the *Smoluchowski region* of very long mean free paths. The existence of such regions (globular coronae around nebulae!) is due to effects analogous to those which cause Smoluckowski "temperature jumps" and "slip regions" in ordinary dilute gases.

The existence of turbulent motions in stellar systems leads to interesting speculations regarding the *turbulent correlation length L*. The properties of the *planetary system* as well as of *groups of stars* which are dynamically related may find their explanation in the analysis of this correlation length.

Nebulae of *small mass* may possess a Smoluchowski structure throughout. These nebulae never can reach a Boltzmann stationary state. They are *irregular*, of low surface brightness and hard to detect. Recent systematic search has resulted in the discovery of several systems of this type. Their incorporation in the statistical survey suggests that the frequency distribution of nebulae commonly adopted will in the near future be subject to some major corrections.

Hydrodynamic considerations may also be applied to *clusters of nebulae*. The important fact, which is apparently irreconcilable with the hypothesis of an expanding universe,[2] that the velocity dispersion of field nebulae is only about half that for cluster nebulae, finds its explanation through an analysis similar to that sketched in this communication.

F. ZWICKY

California Institute of Technology,
Pasadena, California,
July 31, 1940.

[1] F. Zwicky, Astrophys. J. **86**, 217 (1937).
[2] F. Zwicky, Proc. Nat. Acad. Sci. **25**, 604 (1939); **26**, 332 (1940).

Protons from $C^{13}+H^2$

Bower and Burcham[1] and also Pollard[2] have observed a group of protons which they attributed to the reaction $C^{13}+H^2\rightarrow C^{14}+H^1+Q$. Bower and Burcham found a 48-cm group of protons when ordinary carbon was bombarded by 800-kev deuterons. The calculated Q value of this group is 5.9 Mev, which is in satisfactory agreement with the energy release calculated from the change in mass. We have confirmed that the proton group must be attributed to the above reaction by using a target of concentrated C^{13}. The target was prepared by one of us (BEW) from methane in which the C^{13} had been concentrated by thermal diffusion.

We bombarded the target with 1.22-Mev deuterons and used a linear amplifier to detect the protons. Long range protons were found and an absorption curve (Fig. 1) showed that they had a range of 55 cm, as expected. The ratio of the intensity of this group to the intensity of the group of 15-cm protons from the reaction $C^{12}+H^2 \rightarrow C^{13}+H^1$ was found to be 0.11 percent. A target in which C^{13} was depleted was then bombarded and the ratio was only 0.029 percent. This showed that the C^{13} had been concentrated in the first target relative to the second by a factor of 3.8, whereas the separation factor had been calculated from the dimensions of the thermal diffusion apparatus as 3.7. The average of these two ratios (0.07 percent) is consequently the ratio of the yields from ordinary carbon at 1.22 Mev bombarding energy. This ratio would vary considerably with different bombarding voltages since the yield of protons from C^{12} shows resonances at 920 and 1220 kev.[3]

An excitation curve has also been obtained for this reaction and is shown in Fig. 2. The indicated error is the probable error increased by a factor of two, since it was necessary to make observations in two separate runs, which were joined at 1450 kev. The change in range of the protons with bombarding energy might be a source of systematic error in a curve of this type. To avoid this, the bias on the recording circuit was made low enough to count all the protons passing through the ionization chamber, and as an additional precaution absorbers were added as the bombarding voltage was increased to insure that the protons were always counted at the same distance from the end of their range.

The yield curve shows a maximum at about 1500 kev. This may be interpreted as a resonance in the yield, which would indicate an excited state in the intermediate nucleus (N^{15}) at 17.55 Mev. This is a surprisingly high energy at which to find isolated excited states, even in so light a nucleus. However, the experimental distribution might result from a resonance or a group of overlapping resonances of higher intensity than the neighboring overlapping levels which may appear as a continuum.

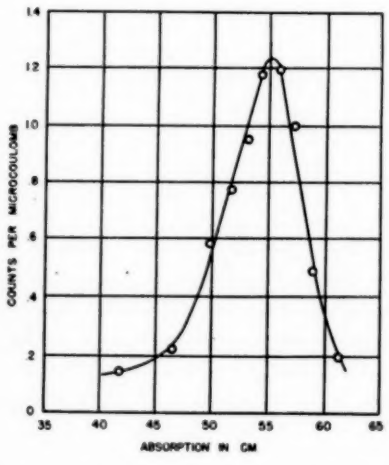

FIG. 1. Range-number curve for protons from $C^{13}+H^2$ at a bombarding energy of 1.22 Mev. The protons were observed with a linear amplifier biased so as to count particles near the end of their range.

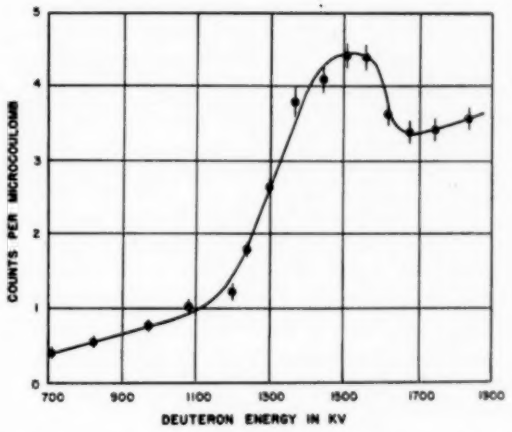

FIG. 2. Excitation curve for protons from the reaction $C^{13}+H^2 \rightarrow C^{14}+H^1$. The maximum in the yield at 1500 kev indicates an excited state in N^{15} at 17.55 Mev.

W. E. BENNETT
T. W. BONNER
EMMETT HUDSPETH
BOB E. WATT

The Rice Institute,
Houston, Texas,
August 13, 1940.

[1] J. C. Bower and W. E. Burcham, Proc. Roy. Soc. **A173**, 379 (1939).
[2] E. Pollard, Phys. Rev. **56**, 1168 (1939).
[3] M. M. Rogers, W. E. Bennett, T. W. Bonner and Emmett Hudspeth, Phys. Rev. **58**, 186 (1940).

Law of Magnus in Single-Crystal Aluminum Wires

By the traveling temperature gradient method of Andrade,[1] good single crystals up to 60 cm length have been produced in 1 mm diameter wires of pure aluminum. The wires were heated internally by a 15-ampere current, the traveling furnace was at 550°C, and moved at about 5 cm per hour along a 1-cm quartz tube evacuated to 0.01 mm Hg, containing the wire supported vertically.

While still unstrained the crystal wires were examined under asymmetrical temperature distributions (140°C peak) for the Benedicks e.m.f. Wires subsequently found by a study of their glide planes to have been uniformly crystallized, gave e.m.f.'s less than 0.02 microvolt, independent of position of the temperature distribution; wires found imperfectly crystallized gave e.m.f.'s greater than 2 microvolts, dependent upon position. Intermediate conditions were not found.

One specimen was deliberately made non-uniform at a selected place, P, by interrupting the motion of the furnace for several minutes when over P. Electromotive forces were produced in this crystal by a small symmetrical heater (110°C) placed at different places near P. On the side from which the traveling furnace had approached, there was a sharp peak of -10 microvolts close

to P, on the other side a less sudden maximum +6 microvolts; e.m.f.'s reduced to zero for positions not near P. The overheated portion P behaved as a thermoelectrically different substance, and was found upon examination to be a hard polycrystalline section in an otherwise uniformly aligned single-crystal wire.

Since aluminum crystals are cubic, changes in orientation cannot cause contact e.m.f.'s, and since the wires were freed from internal strains by the heating processes, the usual causes of heterogeneity were absent.

Benedicks' e.m.f. in ordinary wires[2] is apparently due to electrical disturbances produced by positive emission of impurity nuclei from the wire. In the present work, the slow annealing should have baked out most of the impurity removable by positive emission, the remaining traces of impurity being effectively permanent.

It is suggested now that these permanent impurity nuclei are incorporated in the lattice of the single-crystal part of the wire, their thermoelectric effect being lost; in the polycrystalline section this solid solution does not occur, and the impurity atoms form the "cement" between the polycrystals, and change the thermoelectric properties of the aggregate.

If this interpretation is correct, it can be concluded that there is no contradiction with the law of Magnus in uniformly aligned single-crystal wires of aluminum.

C. Y. Ma
William Band

Department of Physics,
Yenching University,
Peiping, China,
July, 1940.

[1] E. N. Da C. Andrade, Proc. Roy. Soc. **A163**, 16 (1937).
[2] Ch'eng and Band, Proc. Camb. Phys. Soc. **35**, 622 (1939).